Class: RPT
Doc. no.: 1793903
Rev.: A
Prepared by: KNJN
Approved by: JCP

TERMA
CAGE code: R0567

Analysis of Impact on Radar Coverage due to Planned Wind Farm Thor Havmøllepark

Prepared:

Kristian Johnsen 25/05-21

Kristian N. Jakobsen — Date
Systems Architect

Approved: 26/5 2021

Axel C.K. Thomsen — Date
Senior Specialist

Authorized: 26/05-2021

Jens Chr. Pedersen — Date
Senior Director

Record of Changes

ECO	Description	Rev	Date
	Released	A	See Front Page

Contents

1 Introduction 3
1.1 Purpose 3
1.2 Scope 3
2 References 4
3 Definitions and abbreviations 4
4 Summary and Conclusions 5
4.1 Mitigation 8
5 Operational concerns 8
5.1 Background for evaluations and calculations 10
6 Locations and Setups analysed 12
7 Influence on coastal radars surface coverage, evaluations and calculations 20
7.1 Ghost targets 21
7.2 Side lobes 120
7.3 Shadowing 120
7.4 Receiver sensitivity 121
8 Influence on air coverage radars, evaluations and calculations 123
8.1 Overview 124
8.2 Radar line of sight assessment 124
8.3 Top-level engineering assessment – PSR and SSR 134
8.4 Engineering assessment for PSR 136
9 Influence on ship navigational radars 151
9.1 Side lobes 153
10 Mitigation with additional radar(s) 153
10.1 Radar Coverage 155
Annex A Coordinates of Windmills 158
Annex B Formula symbols of Annex C in [1] 190
Annex C Shadow Height Illustrations 191

1 Introduction

1.1 Purpose

Energinet requested Terma A/S to perform an engineering assessment of the projected windmills to be erected at Thor Havmøllepark. The assessment has been requested in anticipation of the hearing process by The Danish Defense Acquisition and Logistics Organization (DALO).

The purpose of this report is to assess the potential impact of Thor Havmøllepark on Radar Surveillance Sensors related to Air and Sea Traffic. The assessment of the potential impact of wind turbines on the air coverage of the Radar Surveillance Sensors will follow the Eurocontrol guidelines, [1]. The maritime coverage will include an assessment of:

1. Coverage / blockage / shadowing
2. Other side effects from the wind farm, including the risk of generating false information.
3. Suggestions on mitigation of possible change in coverage affecting surface targets.

1.2 Scope

The scope is limited to assess the impact on radars defined by DALO. In this case, DALO has requested an assessment of the impact on the air coverage by the long-range PSR/SSR at Karup.

For surface coverage, the KYRA Thyborøn, the potential new KYRA at Hvide Sande and the projected Vesterhav Nord Gap-Filler radar. The potential new KYRA at Hvide Sande is using a projected position, found in agreement with FMI.

The scope is limited to assess the impact from the projected wind farm at Thor Havmøllepark. In order to cover the potential worst case, four different setups have been modelled for two different windmill types, 125 windmills each producing 8MW and 67 windmills each producing 15MW. The first 3 setups describe the wind turbines located in one sector of the area, while the fourth assumes a more distributed pattern.

The scope includes a substation, to be placed in the center of the wind farm. The dimensions and probable location have been provided by Energinet.

The radar line-of-sight (LoS) assessment is based on digital terrain models. Thus, other surface obstructions such as buildings or trees are not included in the analysis. This implies, that the analysis will be based on an ideal radar line-of-sight providing the worst-case criteria for assessing the impact of the wind turbines.

The report assesses the risk of generating false information affecting surface targets. The type of surface targets considered are from small targets to large ocean-going vessels.

Other radars, e.g. onboard ships are not included in the analysis, but effects are mentioned where relevant.

2 References

Ref.	Title
1	EUROCONTROL Guidelines for Assessing the Potential Impact of Wind Turbines on Surveillance Sensors, EUROCONTROL-GUID-0130, Edition Number 1.2, 09/09/2014
2	The International Association of Marine Aids to Navigation and Lighthouse Authorities (IALA): Guideline No. 1111 on Preparation of Operational and Technical Performance Requirements for VTS Systems
3	Report written by Martin Howard and Colin Brown - QINETIQ/03/00297/1.1 - MCA MNA 53/10/366 - 15 November 2004. *Results of the electromagnetic investigations and assessments of marine radar, communications and positioning systems undertaken at the North Hoyle wind farm by QinetiQ and the Maritime and Coastguard Agency.*
4	Article in Seaways, August 2005 by Captain Colin Brown Seaways August 2005 *Offshore wind farms*.
5	Department of Trade & Industry, U.K. Government: *Methodology for Assessing the Marine Navigational Safety Risks of Offshore WindFarms, 7th September 2005*
6	Report written for the Maritime and Coastguard Agency by Colin Brown, MCA Contract MSA 10/6/239, May 2005. *Report of helicopter SAR trials undertaken with Royal Air Force Valley 'C' Flight 22 Squadron on March 22nd, 2005.*
7	L. S. Rashid, A.K. Brown, IET Radar 2007, Edinburgh UK, *Impact Modelling Of Wind Farms On Marine Navigational Radar*
8	A Report compiled by the Port of London Authority based on experience of the Kentish Flats Wind Farm Development: *Interference to radar imagery from offshore wind* farms, 31 March 2005.
9	A.C.K.Thomsen, O.Marqversen, M.Ø.Pedersen, C.Moeller-Hundborg, E.Nielsen, L.J.Jensen, K.Hansen. *Air Traffic Control at Wind Farms with Terma SCANTER 4000/5000*
10	Digital Terrain Model: DK_DTM_10m_OV_L02 Geodatastyrelsen, http://download.kortforsyningen.dk/content/

3 Definitions and abbreviations

Term	Definition
AGL	Above Ground Level
AIS	The Automatic Identification System (AIS) is an automated tracking system used on ships and by Vessel Traffic Services (VTS) for identifying and locating vessels by electronically exchanging data with other nearby ships and VTS stations. AIS information supplements marine radar, which continues to be the primary method of collision avoidance for water transport.
AMSL	Above Mean Sea Level
ARPA	Automatic Radar Plotting Aids

Term	Definition
CFAR	Constant False Alarm Rate is a mechanism in a radar adapting the sensitivity to eliminate noise from in the radar picture, from various sources such as rain or sea clutter.
DALO	The Danish Defense Acquisition and Logistics Organization (In Danish: FMI / Forsvarsministeriets Materiel- og Indkøbsstyrelse)
DSM	Digital Surface Model
FFM	Far-Field Monitor
IALA	International Association of Marine Aids to Navigation and Lighthouse Authorities
KYRA	KYst Radar, a name given to the Danish coastal radars, used for coastal surveillance
LoS	Line-of-Sight
NM	Nautical Miles
PSR	Primary Surveillance Radar
RCS	Radar Cross Section. The RCS is defined as the reflected power from an object [W] divided by power density at the object [W/m^2] and thus has the dimension of square meters [m^2]. The Radar Cross Section cannot be directly related to the physical size of objects.
RMP	Recognized Maritime Picture
SSR	Secondary Surveillance Radar
VTS	Vessel Traffic Services
WGS84	World Geodetic System (1984)

4 Summary and Conclusions

Energinet requested Terma A/S to perform an assessment of the projected Windfarm to be build offshore off Thorsminde. The assessment is done as a preliminary part of the hearing process by The Danish Defense Acquisition and Logistics Organization (DALO).

DALO has requested an assessment of the impact on the long-range PSR/SSR in Karup for the air coverage and the impact on the Thyborøn KYRA, a gap-filler radar at Vesterhav Nord and a potential new KYRA at Hvide Sande for surface coverage.

Four different configurations of Windmill setups have been analyzed. For each configuration, two possible windmill types have been analyzed.

For 8 MW Windmills:

125 wind turbines have been assessed. The wind turbines have a hub height of 105m ASL and a rotor diameter of 167m. The total height of each wind turbine ASL is 190m.

The turbines have been examined in four different setups.

For 15 MW Windmills:

67 wind turbines have been assessed. The wind turbines have a hub height of 150m ASL and a rotor diameter of 260m. The total height of each wind turbine ASL is 280m.

4.1 Air Coverage

Scenario 1:

From Karup TPS PSR, for the 8MW turbines, the turbines are located between 43.95NM to 48.73NM, covering in azimuth 263.3° to 285.5°. For the 15MW turbines, the turbines are located between 43.79NM to 48.80NM, covering in azimuth 264.2° to 285.5°

Scenario 2:

From Karup TPS PSR, for the 8MW turbines, the turbines are located between 43.77NM to 51.65NM, covering in azimuth 267.5° to 285.6°. For the 15MW turbines, the turbines are located between 43.79NM to 51.86NM, covering in azimuth 267.2° to 285.5°

Scenario 3:

From Karup TPS PSR, for the 8MW turbines, the turbines are located between 45.76NM to 57.38NM, covering in azimuth 264.5° to 276.4°. For the 15MW turbines, the turbines are located between 46.27NM to 57.73NM, covering in azimuth 263.3° to 285.5°

Scenario 4:

From Karup TPS PSR, for the 8MW turbines, the turbines are located between 43.48NM to 57.78NM, covering in azimuth 264.2° to 286.3°. For the 15MW turbines, the turbines are located between 43.80NM to 57.73NM, covering in azimuth 264.2° to 285.8°

The assessment methodology will be based on the procedural steps defined in [1].

The impact assessment has the following findings:

1. The PSR have line-of-sight of the turbines in scenario 1, 2, and 4 for the 15MW turbines. For scenario 3 the Karup TPS PSR does not have line of sight. [redacted]

   [redacted]

   [redacted]

   [redacted]

2. The SSR are further away than 16 km, thus needing no assessment according to [1].
3. The guideline recommends a safe-guarding zone for Far-field monitors in azimuth for Karup (TPS) PSR and SSR. The corresponding zones are
   a. Scenario 1: PSR, 259.7° – 289.1°, SSR, 260.9° – 287.9° for the 8MW turbines and PSR, 260.6° – 289.1°, SSR, 261.8° – 287.9° for the 15MW turbines.
   b. Scenario 2: PSR, 263.9° – 289.2°, SSR, 265.1° – 288.0° for the 8MW turbines and PSR, 263.6° – 289.1°, SSR, 264.8° – 287.9° for the 15MW turbines.
   c. Scenario 3: PSR, 260.9° – 280.0°, SSR, 262.1° – 278.8° for the 8MW turbines and PSR, 259.7° – 289.1°, SSR, 260.9° – 287.9° for the 15MW turbines

d. Scenario 3: PSR, 260.6° – 289.9°, SSR, 261.8° – 288.7° for the 8MW turbines and PSR, 260.6° – 289.4°, SSR, 261.8° – 288.2° for the 15MW turbines

[redacted]

[redacted]			[redacted]
			[redacted]
[redacted]	[redacted]	[redacted]	[redacted]
	[redacted]	[redacted]	[redacted]
	[redacted]	[redacted]	[redacted]

[redacted]

8. *No mitigation alternatives have been proposed. This will be provided if found relevant by DALO.*

4.2 Surface Coverage

In summary this leads to the following conclusions in relation to the existing Terma Radars on shore along the coastline.:

1. The main effect will be the risk of ghost echoes and false tracks forming in the area.
    a. These will mostly be associated with large ships such as container carriers, tankers, cruise ships and similar vessels.
    b. The risk of forming ghost echoes associated with other larger ships such as coasters, bulk carriers and fishing trawlers will be less.
    c. Ghosts associated with even smaller ships are expected to be insignificant.

    Furthermore, ghost echoes may occur already when the foundations for the wind turbines have been placed offshore.

    The ghost echoes are mostly seen on large traffic moving very close to the windfarm.
2. Considering the distances involved, the impact from side lobes on coastal radars is evaluated to be insignificant.

3. The effect of the shadowing will be that very small targets may be hidden in shadows in a small area directly behind the wind turbine towers. The effect on larger targets may be a marginal variation in the detection probability, in accordance with diminished/increased echo power.
4. The signal processing of the existing radars will not be affected by the typical wind farm layout.

In addition, interfering side lobes, multiple and reflected echoes (ghosts) may be on shipborne (navigational) radar systems, where:

9. Calculations and experience from other wind farms show that generation of ghosts as complete ships images could lead to confusion onboard ships when ships are within 0.5 nautical mile distance from a wind turbine.

Side lobes caused by imperfect antenna radiation diagrams of radars onboard ships typically occur at angles up to 10 degrees on both sides of the individual wind turbine and at distances up to several nautical miles. However, such mechanisms are known by navigators and they are therefore unlikely to cause confusion.

4.3 Mitigation

Ghost echoes can be eliminated by combining information from more than one radar. However, it is unknown if this lies within the capability of the VTS/coastal radar system.

Guidance from VTS should also reduce risk to shipping in the area. Possible add-on requirements to radar coverage due to the revised shipping is considered by paragraph 10 this report. Refer to IALA recommendations, including [2] for further guidance on this subject.

5 Operational concerns

For surface surveillance AIS may provide important additional information to produce the right RMP.

Figure 1 shows the traffic density in 2017 as measured by AIS, obtained from www.marinetraffic.com/en, with the approximate area of concern circled in.

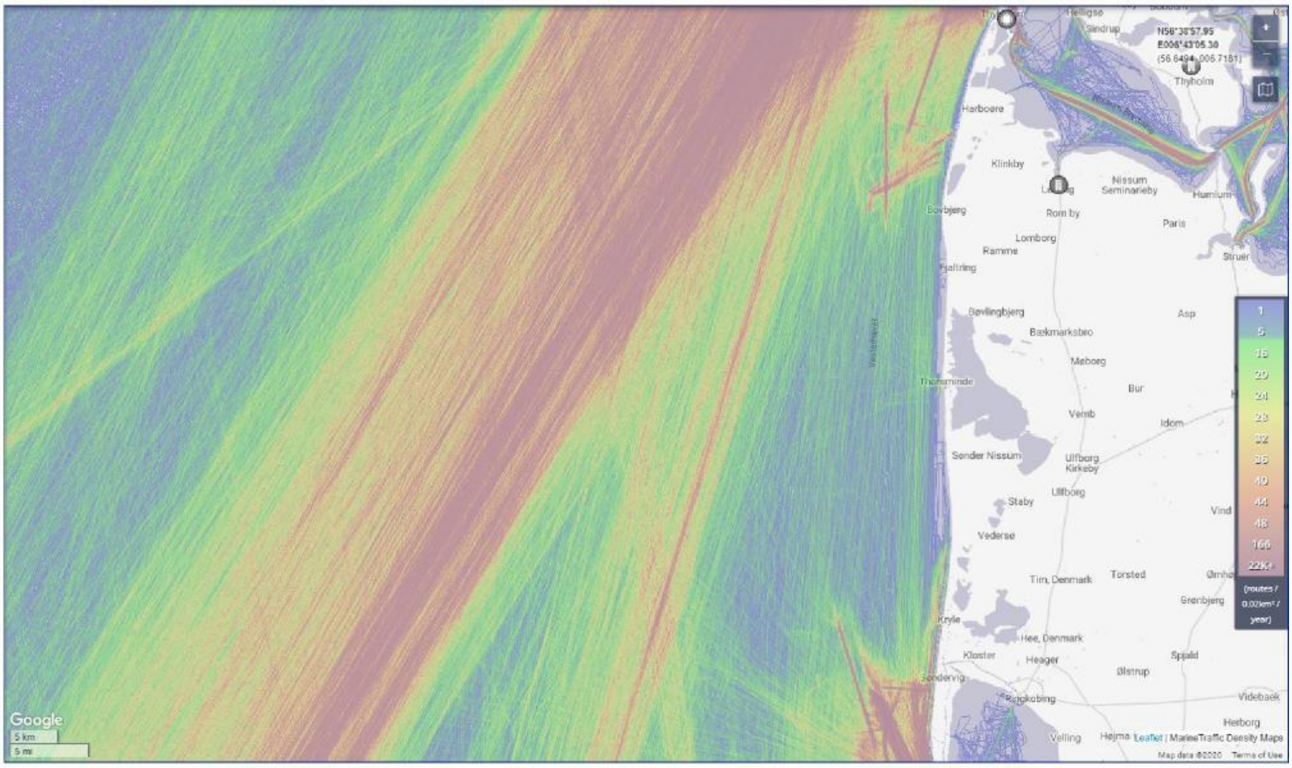

Figure 1 Traffic density in the area of concern, data from 2017

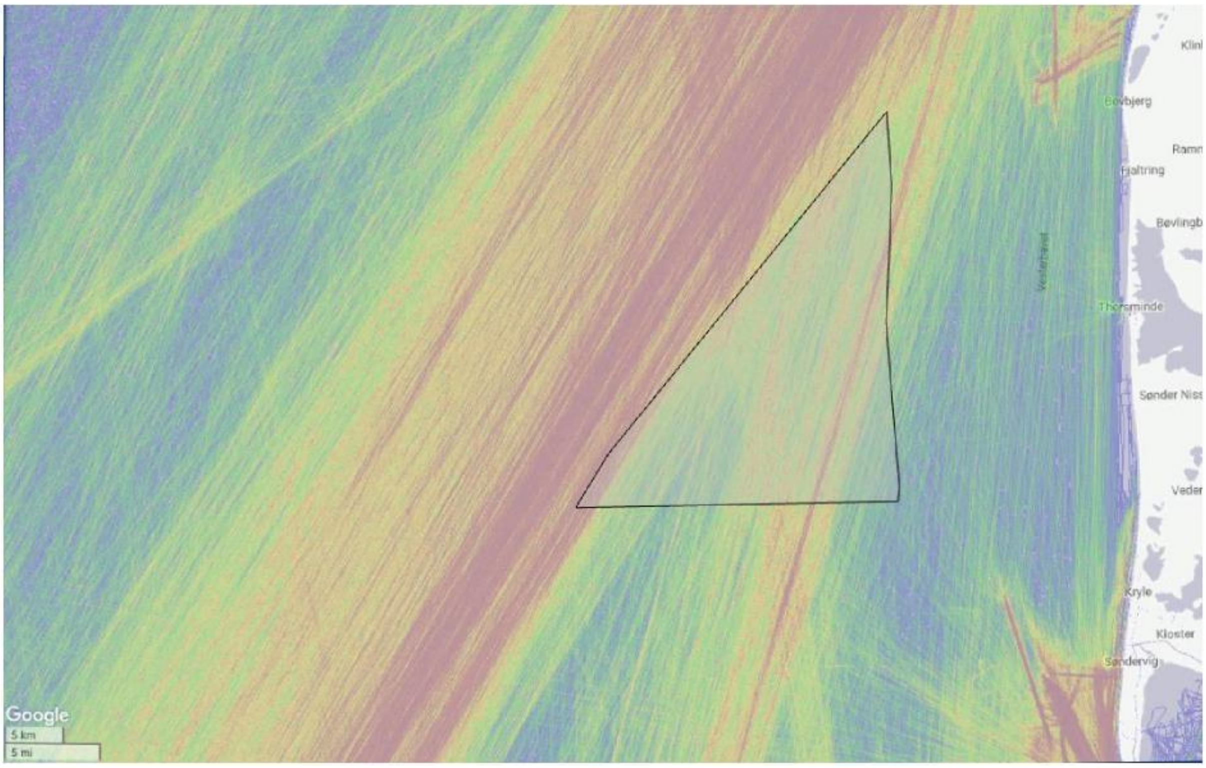

Figure 2 Traffic density with the windfarm area included - data from 2017

The following concerns, relative to radar coverage, are addressed:

a) False information (ghost targets and side lobes) may be presented on VTS/coastal radars.

b) False information (ghost targets and side lobes) may be presented on navigational radars onboard ships, which may confuse navigators and lead to improper measures taken.

c) Sensitivity in the ability of small targets detection by radars may be reduced as a result of small targets being masked behind wind turbine towers or due to influence on radar signal processing.

The mechanisms are described as follows.

5.1 Background for evaluations and calculations

5.1.1 Surface Evaluation

Basis for the work on influence on surface radar by wind turbines was published by UK specialists, see publications [3], [4], [5], [6], [7], and [8]. The publications describe the experience and experimental field tests from the establishment of the first large-scale, offshore wind farms in the United Kingdom, with respect to their potential effect on marine radar, communications and navigation systems.

Basis for the work on influence on the aerial coverage is based on Eurocontrol guidelines [1]

In addition to the published tests, Terma A/S has gained substantial experience as seen from the effects of wind turbines observed on several locations, concluding that the dominating operational influence is the presence of ghost echoes, where:

- Several ghost echoes may appear on ships and VTS/coastal radars when ships pass close by wind turbines – at short and longer ranges. Also indicated by [8].
- The tower of wind turbines, especially large new designs, give substantially stronger radar returns than anticipated by [6]. [2] reveals RCS up to 60 dBm however, the individual windfarm will only be illuminated by a fraction of the radar beam at typical distances from a shore-based radar, and the geometry of the towers means that less energy is reflected towards targets on the surface. The best evaluation and experience are that modelling with 40 dBm (10.000 m2) for the 8 MW turbines and 43 dBm (20.000 m2) for the 15 MW turbines will provide representative results.
- The RCS of oceangoing ships may be as large as 63 dBm, however the likelihood of the entire target being illuminated by the radar beam from a land-based radar is small (or the reflected energy from a wind turbine is small). The best evaluation and experience are that modelling with 50 dBm (100.000 m2) will provide representative results.
- In addition to what is considered as representative calculations, worst case calculations assuming 6 dB higher RCS of ships and wind turbines.

NOTE: *Due to the large physical size of the turbines and ships under analysis, the effect of phase front curvature causes a reduction of the apparent RCS at significant distances compared to the theoretical RCS for infinite distance, see [9].*

Effects in relation to detection of surface targets (ships) are virtually unchanged as a result of aspect angle of the individual rotor and whether the rotors were turning or not.

Radar returns for airspace monitoring can be substantially affected as a result of aspect angle of the individual rotor and whether the rotors were turning or not.

5.1.2 Air Detection methodology

The assessment methodology will be based on the procedural steps defined in [1].

5.1.2.1 Radar line of sight assessment (PSR and SSR)

Can be performed in accordance with [1] section 4.1.

The line of sight is analyzed based on a public available terrain model [10]. The applied model is a digital terrain model (DTM) with a horizontal resolution of 10m provided by Geodatastyrelsen. The line of sight analysis is based on a 30m cell size.

To simulate the radar line of sight, a factor k (4/3) is included to account for electromagnetic wave propagation. This is simulated in ArcGIS Pro using line-of-sight analysis (viewshed) with a refractivity coefficient of 0.25.

5.1.2.2 PSR Probability of Detection

When a wind turbine lies in the line of sight of the PSR, the probability of detection can be reduced in two ways:

I. In a shadow region directly behind the wind turbine
II. In a volume located above and around the wind turbine
III. In a larger volume located above and around the wind turbine if the radar has signal processing, plot extractor or mono-radar tracking techniques which can be affected by the wind turbine.

The first effect is caused by the attenuation due to the wind turbine being an obstacle for the electromagnetic field. The second effect is caused by the large amount of energy reflected by the wind turbine, causing an increase in the radar’s detection threshold (CFAR) in the range azimuth cell, or in worst cases receiver saturation, where the wind turbine is located and in some adjacent cells.

Shadow Region

The shadow region can be determined by calculation of the shadow height and shadow width. The shadow height can be calculated according to formula provided in [1] section A.2.

The shadow height is calculated prior and after deployment, to determine the relative loss in minimum detection altitude.

The half-shadow width can be calculated according to Equation 5 provided in [1] section A.3. The typical cross-section of the shadow effect is shown in Figure 4. The formula provides an approximation of the path difference at the center azimuth angle behind an obstruction (point A) and point B where the direct and reflected signal will combine constructive to give maxima.

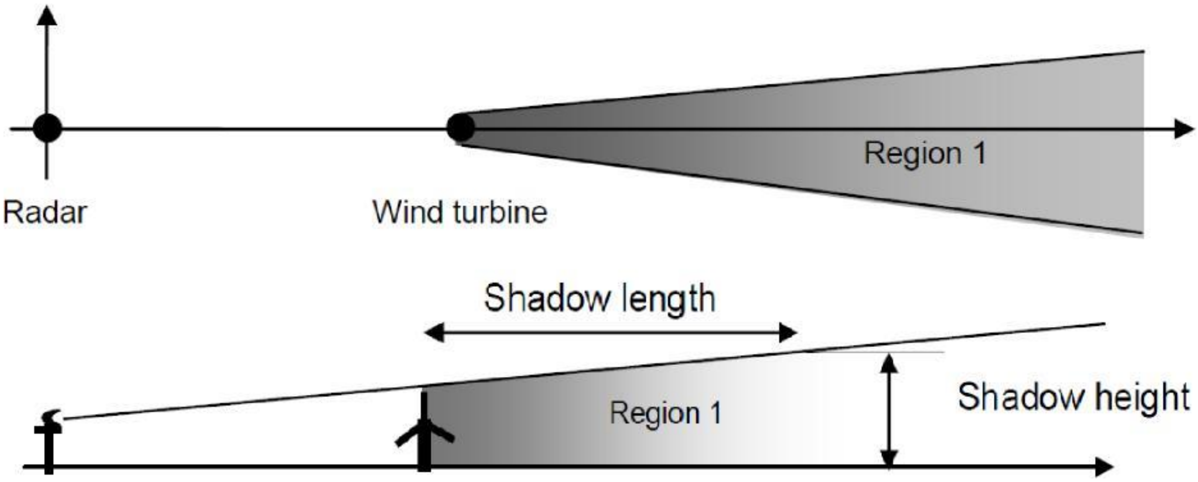

Figure 3 – Illustration of shadow region, taken from [1]

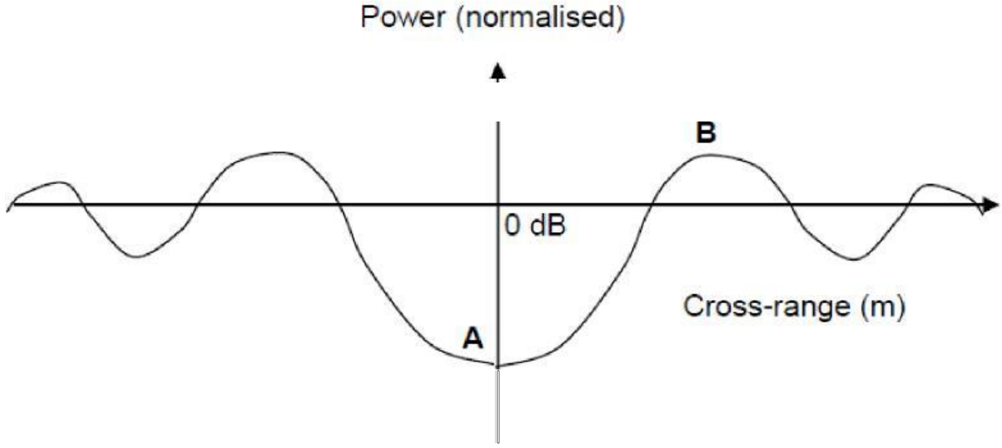

Figure 4 – Illustration of shadow width according to [1]

6 Locations and Setups analysed

There are four types of setups analysed in this report; Scenario 1 with the turbines located mostly on the eastern edge of the project area, Scenario 2 with the turbines focused on the northern side, Scenario 3 with the turbines located in the southwestern part of the project area and Scenario 4 with the turbines spread over the project area. As the final locations of the wind turbines have not yet been decided, these setups should cover all extremes and thus the worst-case scenario. For each scenario, the windfarm can either be construed of 125 8MW turbines or 67 15MW turbines. The heights and locations for the different scenarios can be seen in Annex A Coordinates of Windmills. [redacted]

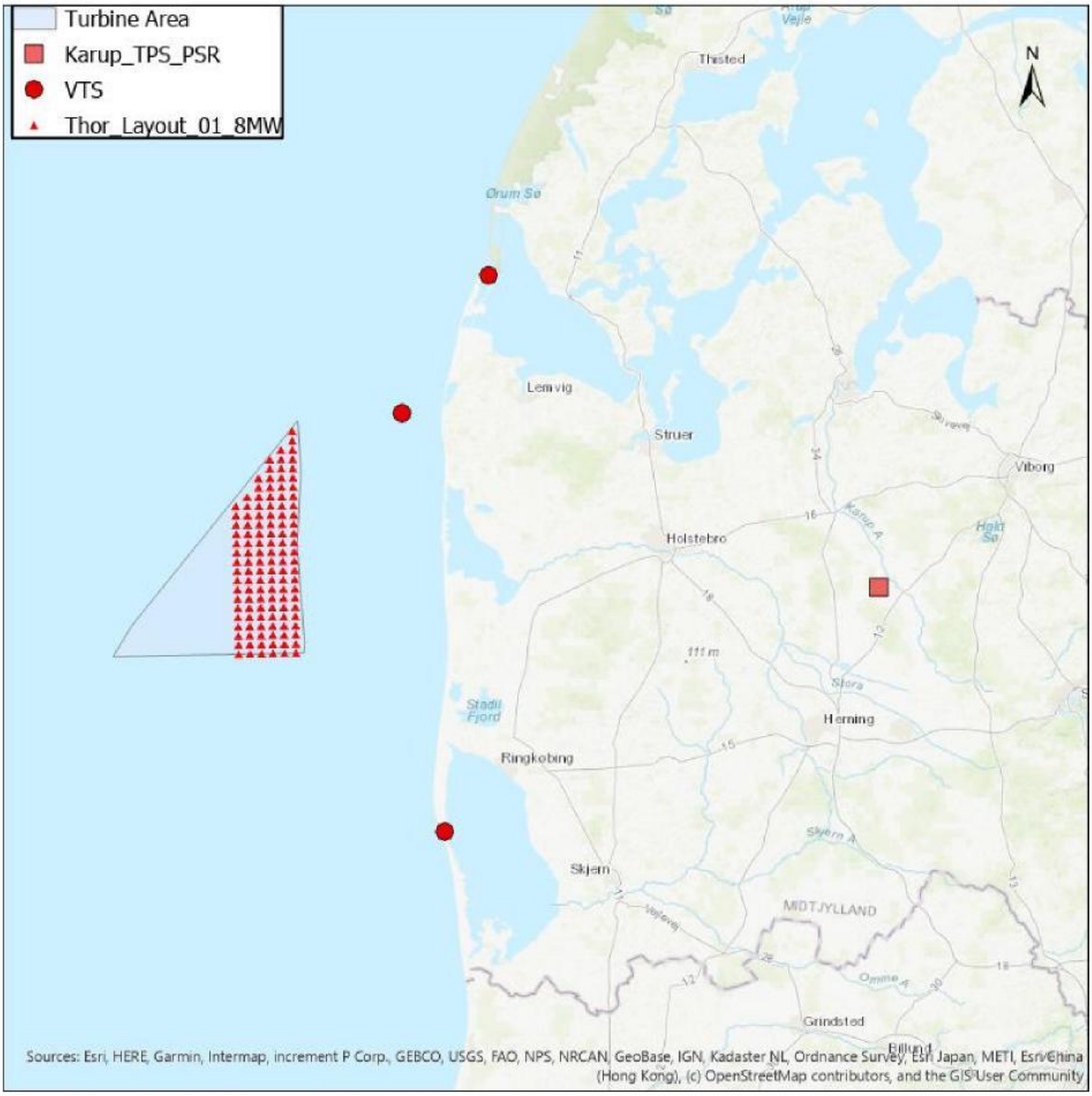

Figure 5 – Scenario 1: 8MW Windmills

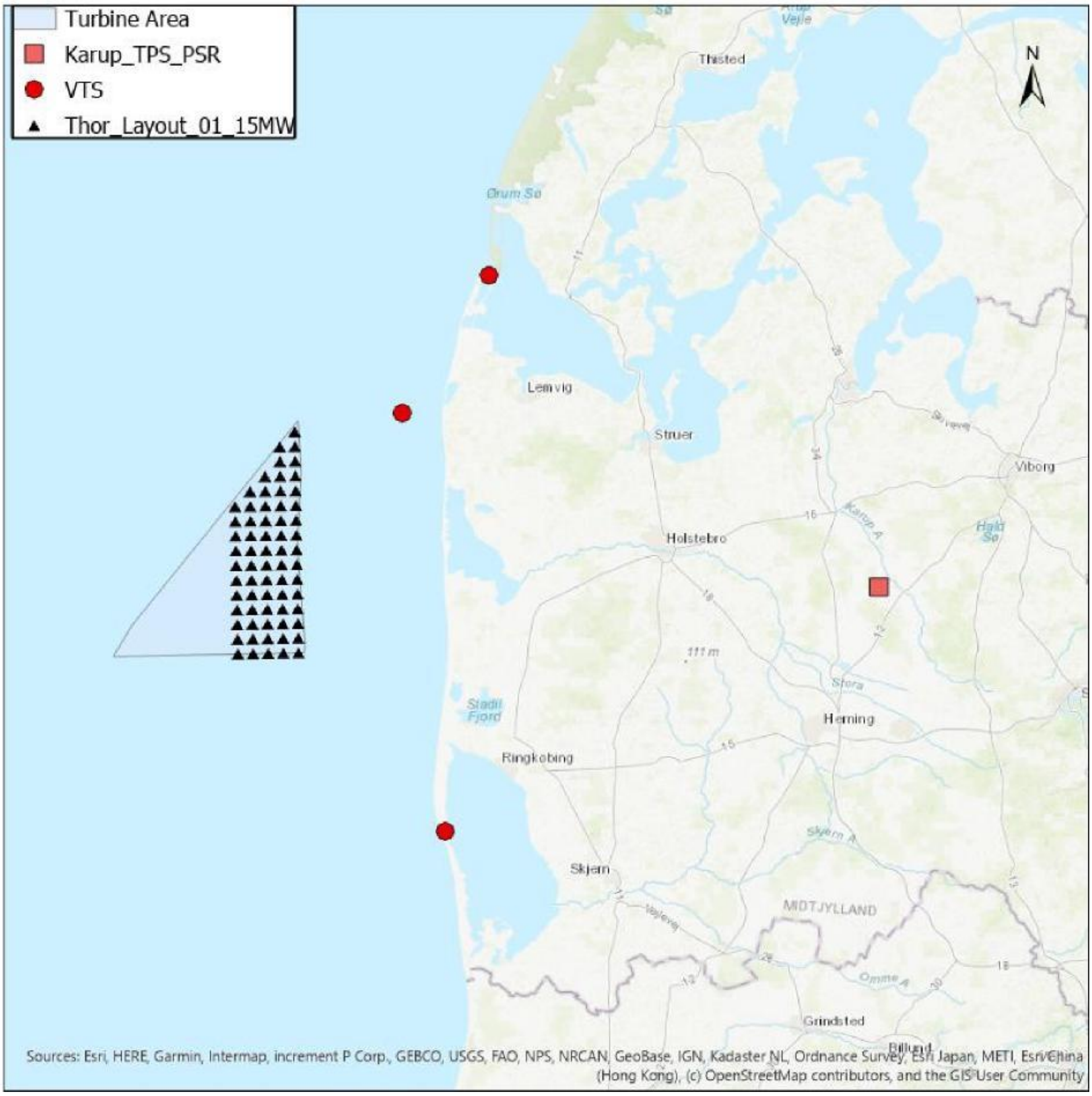

Figure 6 – Scenario 1: 15MW Windmills

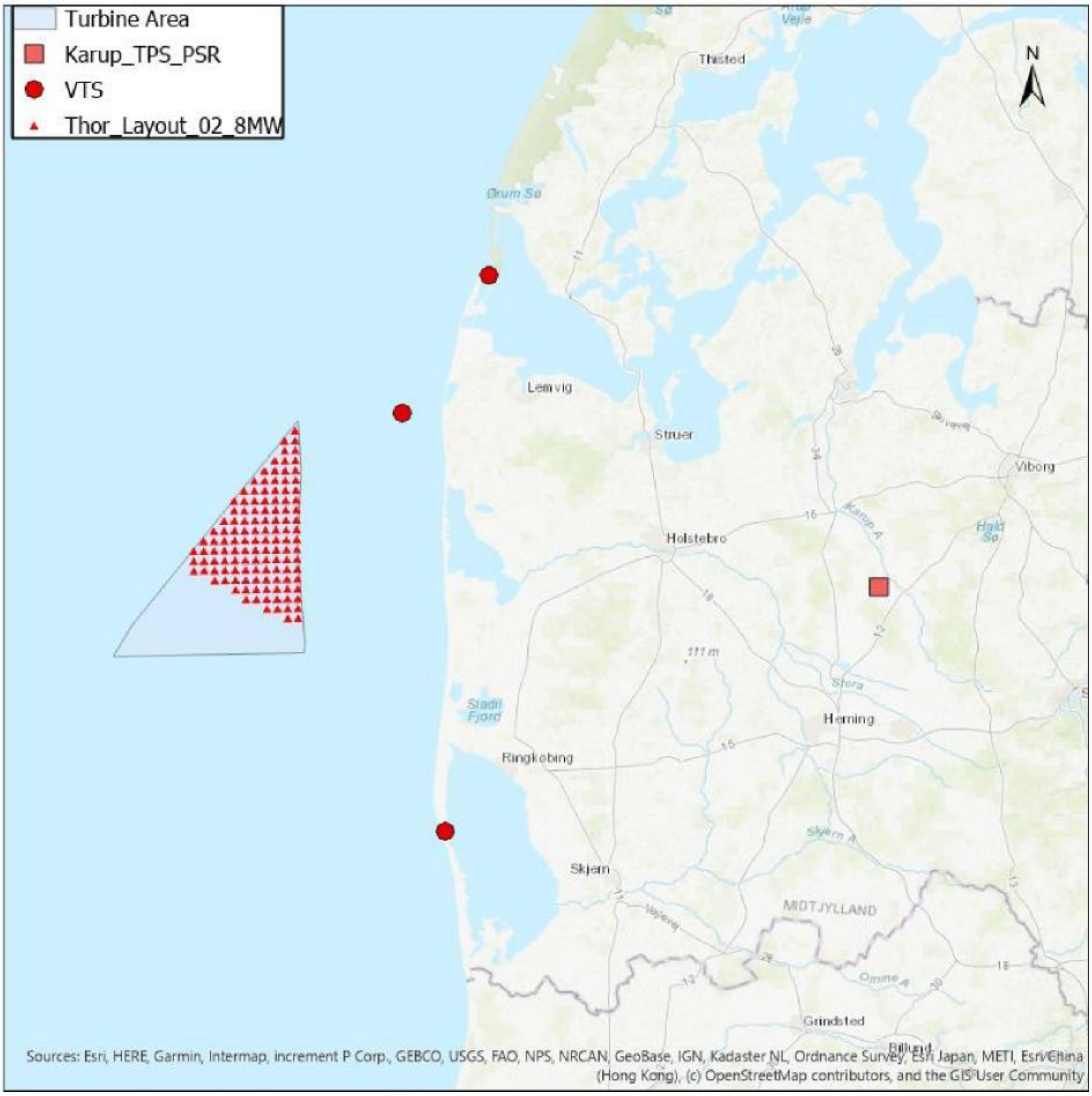

Figure 7 – Scenario 2: 8MW Windmills

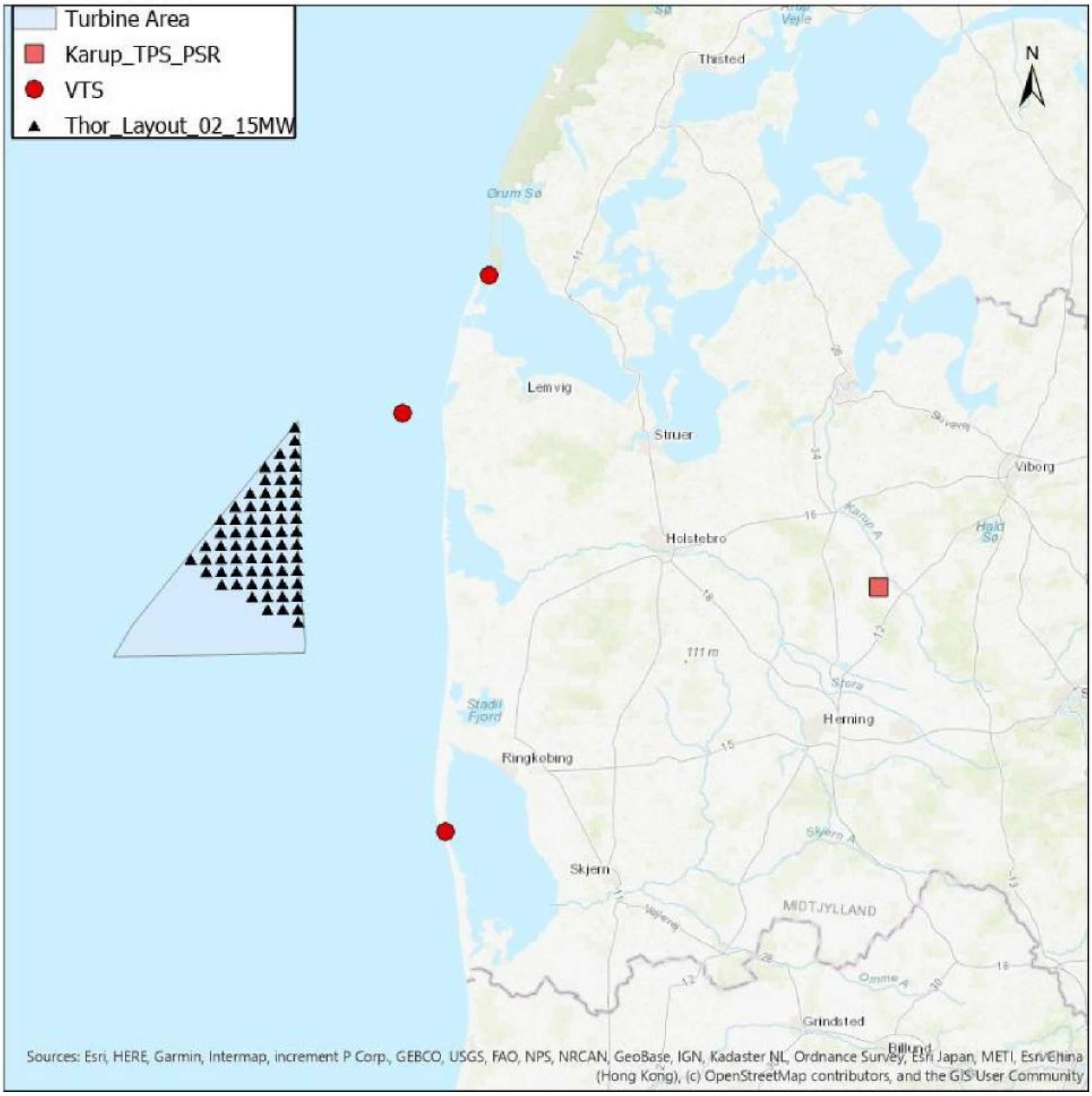

Figure 8 – Scenario 2: 15MW Windmills

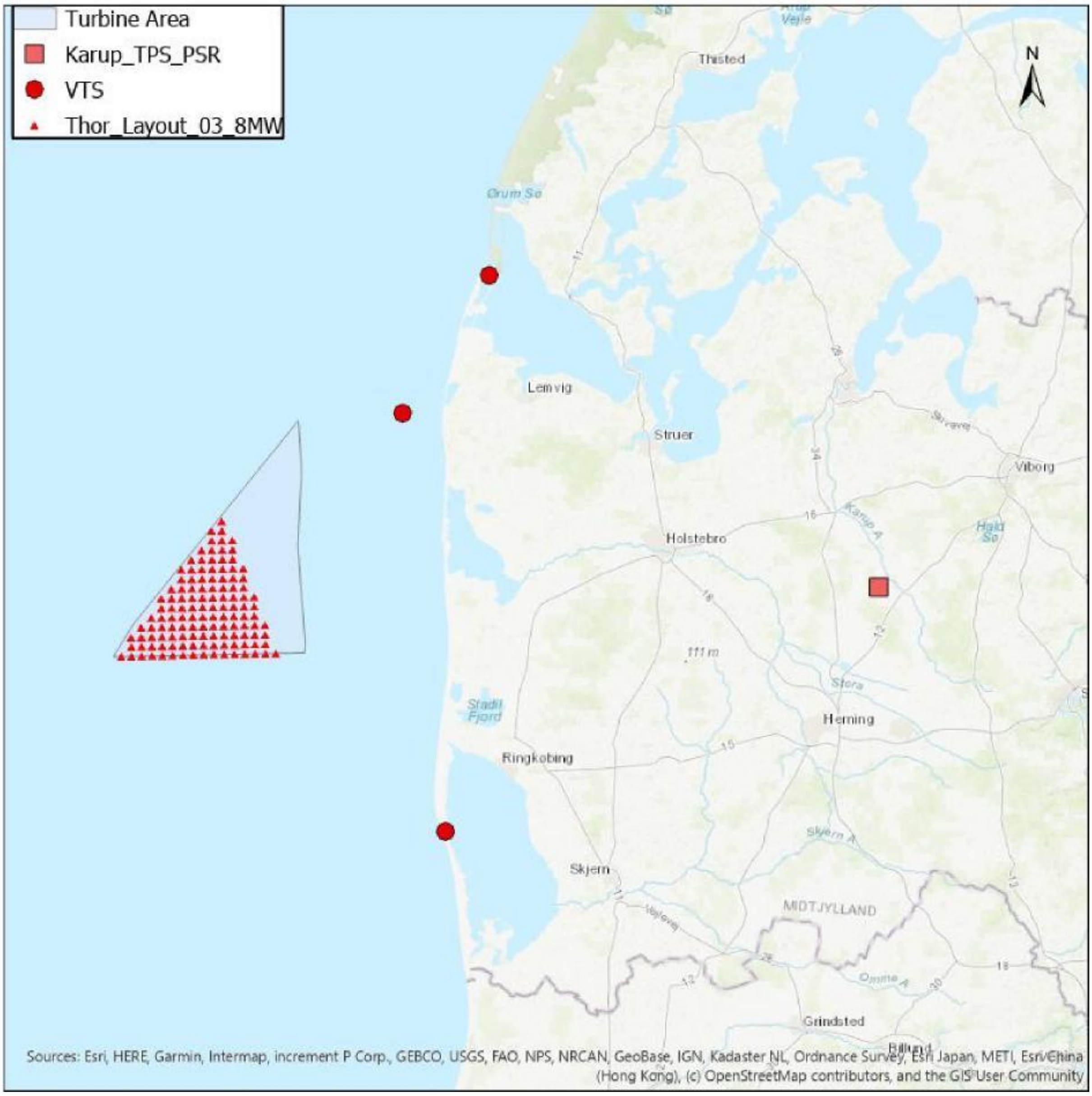

Figure 9 – Scenario 3: 8MW Windmills

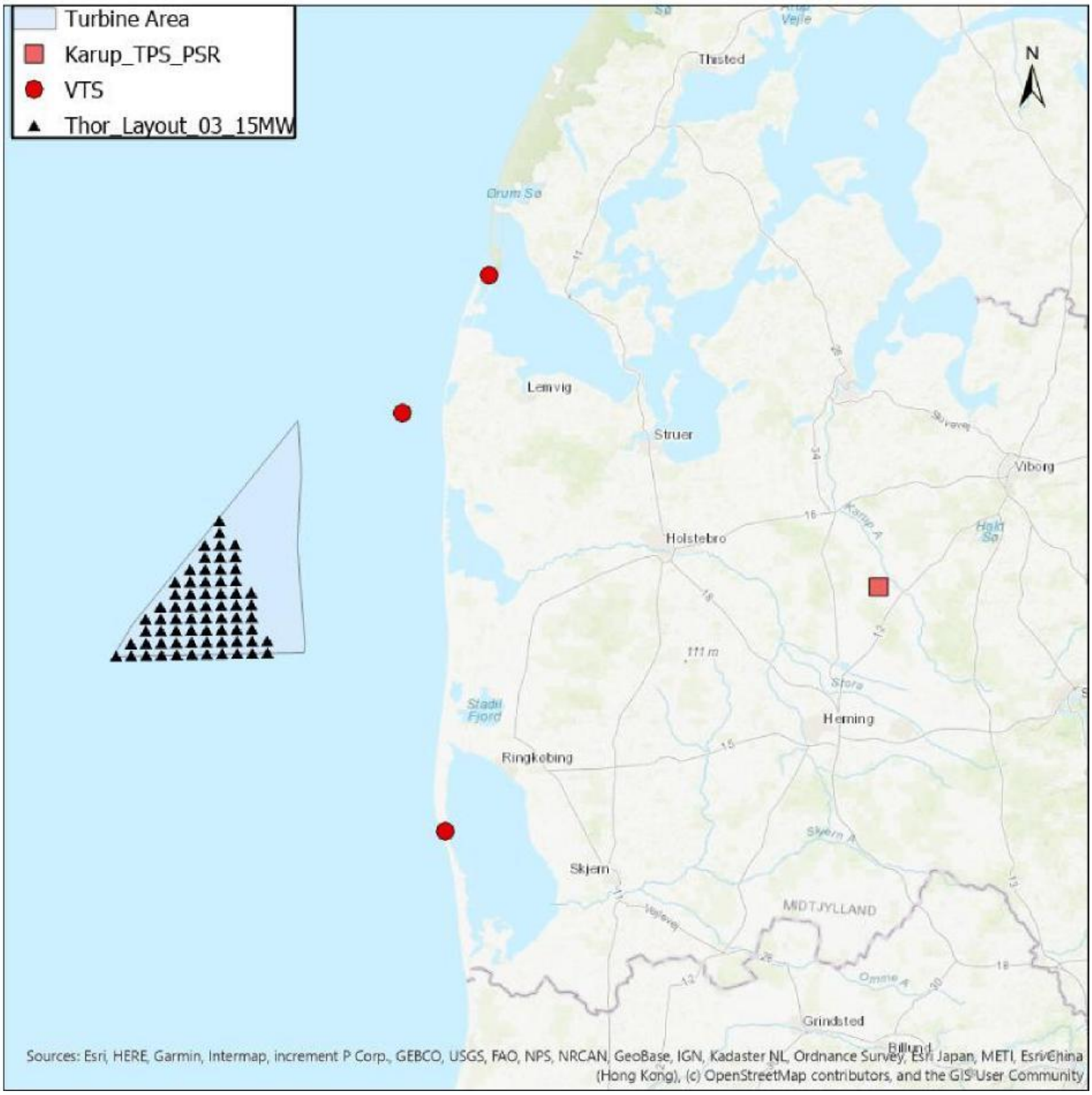

Figure 10 – Scenario 3: 15MW Windmills

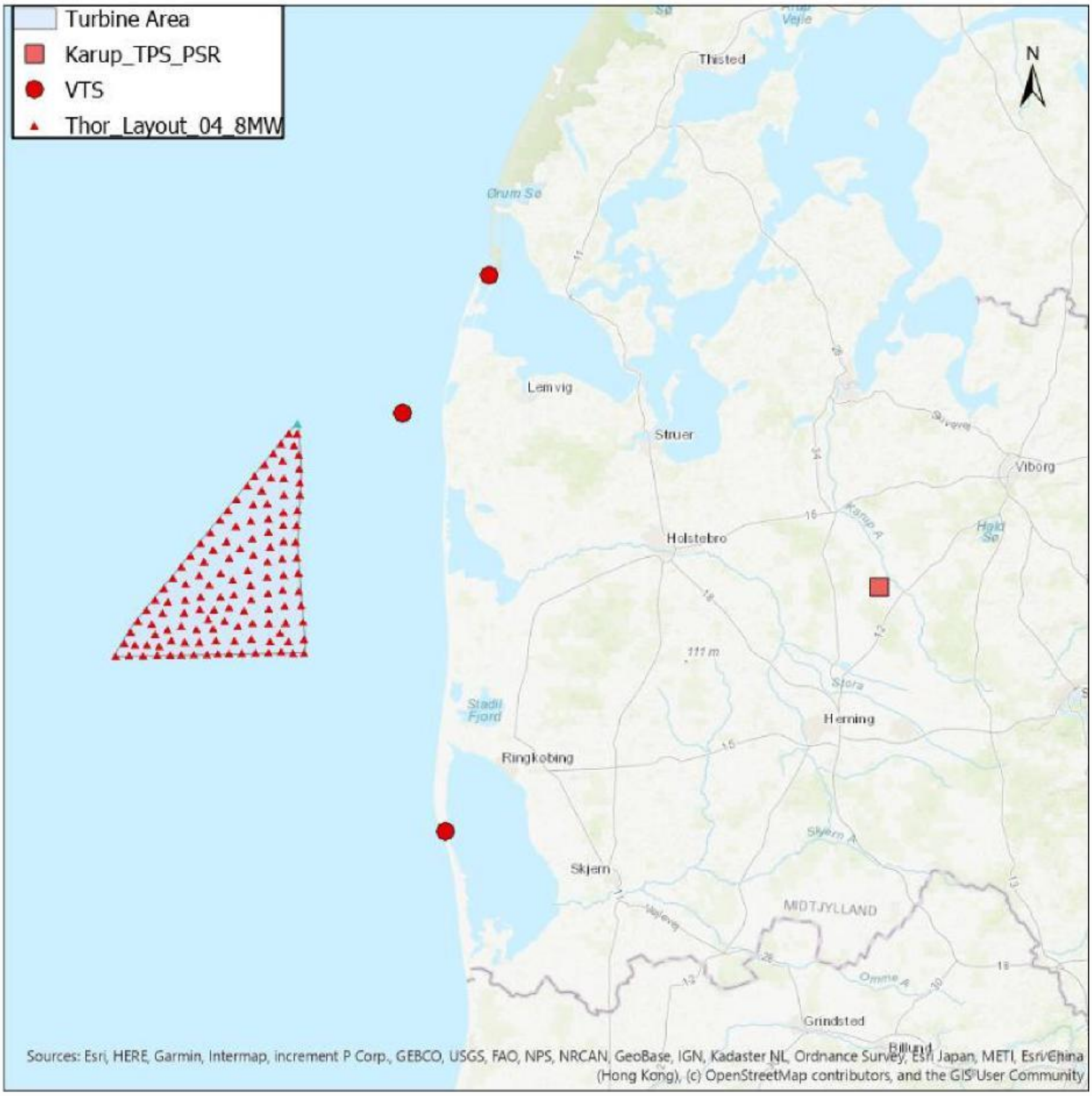

Figure 11 – Scenario 4: 8MW Windmills

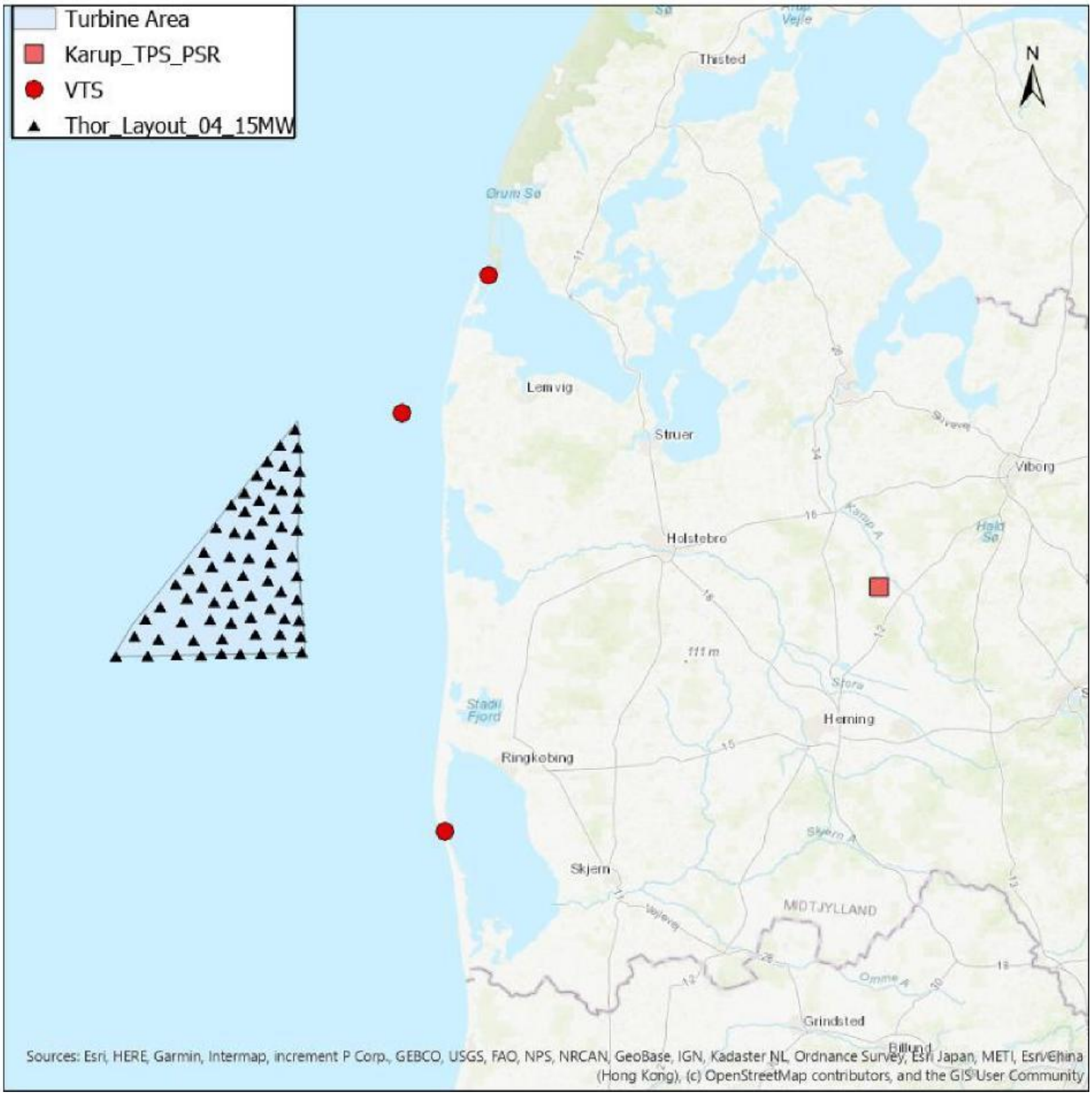

Figure 12 – Scenario 4: 15MW Windmills

7 Influence on coastal radars surface coverage, evaluations and calculations

The local situation was mathematically modelled using the following coordinates for the radar stations. (Refer to Section 6 Locations and Setups analysed for visual representation).

Table 2: The provided coordinates for the 3 surface radar stations overlooking the wind farm

CG radar station	Long	Lat	Height [AMSL]	Detection Range [NMi]
[redacted]	[redacted]	[redacted]	[redacted]	[redacted]

[redacted]	[redacted]	[redacted]	[redacted]	[redacted]
[redacted]	[redacted]	[redacted]	[redacted]	[redacted]

The locations of the Wind Turbines in the four different scenarios are in Annex A Coordinates of Windmills.

The radar KYRA Hvide Sande is yet not constructed, and the analysis is based on a projected location found in collaboration with FMI. [redacted]

7.1 Ghost targets

Experience shows that the risk of forming ghost echoes, creating false tacks will mostly be associated with large ships such as container carriers, tankers and similar vessels, as defined by [2], table 9. This includes cruise ships.

Experience also shows that the risk of forming ghost echoes associated with other larger ships such as coasters, bulk carriers and fishing trawlers will be lower. Ghosts associated with even smaller ships are expected to be insignificant. This includes smaller ships such as fishing ships, pilot boats and crew transfer vessels.

Furthermore, ghost echoes may occur as soon as the foundations for the wind turbines have been placed offshore.

Ghost echoes tend to be more "blurred" than real echoes, and trained operators may be able to distinguish these from real targets. However, the load on operators may become extensive, and human error will factor in.

Signal processing and tracking algorithms will in general tend to filter "blurred" echoes out, depending on statistics.

The issue is therefore very complex and statistical in nature, where the following provides simulated images of what is judged to be representative and worst case for the actual situation.

7.1.1 Calculation method

To calculate the estimated amount of ghost targets, as well as the ghost targets size in RCS, there are three scenarios to consider, shown in Figure 13:

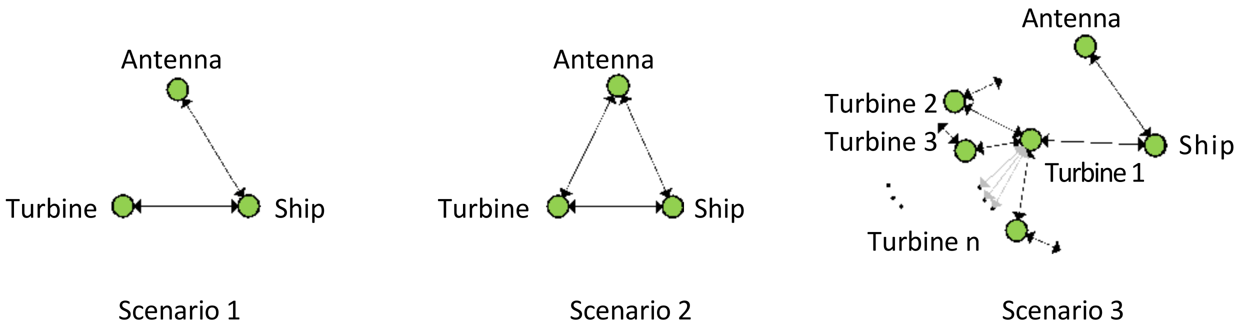

Figure 13 Possible scenarios for ghost target analysis

For scenario 1, the radar wave bounces from Antenna->Ship->Turbine->Ship->Antenna. In scenario 2, the radar wave bounces from Antenna->Ship->Turbine->Antenna. In scenario 3, the radar wave bounces from Antenna->Ship->Turbine 1->Turbine 2 -> ... -> Turbine n ->Antenna.

As the beam loses power during propagation and through each bounce, in order to estimate the worst-case scenario, the situation with the least amount of wave travel length and fewest bounces, is considered, since that scenario has the largest returned power, leaving the others negligible in comparison. In this case, scenario 2 is the focus for this report, due to fewest bounces and shortest wave travel.

Looking at the scenarios described above, scenario 2 as detailed by Figure 14 is the basis for this analysis, since this scenario will produce the strongest ghost targets. The radar wave travels from the antenna to the ship (range r_1) and bounces off the ship to the wind turbine (range r_2) and bounces off the wind turbine back to the antenna (range r_3).
This will result in a ghost target (Ghost Target 1) at range $(r_1 + r_2 + r_3)/2$ with bearing towards the ship. It can also travel in the opposite direction – antenna->wind turbine->ship->antenna, which will result in a ghost target (Ghost Target 2), also at range $(r_1 + r_2 + r_3)/2$, but with a bearing towards the wind turbine.

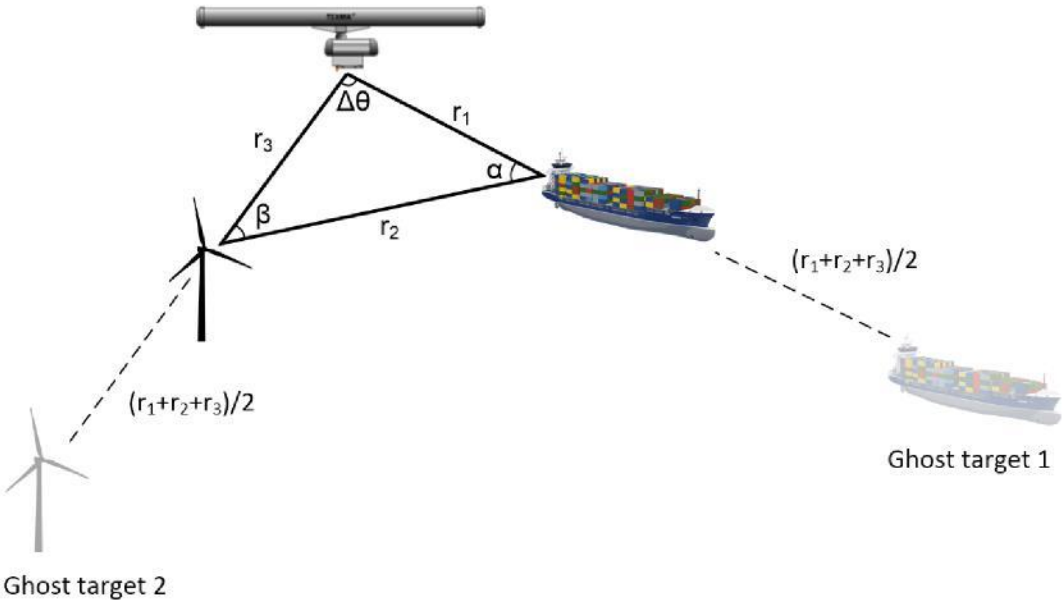

Figure 14: Scenario 2 details

From the radar equation, we get the following basic returned power from antenna->ship->antenna: (simplified without external losses from e.g. atmosphere etc. as well as internal losses, waveguide losses etc.)

$$= \times \frac{1}{4r^4} \times_h \frac{1}{4r^4} \times \times 4^2$$

Where:
= or riv'
= or transmitt (iv'ant a or)
= ntnna ain (transmission)

$h = h'$,
= ( )
= h
=

In the above equation, and are equal, since both transmission and reception happen in the main lobe of the antenna, so it can be reduced to:

$$= \times \frac{^2 \times h \times ^2}{(4)^3{}^4}$$

Applying the same principles, where the wave returns to the antenna via a reflection (refer to Figure 14), we get:

$$= \times \times \frac{1}{4_1} {}^2 \times h() \times \frac{1}{4_2} {}^2 \times () \times (\Delta) \times_4 {}^2 \times \frac{1}{4_3^2}$$

Where (refer to Figure 14):

=
= ( )
= ( )
$h = h'$
= $'$
= ( )
= h
$_1$ = , → h
$_2$ = , h →
3 = , →
= h
=
Δ =

This can be reduced to:

$$= \times \times (\Delta) \frac{2}{(4)^4{}_1{}^2{}_2 \; 23 \; 2 \times h() \times ()}$$

The range to the ghost target will be $h = \frac{_1 + _2 + _3}{2}$ and with the assumption that ≅ , we can write the following equation:

$$= \times {}^2 \times \frac{^2 h}{(4)^4{}_1{}^2{}_2{}^2{}_3} {}^2 \times \times [(\Delta)]$$

Which can be written as:

$$\frac{^2 h}{(4)^4 h} \; 4 \; \times [h \; \frac{4}{_1{}^2{}_2{}^2{}_3} \; = \times {}^2 \times \; 2 \times \times (\Delta) \;] = h$$

This is the equation used, to calculate the power returned from the ghost target - h.

To calculate the RCS of the ghost targets, as if it was a real target at the ghost target's position, we use the returned power (h) as if it was received at $\Delta = 0 \Longrightarrow (\Delta) = \Longrightarrow (\Delta) = 1$ and we get:

$$h = \frac{(4)^4 \times h}{4 \times {}_2 \times {}^2}$$

The result of h is the data used for estimating the amount and size of the ghost targets, resulting from the wind turbines. The ghost targets are calculated assuming homogeneous scattering, thus the ships will scatter in all directions This will give a conservative estimate of the ghost echoes, thus cover the worst-case estimation.

7.1.2 Calculations

The ghost echoes have been analysed based on likely scenario following the AIS data. The most likely scenarios are:

1. Traffic West of Thor Havmøllepark 1 Nautical mile out from the windfarm area
2. Traffic East of Thor Havmøllepark 1 Nautical mile out from the windfarm area
3. Traffic South of Thor Havmøllepark 1 Nautical mile out from the windfarm area
4. Traffic West of Thor Havmøllepark 2 Nautical miles out from the windfarm area
5. Traffic East of Thor Havmøllepark 2 Nautical miles out from the windfarm area
6. Traffic South of Thor Havmøllepark 2 Nautical miles out from the windfarm

area This is illustrated by Figure 15:

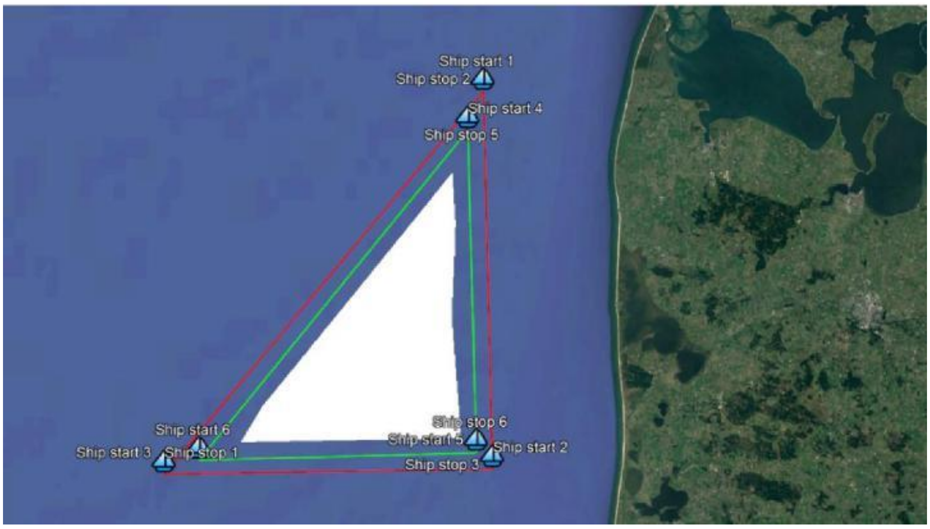

Figure 15 Trajectories used for calculations. Red are 2 Nautical miles out, green is 1 Nautical mile out from the windfarm area

Offshore work vessels are likely to navigate very close to the wind turbines and will therefore tend to create more and stronger ghosts than other vessels. However, this is expected to be an acceptable side effect with no need for VTS or coastal surveillance.

Fishing vessels etc. operating close to shore have a small RCS and are therefore not considered as a source for ghost targets.

Each route has been calculated for each of the four possible windfarm configurations.

7.1.1 Scenario 1 8MW Windmills

Likelihood of ghosts originating from southwest bound traffic West of Thor Havmøllepark 1 Nautical mile out from the windfarm area

Below images indicate that there is a high likelihood of ghosts originating from ships travelling Northwest of Thor Havmøllepark.

The ghosts may be pronounced (> 5 m2 in RCS) and are therefore likely to cause significant false tracks or significant disturbance on operational displays.

Due to the large distance, KYRA Hvide Sande is calculated to not produce prominent ghost echoes.

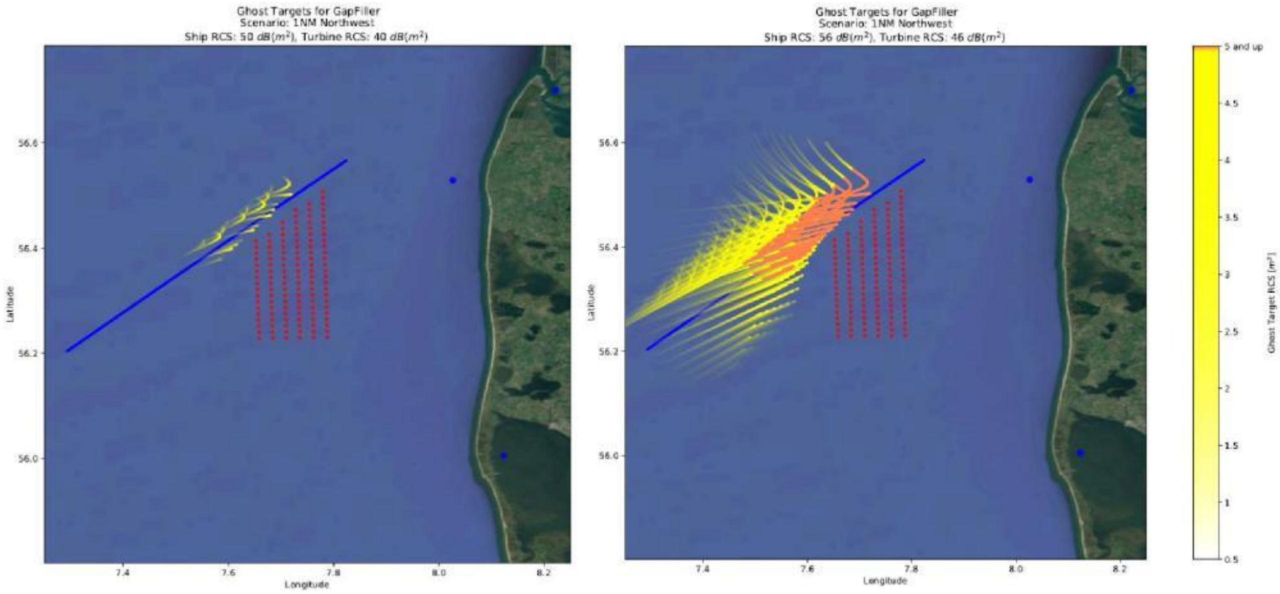

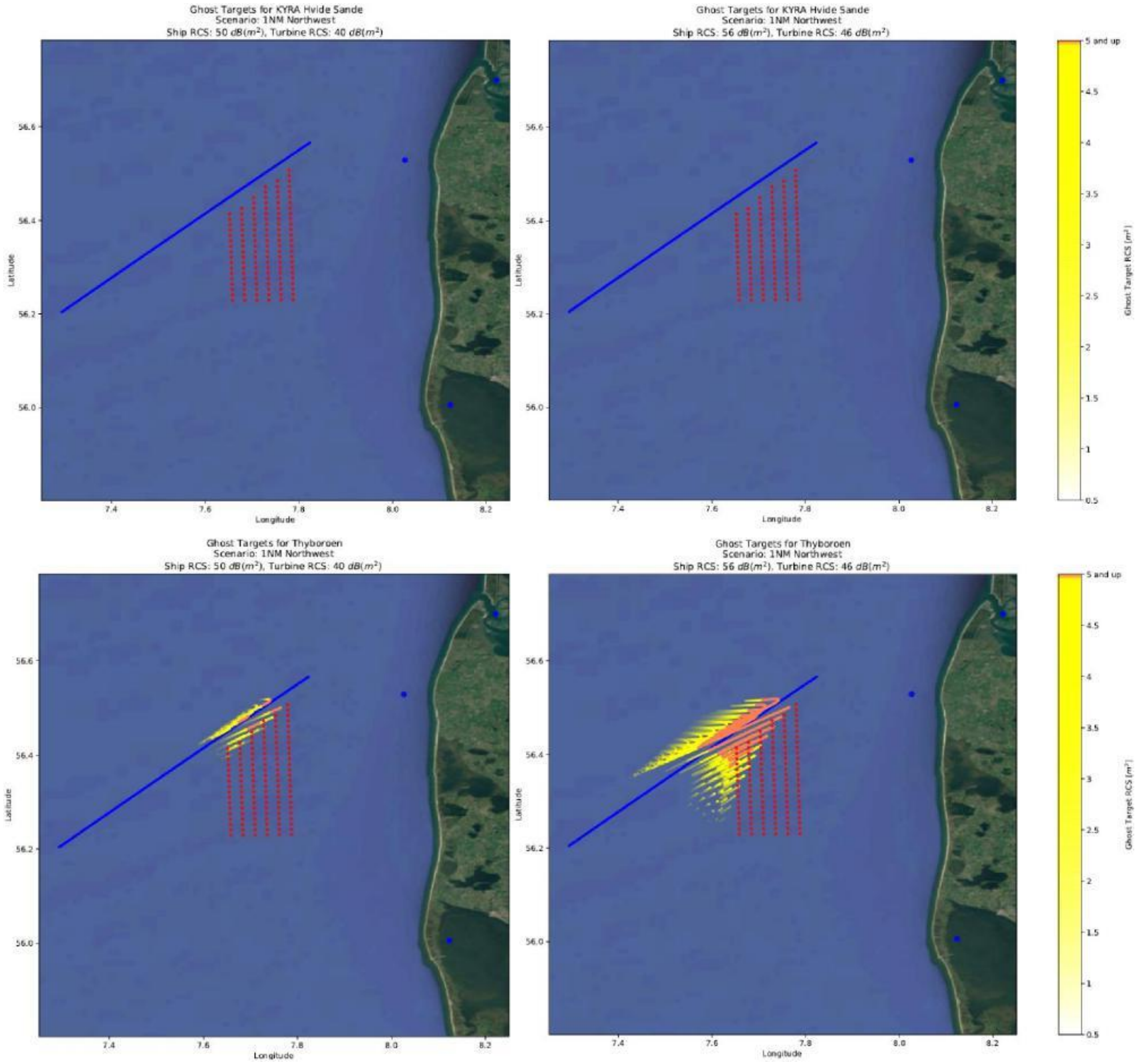

Figure 16 Calculation of ghost targets originating from large vessels, southwest bound west of Thor Havmøllepark 1 Nautical mile out from the windfarm area. Radar sites from top to bottom are: Gapfiller Radar at Vesterhav Nord, KYRA Hvide Sande, and KYRA Thyborøn. Representative (left) and Worst case (right)

Likelihood of ghosts originating from north bound traffic east of Thor Havmøllepark 1 Nautical mile out from the windfarm area

Below images indicate that here is some likelihood of ghosts originating from ships travelling east of Thor Havmøllepark. The ghosts may be pronounced (> 5 m2 in RCS) and are therefore likely to cause significant false tracks or significant disturbance on operational displays.

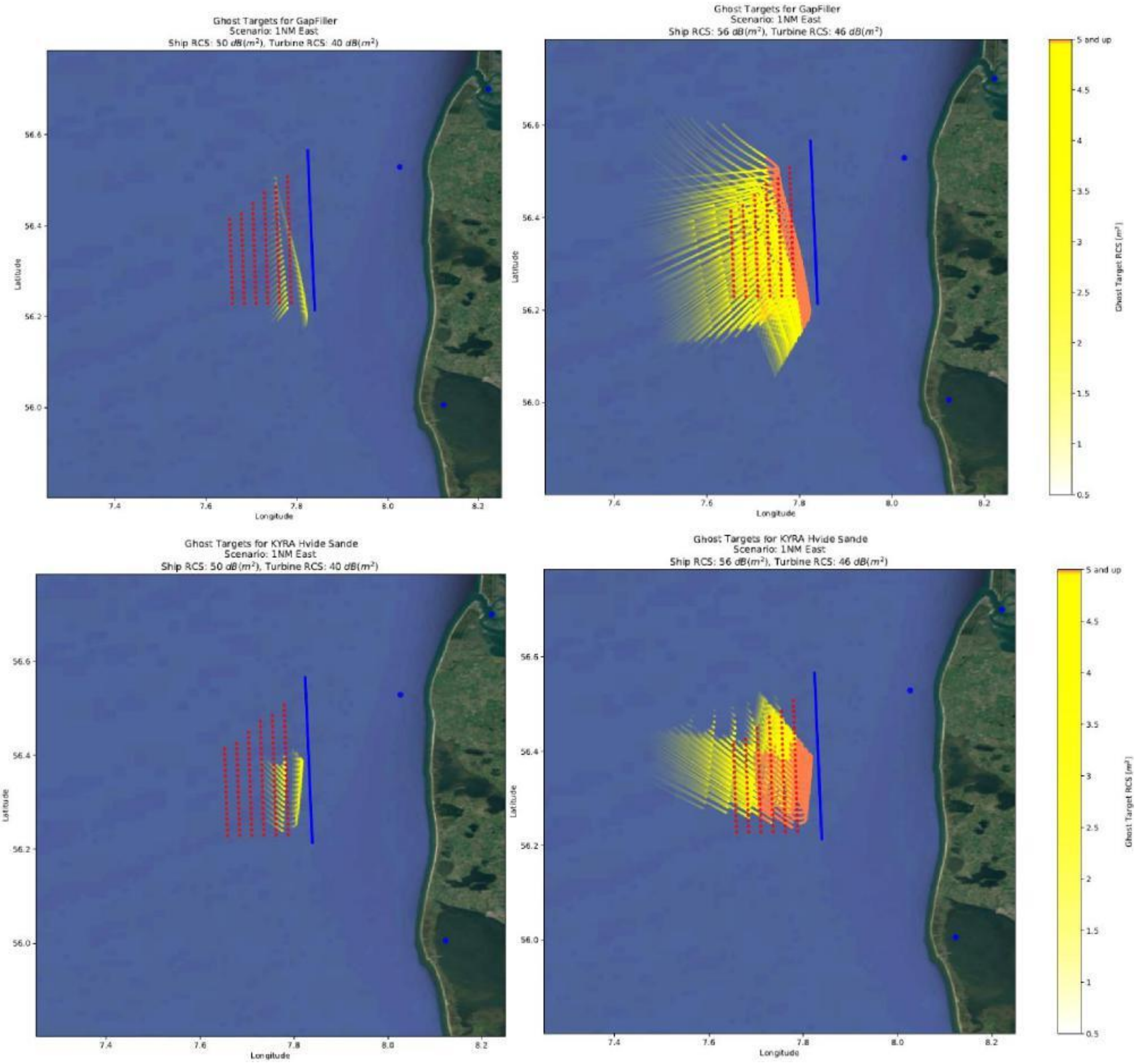

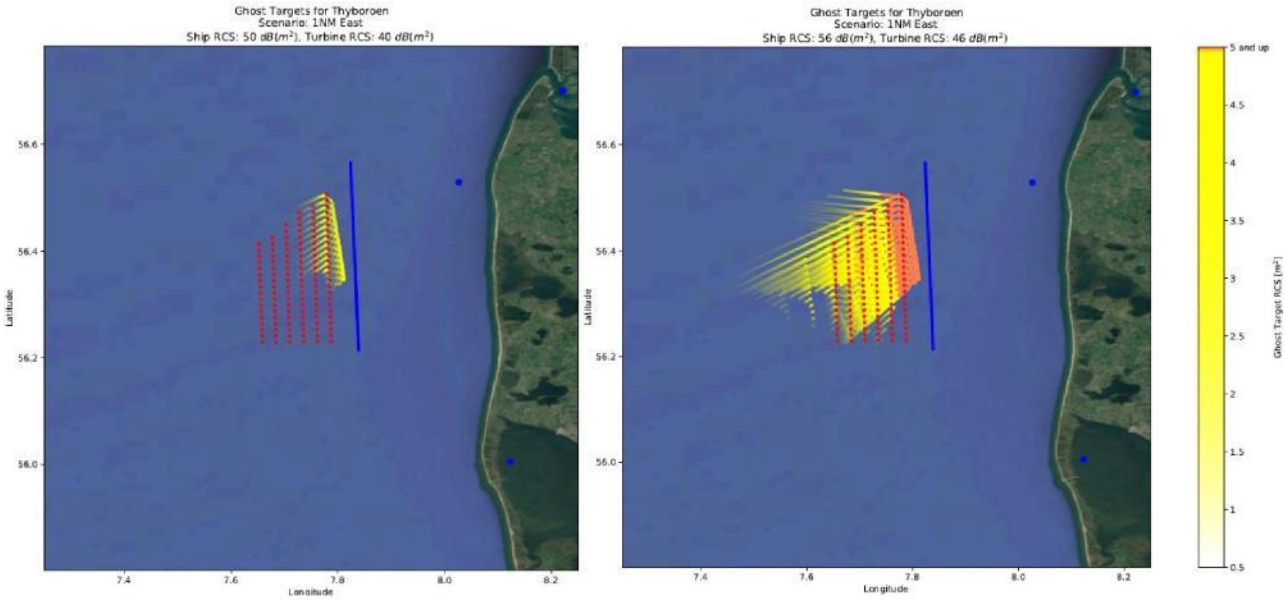

Figure 17 Calculation of ghost targets originating from large vessels, north bound east of Thor Havmøllepark 1 Nautical mile out from the windfarm area. Radar sites from top to bottom are: Gapfiller Radar at Vesterhav Nord, KYRA Hvide Sande, and KYRA Thyborøn. Representative (left) and Worst case (right)

Likelihood of ghosts originating from east bound traffic south of Thor Havmøllepark 1 Nautical mile out from the windfarm area

Below images indicate that here is some likelihood of ghosts originating from ships travelling south of Thor Havmøllepark. The ghosts may be pronounced (> 5 m2 in RCS) and are therefore likely to cause significant false tracks or significant disturbance on operational displays.

Due to the large distance, KYRA Thyborøn is calculated to not produce prominent ghost echoes.

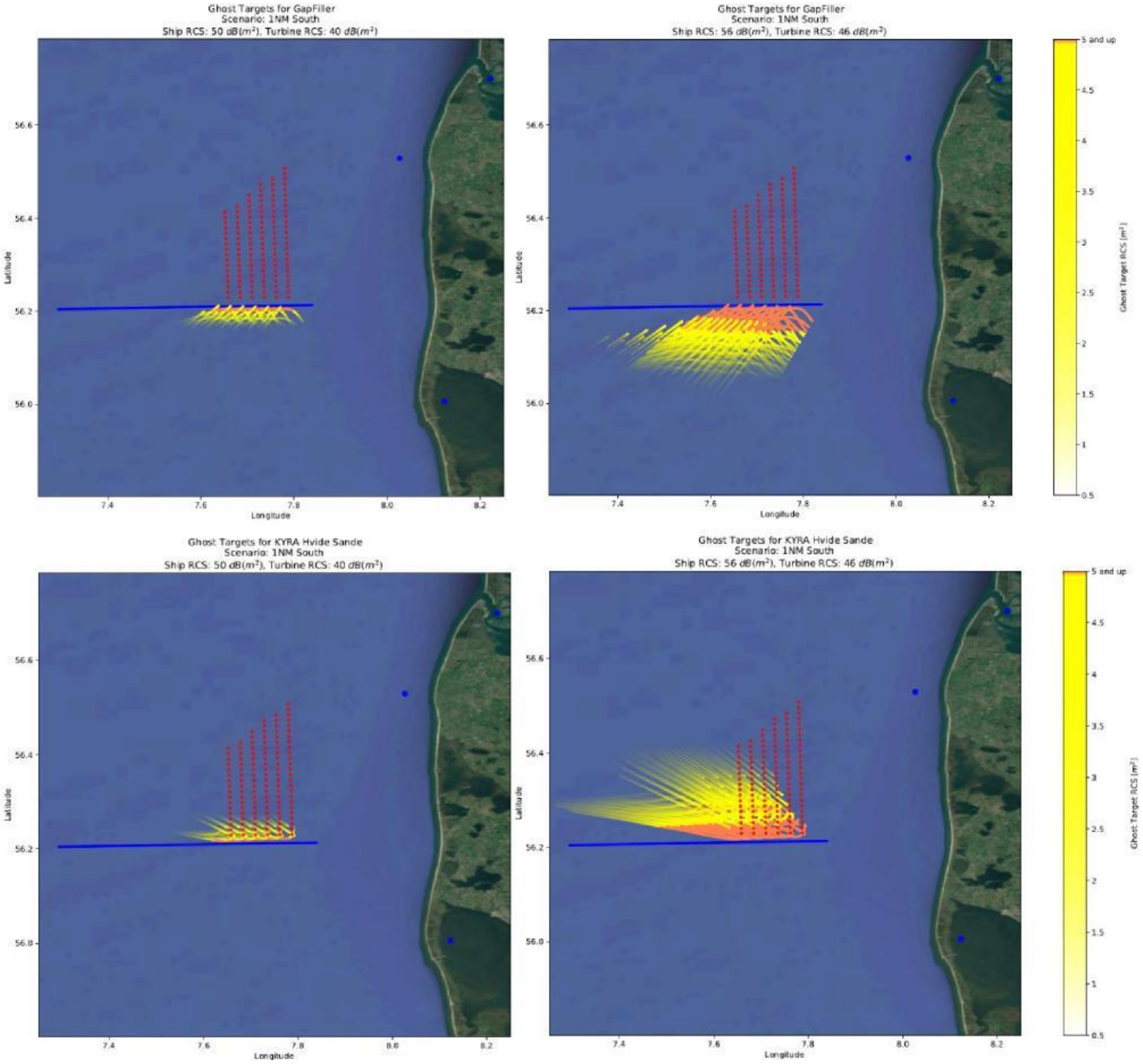

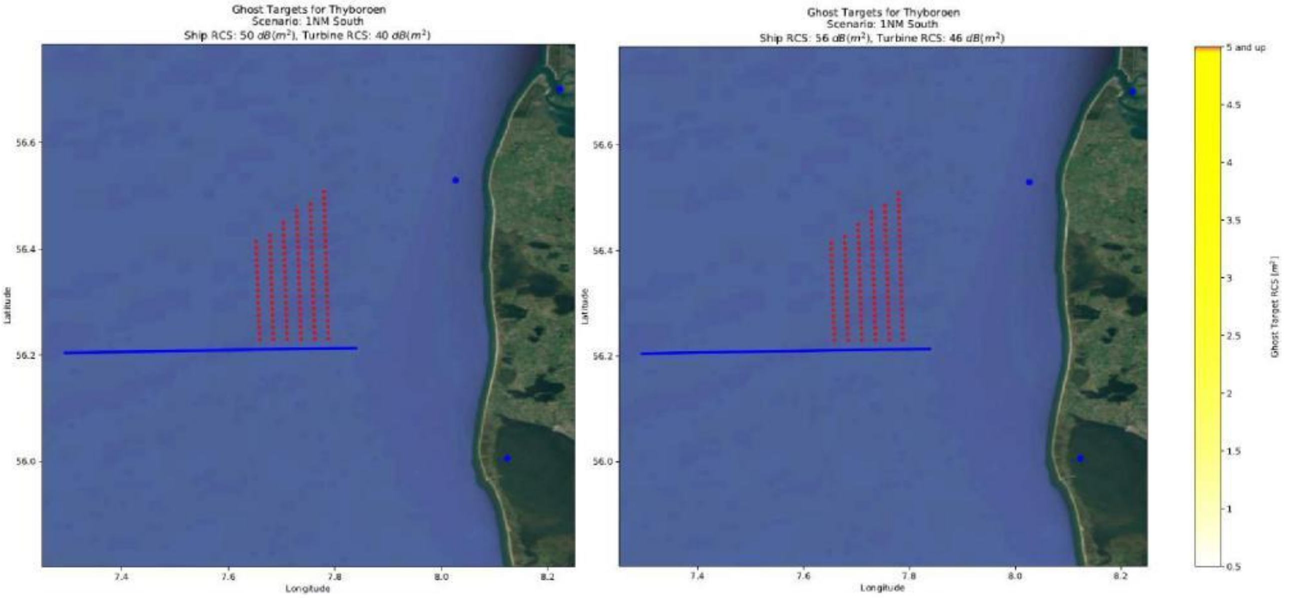

Figure 18 Calculation of ghost targets originating from large vessels, east bound south of Thor Havmøllepark 1 Nautical mile out from the windfarm area. Radar sites from top to bottom are: Gapfiller Radar at Vesterhav Nord, KYRA Hvide Sande, and KYRA Thyborøn. Representative (left) and Worst case (right)

Likelihood of ghosts originating from southwest bound traffic West of Thor Havmøllepark 2 Nautical miles out from the windfarm area

Below images indicate that there is a high likelihood of ghosts originating from ships travelling Northwest of Thor Havmøllepark.

Possible ghost echoes are calculated to be weak and diffuse for smaller ships, however in the worst case, ghost echoes of more than 5 m^2 in RCS are seen and therefore are likely to cause false tracks or to be displayed on operational displays.

Due to the large distance, KYRA Hvide Sande is calculated to not produce prominent ghost echoes.

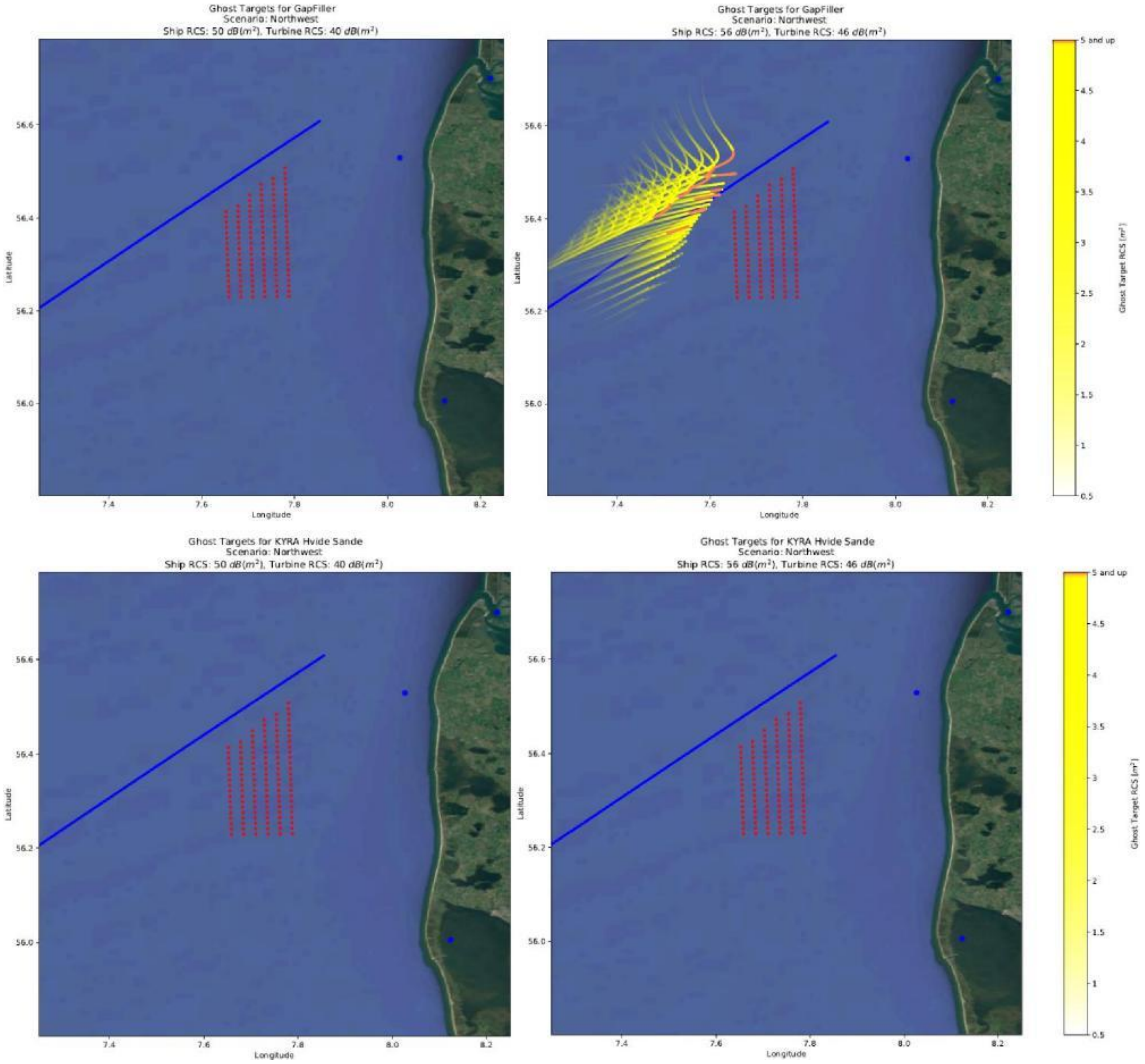

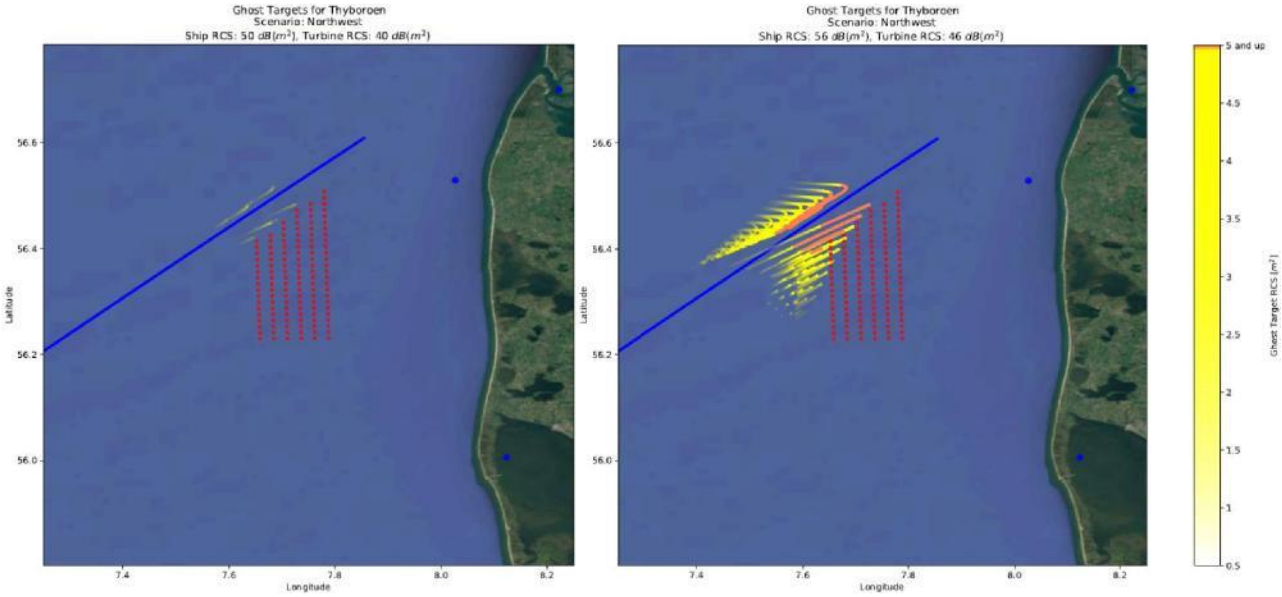

Figure 19 Calculation of ghost targets originating from large vessels, southwest bound north of Thor Havmøllepark 2 Nautical miles out from the windfarm area. Radar sites from top to bottom are: Gapfiller Radar at Vesterhav Nord, KYRA Hvide Sande, and KYRA Thyborøn. Representative (left) and Worst case (right)

Likelihood of ghosts originating from north bound traffic east of Thor Havmøllepark 2 Nautical miles out from the windfarm area

Below images indicate that here is some likelihood of ghosts originating from ships east of Thor Havmøllepark. Possible ghost echoes are calculated to be weak and diffuse for smaller ships, however in the worst case, ghost echoes of more than 5 m^2 in RCS are seen and therefore are likely to cause false tracks or to be displayed on operational displays.

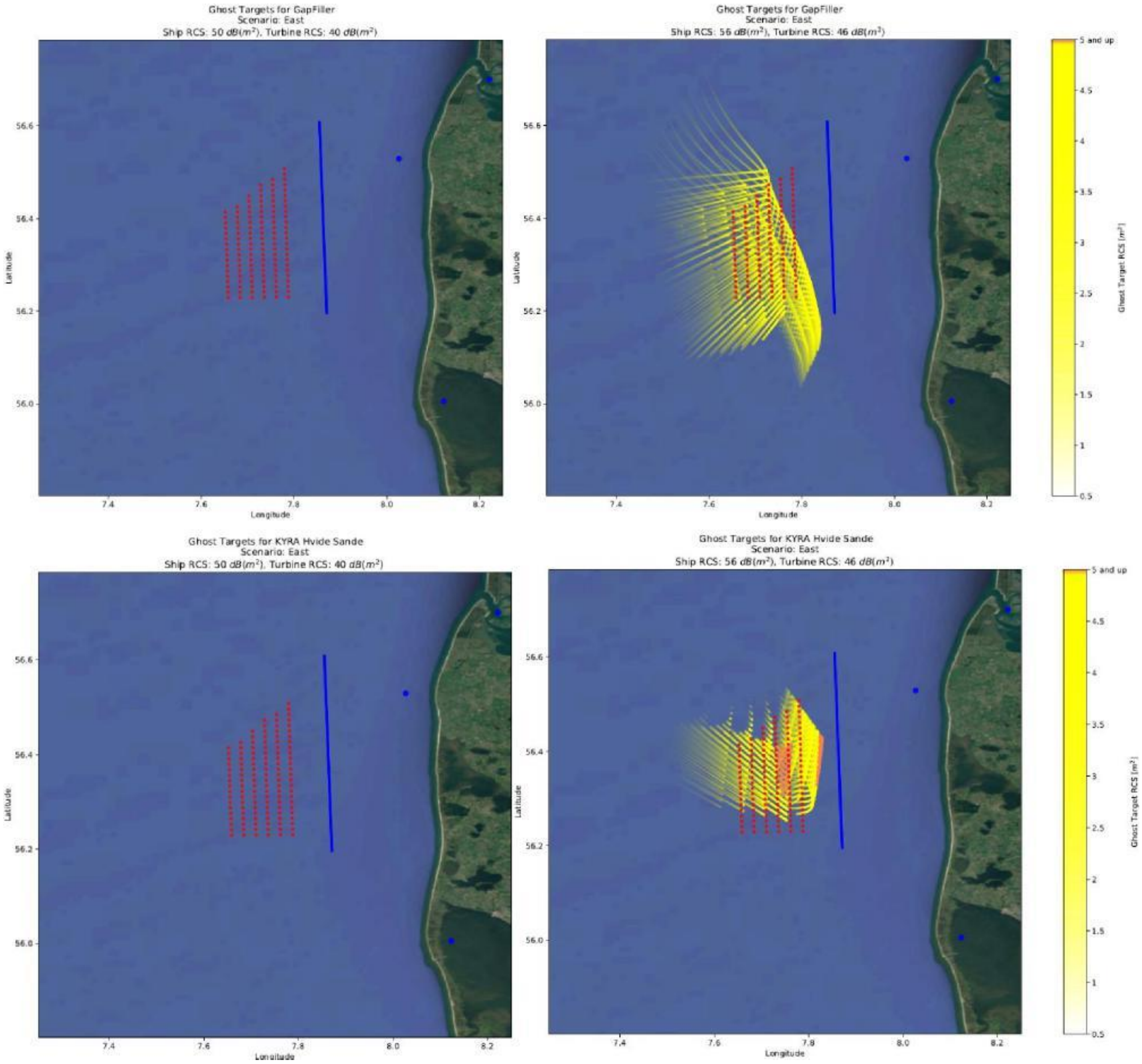

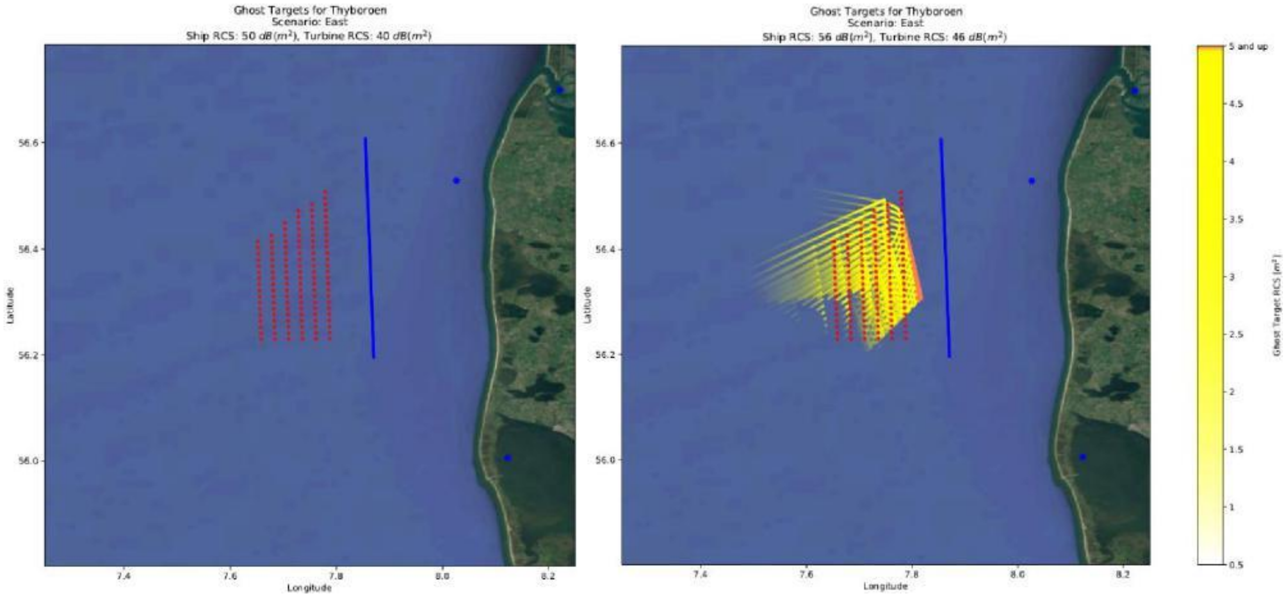

Figure 20 Calculation of ghost targets originating from large vessels, north bound east of Thor Havmøllepark 2 Nautical miles out from the windfarm area. Radar sites from top to bottom are: Gapfiller Radar at Vesterhav Nord, KYRA Hvide Sande, and KYRA Thyborøn. Representative (left) and Worst case (right)

Likelihood of ghosts originating from east bound traffic south of Thor Havmøllepark 2 Nautical miles out from the windfarm area

Below images indicate that here is some likelihood of ghosts originating from ships travelling east of Thor Havmøllepark. The ghosts may be pronounced (> 5 m2 in RCS) and are therefore likely to cause significant false tracks or significant disturbance on operational displays.

This will be more pronounced with shipping, also smaller ships, even closer to the wind farms.

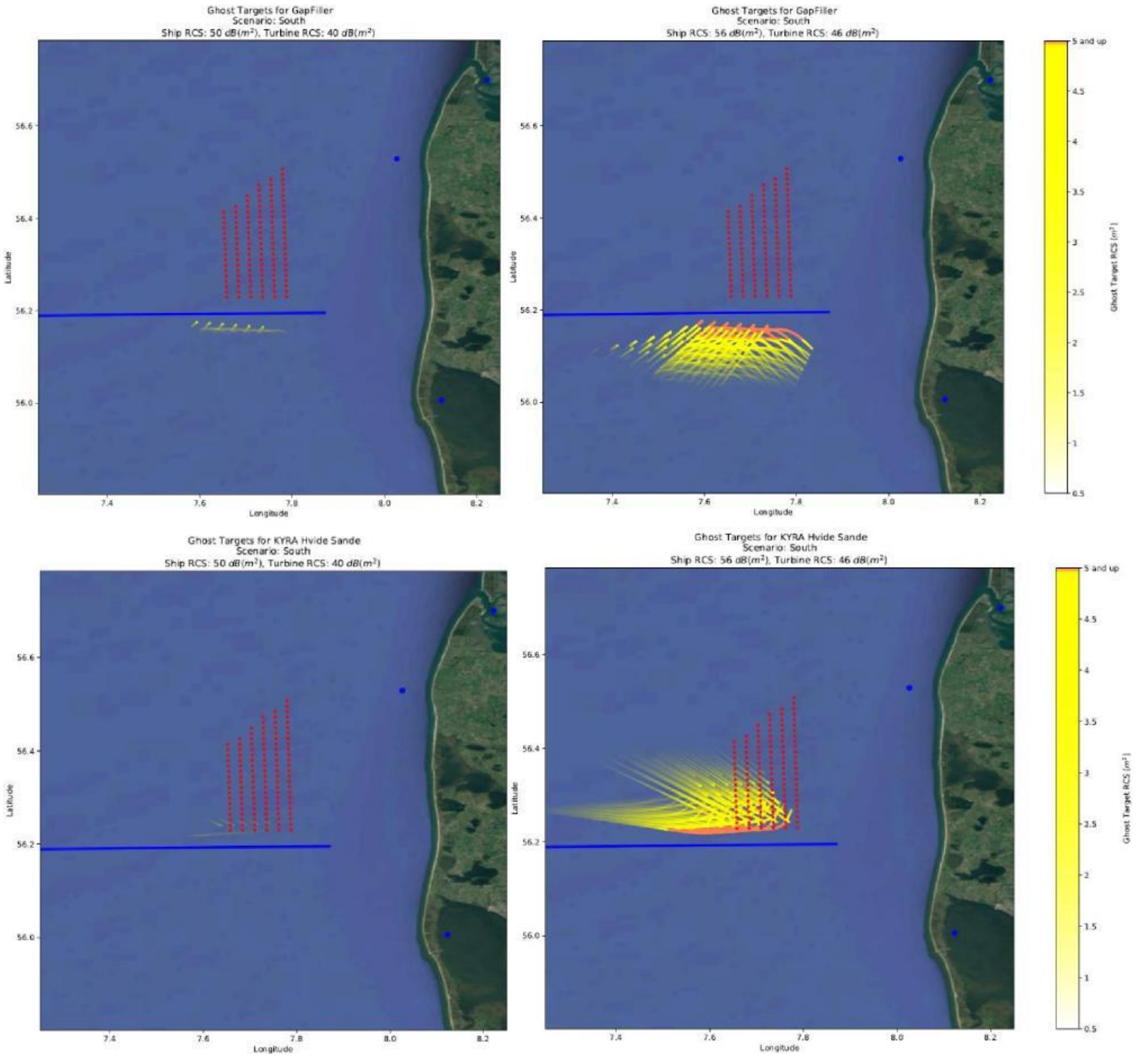

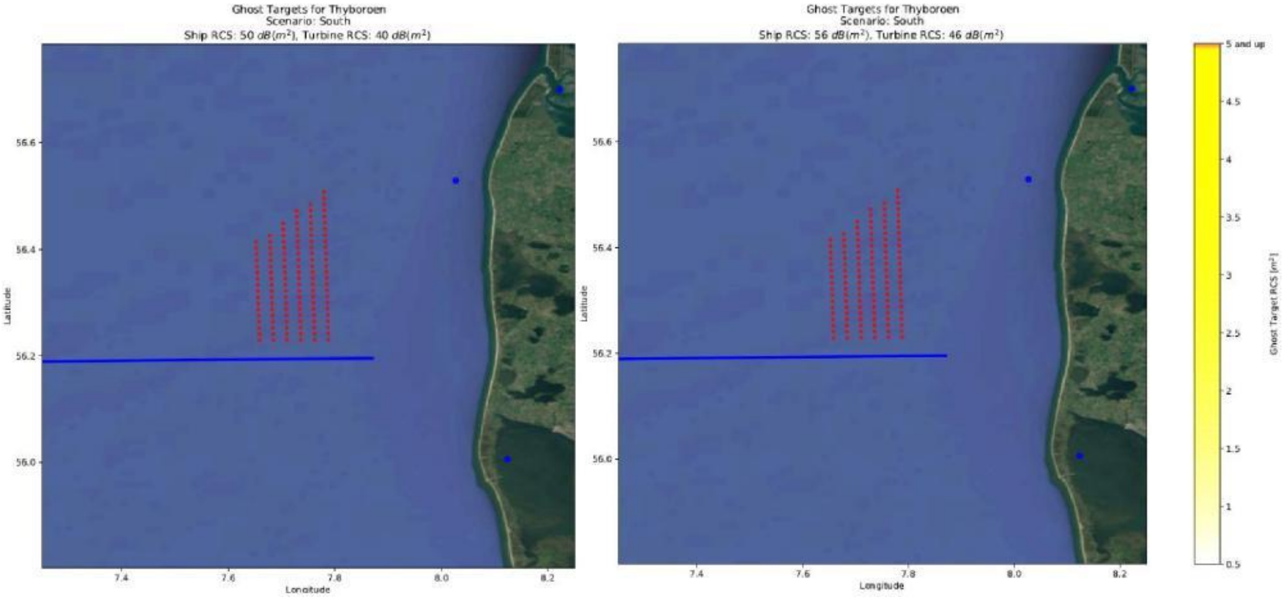

Figure 21 Calculation of ghost targets originating from large vessels, east bound south of Thor Havmøllepark 2 Nautical miles out from the windfarm area. Radar sites from top to bottom are: Gapfiller Radar at Vesterhav Nord, KYRA Hvide Sande, and KYRA Thyborøn. Representative (left) and Worst case (right)

7.1.2 Scenario 1 15MW Windmills

Likelihood of ghosts originating from southwest bound traffic West of Thor Havmøllepark 1 Nautical mile out from the windfarm area

Below images indicate that there is a high likelihood of ghosts originating from ships travelling Northwest of Thor Havmøllepark.

The ghosts may be pronounced (> 5 m2 in RCS) and are therefore likely to cause significant false tracks or significant disturbance on operational displays.

Due to the large distance, KYRA Hvide Sande is calculated to not produce prominent ghost echoes.

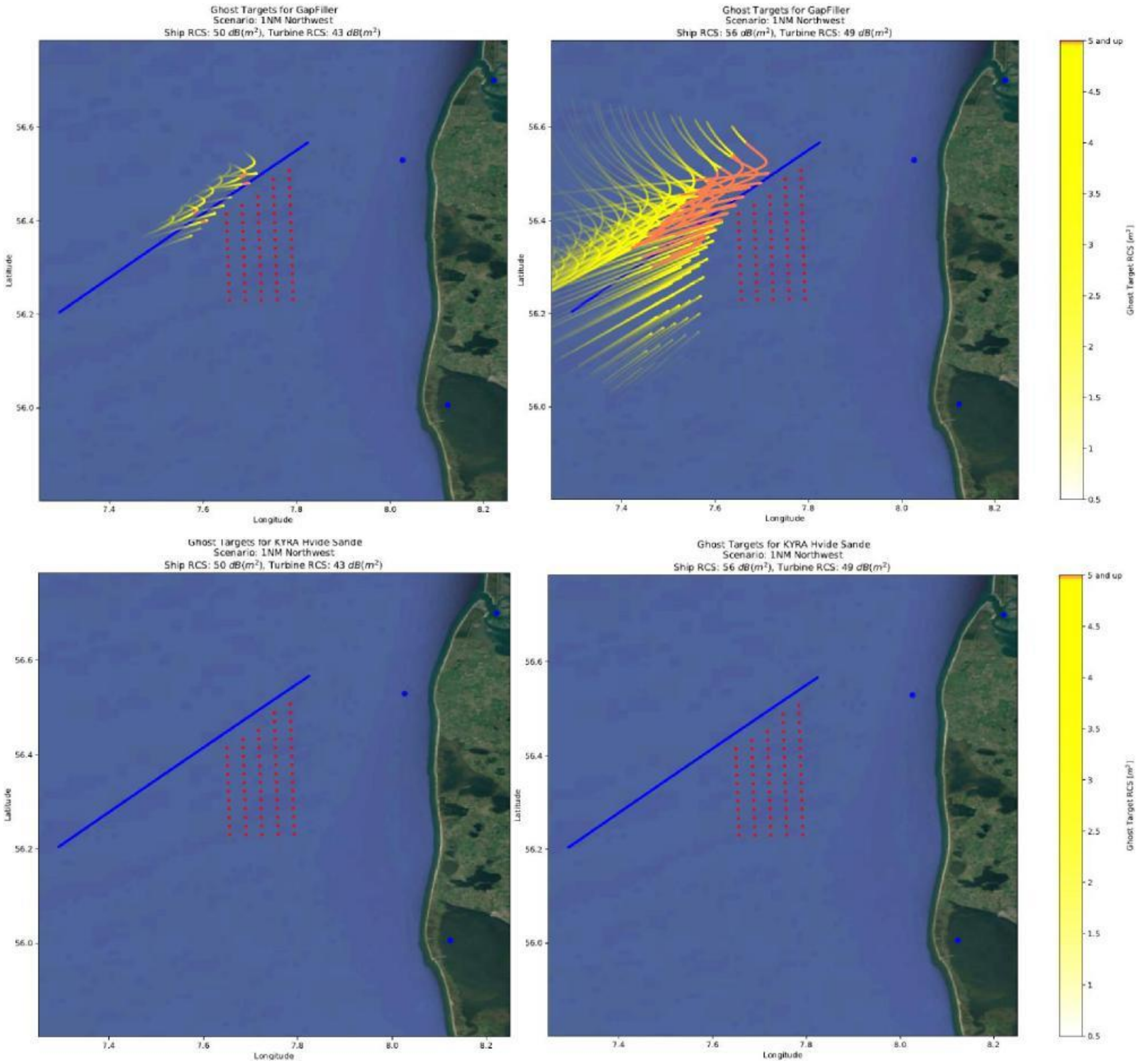

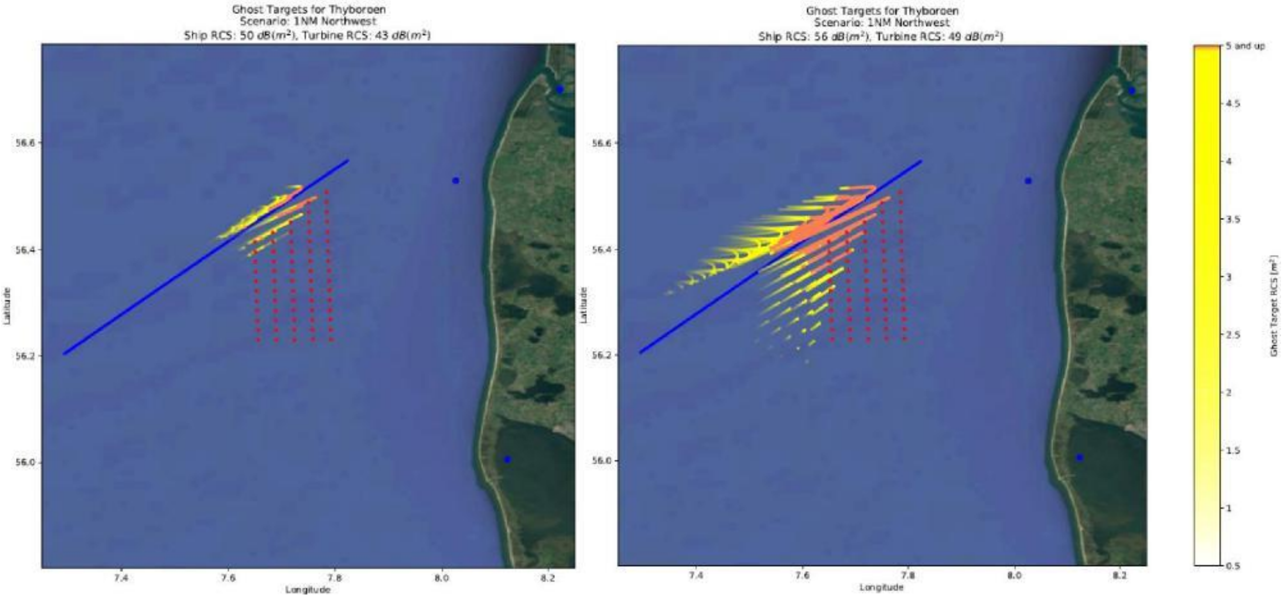

Figure 22 Calculation of ghost targets originating from large vessels, southwest bound west of Thor Havmøllepark 1 Nautical mile out from the windfarm area. Radar sites from top to bottom are: Gapfiller Radar at Vesterhav Nord, KYRA Hvide Sande, and KYRA Thyborøn. Representative (left) and Worst case (right)

Likelihood of ghosts originating from north bound traffic east of Thor Havmøllepark 1 Nautical mile out from the windfarm area

Below images indicate that here is some likelihood of ghosts originating from ships travelling east of Thor Havmøllepark. The ghosts may be pronounced (> 5 m2 in RCS) and are therefore likely to cause significant false tracks or significant disturbance on operational displays.

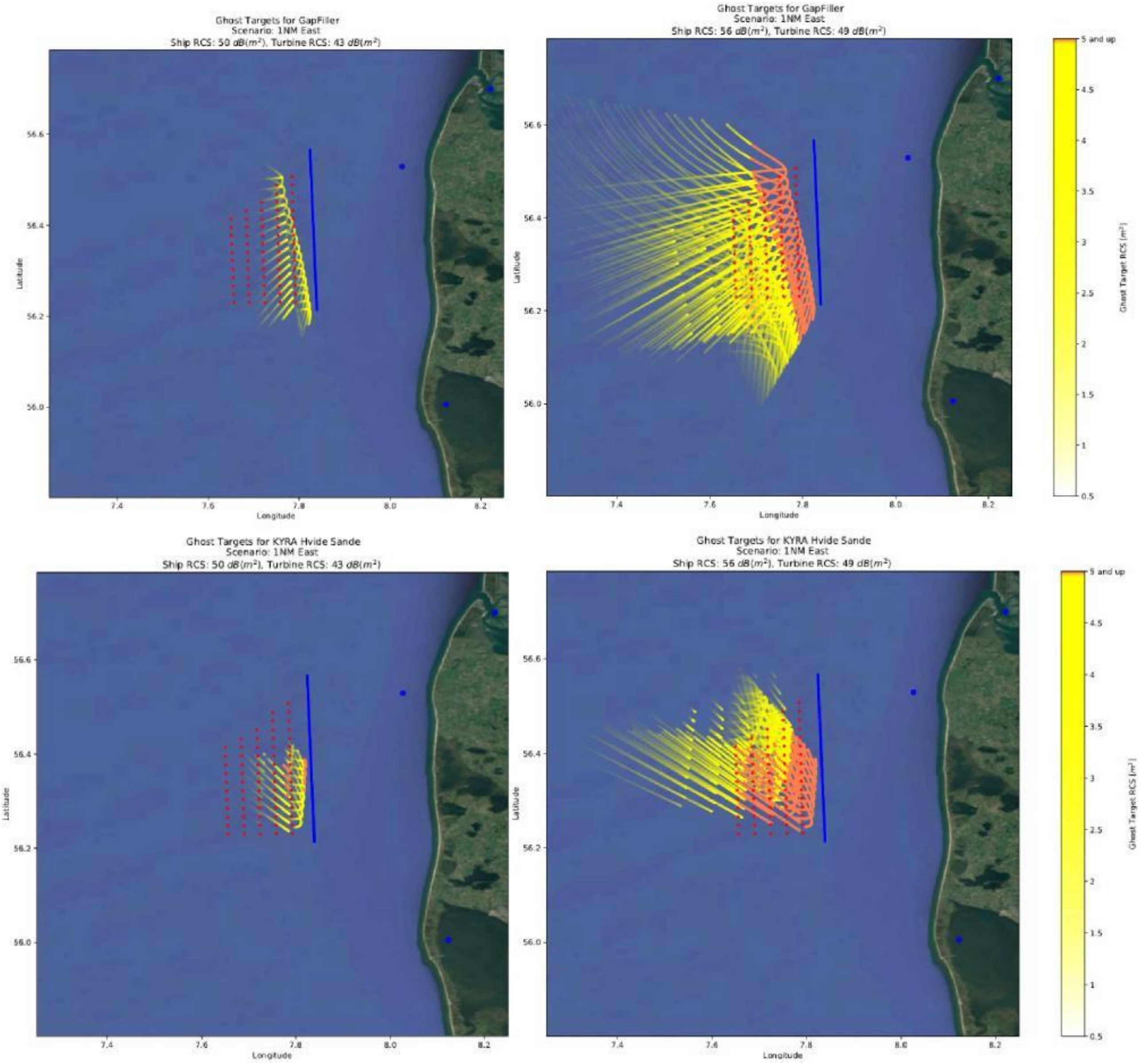

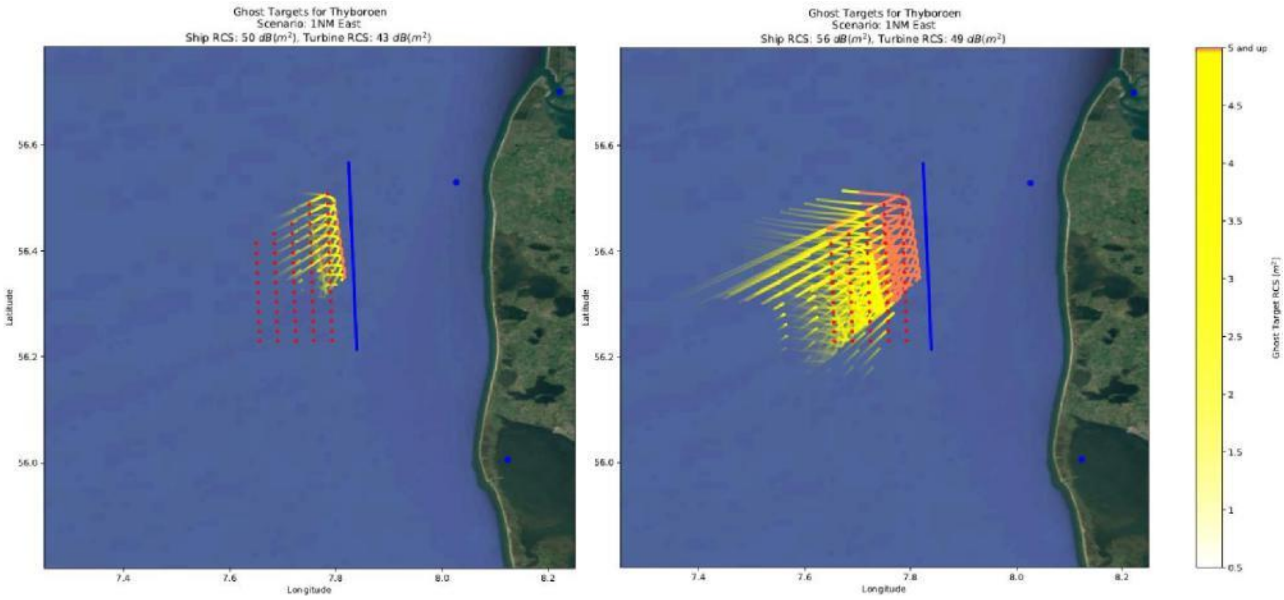

Figure 23 Calculation of ghost targets originating from large vessels, north bound east of Thor Havmøllepark 1 Nautical mile out from the windfarm area. Radar sites from top to bottom are: Gapfiller Radar at Vesterhav Nord, KYRA Hvide Sande, and KYRA Thyborøn. Representative (left) and Worst case (right)

Likelihood of ghosts originating from east bound traffic south of Thor Havmøllepark 1 Nautical mile out from the windfarm area

Below images indicate that here is some likelihood of ghosts originating from ships travelling south of Thor Havmøllepark. The ghosts may be pronounced (> 5 m2 in RCS) and are therefore likely to cause significant false tracks or significant disturbance on operational displays.

Due to the large distance, KYRA Thyborøn is calculated to not produce prominent ghost echoes.

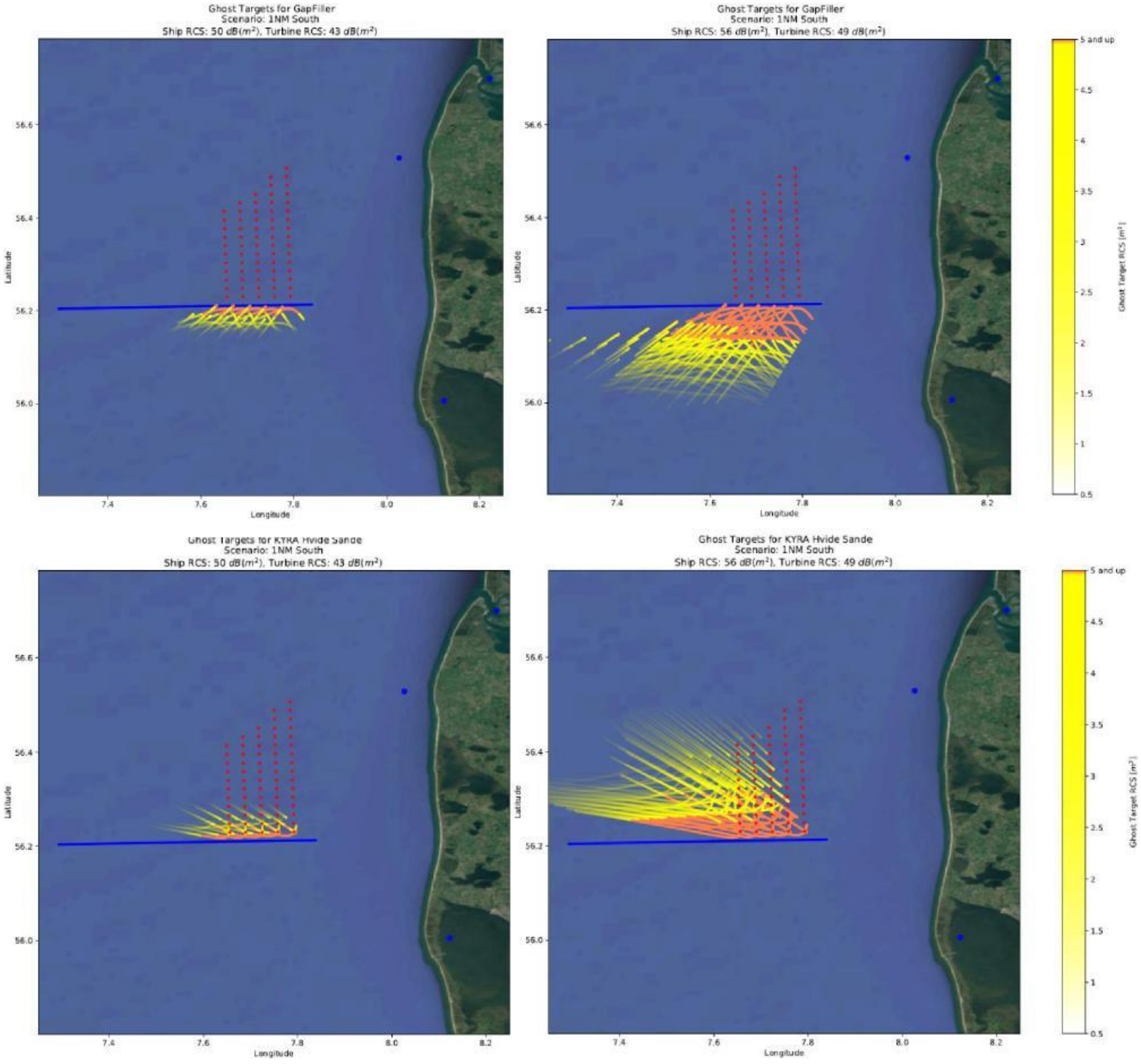

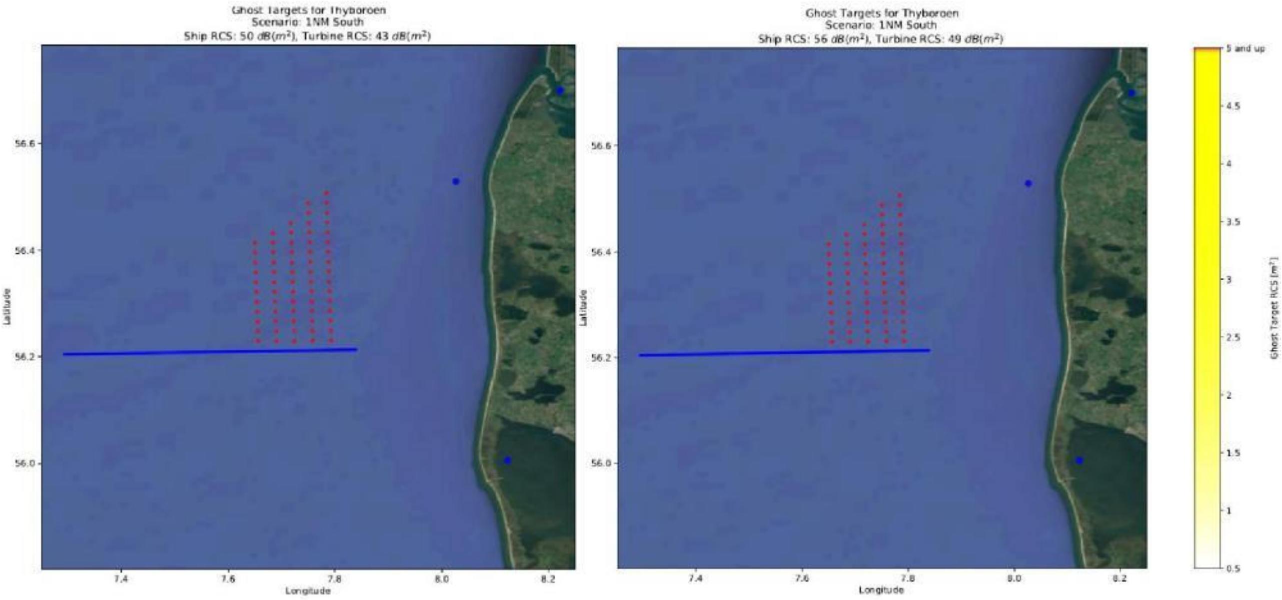

Figure 24 Calculation of ghost targets originating from large vessels, east bound south of Thor Havmøllepark 1 Nautical mile out from the windfarm area. Radar sites from top to bottom are: Gapfiller Radar at Vesterhav Nord, KYRA Hvide Sande, and KYRA Thyborøn. Representative (left) and Worst case (right)

Likelihood of ghosts originating from southwest bound traffic West of Thor Havmøllepark 2 Nautical miles out from the windfarm area

Below images indicate that there is a high likelihood of ghosts originating from ships travelling Northwest of Thor Havmøllepark.

Possible ghost echoes are calculated to be weak and diffuse for smaller ships, however in the worst case, ghost echoes of more than 5 m^2 in RCS are seen and therefore are likely to cause false tracks or to be displayed on operational displays.

Due to the large distance, KYRA Hvide Sande is calculated to not produce prominent ghost echoes.

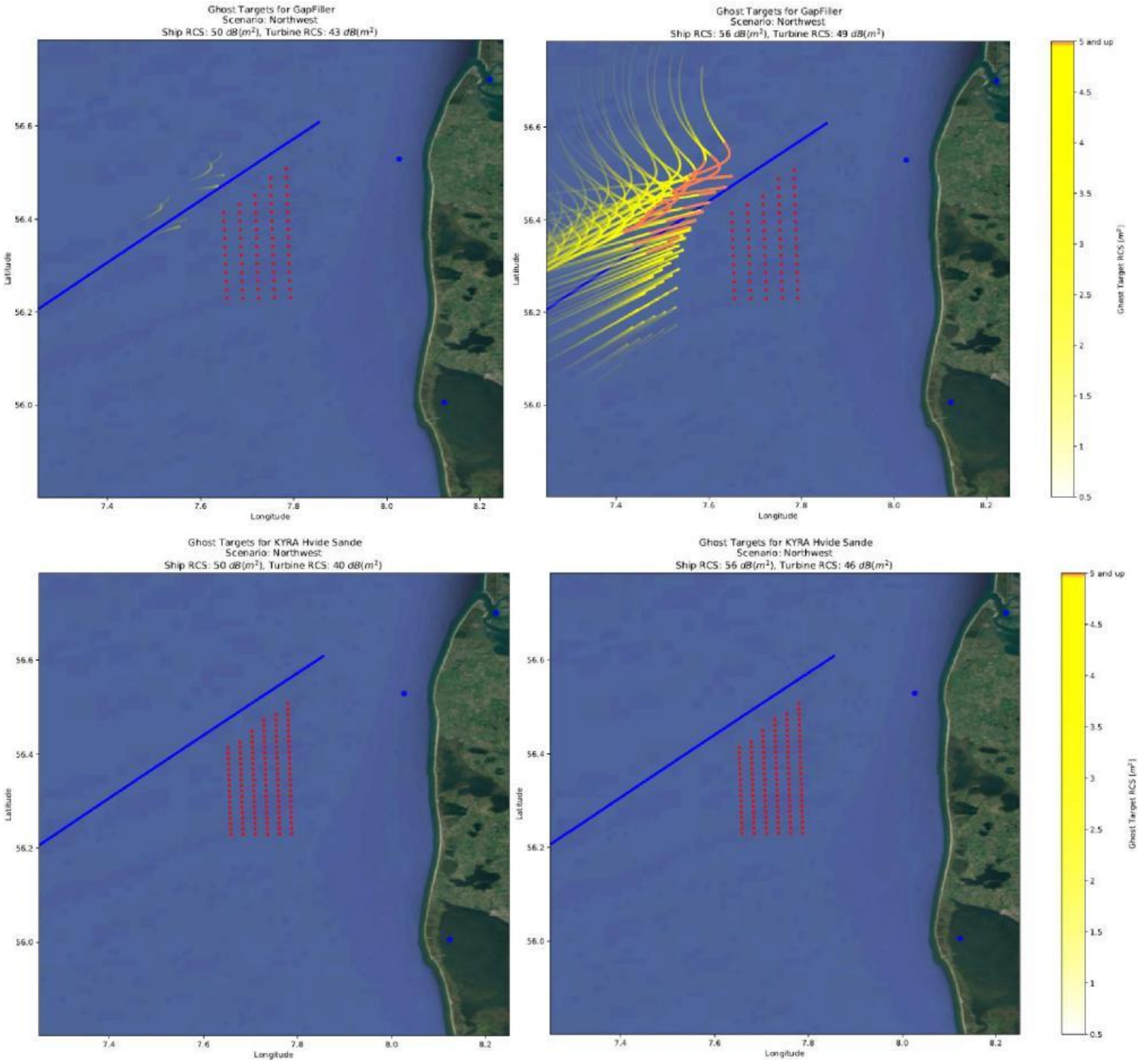

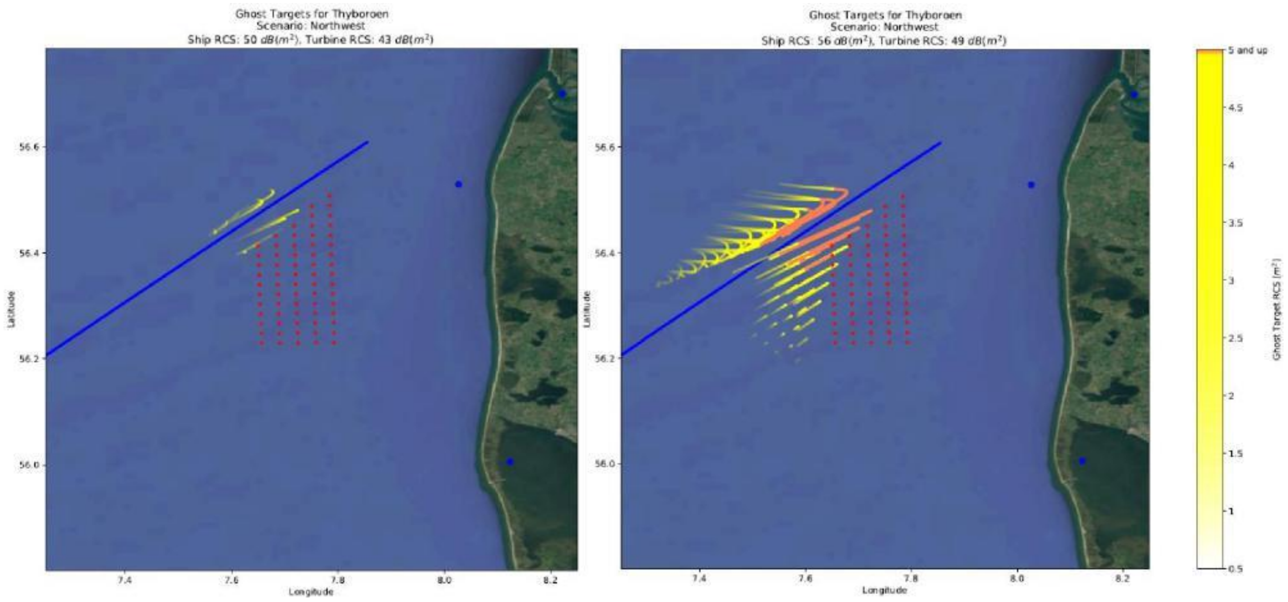

Figure 25 Calculation of ghost targets originating from large vessels, southwest bound north of Thor Havmøllepark 2 Nautical miles out from the windfarm area. Radar sites from top to bottom are: Gapfiller Radar at Vesterhav Nord, KYRA Hvide Sande, and KYRA Thyborøn. Representative (left) and Worst case (right)

Likelihood of ghosts originating from north bound traffic east of Thor Havmøllepark 2 Nautical miles out from the windfarm area

Below images indicate that here is some likelihood of ghosts originating from ships travelling east of Thor Havmøllepark. Possible ghost echoes are calculated to be weak and diffuse for smaller ships, however in the worst case, ghost echoes of more than 5 m^2 in RCS are seen and therefore are likely to cause false tracks or to be displayed on operational displays.

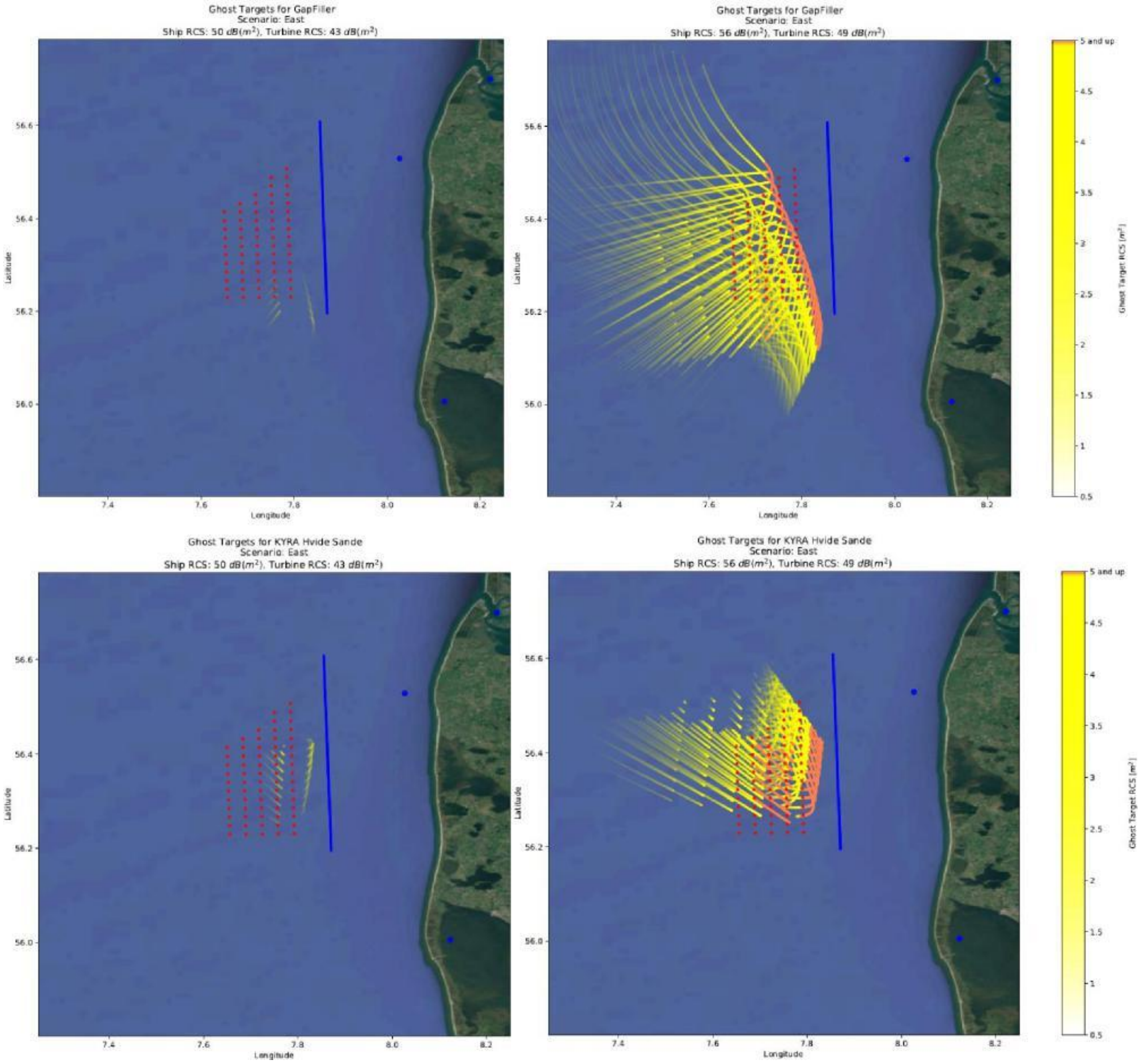

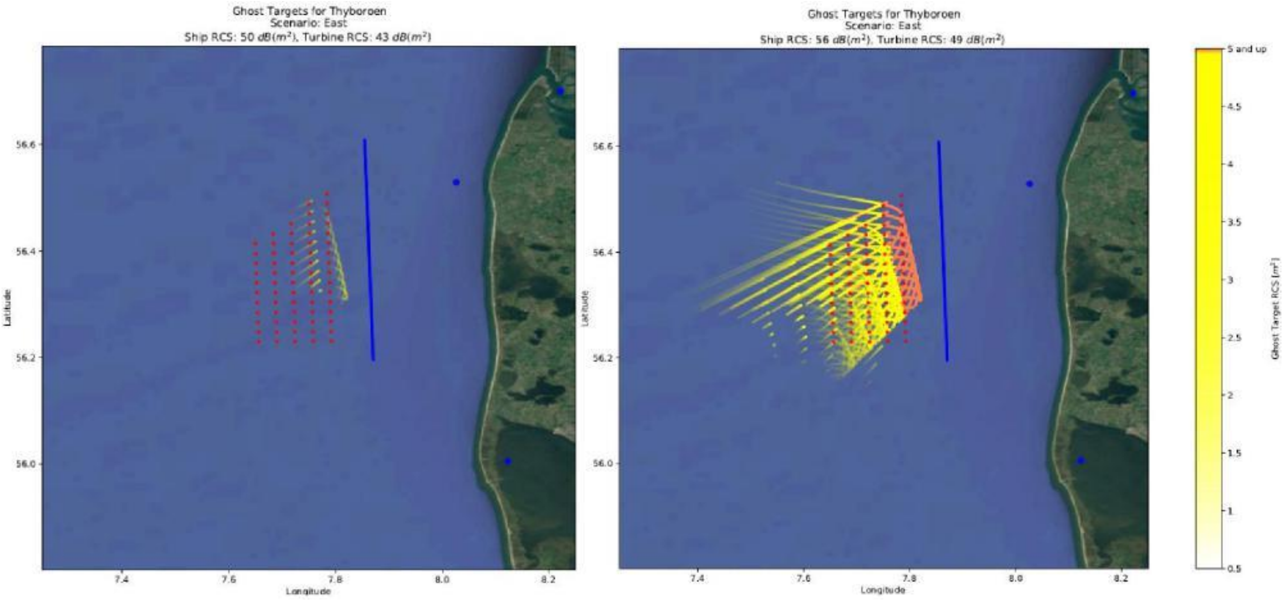

Figure 26 Calculation of ghost targets originating from large vessels, north bound east of Thor Havmøllepark 2 Nautical miles out from the windfarm area. Radar sites from top to bottom are: Gapfiller Radar at Vesterhav Nord, KYRA Hvide Sande, and KYRA Thyborøn. Representative (left) and Worst case (right)

Likelihood of ghosts originating from east bound traffic south of Thor Havmøllepark 2 Nautical miles out from the windfarm area

Below images indicate that there is likelihood of ghosts originating from large ships operating south of Thor Havmøllepark. The ghosts are calculated to be weak and diffuse, however the ghosts may be pronounced (> 5 m2 in RCS) in the worst case and are therefore likely to cause significant false tracks or significant disturbance on operational displays.

This will be more pronounced with shipping, also smaller ships, even closer to the wind farms.

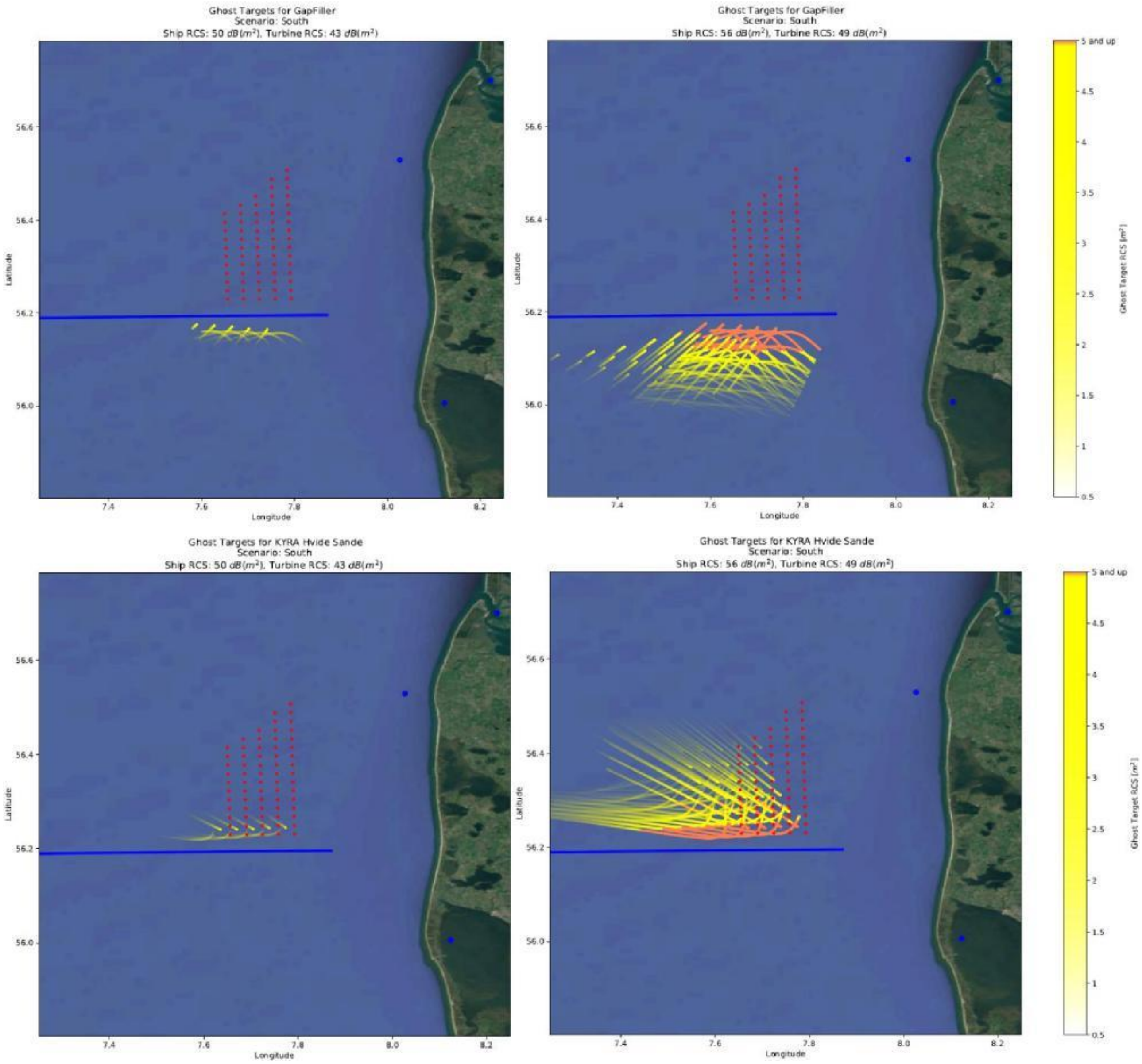

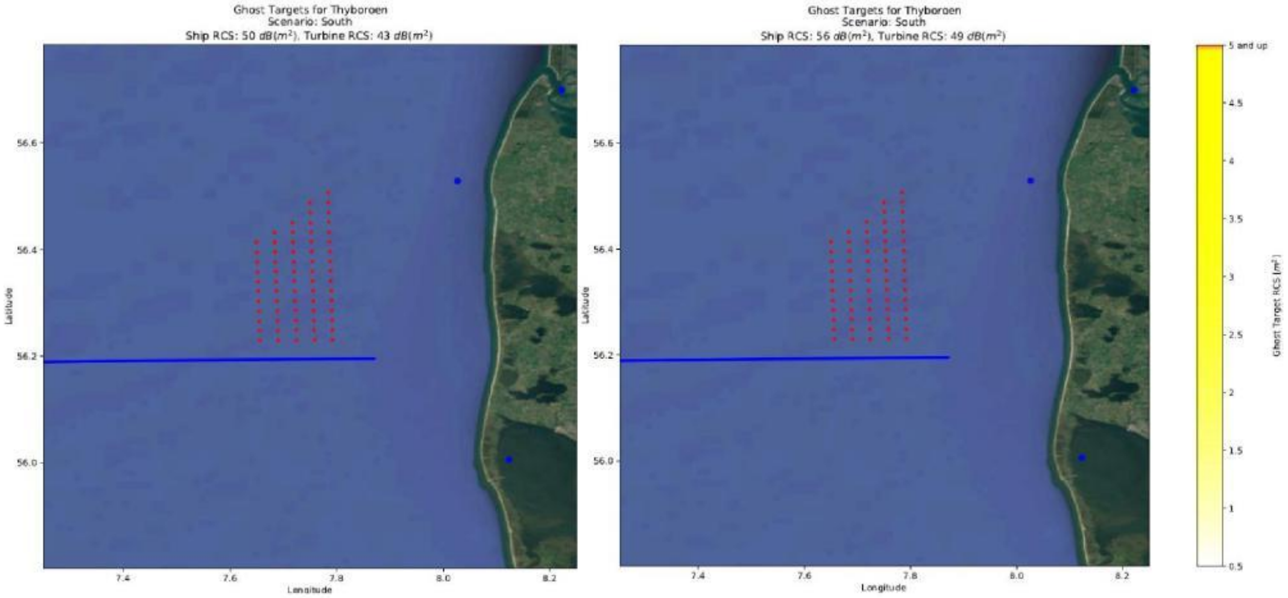

Figure 27 Calculation of ghost targets originating from large vessels, east bound south of Thor Havmøllepark 2 Nautical miles out from the windfarm area. Radar sites from top to bottom are: Gapfiller Radar at Vesterhav Nord, KYRA Hvide Sande, and KYRA Thyborøn. Representative (left) and Worst case (right)

7.1.3 Scenario 2 8MW Windmills

Likelihood of ghosts originating from southwest bound traffic West of Thor Havmøllepark 1 Nautical mile out from the windfarm area

Below images indicate that there is a high likelihood of ghosts originating from ships travelling Northwest of Thor Havmøllepark.

The ghosts may be pronounced (> 5 m2 in RCS) and are therefore likely to cause significant false tracks or significant disturbance on operational displays.

Due to the large distance, KYRA Hvide Sande is calculated to not produce prominent ghost echoes.

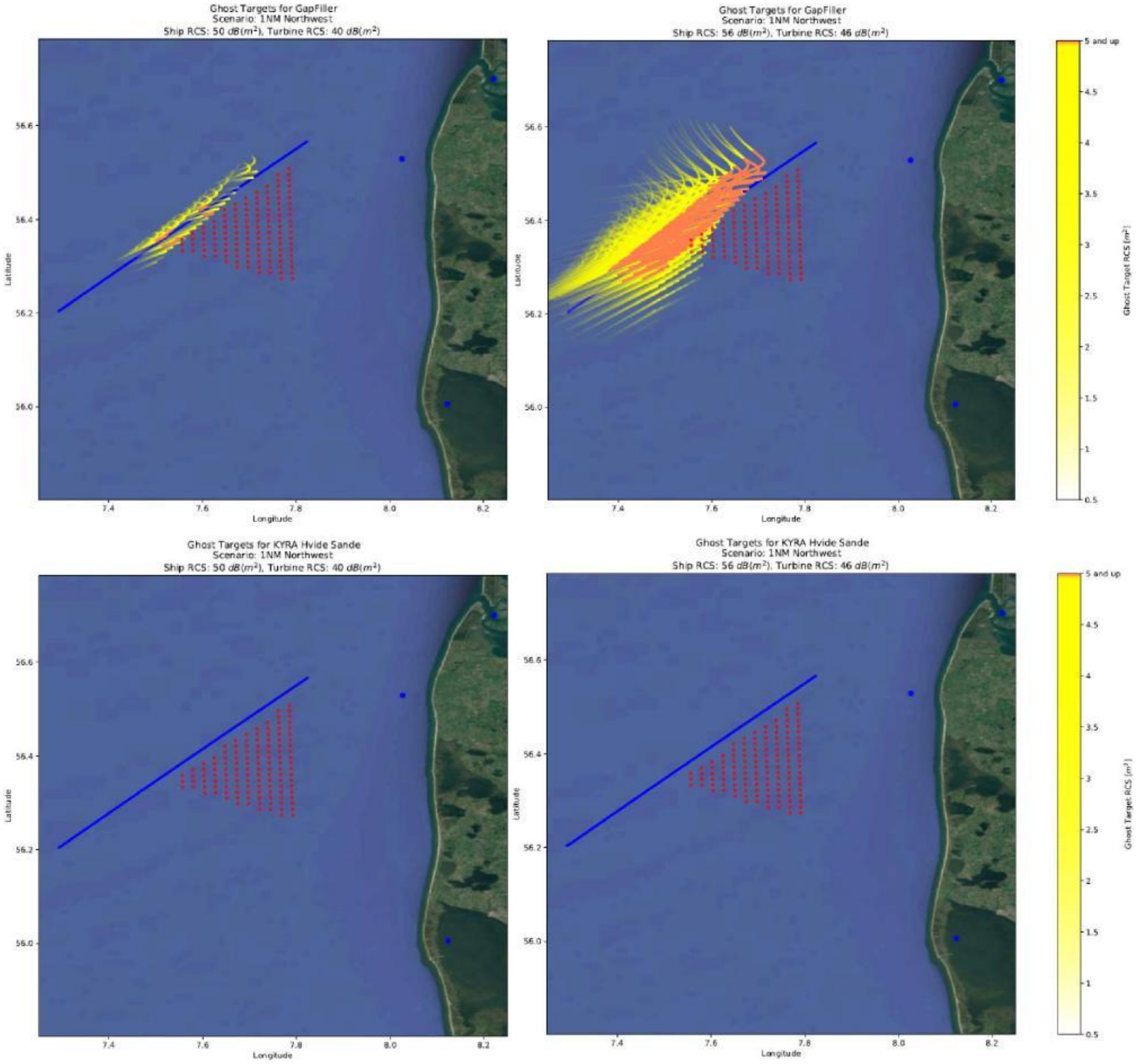

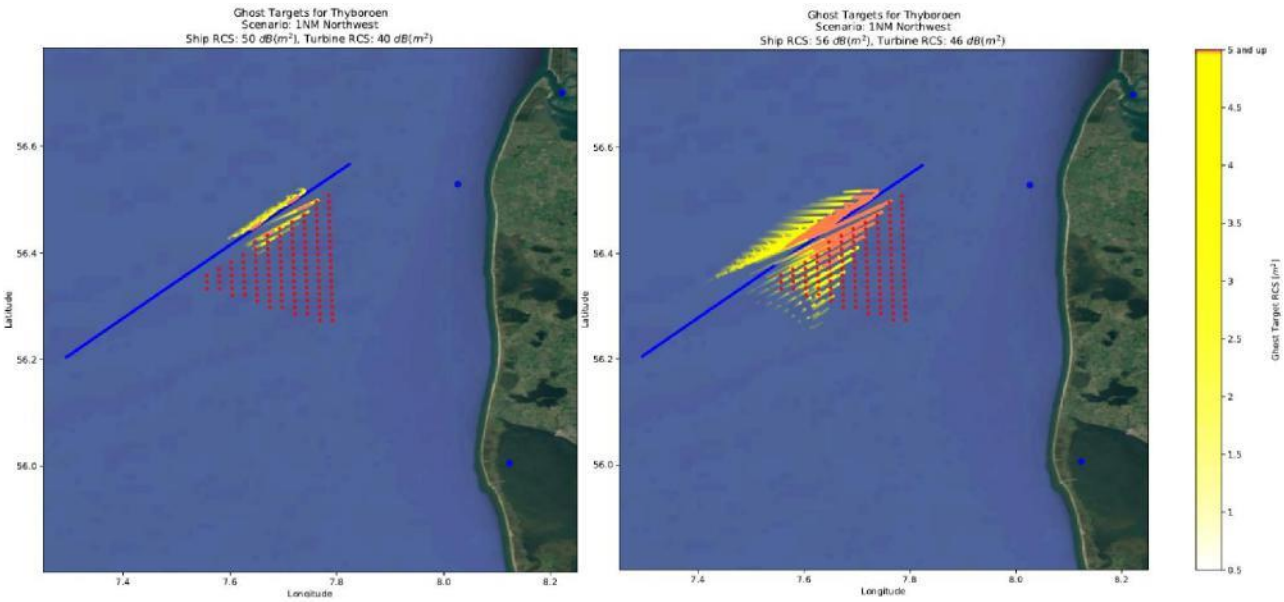

Figure 28 Calculation of ghost targets originating from large vessels, southwest bound west of Thor Havmøllepark 1 Nautical mile out from the windfarm area. Radar sites from top to bottom are: Gapfiller Radar at Vesterhav Nord, KYRA Hvide Sande, and KYRA Thyborøn. Representative (left) and Worst case (right)

Likelihood of ghosts originating from north bound traffic east of Thor Havmøllepark 1 Nautical mile out from the windfarm area

Below images indicate that here is some likelihood of ghosts originating from ships travelling east of Thor Havmøllepark. The ghosts may be pronounced (> 5 m2 in RCS) and are therefore likely to cause significant false tracks or significant disturbance on operational displays.

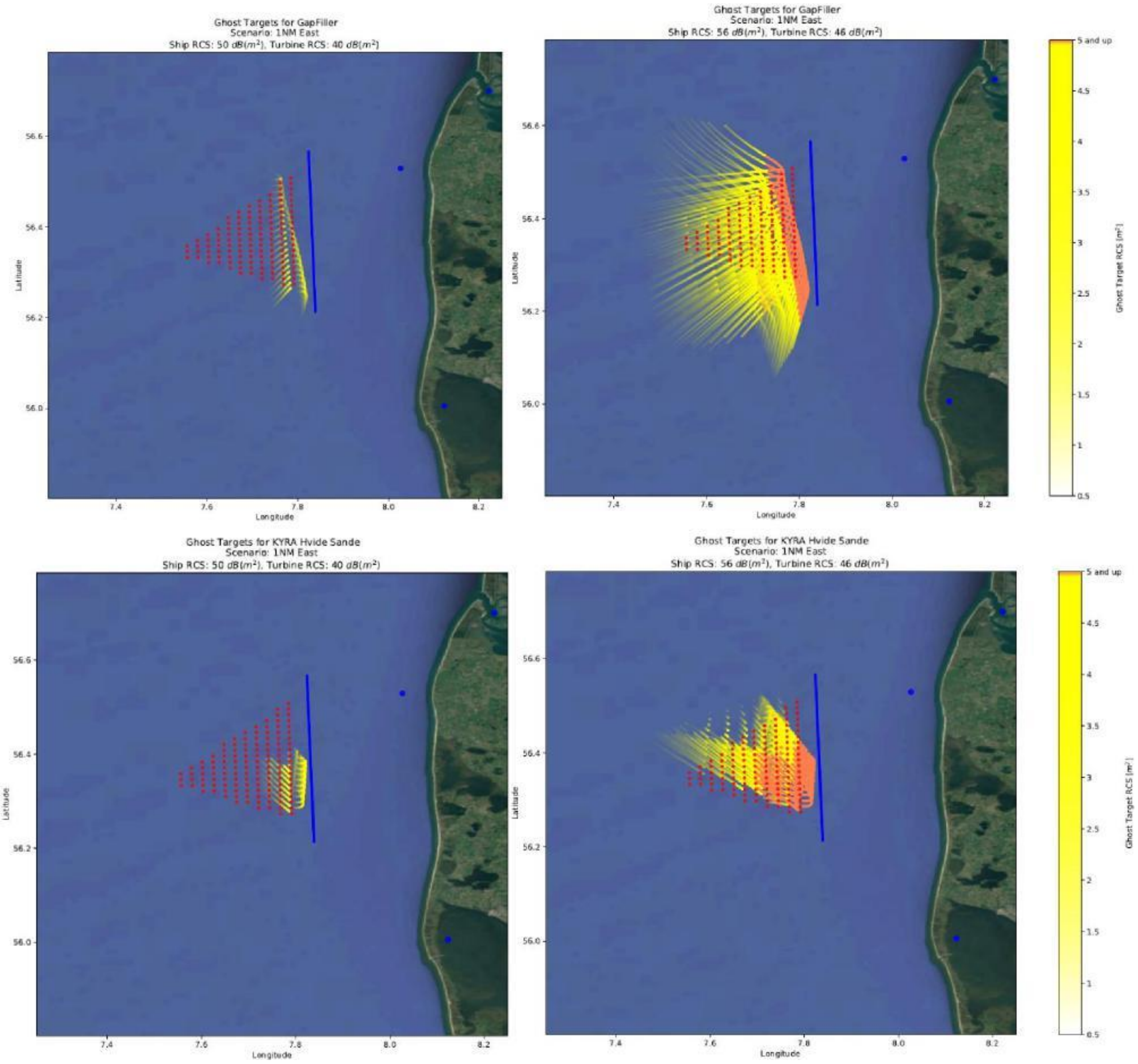

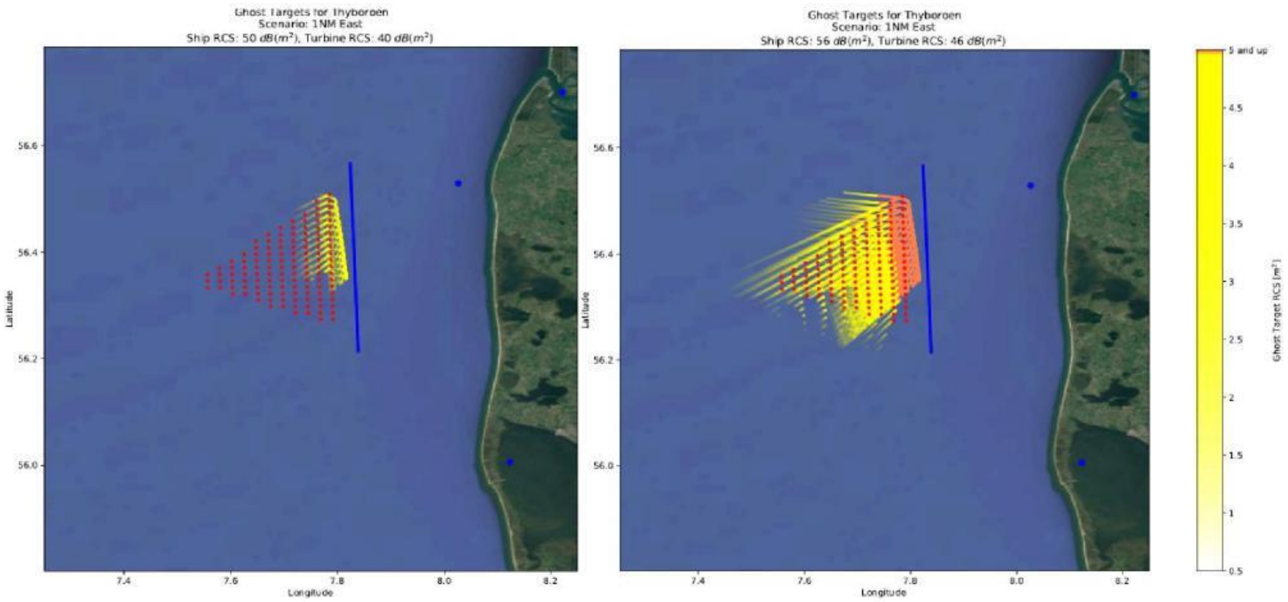

Figure 29 Calculation of ghost targets originating from large vessels, north bound east of Thor Havmøllepark 1 Nautical mile out from the windfarm area. Radar sites from top to bottom are: Gapfiller Radar at Vesterhav Nord, KYRA Hvide Sande, and KYRA Thyborøn. Representative (left) and Worst case (right)

Likelihood of ghosts originating from east bound traffic south of Thor Havmøllepark 1 Nautical mile out from the windfarm area

Below images indicate that here is low likelihood of ghosts originating from ships travelling south of Thor Havmøllepark. The ghosts are weak and diffuse (< 5 m2 in RCS) and are therefore unlikely to cause significant false tracks or significant disturbance on operational displays.

Due to the large distance, KYRA Thyborøn is calculated to not produce prominent ghost echoes.

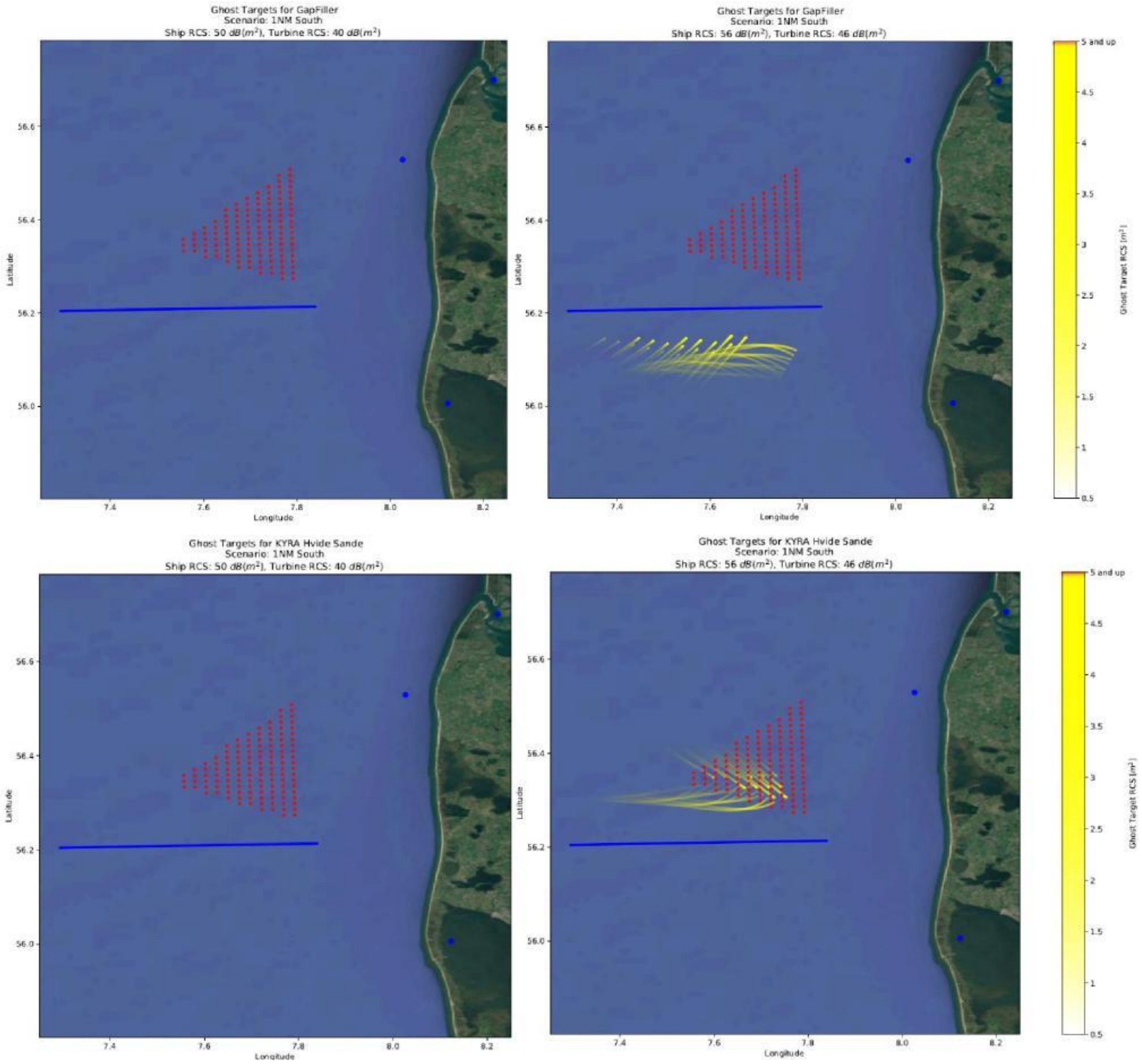

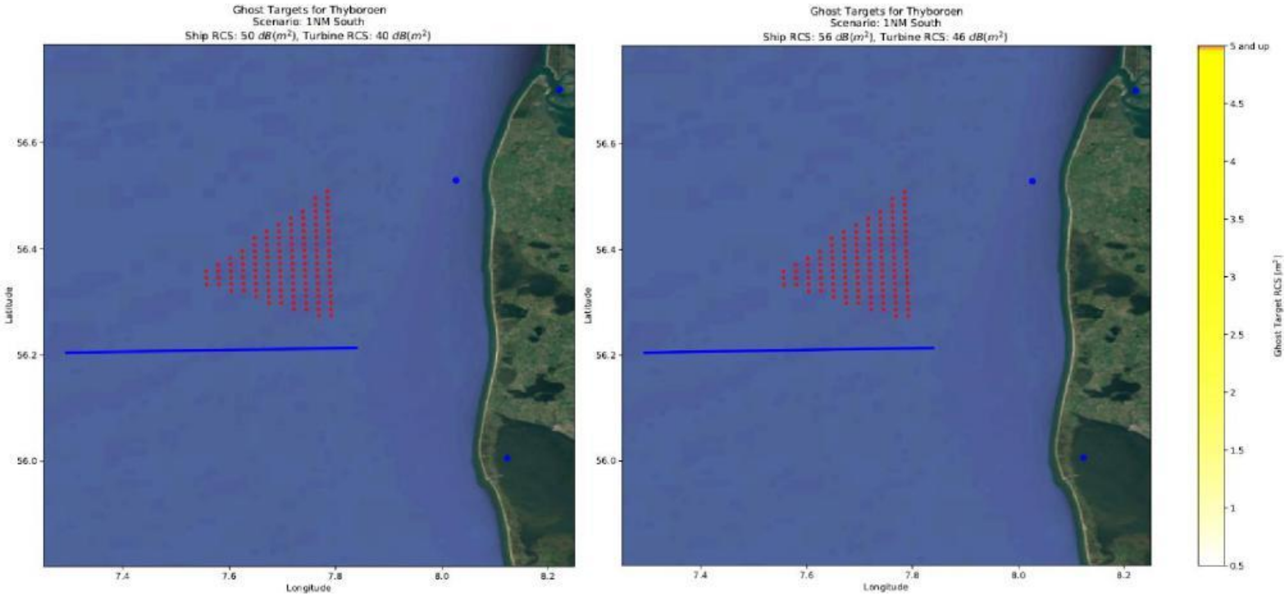

Figure 30 Calculation of ghost targets originating from large vessels, east bound south of Thor Havmøllepark 1 Nautical mile out from the windfarm area. Radar sites from top to bottom are: Gapfiller Radar at Vesterhav Nord, KYRA Hvide Sande, and KYRA Thyborøn. Representative (left) and Worst case (right)

Likelihood of ghosts originating from southwest bound traffic West of Thor Havmøllepark 2 Nautical miles out from the windfarm area

Below images indicate that there is a high likelihood of ghosts originating from ships travelling Northwest of Thor Havmøllepark.

Possible ghost echoes are calculated to be weak and diffuse for smaller ships, however in the worst case, ghost echoes of more than 5 m^2 in RCS are seen and therefore are likely to cause false tracks or to be displayed on operational displays.

Due to the large distance, KYRA Hvide Sande is calculated to not produce prominent ghost echoes.

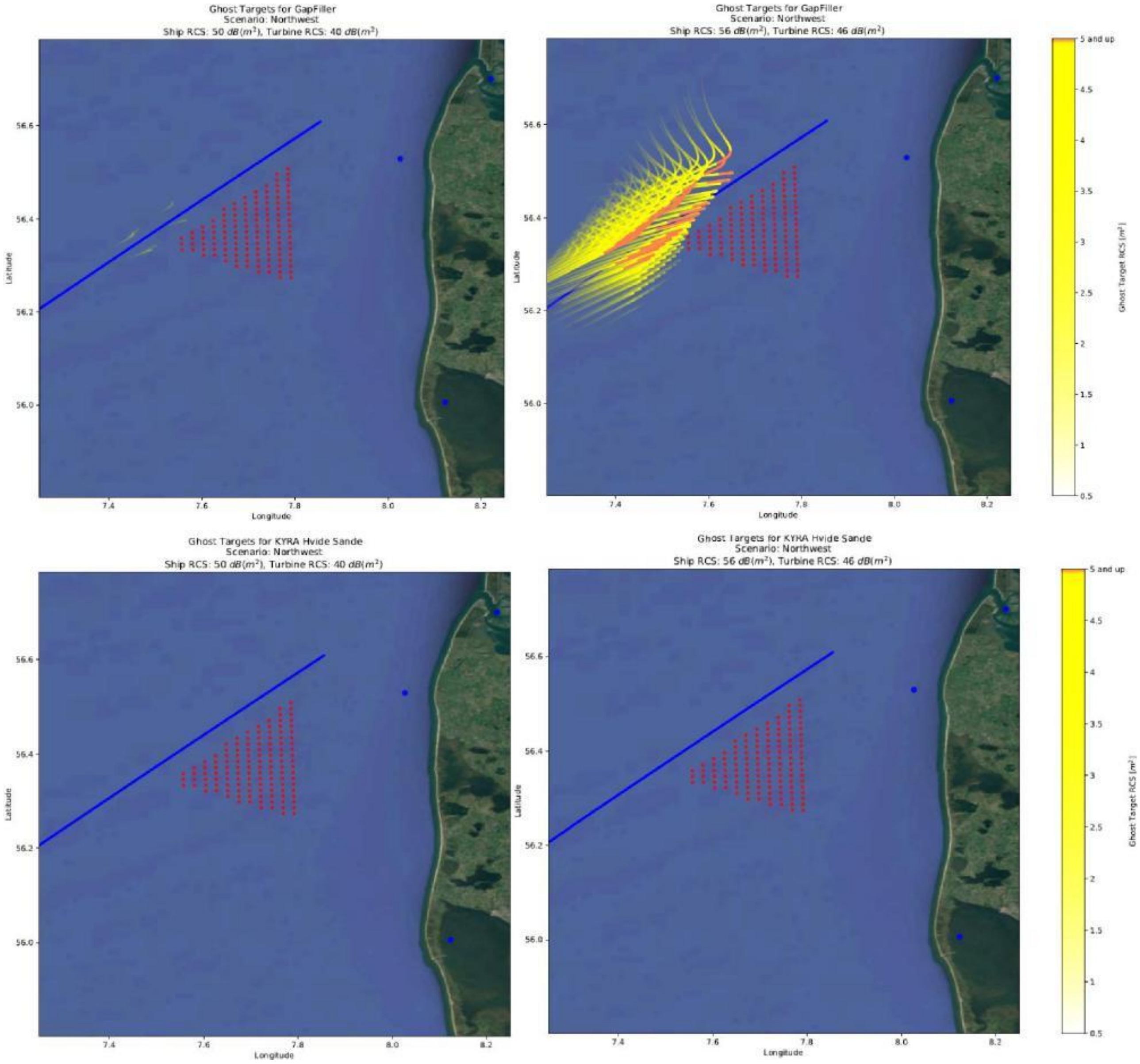

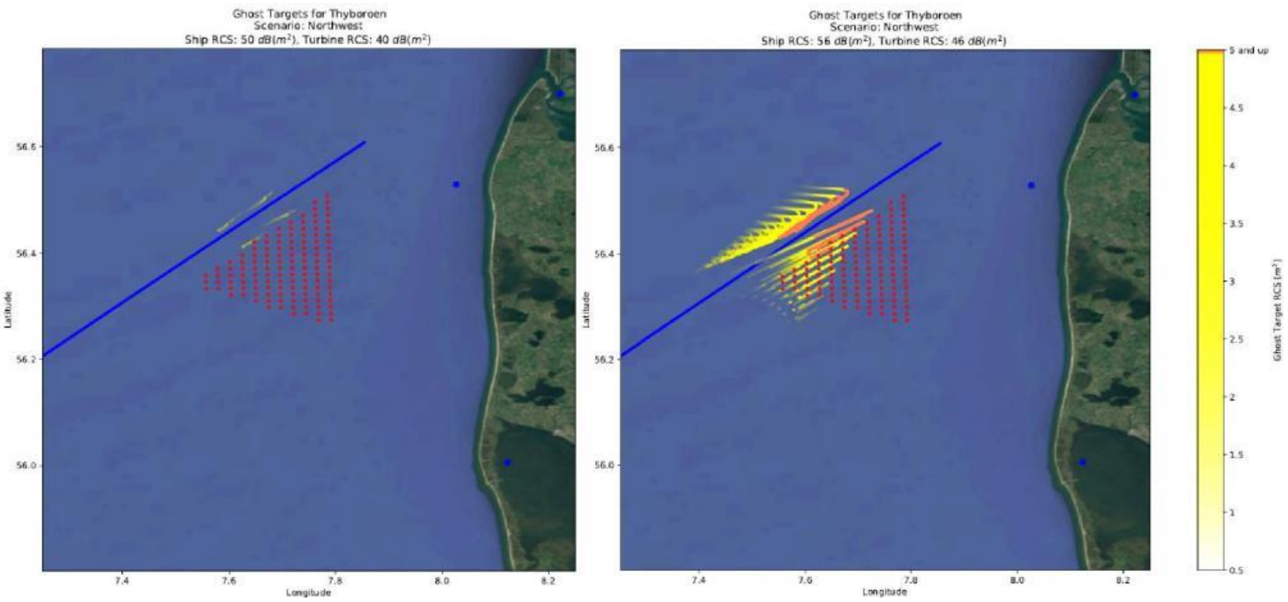

Figure 31 Calculation of ghost targets originating from large vessels, southwest bound north of Thor Havmøllepark 2 Nautical miles out from the windfarm area. Radar sites from top to bottom are: Gapfiller Radar at Vesterhav Nord, KYRA Hvide Sande, and KYRA Thyborøn. Representative (left) and Worst case (right)

Likelihood of ghosts originating from north bound traffic east of Thor Havmøllepark 2 Nautical miles out from the windfarm area

Below images indicate that here is some likelihood of ghosts originating from ships travelling east of Thor Havmøllepark. Possible ghost echoes are calculated to be weak and diffuse for smaller ships, however in the worst case, ghost echoes of more than 5 m^2 in RCS are seen and therefore are likely to cause false tracks or to be displayed on operational displays.

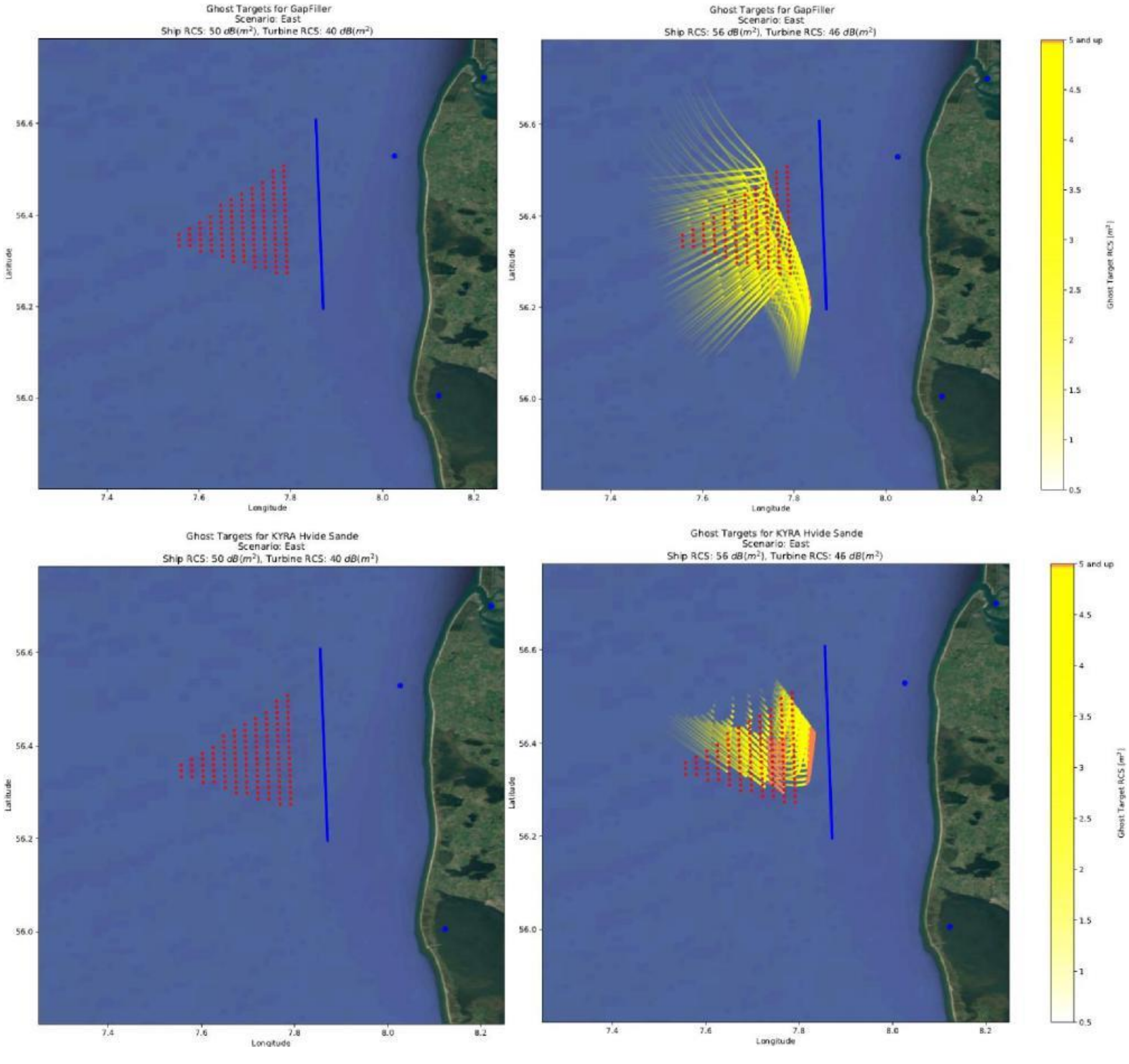

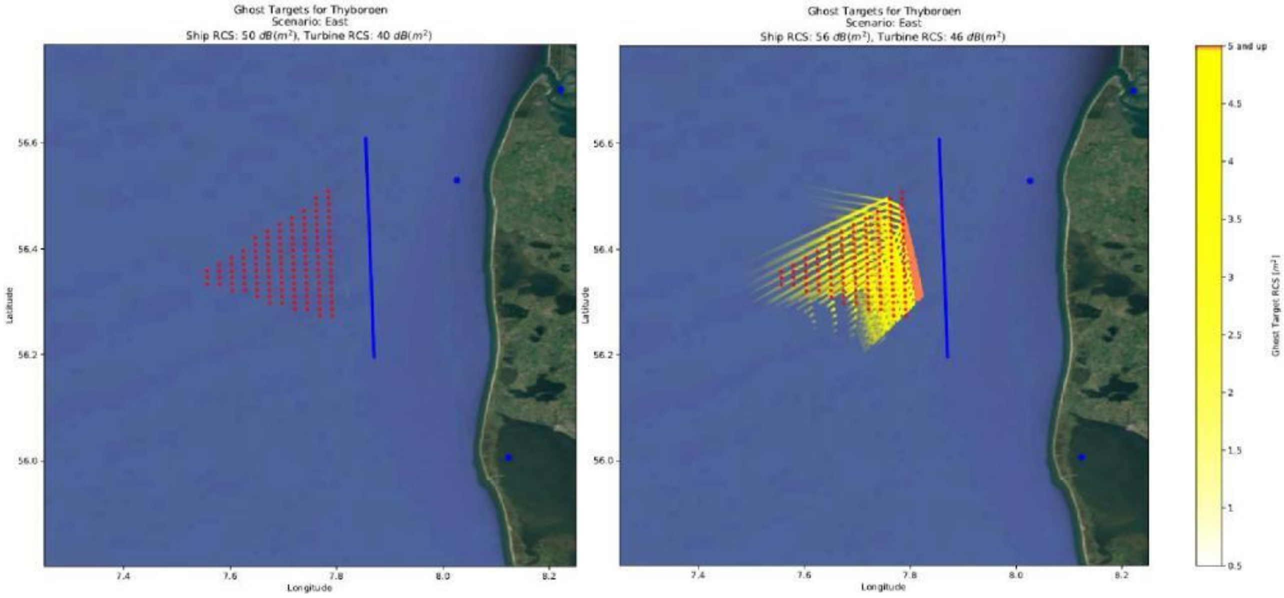

Figure 32 Calculation of ghost targets originating from large vessels, north bound east of Thor Havmøllepark 2 Nautical miles out from the windfarm area. Radar sites from top to bottom are: Gapfiller Radar at Vesterhav Nord, KYRA Hvide Sande, and KYRA Thyborøn. Representative (left) and Worst case (right)

Likelihood of ghosts originating from east bound traffic south of Thor Havmøllepark 2 Nautical miles out from the windfarm area

Below images indicate that here is likelihood of ghosts originating from large ships operating south of Thor Havmøllepark. The ghosts are weak and diffuse, in the worst case (< 5 m2 in RCS) and are therefore unlikely to cause significant false tracks or significant disturbance on operational displays.

This will be more pronounced with shipping, also smaller ships, even closer to the wind farms.

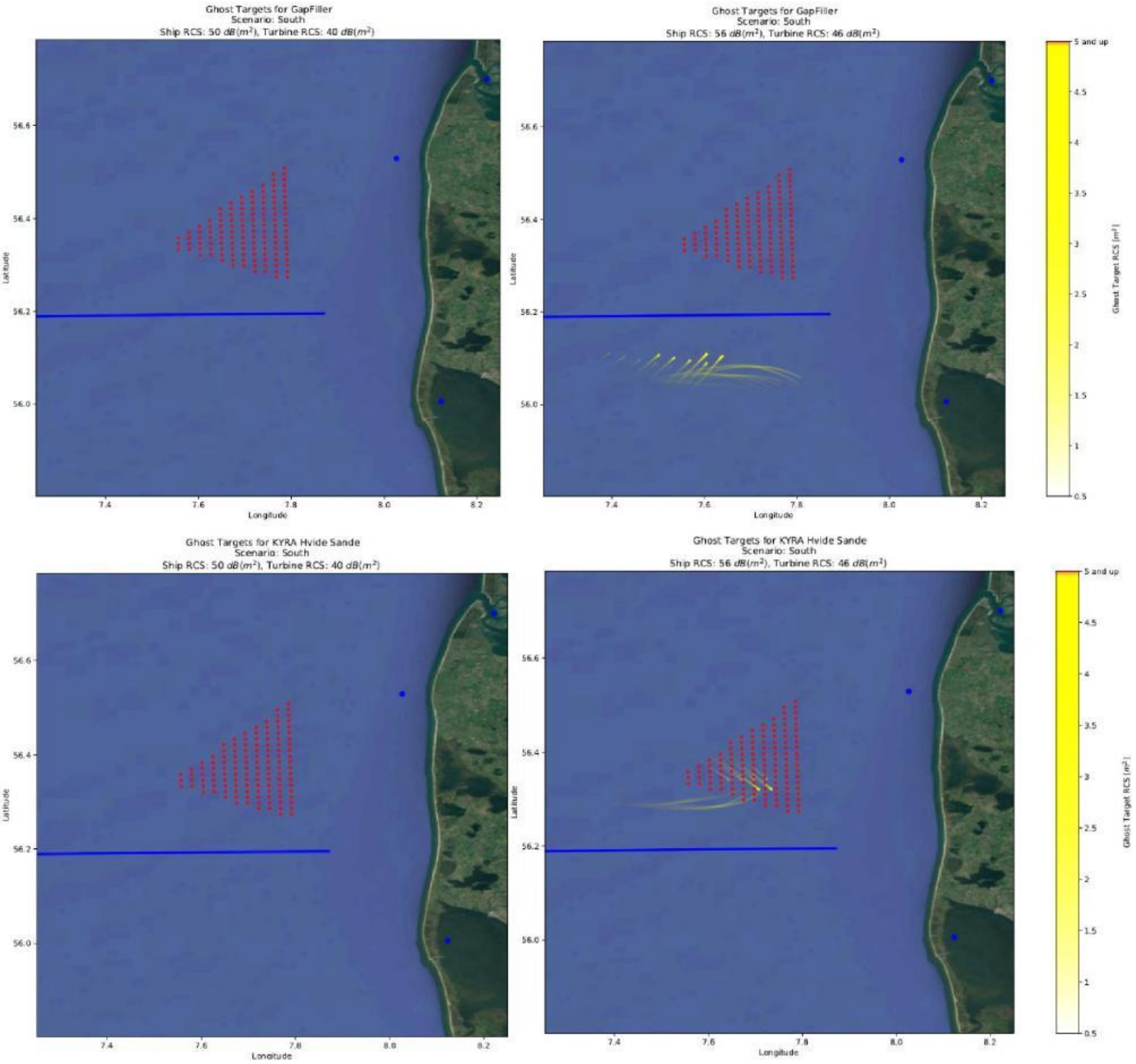

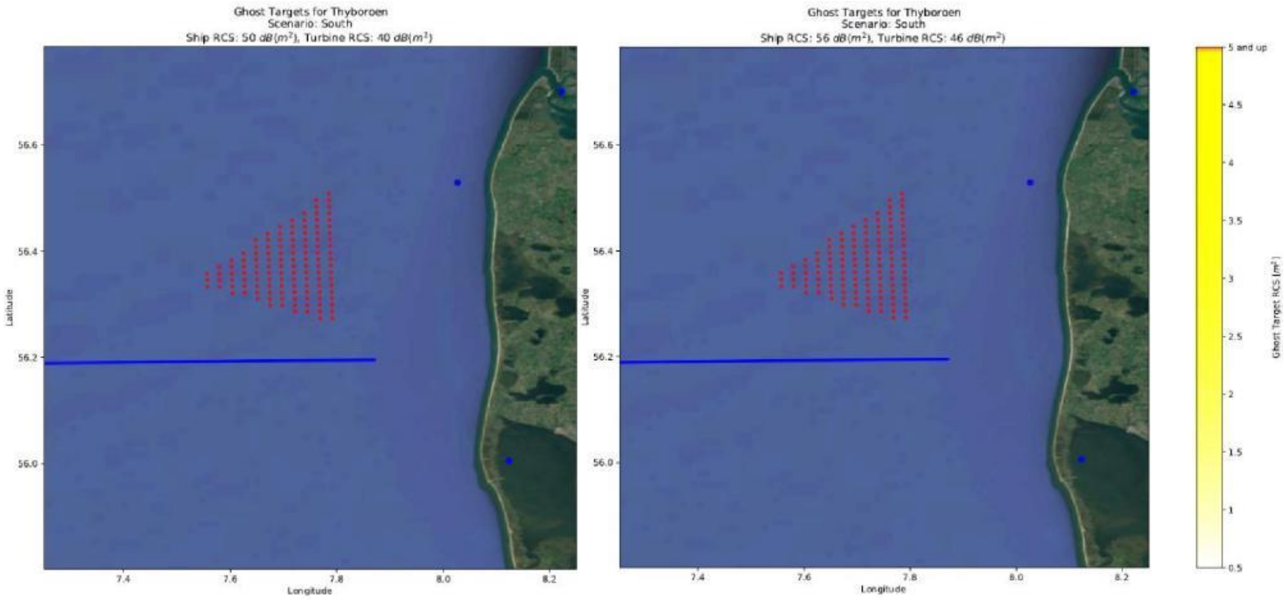

Figure 33 Calculation of ghost targets originating from large vessels, east bound south of Thor Havmøllepark 2 Nautical miles out from the windfarm area. Radar sites from top to bottom are: Gapfiller Radar at Vesterhav Nord, KYRA Hvide Sande, and KYRA Thyborøn. Representative (left) and Worst case (right)

7.1.1 Scenario 2 15MW Windmills

Likelihood of ghosts originating from southwest bound traffic West of Thor Havmøllepark 1 Nautical mile out from the windfarm area

Below images indicate that there is a high likelihood of ghosts originating from ships travelling Northwest of Thor Havmøllepark.

The ghosts may be pronounced (> 5 m2 in RCS) and are therefore likely to cause significant false tracks or significant disturbance on operational displays.

Due to the large distance, KYRA Hvide Sande is calculated to not produce prominent ghost echoes.

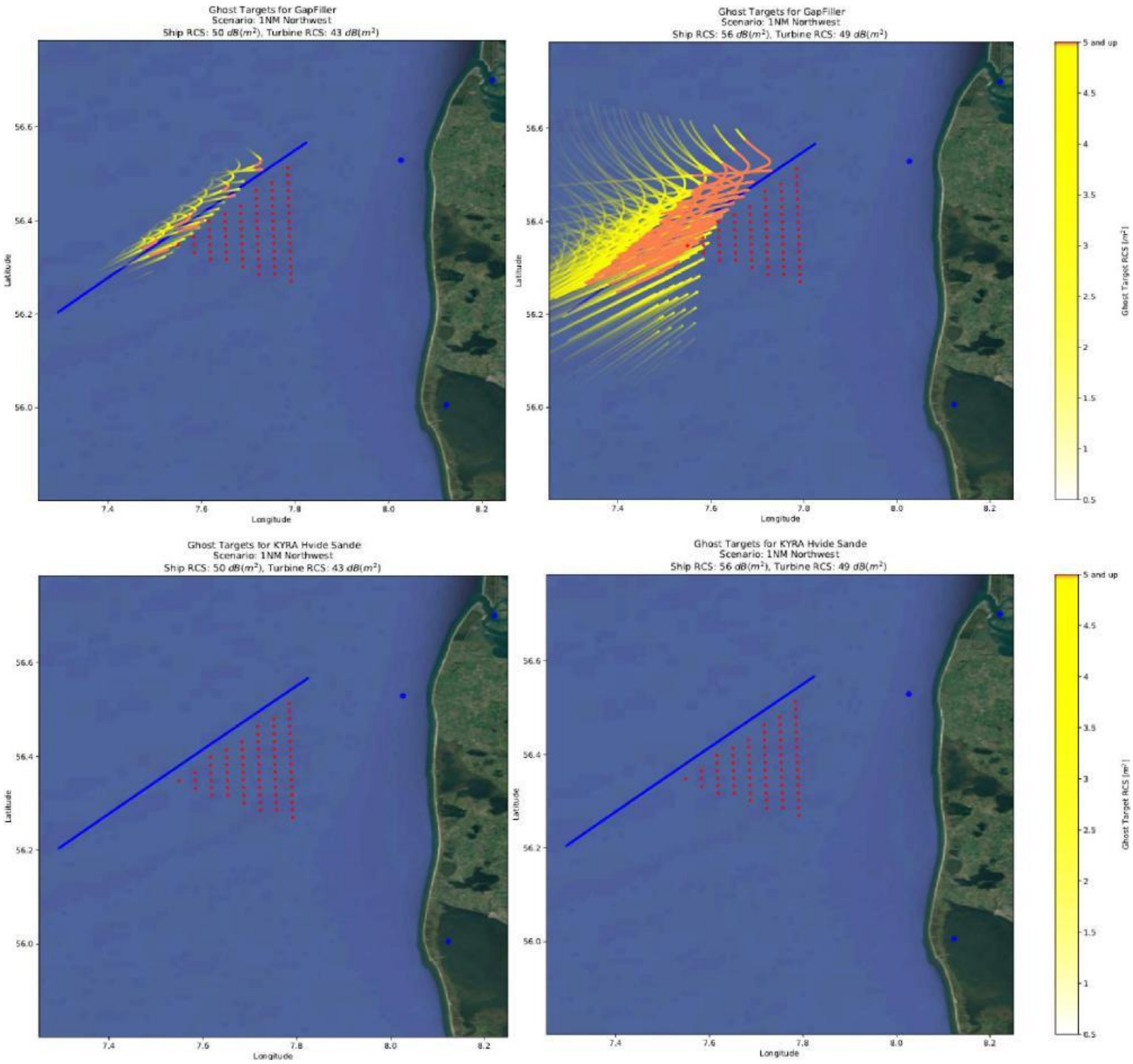

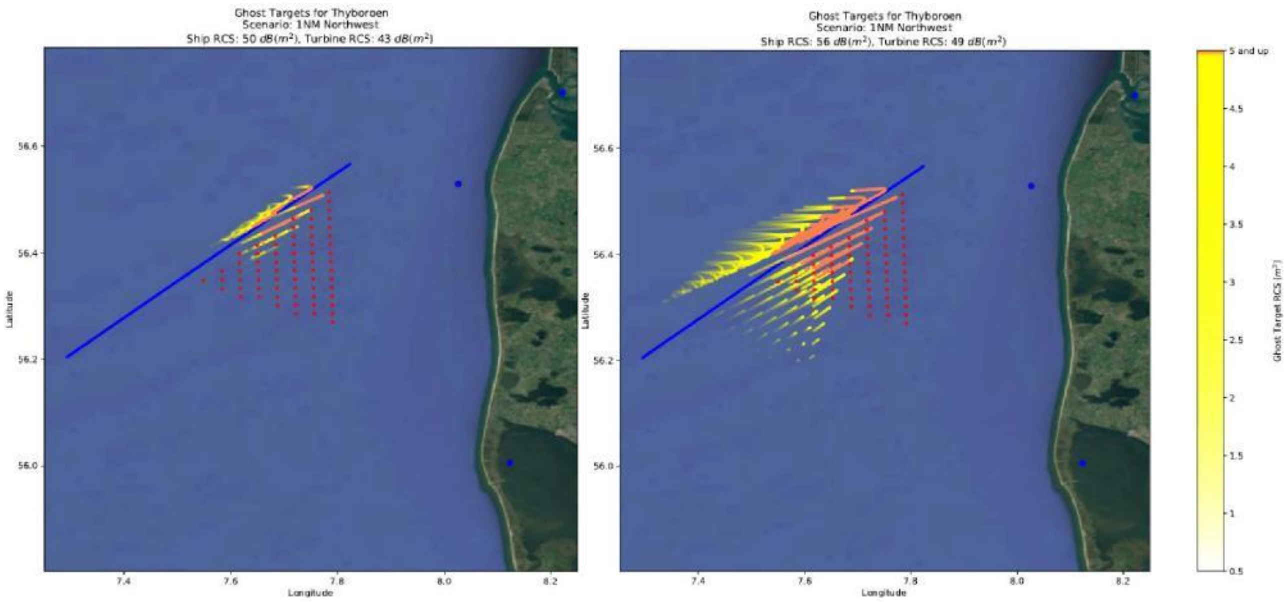

Figure 34 Calculation of ghost targets originating from large vessels, southwest bound west of Thor Havmøllepark 1 Nautical mile out from the windfarm area. Radar sites from top to bottom are: Gapfiller Radar at Vesterhav Nord, KYRA Hvide Sande, and KYRA Thyborøn. Representative (left) and Worst case (right)

Likelihood of ghosts originating from north bound traffic east of Thor Havmøllepark 1 Nautical mile out from the windfarm area

Below images indicate that here is some likelihood of ghosts originating from ships travelling east of Thor Havmøllepark. The ghosts may be pronounced (> 5 m2 in RCS) and are therefore likely to cause significant false tracks or significant disturbance on operational displays.

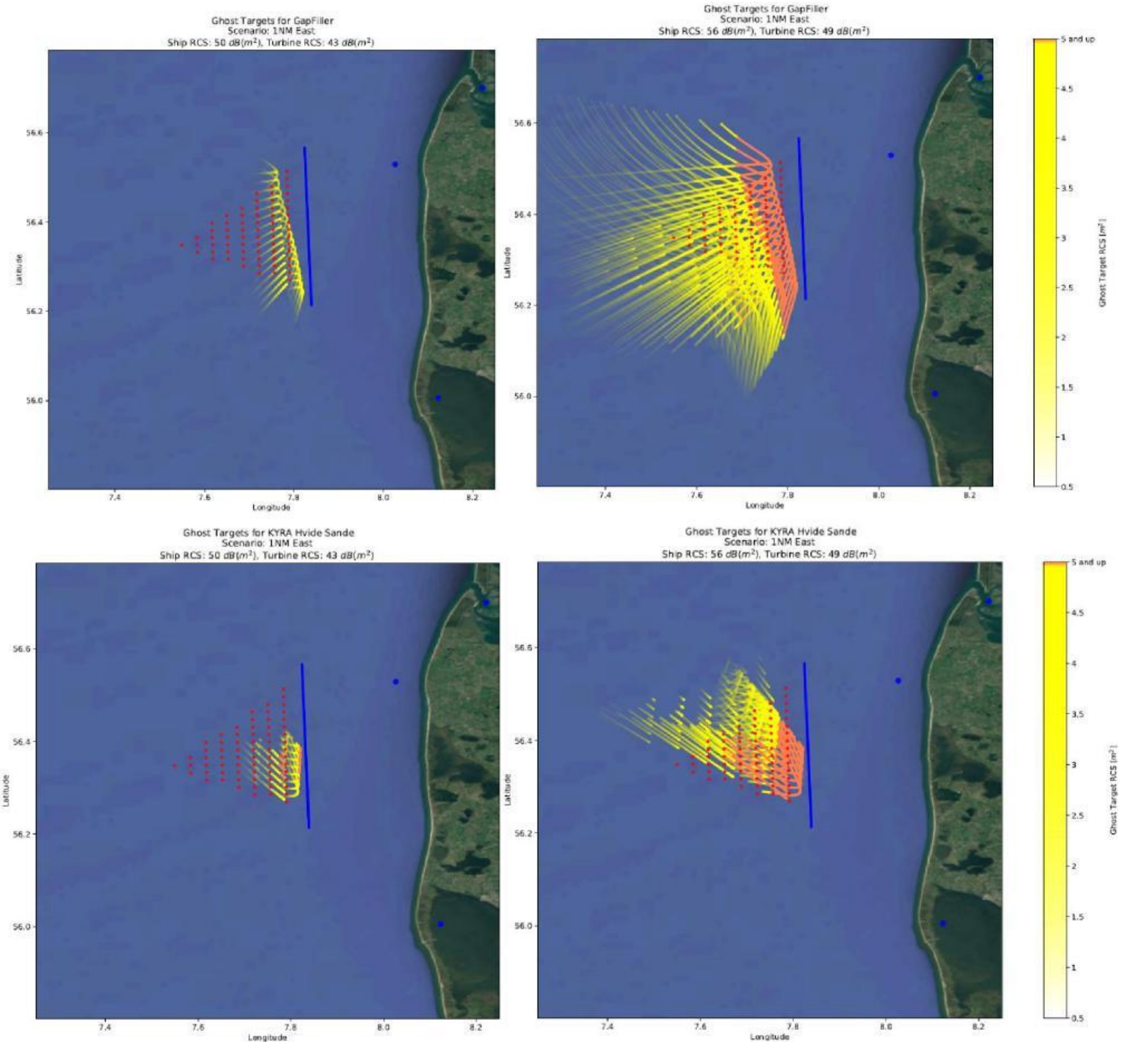

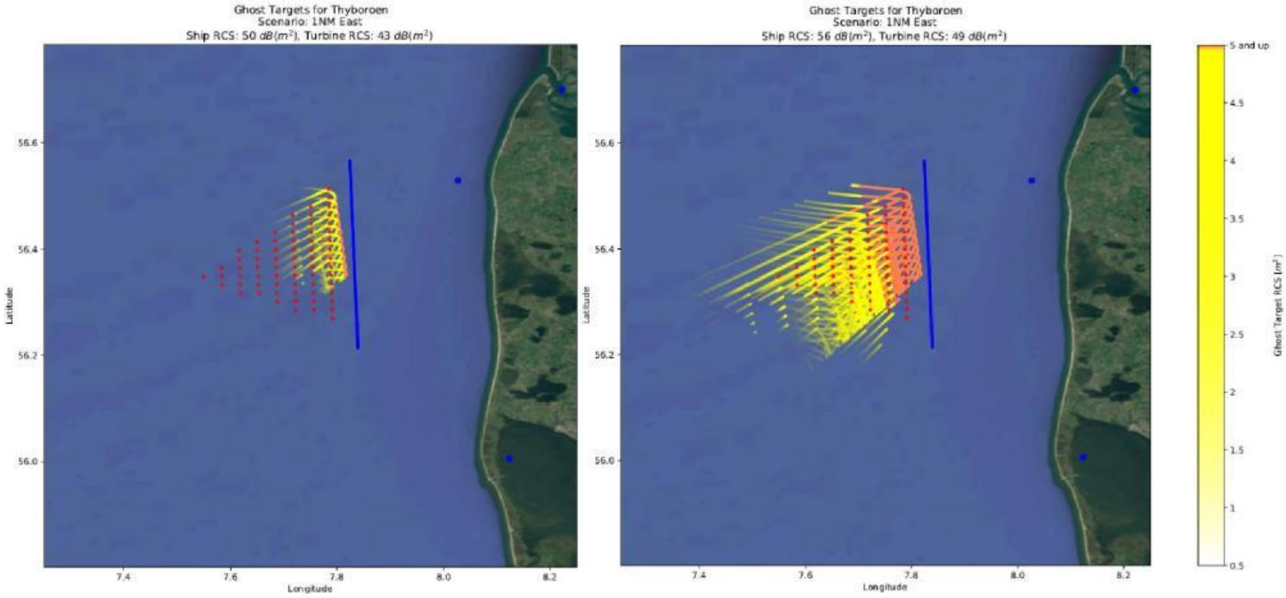

Figure 35 Calculation of ghost targets originating from large vessels, north bound east of Thor Havmøllepark 1 Nautical mile out from the windfarm area. Radar sites from top to bottom are: Gapfiller Radar at Vesterhav Nord, KYRA Hvide Sande, and KYRA Thyborøn. Representative (left) and Worst case (right)

Likelihood of ghosts originating from east bound traffic south of Thor Havmøllepark 1 Nautical mile out from the windfarm area

Below images indicate that here is some likelihood of ghosts originating from ships travelling south of Thor Havmøllepark. The ghosts may be pronounced (> 5 m2 in RCS) and are therefore likely to cause significant false tracks or significant disturbance on operational displays.

Due to the large distance, KYRA Thyborøn is calculated to not produce prominent ghost echoes.

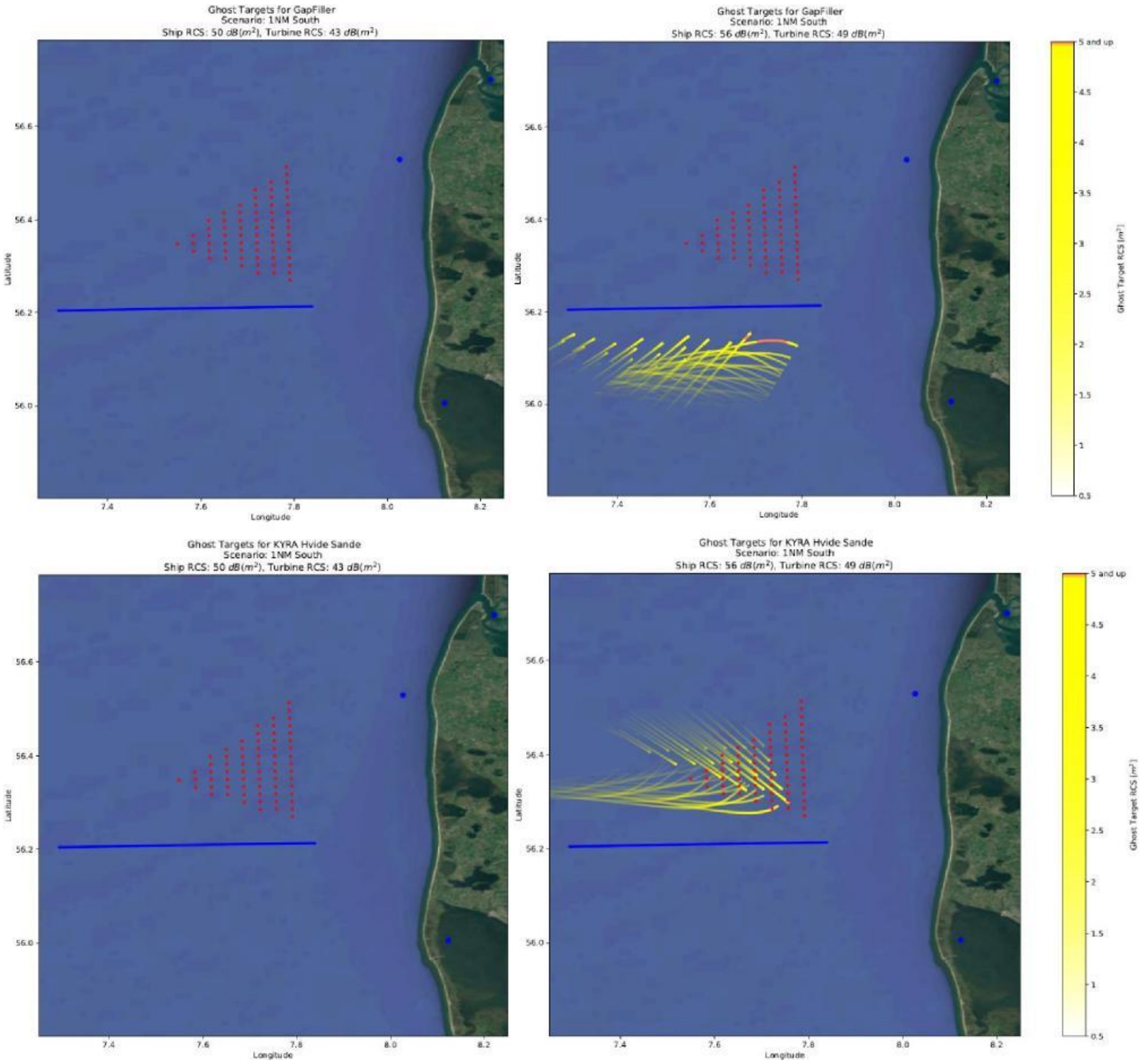

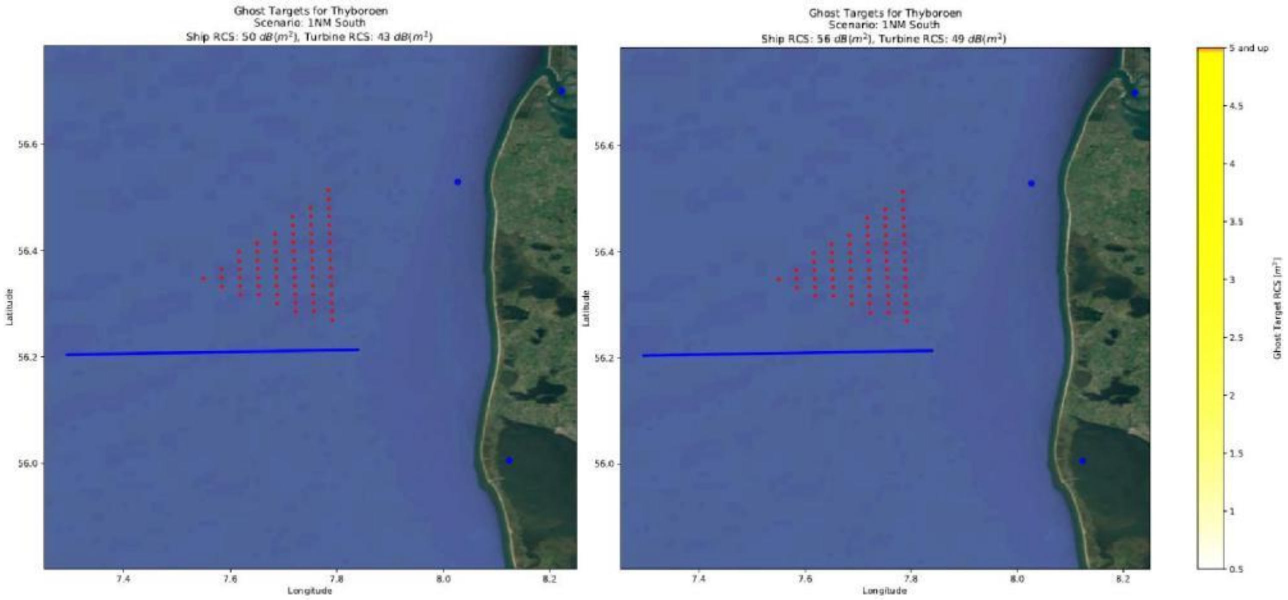

Figure 36 Calculation of ghost targets originating from large vessels, east bound south of Thor Havmøllepark 1 Nautical mile out from the windfarm area. Radar sites from top to bottom are: Gapfiller Radar at Vesterhav Nord, KYRA Hvide Sande, and KYRA Thyborøn. Representative (left) and Worst case (right)

Likelihood of ghosts originating from southwest bound traffic West of Thor Havmøllepark 2 Nautical miles out from the windfarm area

Below images indicate that there is a high likelihood of ghosts originating from ships travelling Northwest of Thor Havmøllepark.

Possible ghost echoes are calculated to be weak and diffuse for smaller ships, however in the worst case, ghost echoes of more than 5 m^2 in RCS are seen and therefore are likely to cause false tracks or to be displayed on operational displays.

Due to the large distance, KYRA Hvide Sande is calculated to not produce prominent ghost echoes.

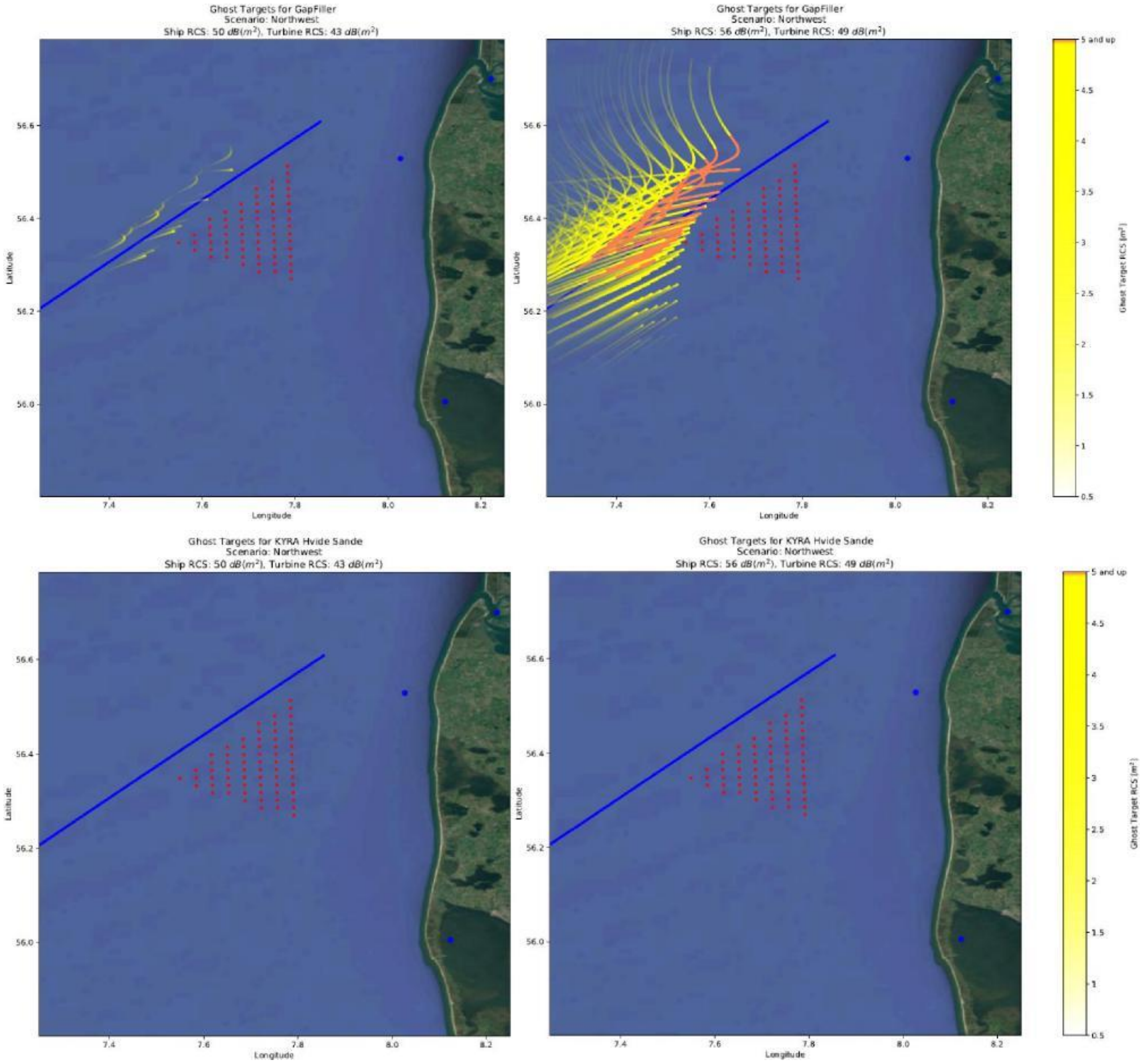

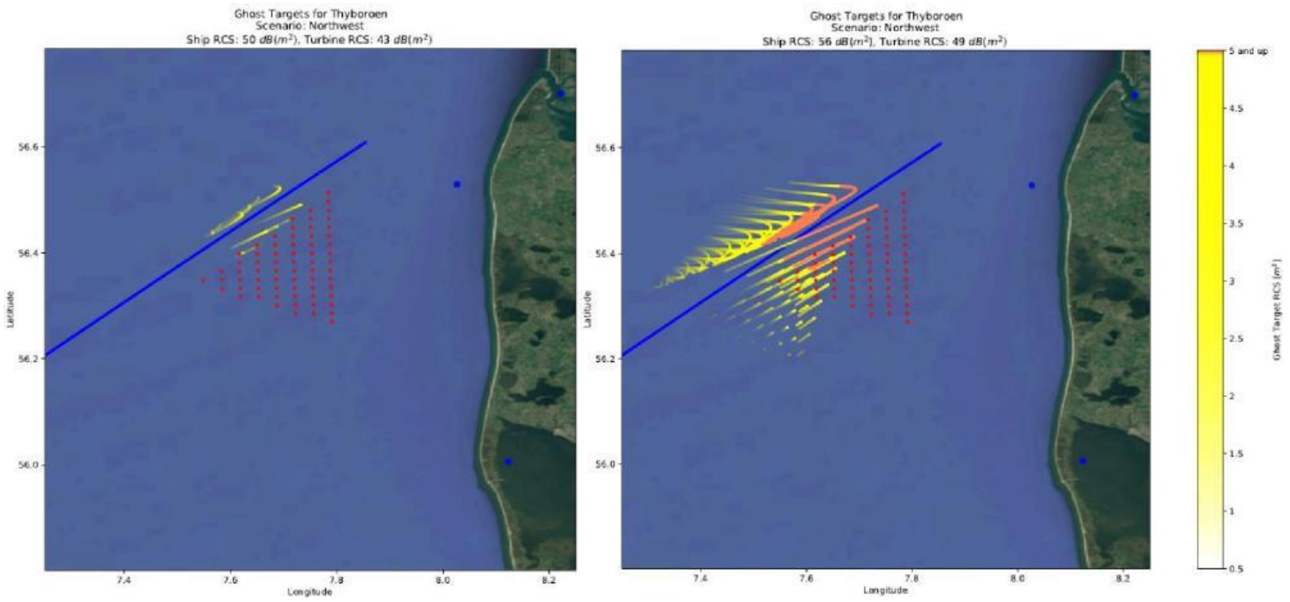

Figure 37 Calculation of ghost targets originating from large vessels, southwest bound north of Thor Havmøllepark 2 Nautical miles out from the windfarm area. Radar sites from top to bottom are: Gapfiller Radar at Vesterhav Nord, KYRA Hvide Sande, and KYRA Thyborøn. Representative (left) and Worst case (right)

Likelihood of ghosts originating from north bound traffic east of Thor Havmøllepark 2 Nautical miles out from the windfarm area

Below images indicate that here is some likelihood of ghosts originating from ships in the northbound east of Thor Havmøllepark. Possible ghost echoes are calculated to be weak and diffuse for smaller ships, however in the worst case, ghost echoes of more than 5 m^2 in RCS are seen and therefore are likely to cause false tracks or to be displayed on operational displays.

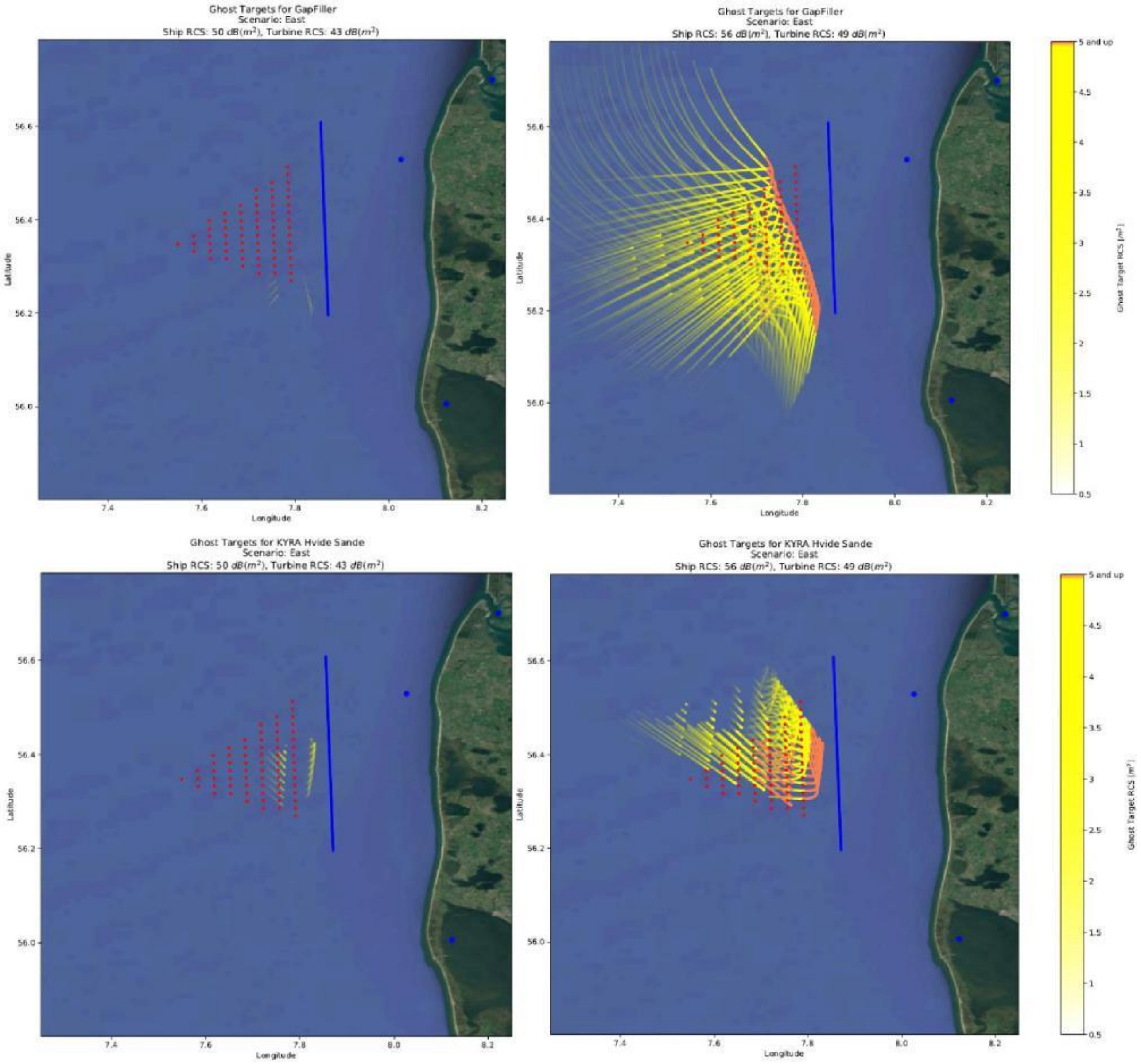

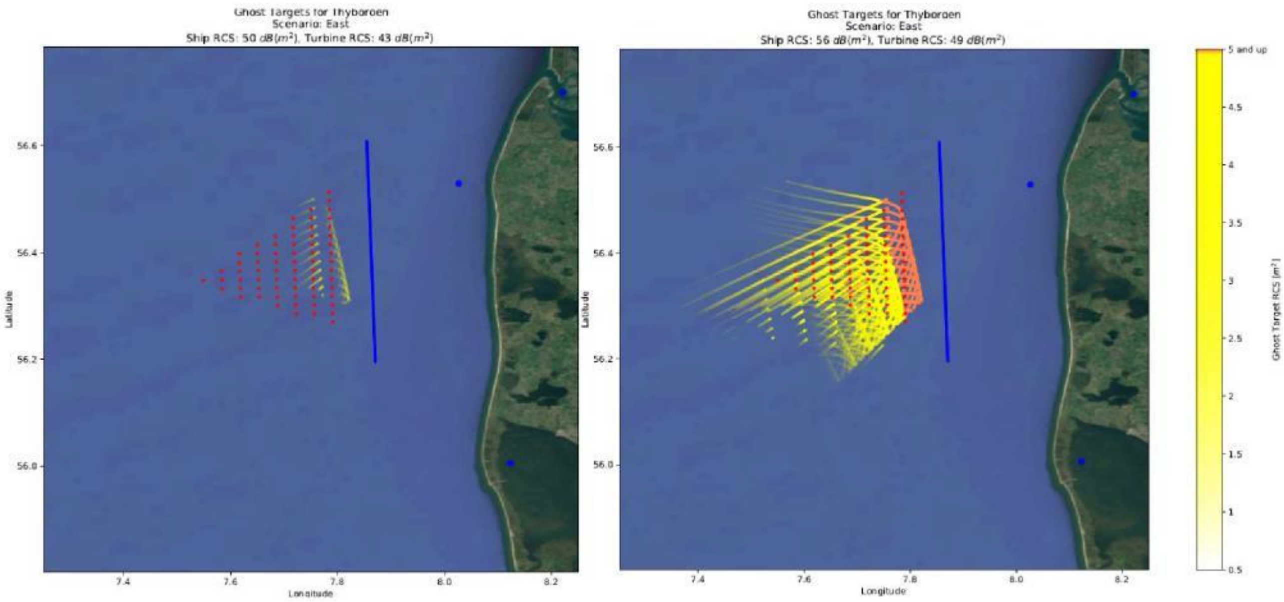

Figure 38 Calculation of ghost targets originating from large vessels, north bound east of Thor Havmøllepark 2 Nautical miles out from the windfarm area. Radar sites from top to bottom are: Gapfiller Radar at Vesterhav Nord, KYRA Hvide Sande, and KYRA Thyborøn. Representative (left) and Worst case (right)

Likelihood of ghosts originating from east bound traffic south of Thor Havmøllepark 2 Nautical miles out from the windfarm area

Below images indicate that there is alow likelihood of ghosts originating from large ships operating south of Thor Havmøllepark. The ghosts may in the worst case be diffuse the ghosts will be weak (< 5 m2 in RCS) and diffuse and are therefore unlikely to cause significant false tracks or significant disturbance on operational displays.

KYRA Thyborøn does not produce prominent ghost echoes due to the large distance.

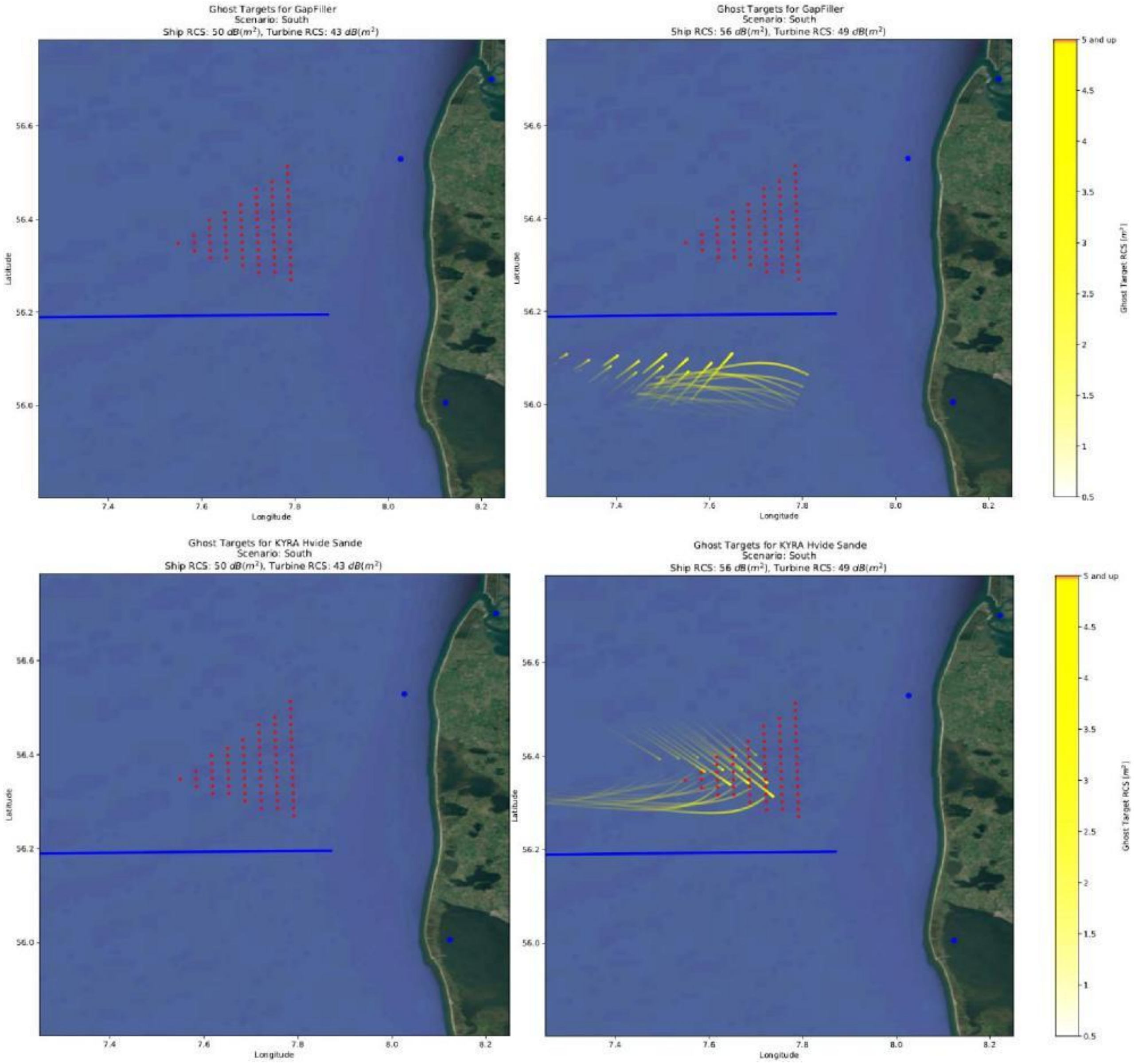

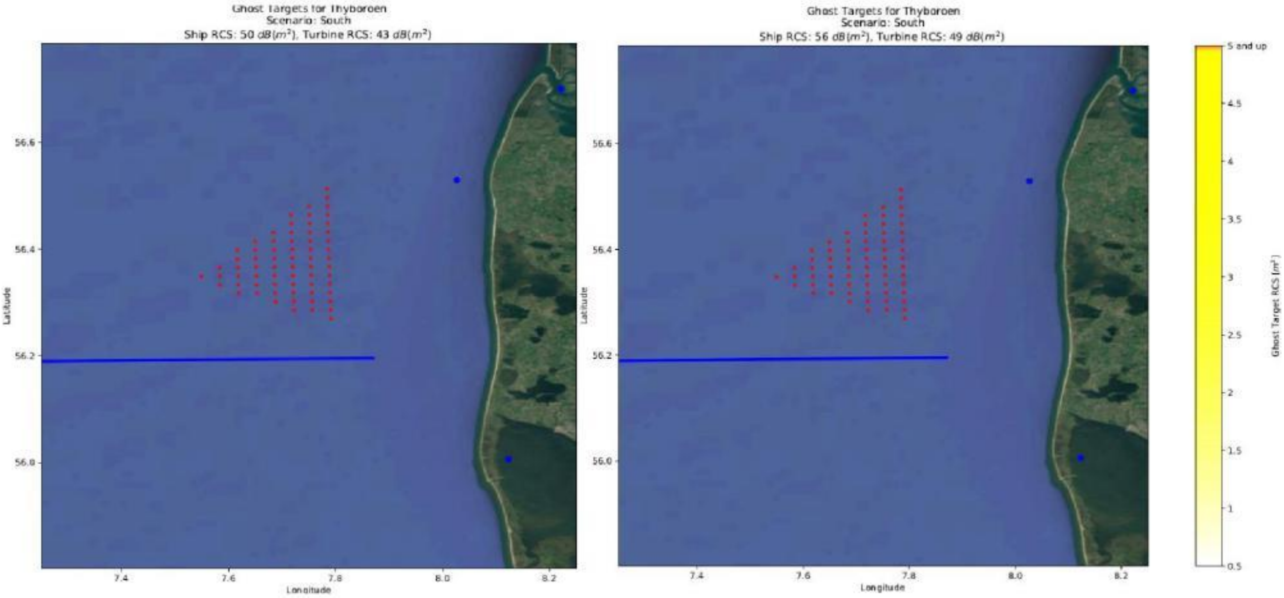

Figure 39 Calculation of ghost targets originating from large vessels, east bound south of Thor Havmøllepark 2 Nautical miles out from the windfarm area. Radar sites from top to bottom are: Gapfiller Radar at Vesterhav Nord, KYRA Hvide Sande, and KYRA Thyborøn. Representative (left) and Worst case (right)

7.1.2 Scenario 3 8MW Windmills

Likelihood of ghosts originating from southwest bound traffic West of Thor Havmøllepark 1 Nautical mile out from the windfarm area

Below images indicate that there is a high likelihood of ghosts originating from ships travelling Northwest of Thor Havmøllepark.

The ghosts may be pronounced (> 5 m2 in RCS) and are therefore likely to cause significant false tracks or significant disturbance on operational displays.

Due to the large distance, neither KYRA Hvide Sande or KYRA Thyborøn are calculated to produce prominent ghost echoes.

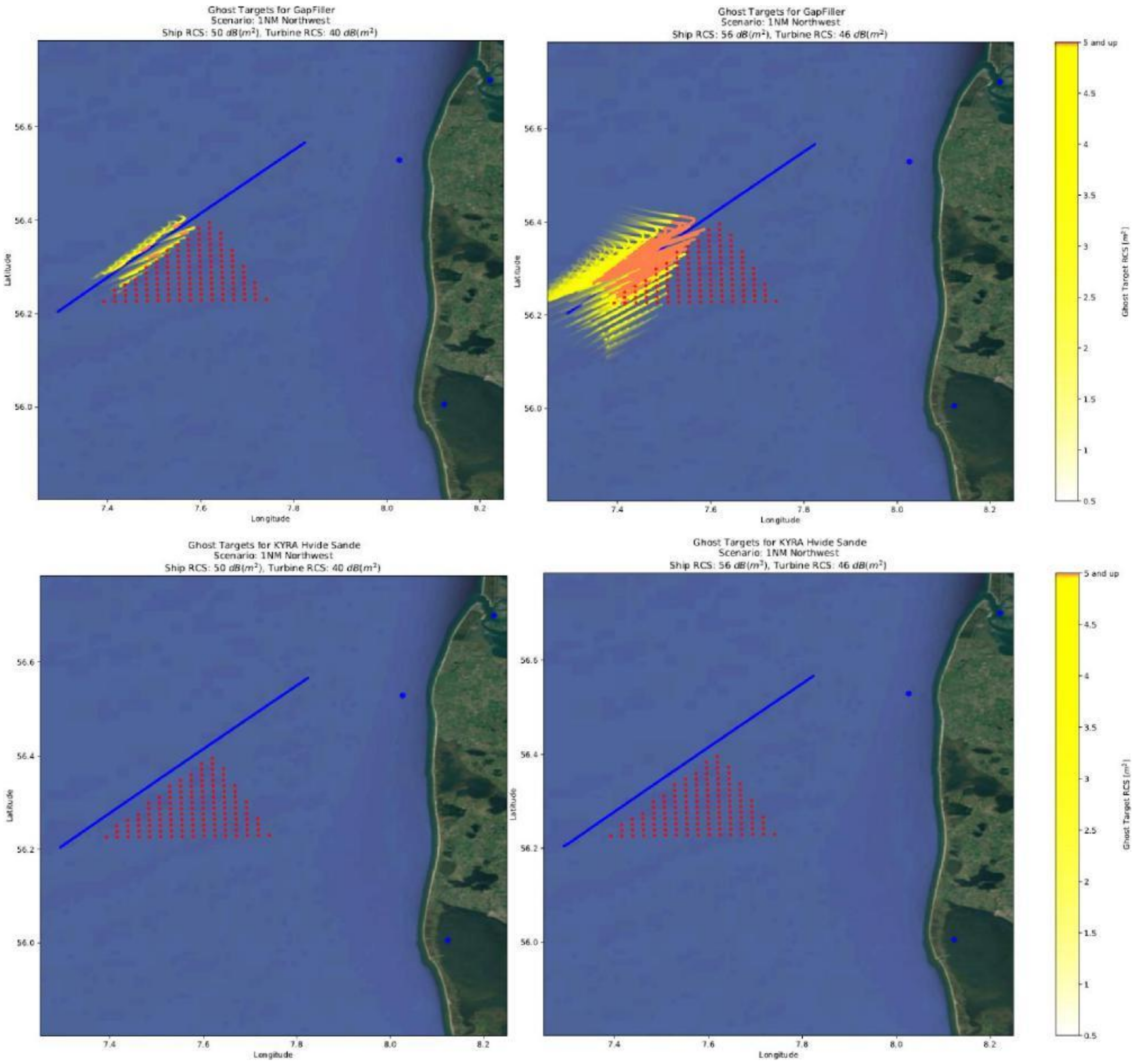

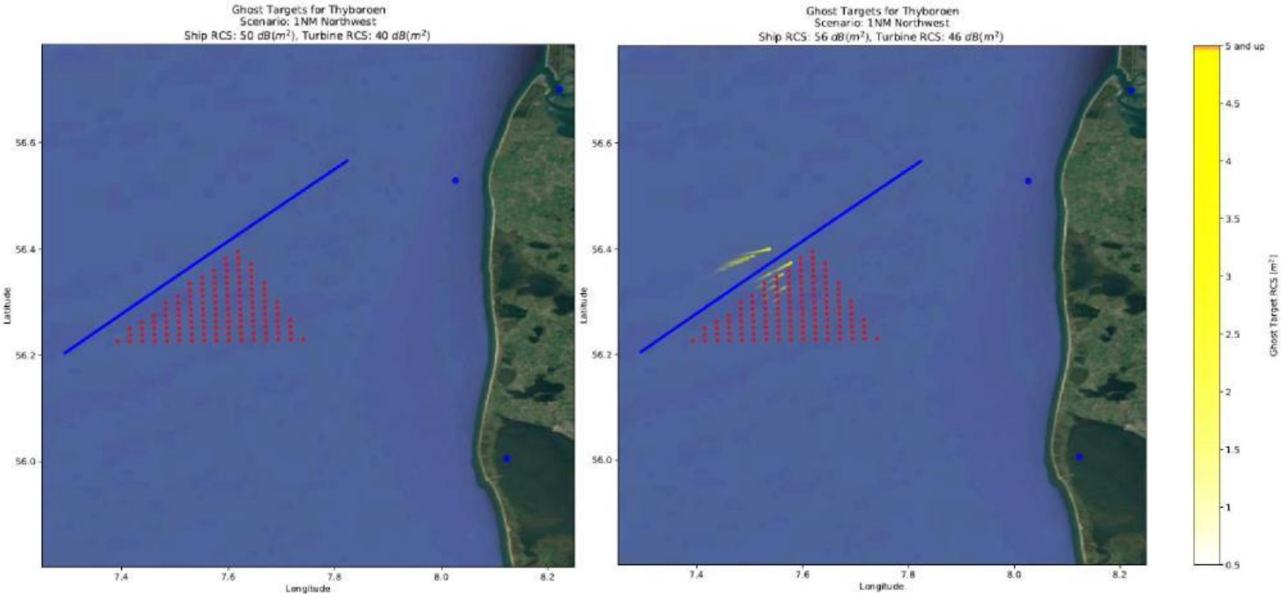

Figure 40 Calculation of ghost targets originating from large vessels, southwest bound west of Thor Havmøllepark 1 Nautical mile out from the windfarm area. Radar sites from top to bottom are: Gapfiller Radar at Vesterhav Nord, KYRA Hvide Sande, and KYRA Thyborøn. Representative (left) and Worst case (right)

Likelihood of ghosts originating from north bound traffic east of Thor Havmøllepark
1 Nautical mile out from the windfarm area

Below images indicate that here is a low likelihood of ghosts originating from ships travelling east of the Thor Havmøllepark area. The ghosts are weak (< 5 m2 in RCS) and are therefore unlikely to cause significant false tracks or significant disturbance on operational displays.

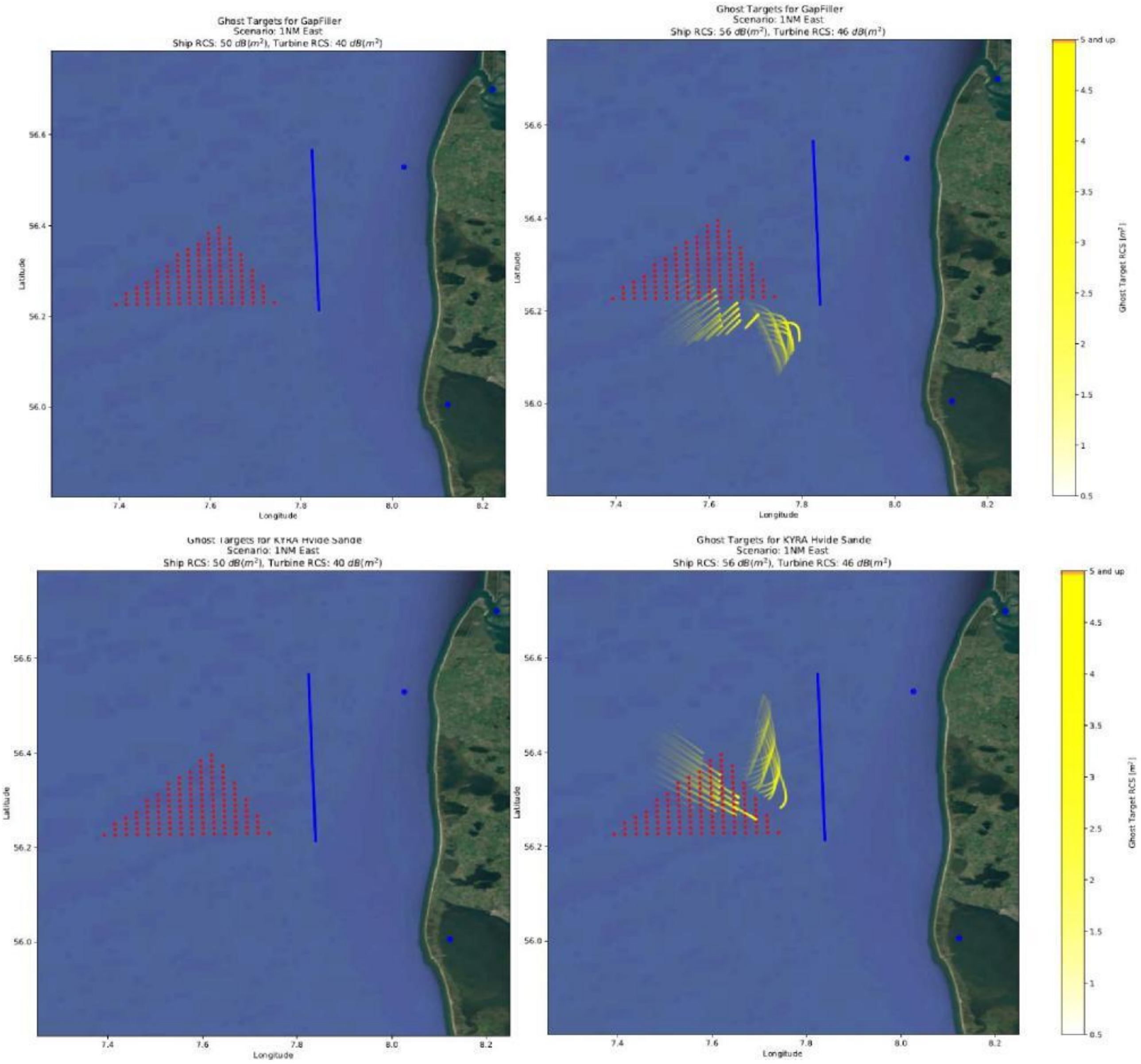

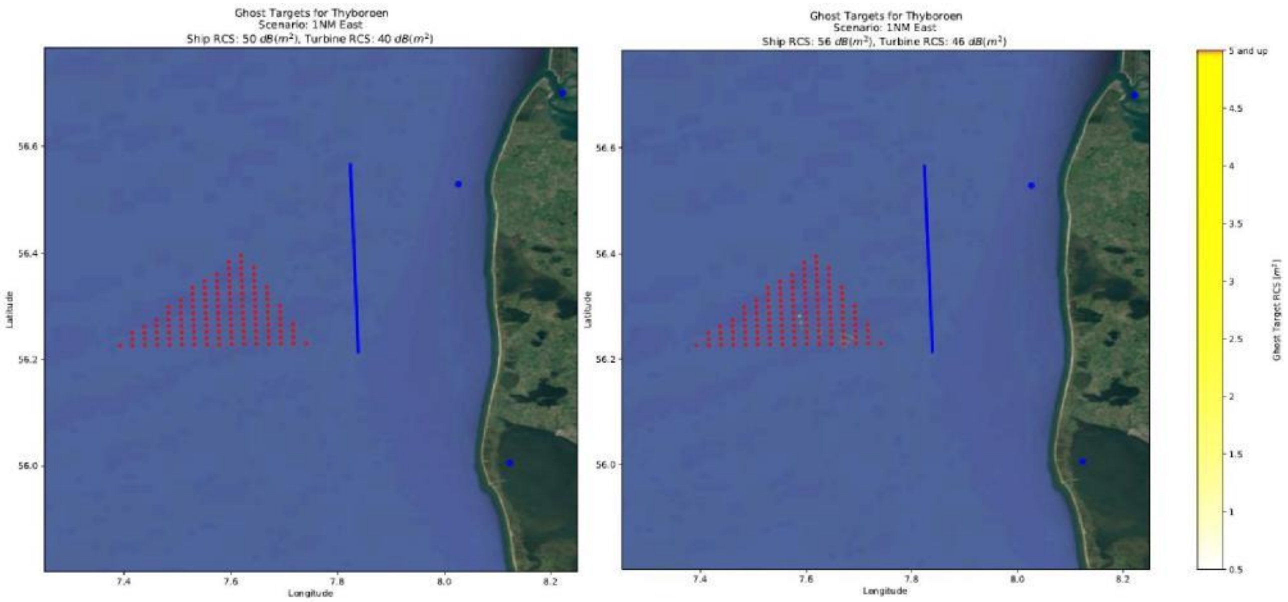

Figure 41 Calculation of ghost targets originating from large vessels, north bound east of Thor Havmøllepark 1 Nautical mile out from the windfarm area. Radar sites from top to bottom are: Gapfiller Radar at Vesterhav Nord, KYRA Hvide Sande, and KYRA Thyborøn. Representative (left) and Worst case (right)

Likelihood of ghosts originating from east bound traffic south of Thor Havmøllepark 1 Nautical mile out from the windfarm area

Below images indicate that there is high likelihood of ghosts originating from ships travelling south of Thor Havmøllepark. The ghosts are prominent (> 5 m2 in RCS) and are therefore likely to cause significant false tracks or significant disturbance on operational displays.

Due to the large distance, KYRA Thyborøn is calculated to not produce prominent ghost echoes.

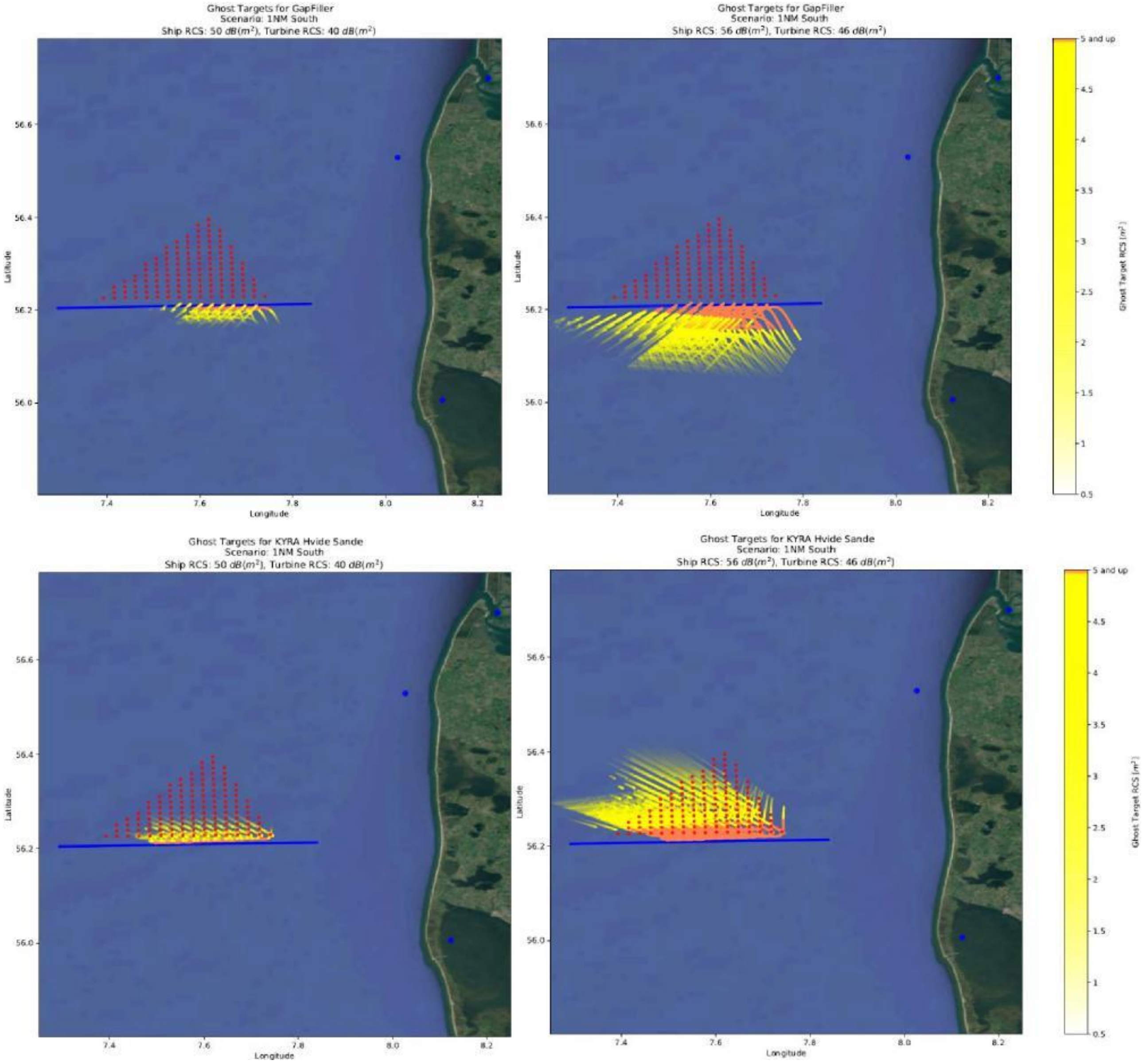

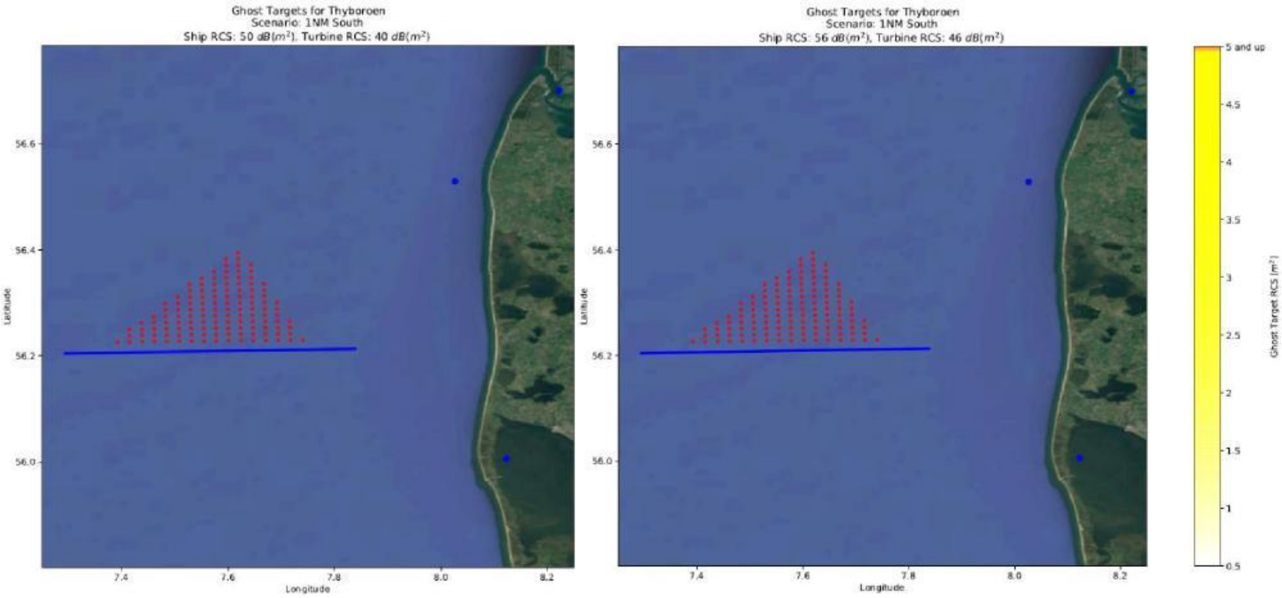

Figure 42 Calculation of ghost targets originating from large vessels, east bound south of Thor Havmøllepark 1 Nautical mile out from the windfarm area. Radar sites from top to bottom are: Gapfiller Radar at Vesterhav Nord, KYRA Hvide Sande, and KYRA Thyborøn. Representative (left) and Worst case (right)

Likelihood of ghosts originating from southwest bound traffic West of Thor Havmøllepark 2 Nautical miles out from the windfarm area

Below images indicate that there is a high likelihood of ghosts originating from ships travelling Northwest of Thor Havmøllepark.

Possible ghost echoes are calculated to be weak and diffuse for smaller ships, however in the worst case, ghost echoes of more than 5 m^2 in RCS are seen and therefore are likely to cause false tracks or to be displayed on operational displays.

Due to the large distance, KYRA Hvide Sande is calculated to not produce prominent ghost echoes.

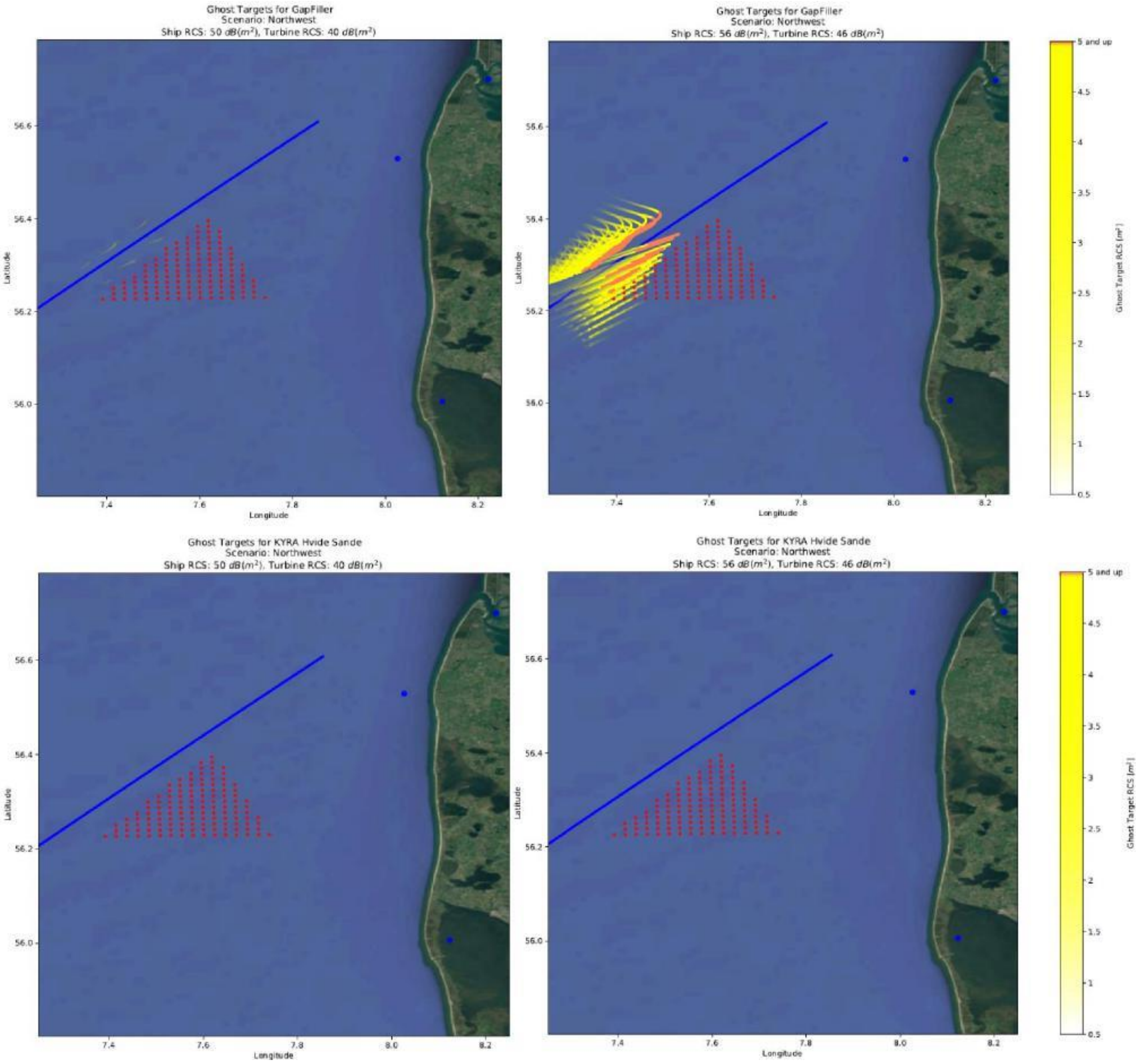

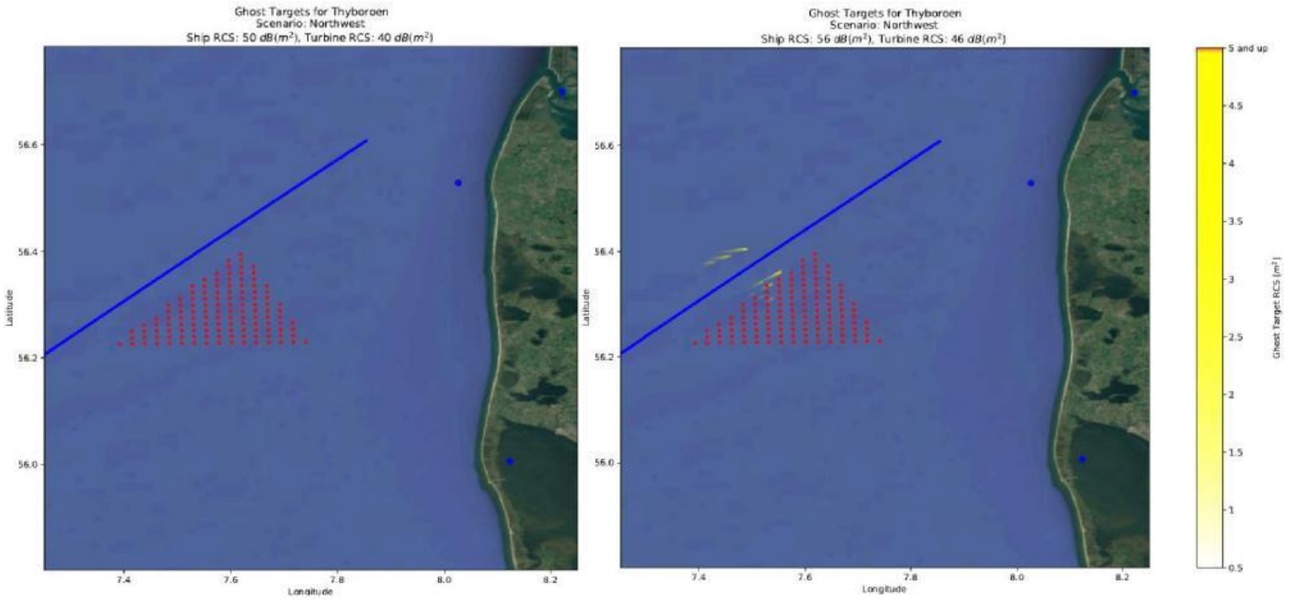

Figure 43 Calculation of ghost targets originating from large vessels, southwest bound north of Thor Havmøllepark 2 Nautical miles out from the windfarm area. Radar sites from top to bottom are: Gapfiller Radar at Vesterhav Nord, KYRA Hvide Sande, and KYRA Thyborøn. Representative (left) and Worst case (right)

Likelihood of ghosts originating from north bound traffic east of Thor Havmøllepark
2 Nautical miles out from the windfarm area

Below images indicate that here is a low likelihood of ghosts originating from ships travelling east of Thor Havmøllepark. Possible ghost echoes are calculated to be weak and diffuse and therefore are likely to cause false tracks or to be displayed on operational displays.

It is possible that the vessel traffic will move closer to the turbines if such a large part of Thor Havmøllepark is unfilled.

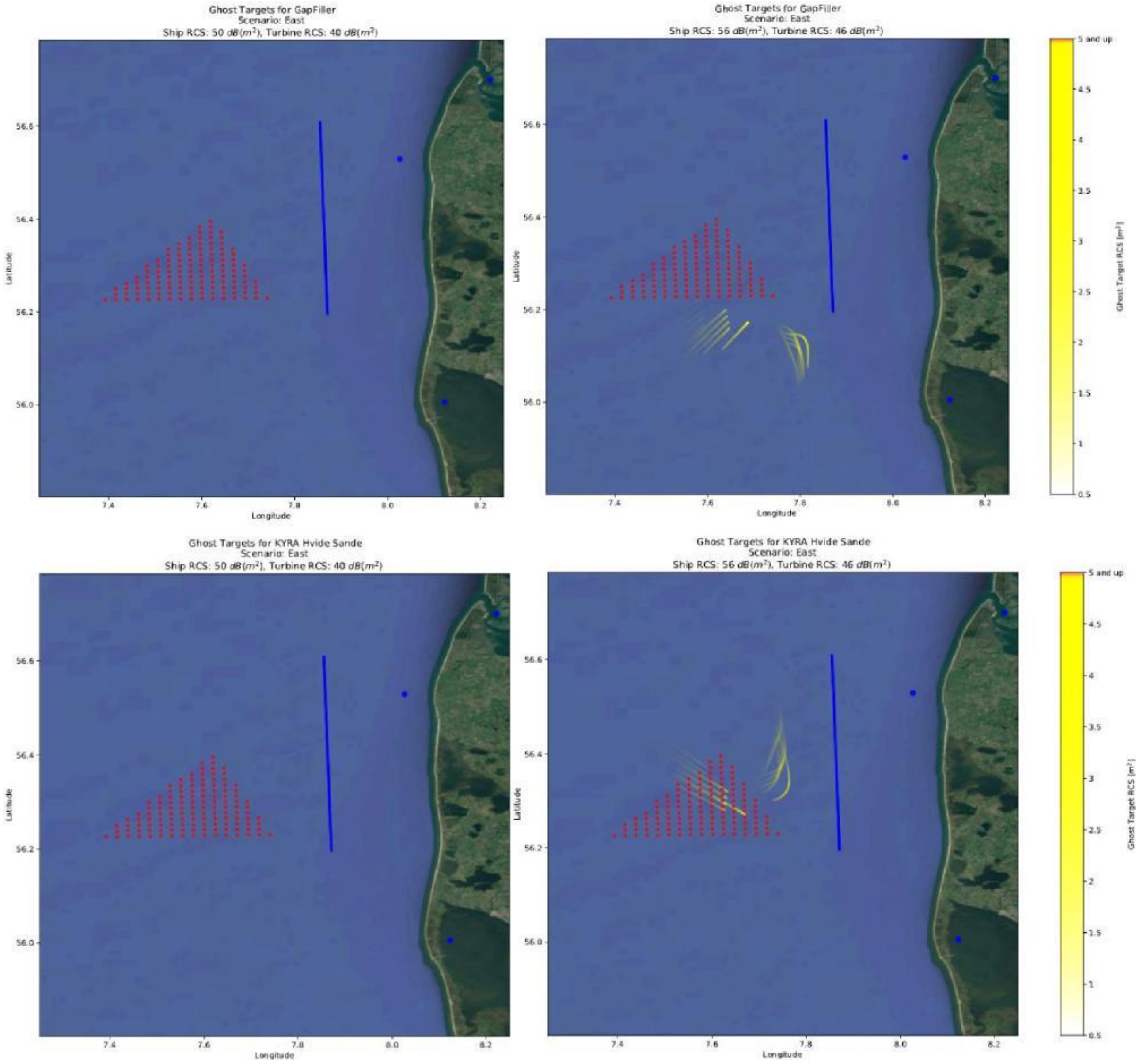

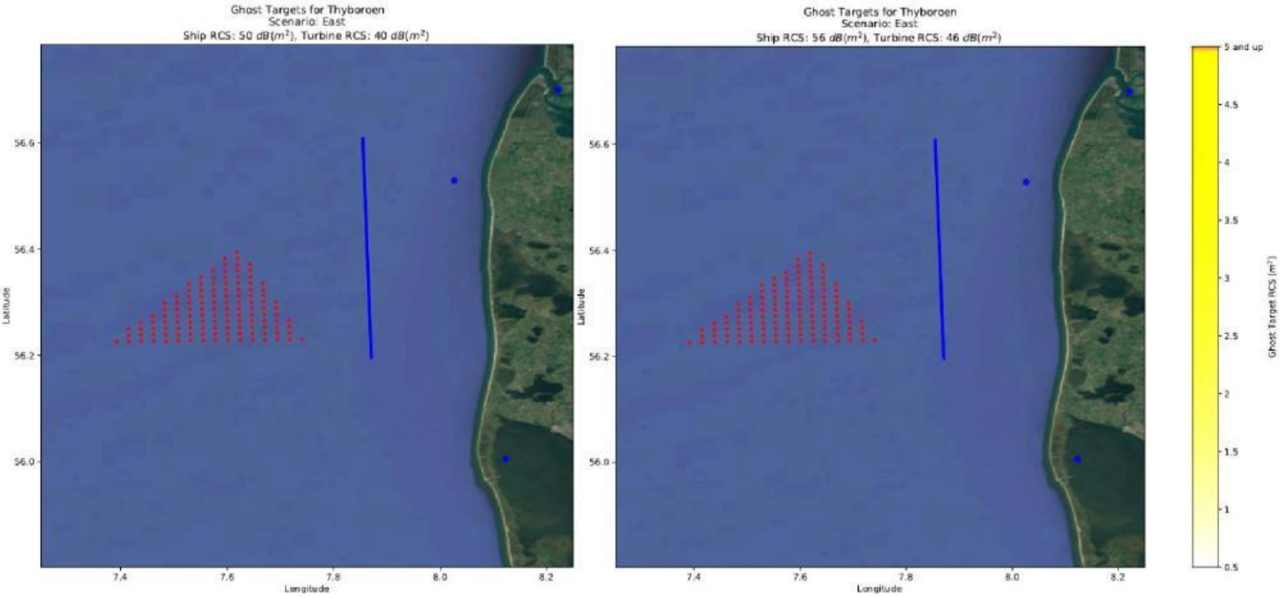

Figure 44 Calculation of ghost targets originating from large vessels, north bound east of Thor Havmøllepark 2 Nautical miles out from the windfarm area. Radar sites from top to bottom are: Gapfiller Radar at Vesterhav Nord, KYRA Hvide Sande, and KYRA Thyborøn. Representative (left) and Worst case (right)

Likelihood of ghosts originating from east bound traffic south of Thor Havmøllepark 2 Nautical miles out from the windfarm area

Below images indicate that there is likelihood of ghosts originating from large ships operating south of Thor Havmøllepark. The ghosts are weak and diffuse for the smaller ships, however in the worst case prominent ghost echoes can be seen (> 5 m2 in RCS) and can therefore cause significant false tracks or significant disturbance on operational displays.

Due to the large distance from the radar to the turbines, KYRA Thyborøn does not indicate prominent ghost echoes.

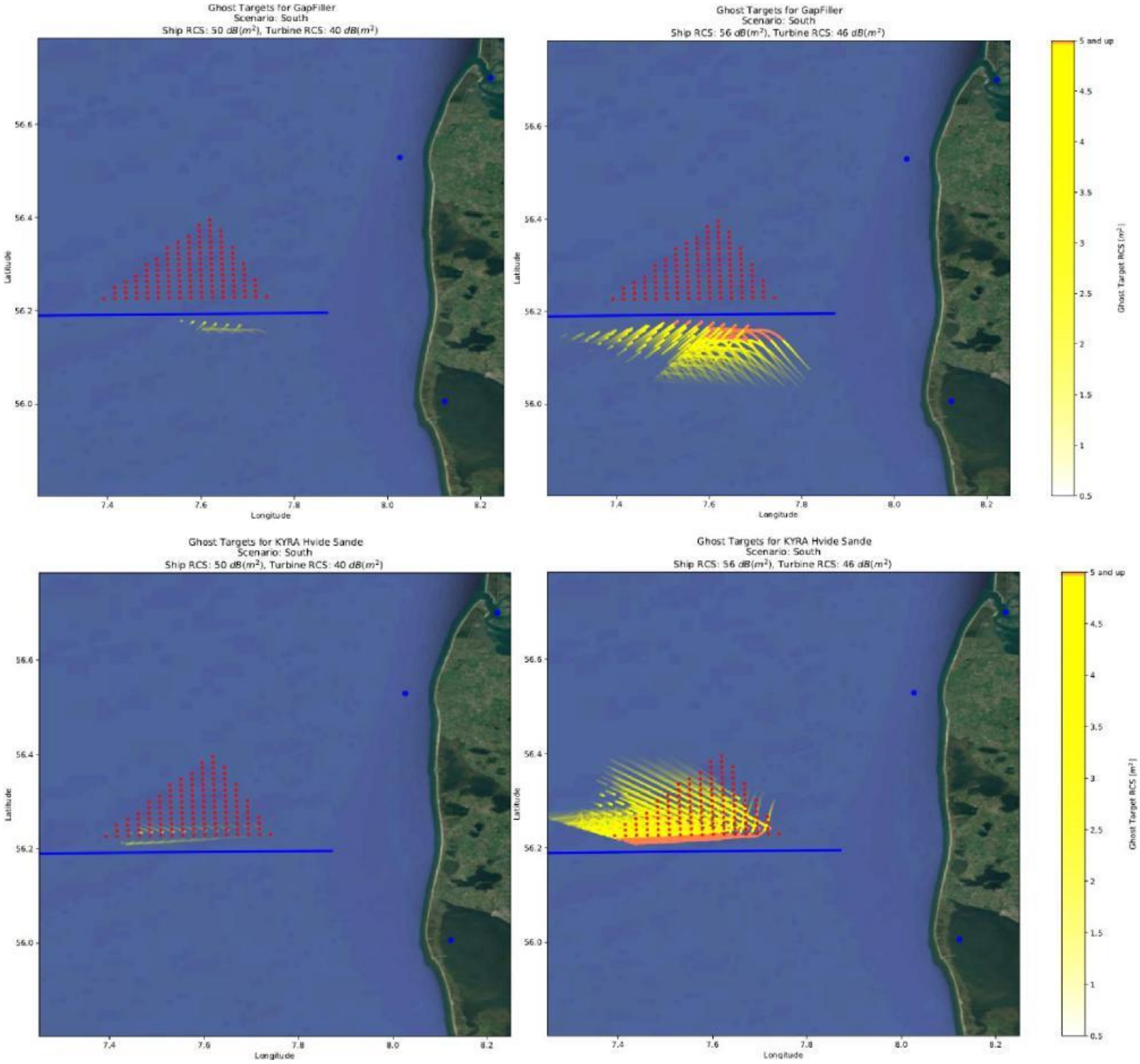

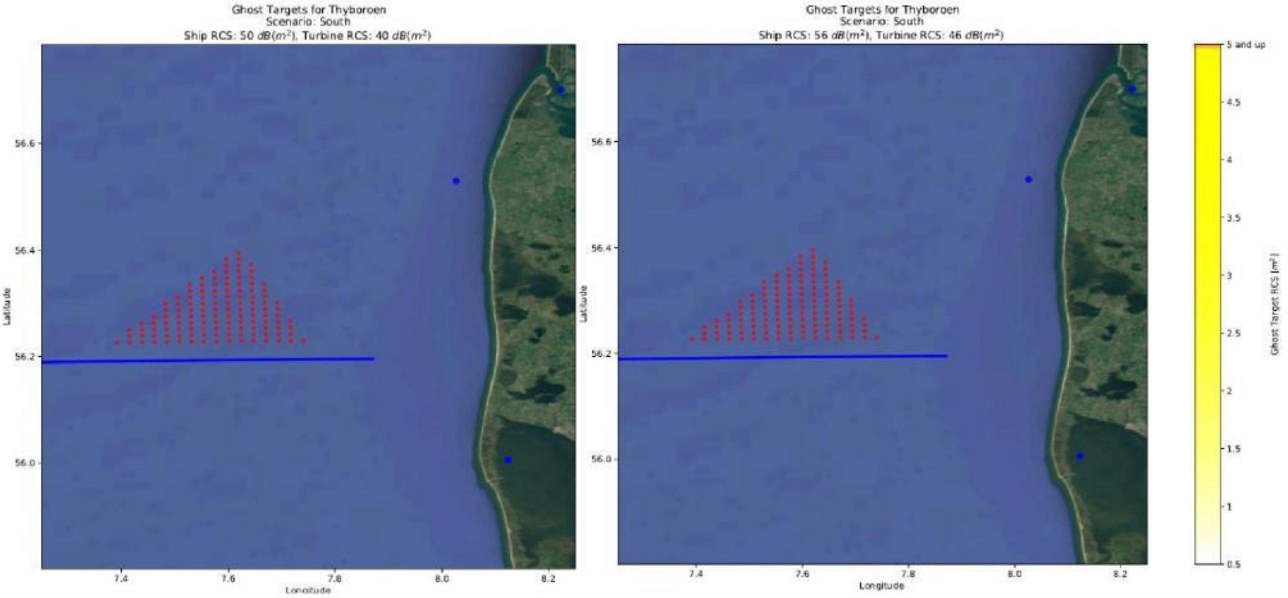

Figure 45 Calculation of ghost targets originating from large vessels, east bound south of Thor Havmøllepark 2 Nautical miles out from the windfarm area. Radar sites from top to bottom are: Gapfiller Radar at Vesterhav Nord, KYRA Hvide Sande, and KYRA Thyborøn. Representative (left) and Worst case (right)

7.1.1 Scenario 3 15MW Windmills

Likelihood of ghosts originating from southwest bound traffic West of Thor Havmøllepark 1 Nautical mile out from the windfarm area

Below images indicate that there is a high likelihood of ghosts originating from ships travelling Northwest of Thor Havmøllepark.

The ghosts may be pronounced (> 5 m2 in RCS) and are therefore likely to cause significant false tracks or significant disturbance on operational displays.

Due to the large distance, KYRA Hvide Sande is calculated to not produce prominent ghost echoes.

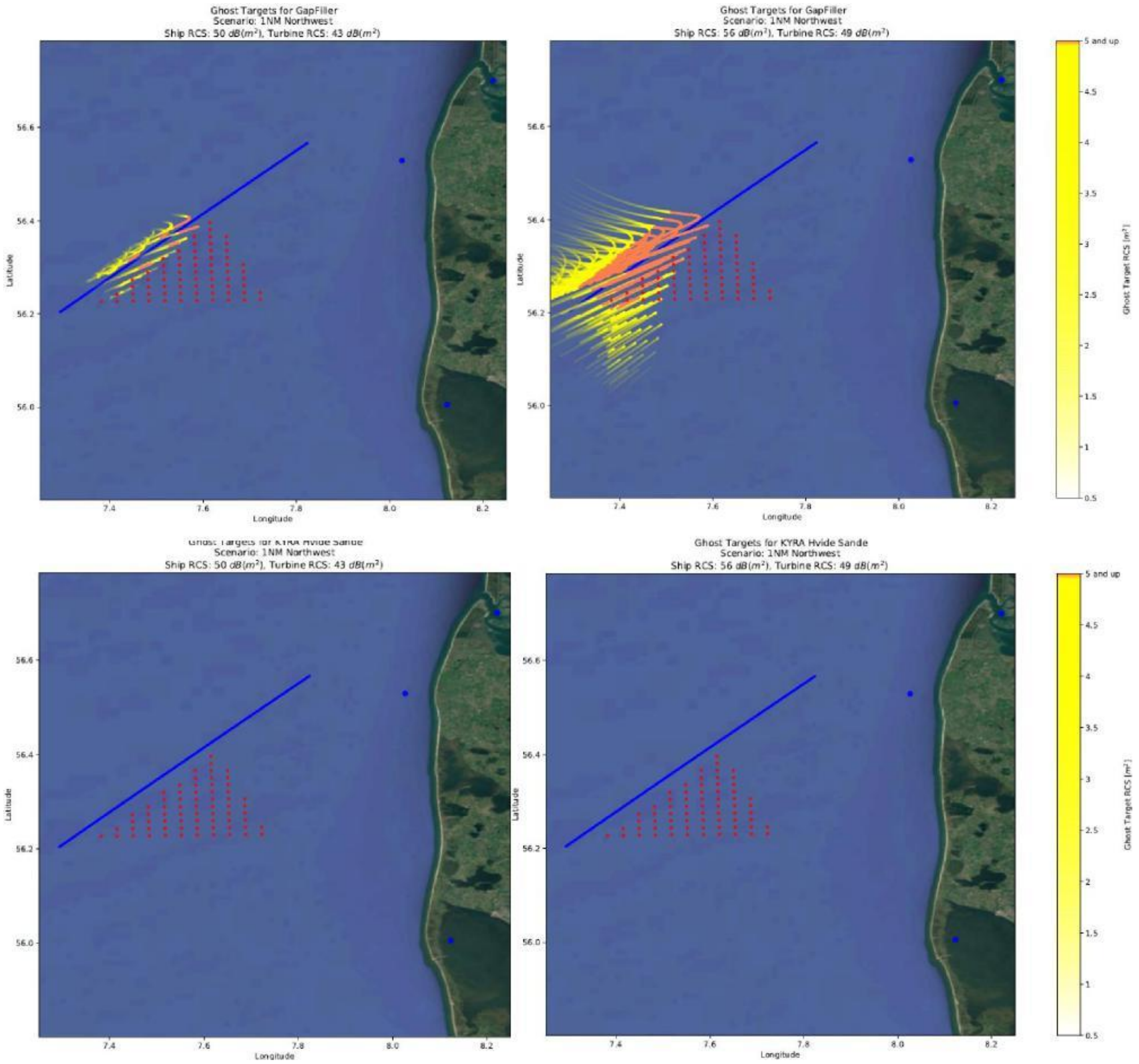

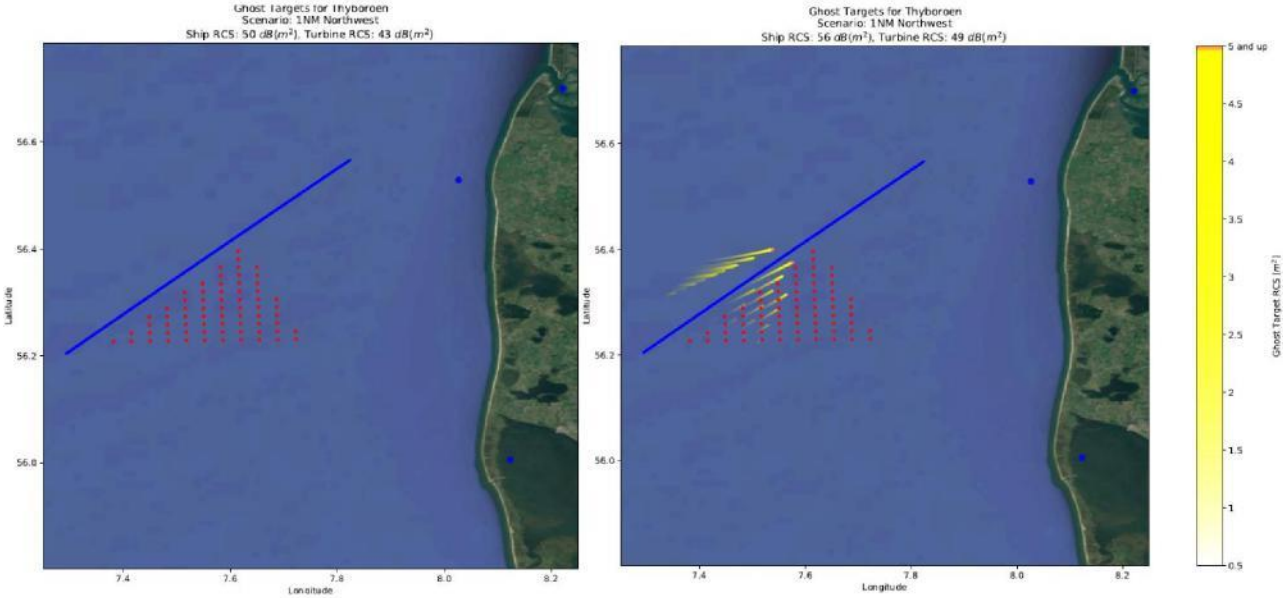

Figure 46 Calculation of ghost targets originating from large vessels, southwest bound west of Thor Havmøllepark 1 Nautical mile out from the windfarm area. Radar sites from top to bottom are: Gapfiller Radar at Vesterhav Nord, KYRA Hvide Sande, and KYRA Thyborøn. Representative (left) and Worst case (right)

Likelihood of ghosts originating from north bound traffic east of Thor Havmøllepark 1 Nautical mile out from the windfarm area

Below images indicate that here is a low likelihood of ghosts originating from ships travelling east of Thor Havmøllepark. Possible ghost echoes are calculated to be weak and diffuse and therefore are likely to cause false tracks or to be displayed on operational displays.

It is possible that the vessel traffic will move closer to the turbines if such a large part of Thor Havmøllepark is unfilled.

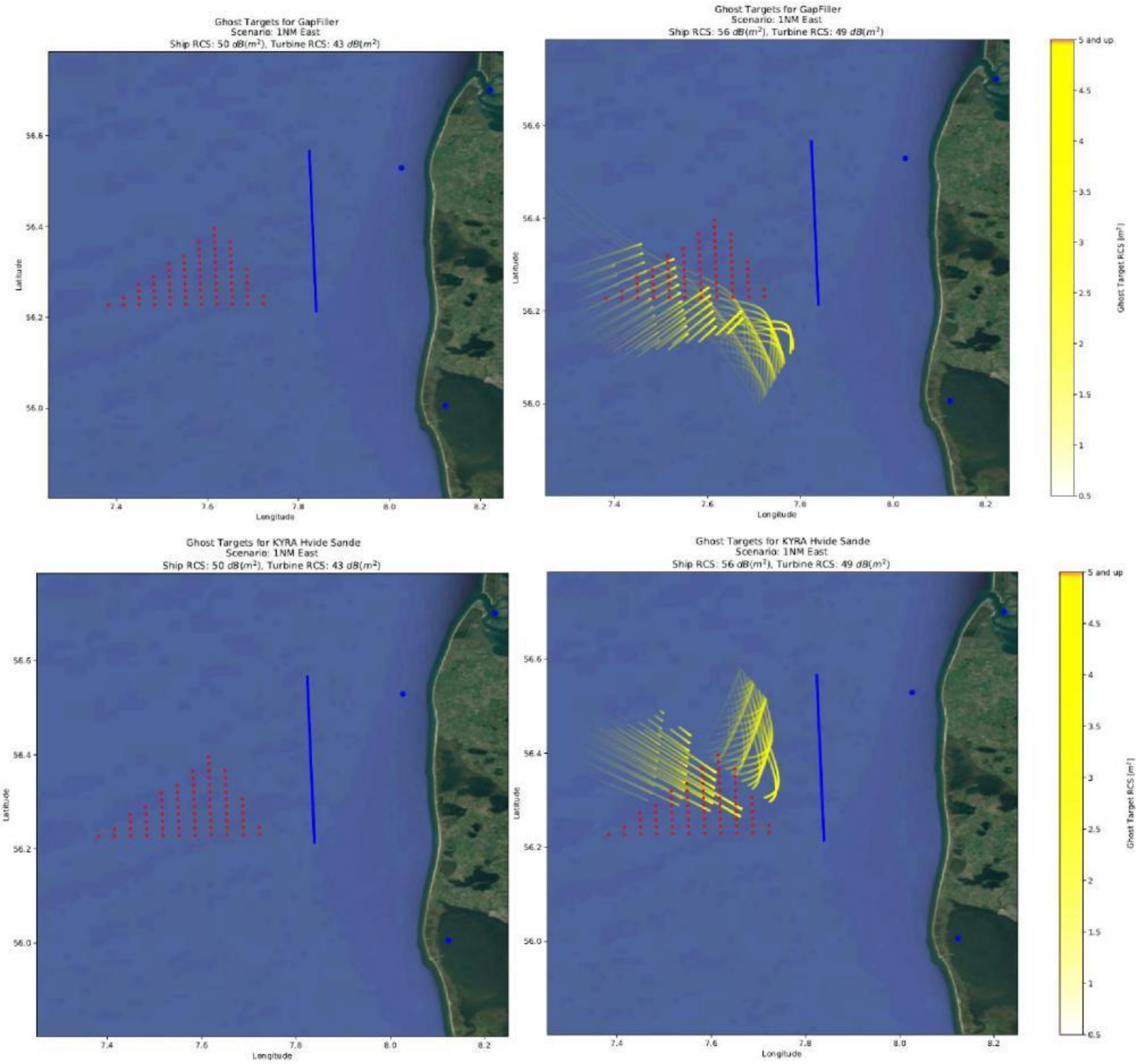

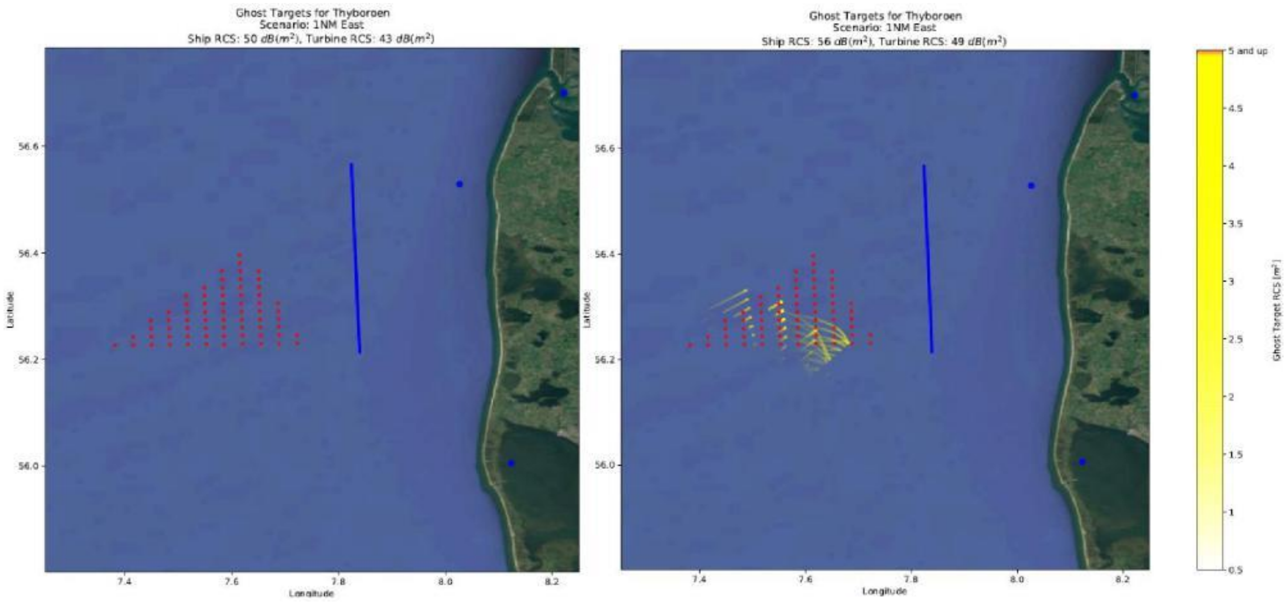

Figure 47 Calculation of ghost targets originating from large vessels, north bound east of Thor Havmøllepark 1 Nautical mile out from the windfarm area. Radar sites from top to bottom are: Gapfiller Radar at Vesterhav Nord, KYRA Hvide Sande, and KYRA Thyborøn. Representative (left) and Worst case (right)

Likelihood of ghosts originating from east bound traffic south of Thor Havmøllepark 1 Nautical mile out from the windfarm area

Below images indicate that here is a high likelihood of ghosts originating from ships travelling south of Thor Havmøllepark. The ghosts may be pronounced (> 5 m2 in RCS) and are thereby likely to cause significant false tracks or significant disturbance on operational displays.

Due to the large distance, KYRA Thyborøn is calculated to not produce prominent ghost echoes.

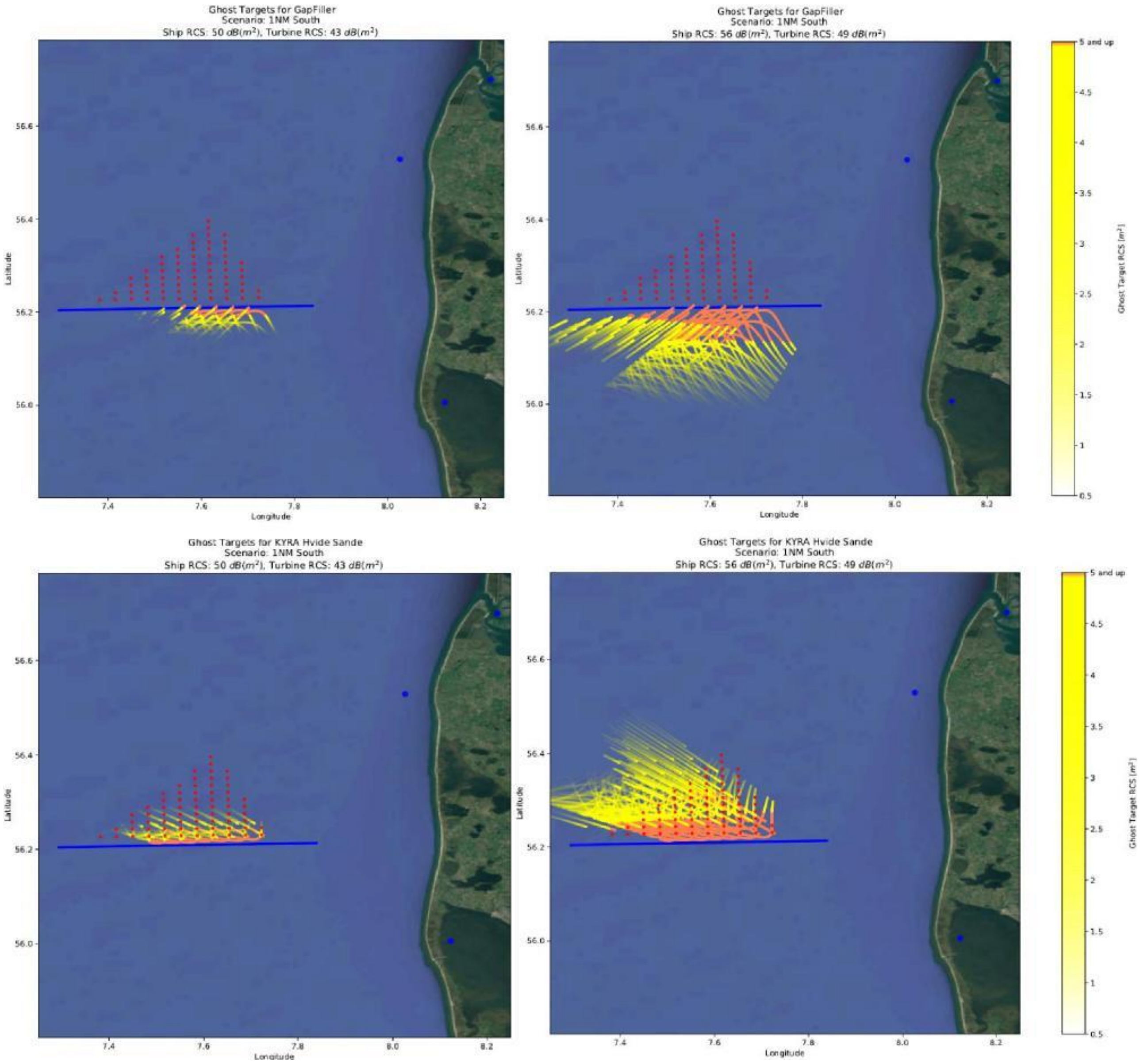

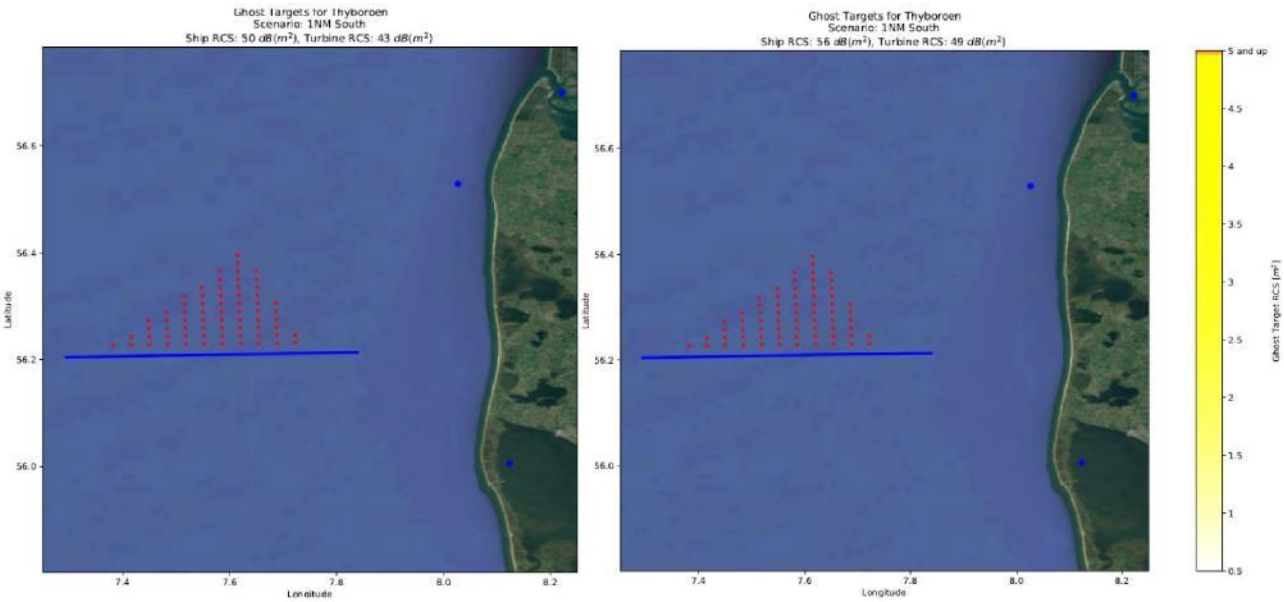

Figure 48 Calculation of ghost targets originating from large vessels, east bound south of Thor Havmøllepark 1 Nautical mile out from the windfarm area. Radar sites from top to bottom are: Gapfiller Radar at Vesterhav Nord, KYRA Hvide Sande, and KYRA Thyborøn. Representative (left) and Worst case (right)

Likelihood of ghosts originating from southwest bound traffic West of Thor Havmøllepark 2 Nautical miles out from the windfarm area

Below images indicate that there is possibility of ghosts originating from ships travelling Northwest of Thor Havmøllepark.

Possible ghost echoes are calculated to be weak and diffuse for smaller ships, however in the worst case, ghost echoes of more than 5 m^2 in RCS are seen and therefore are likely to cause false tracks or to be displayed on operational displays.

Due to the large distance, KYRA Hvide Sande is calculated to not produce prominent ghost echoes.

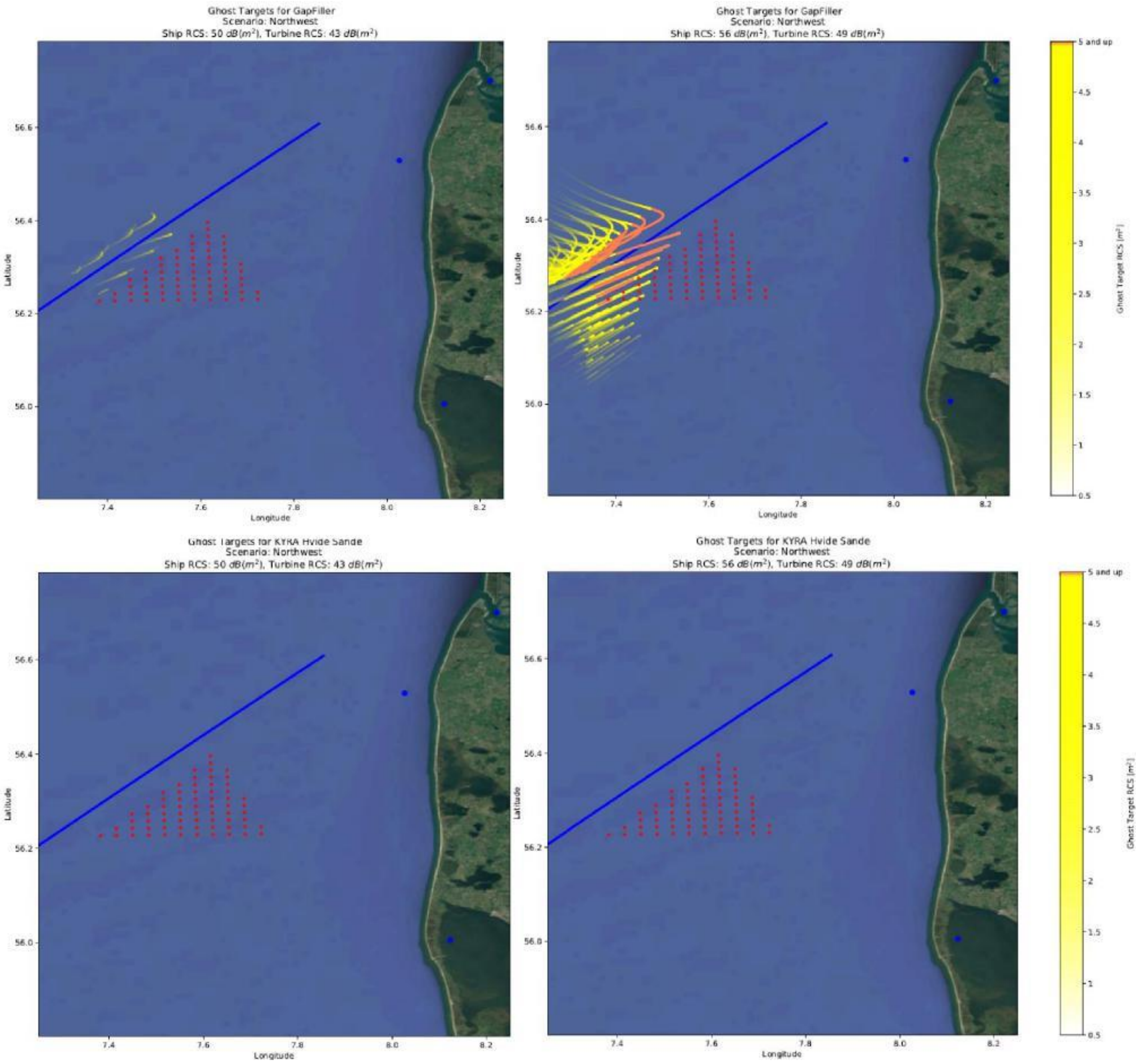

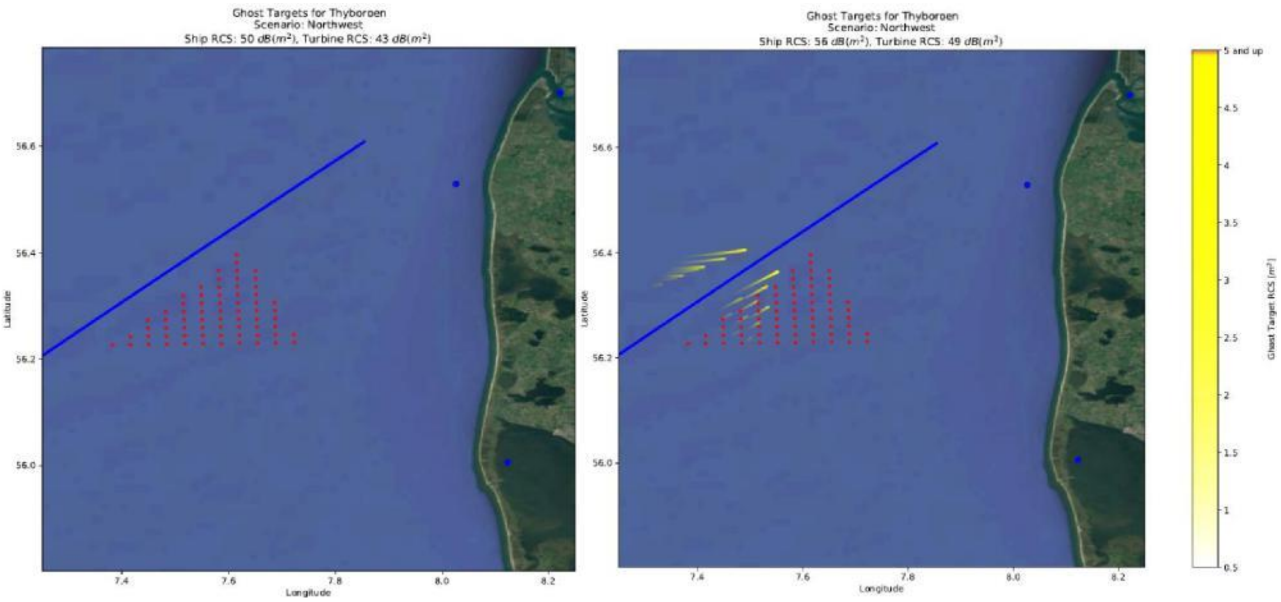

Figure 49 Calculation of ghost targets originating from large vessels, southwest bound north of Thor Havmøllepark 2 Nautical miles out from the windfarm area. Radar sites from top to bottom are: Gapfiller Radar at Vesterhav Nord, KYRA Hvide Sande, and KYRA Thyborøn. Representative (left) and Worst case (right)

Likelihood of ghosts originating from north bound traffic east of Thor Havmøllepark
2 Nautical miles out from the windfarm area

Below images indicate that here is a low likelihood of ghosts originating from ships travelling east of Thor Havmøllepark. Possible ghost echoes are calculated to be weak and diffuse (<5 m^2 in RCS) and therefore are unlikely to cause false tracks or to be displayed on operational displays.

It is possible that the vessel traffic will move closer to the turbines if such a large part of Thor Havmøllepark is unfilled. Especially smaller ships and fishing vessels.

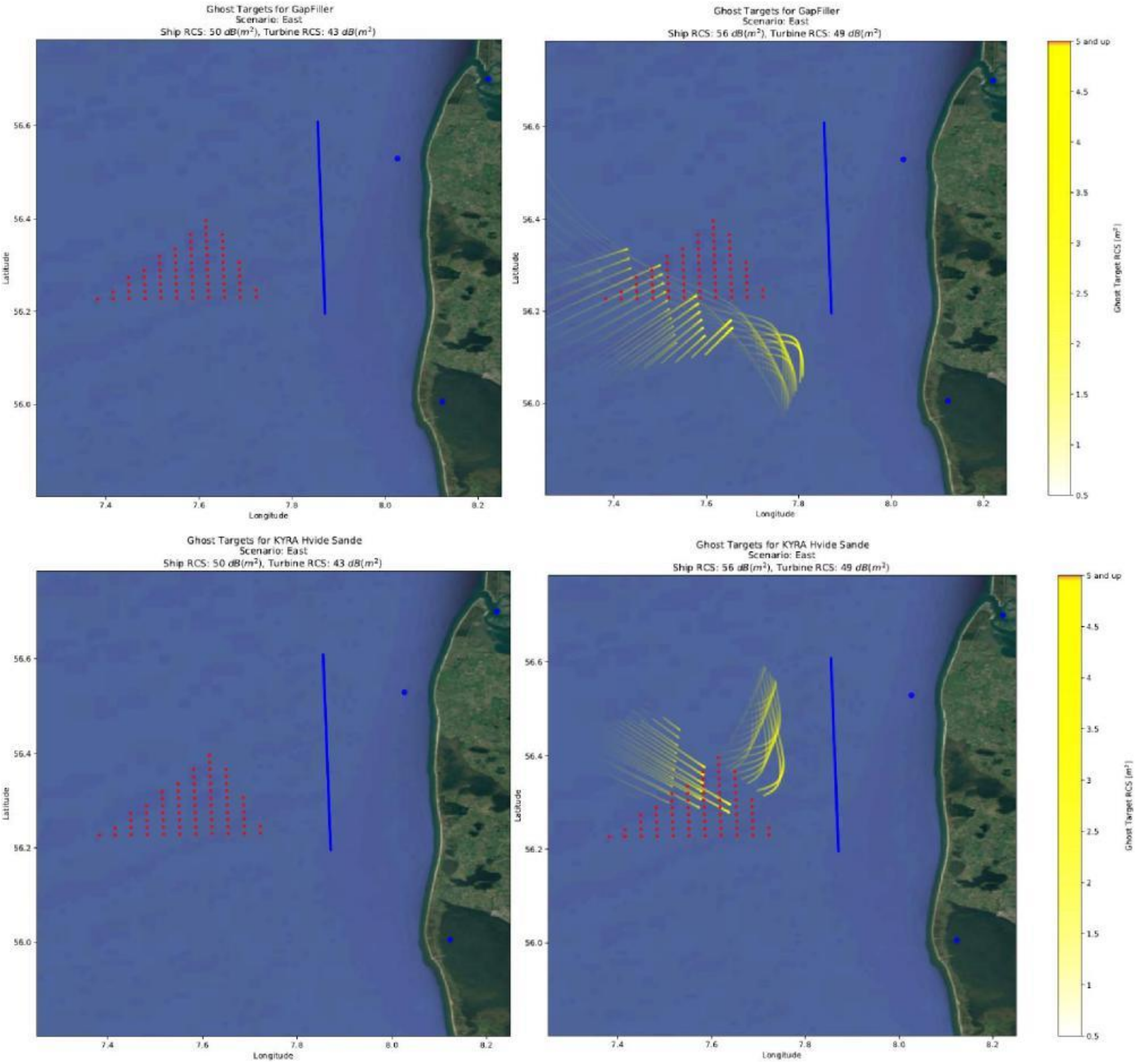

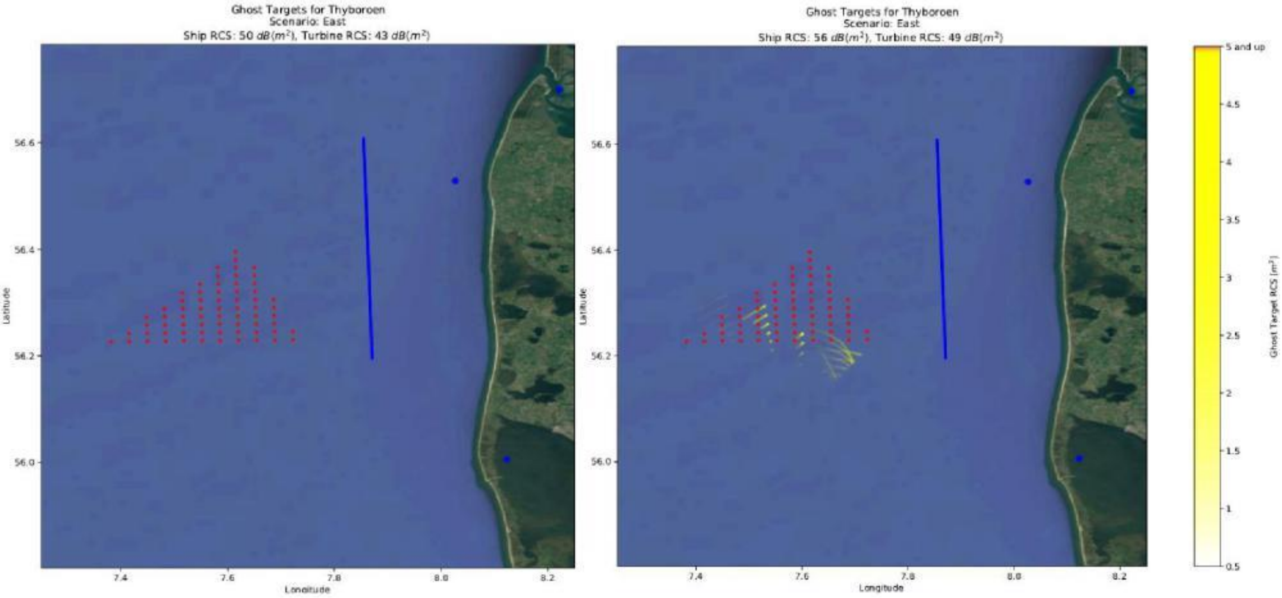

Figure 50 Calculation of ghost targets originating from large vessels, north bound east of Thor Havmøllepark 2 Nautical miles out from the windfarm area. Radar sites from top to bottom are: Gapfiller Radar at Vesterhav Nord, KYRA Hvide Sande, and KYRA Thyborøn. Representative (left) and Worst case (right)

Likelihood of ghosts originating from east bound traffic south of Thor Havmøllepark 2 Nautical miles out from the windfarm area

Below images indicate that there is high likelihood of ghosts originating from large ships operating south of Thor Havmøllepark. The ghosts are in the worst case be prominent (> 5 m2 in RCS) and are therefore likely to cause significant false tracks or significant disturbance on operational displays.

KYRA Thyborøn does not produce prominent ghost echoes due to the large distance.

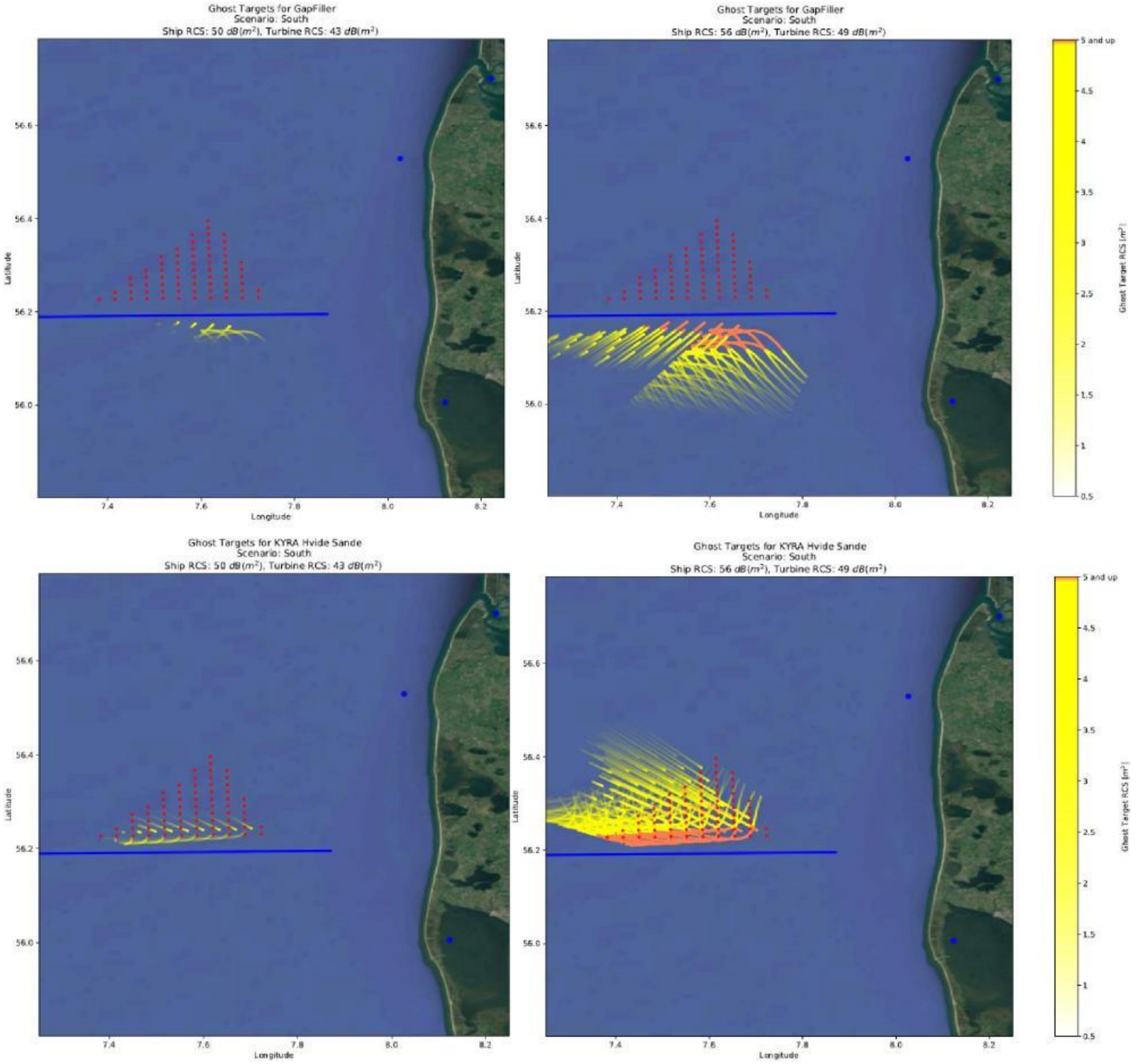

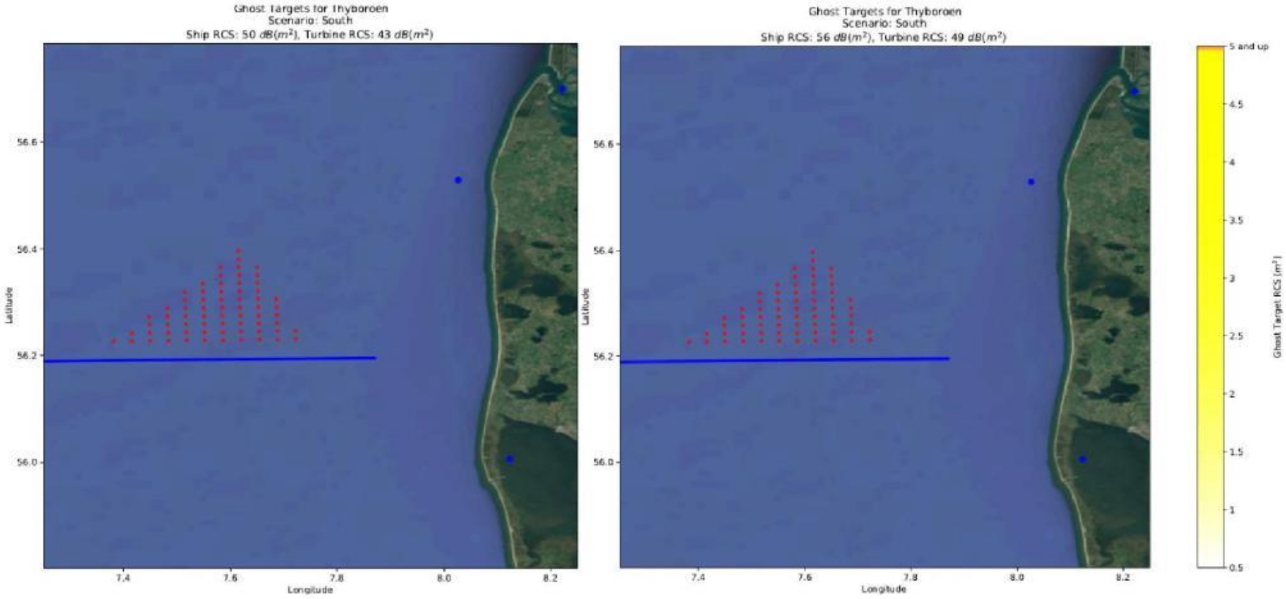

Figure 51 Calculation of ghost targets originating from large vessels, east bound south of Thor Havmøllepark 2 Nautical miles out from the windfarm area. Radar sites from top to bottom are: Gapfiller Radar at Vesterhav Nord, KYRA Hvide Sande, and KYRA Thyborøn. Representative (left) and Worst case (right)

7.1.2 Scenario 4 8MW Windmills

Likelihood of ghosts originating from southwest bound traffic West of Thor Havmøllepark 1 Nautical mile out from the windfarm area

Below images indicate that there is a high likelihood of ghosts originating from ships travelling Northwest of Thor Havmøllepark.

The ghosts may be pronounced (> 5 m2 in RCS) and are therefore likely to cause significant false tracks or significant disturbance on operational displays.

Due to the large distance, KYRA Hvide Sande is estimated to not produce prominent ghost echoes.

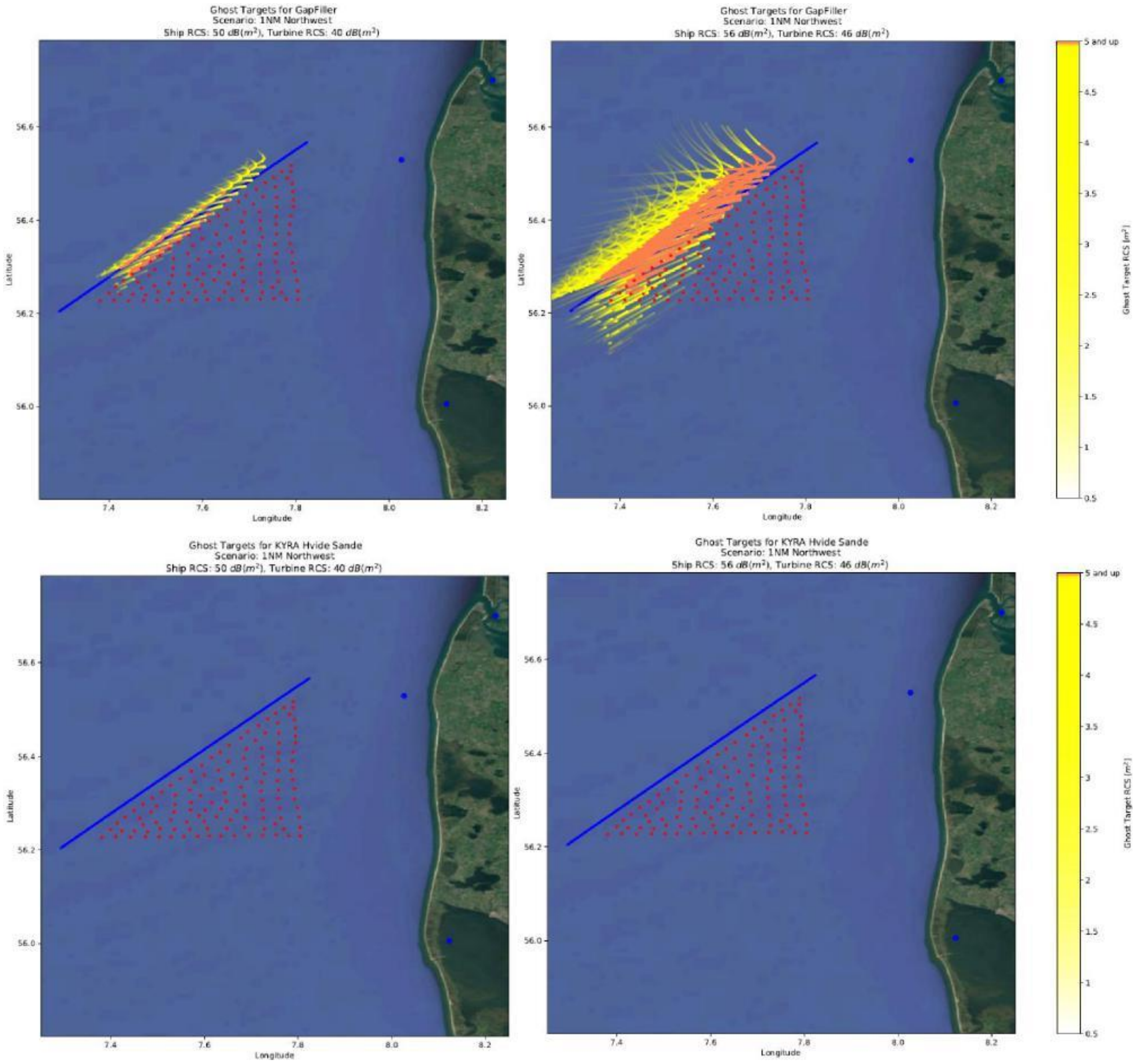

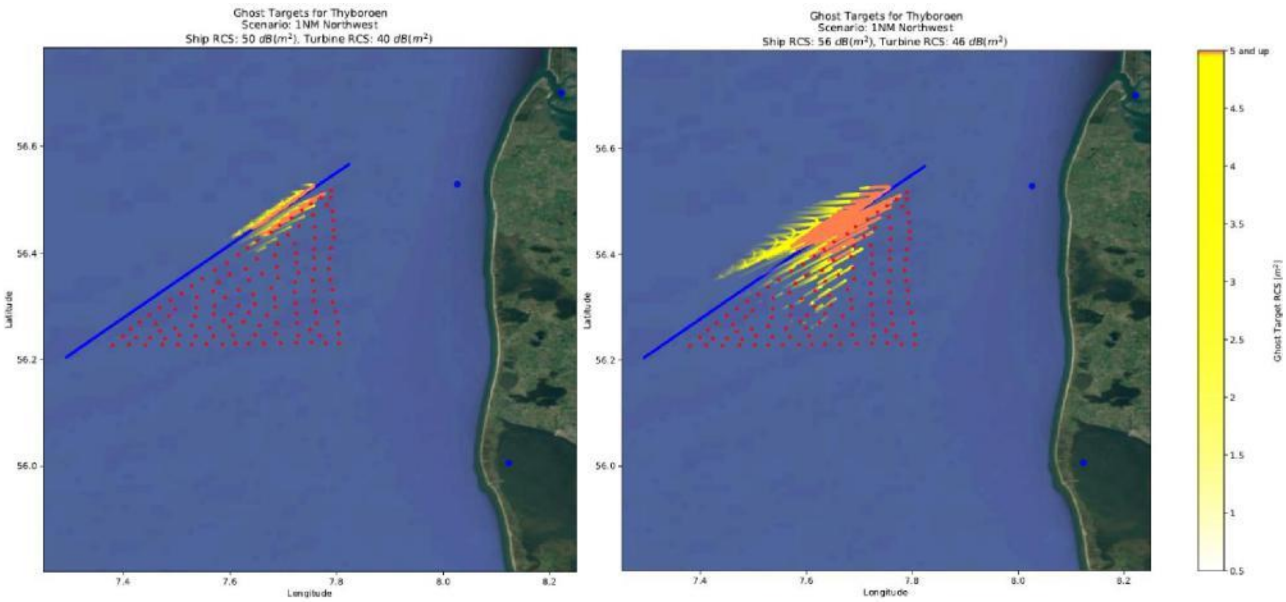

Figure 52 Calculation of ghost targets originating from large vessels, southwest bound west of Thor Havmøllepark 1 Nautical mile out from the windfarm area. Radar sites from top to bottom are: Gapfiller Radar at Vesterhav Nord, KYRA Hvide Sande, and KYRA Thyborøn. Representative (left) and Worst case (right)

Likelihood of ghosts originating from north bound traffic east of Thor Havmøllepark
1 Nautical mile out from the windfarm area

Below images indicate that here is a high likelihood of ghosts originating from ships travelling east of the Thor Havmøllepark area. The ghosts are prominent (> 5 m2 in RCS) and are therefore likely to cause significant false tracks or significant disturbance on operational displays.

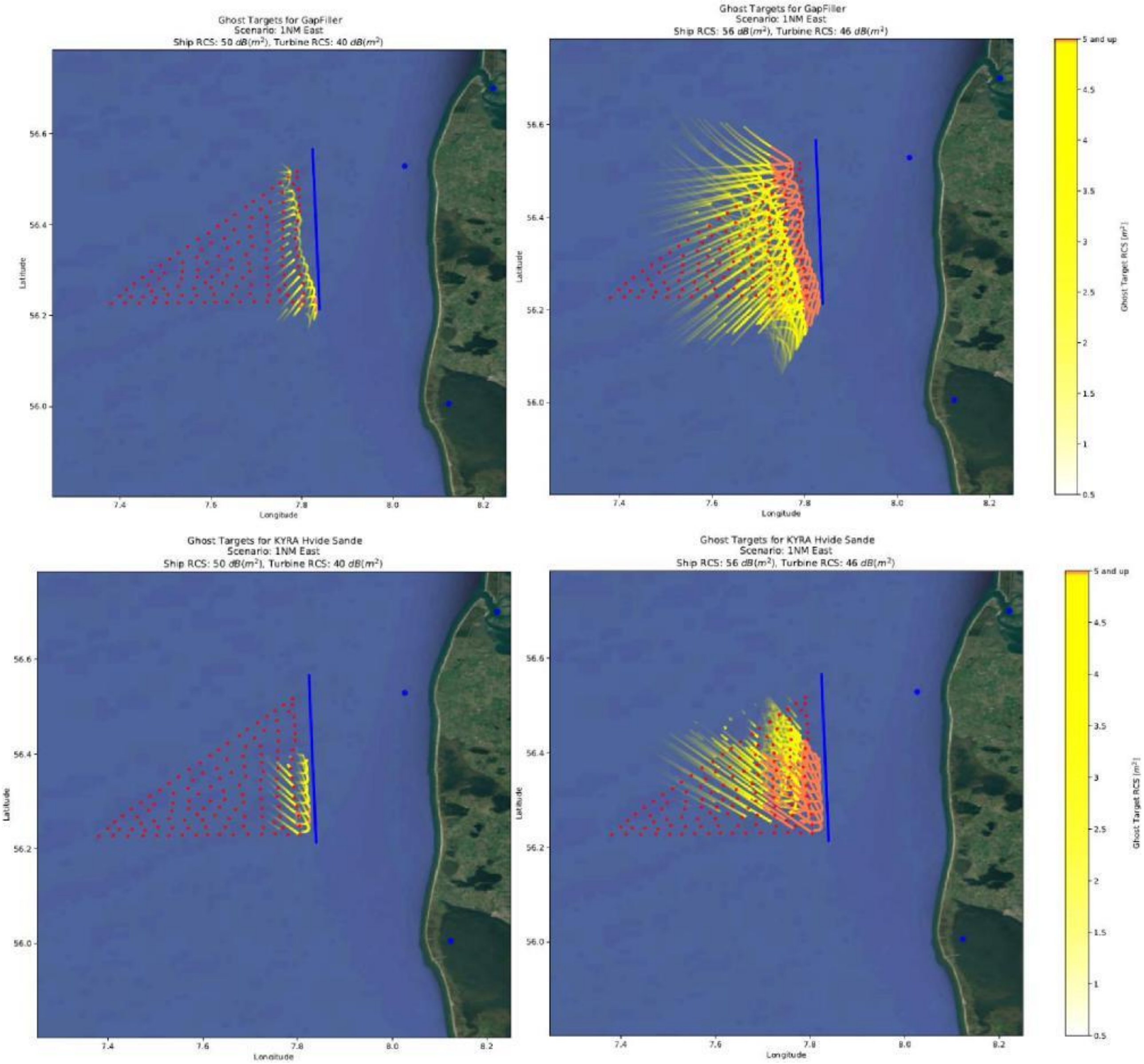

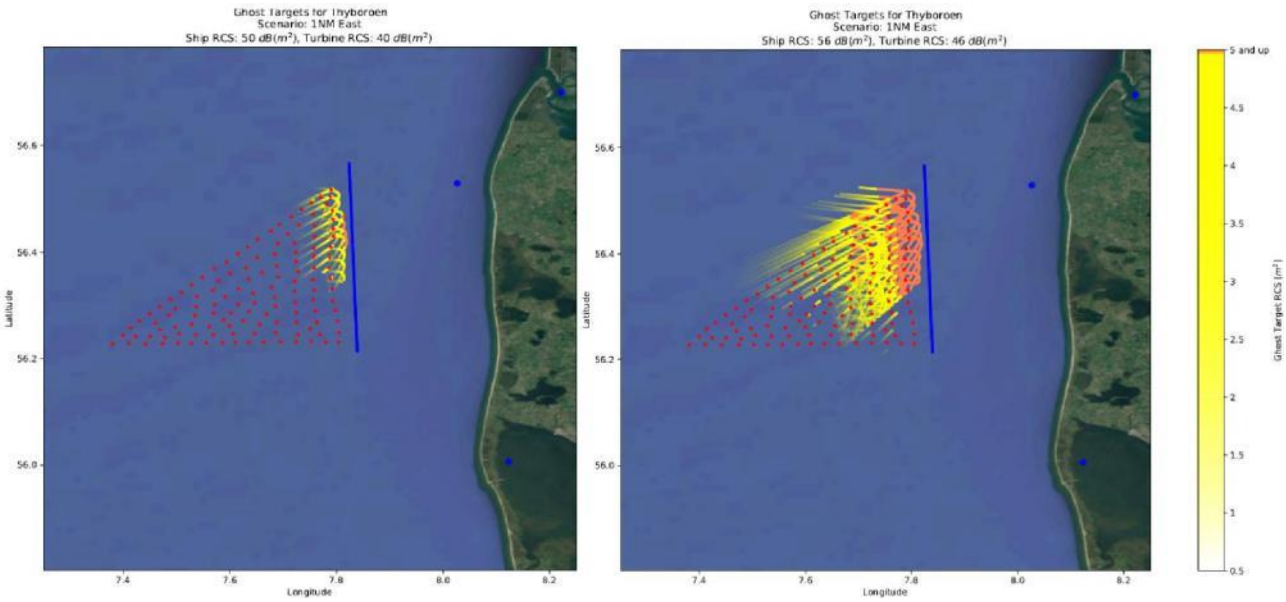

Figure 53 Calculation of ghost targets originating from large vessels, north bound east of Thor Havmøllepark 1 Nautical mile out from the windfarm area. Radar sites from top to bottom are: Gapfiller Radar at Vesterhav Nord, KYRA Hvide Sande, and KYRA Thyborøn. Representative (left) and Worst case (right)

Likelihood of ghosts originating from east bound traffic south of Thor Havmøllepark 1 Nautical mile out from the windfarm area

Below images indicate that there is high likelihood of ghosts originating from ships travelling south of Thor Havmøllepark. The ghosts are prominent (> 5 m2 in RCS) and are therefore likely to cause significant false tracks or significant disturbance on operational displays.

Due to the large distance, KYRA Thyborøn is calculated to not produce prominent ghost echoes.

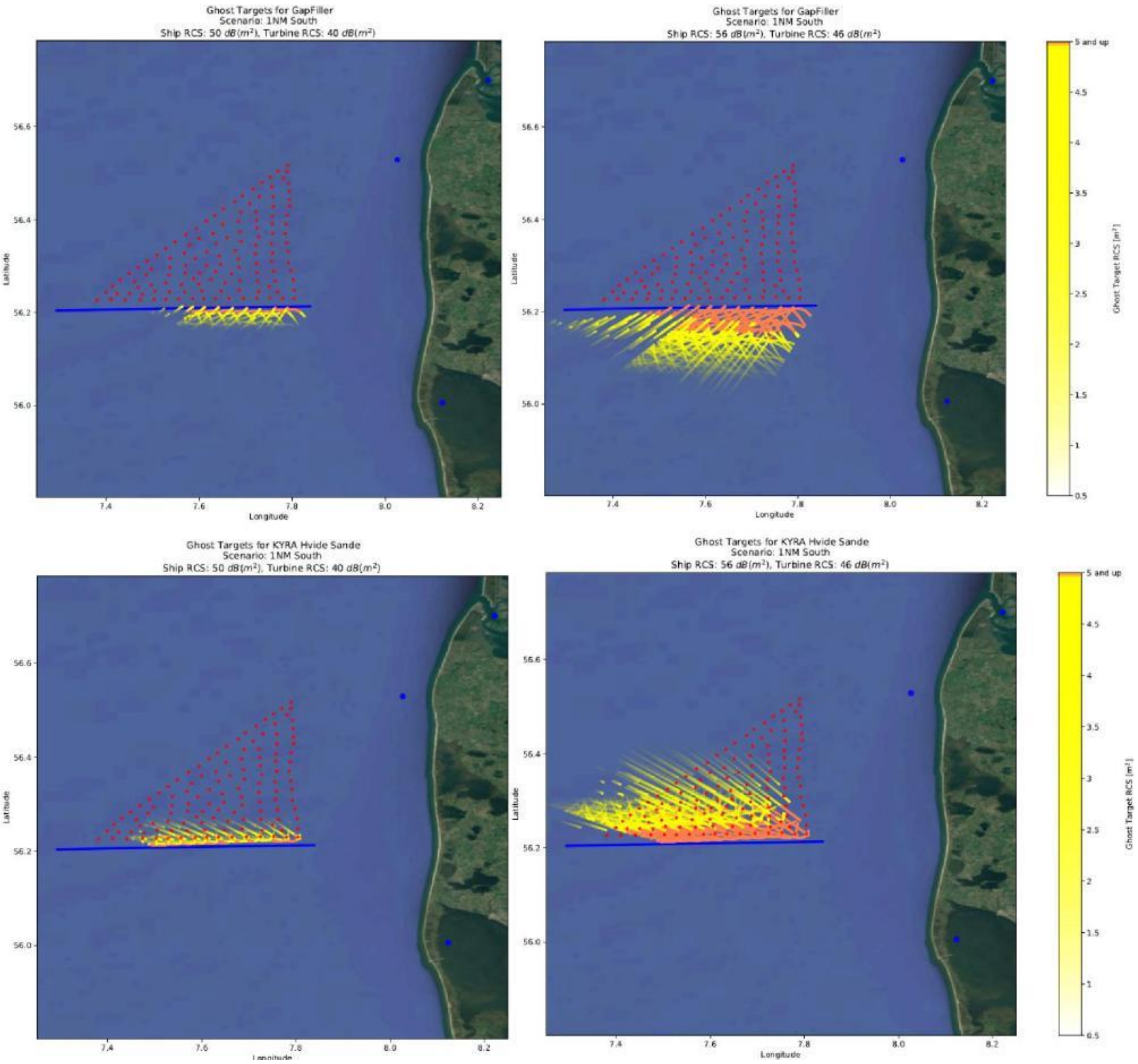

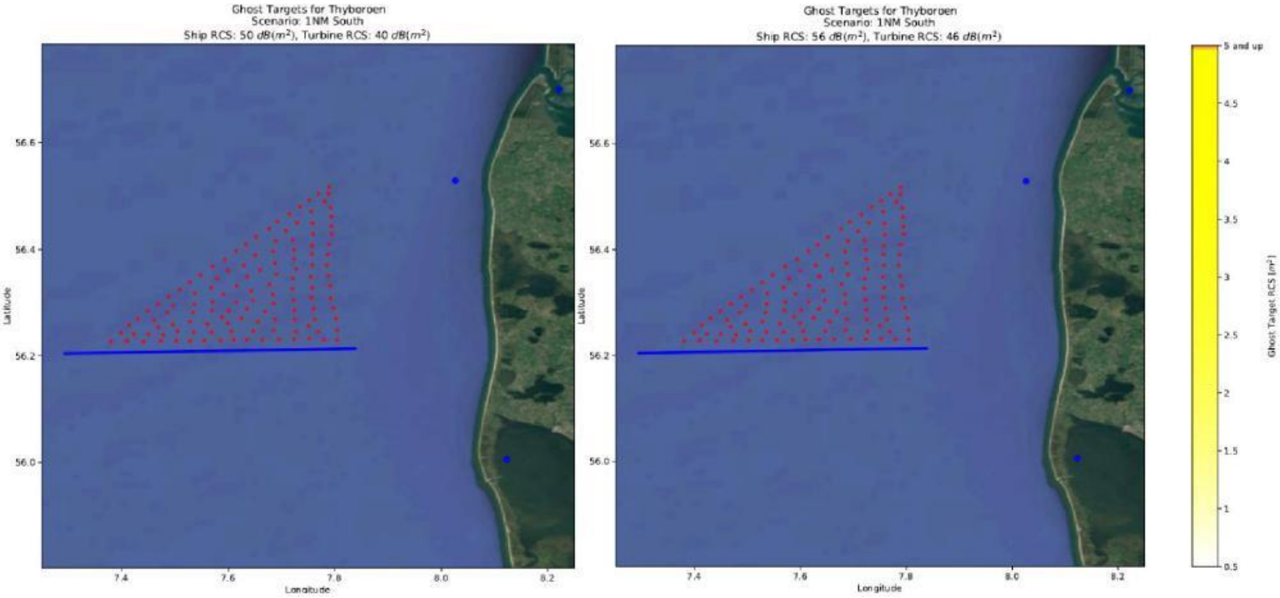

Figure 54 Calculation of ghost targets originating from large vessels, east bound south of Thor Havmøllepark 1 Nautical mile out from the windfarm area. Radar sites from top to bottom are: Gapfiller Radar at Vesterhav Nord, KYRA Hvide Sande, and KYRA Thyborøn. Representative (left) and Worst case (right)

Likelihood of ghosts originating from southwest bound traffic West of Thor Havmøllepark 2 Nautical miles out from the windfarm area

Below images indicate that there is a high likelihood of ghosts originating from ships travelling Northwest of Thor Havmøllepark.

Possible ghost echoes are calculated to be weak and diffuse for smaller ships, however in the worst case, ghost echoes of more than 5 m^2 in RCS are seen and therefore are likely to cause false tracks or to be displayed on operational displays.

Due to the large distance, KYRA Hvide Sande is calculated to not produce prominent ghost echoes.

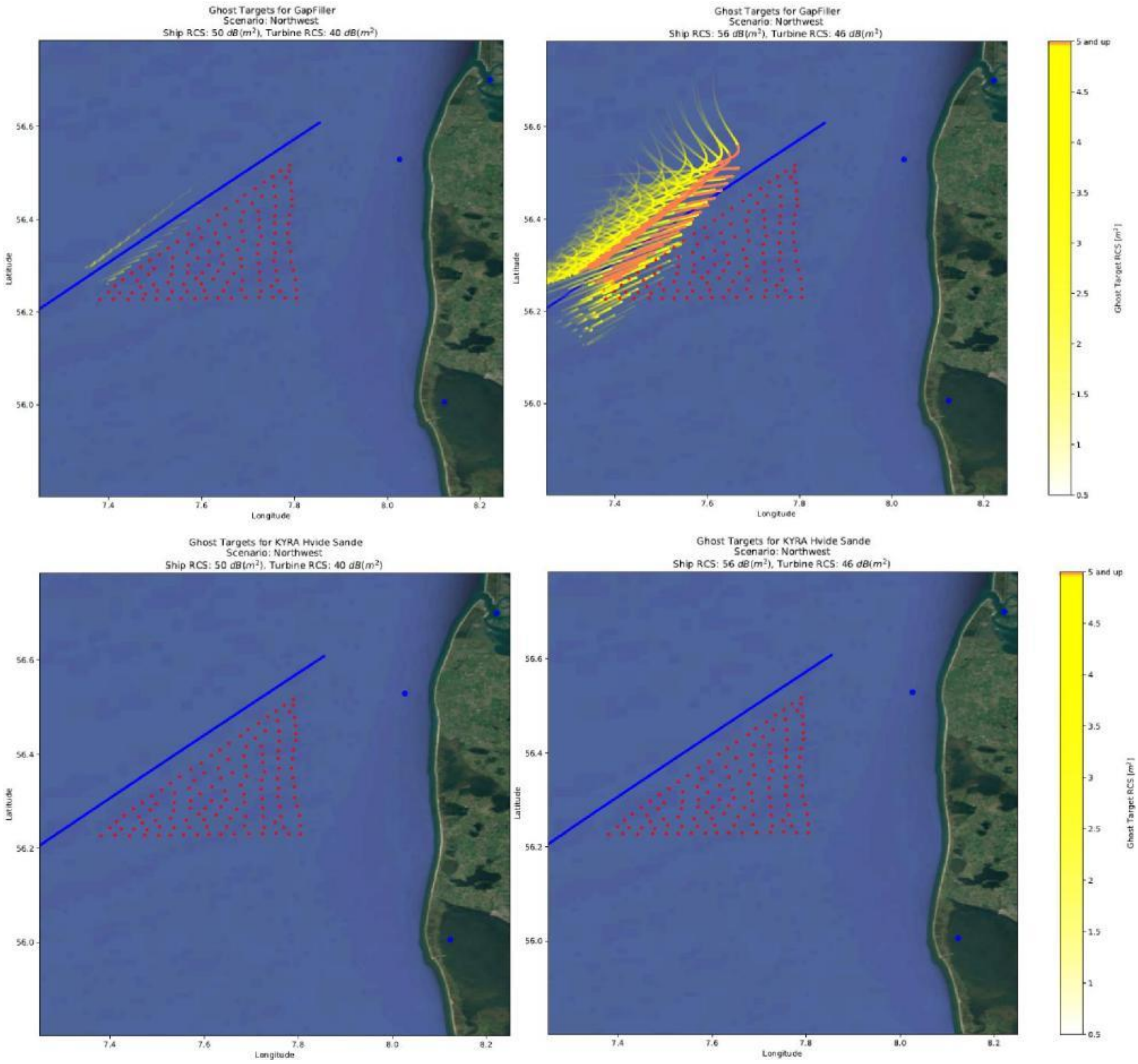

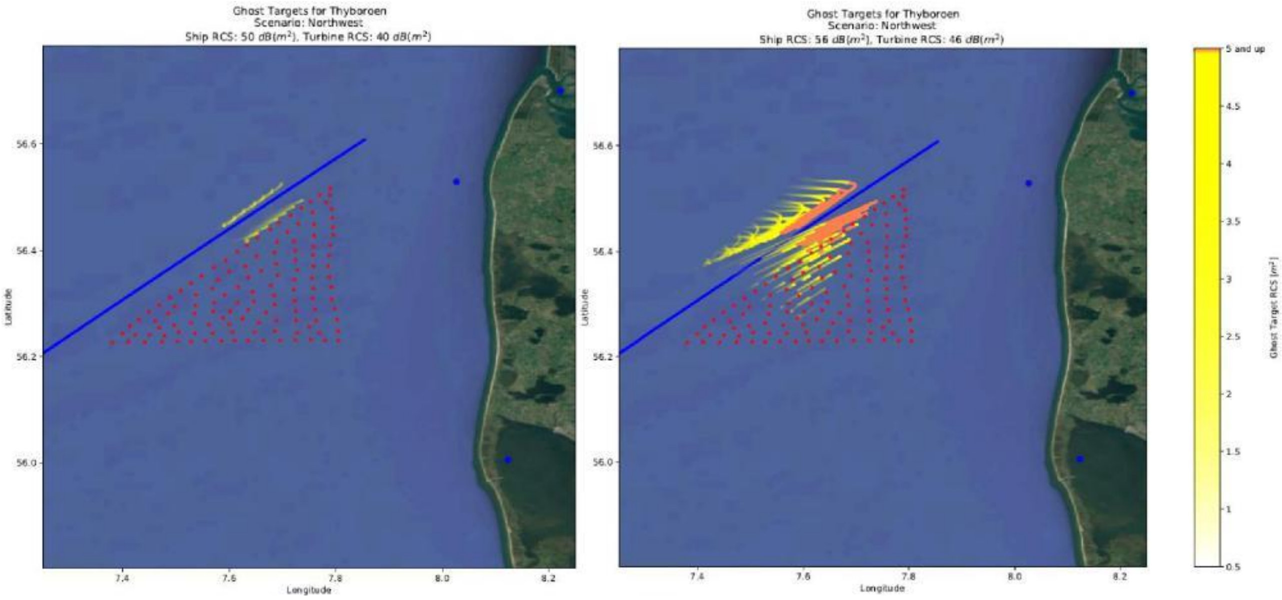

Figure 55 Calculation of ghost targets originating from large vessels, southwest bound north of Thor Havmøllepark 2 Nautical miles out from the windfarm area. Radar sites from top to bottom are: Gapfiller Radar at Vesterhav Nord, KYRA Hvide Sande, and KYRA Thyborøn. Representative (left) and Worst case (right)

Likelihood of ghosts originating from north bound traffic east of Thor Havmøllepark
2 Nautical miles out from the windfarm area

Below images indicate that there is a high likelihood of ghosts originating from ships travelling east of Thor Havmøllepark. The possible ghosts may be pronounced (> 5 m^2 in RCS) and therefore likely to cause false tracks or to be displayed on operational displays.

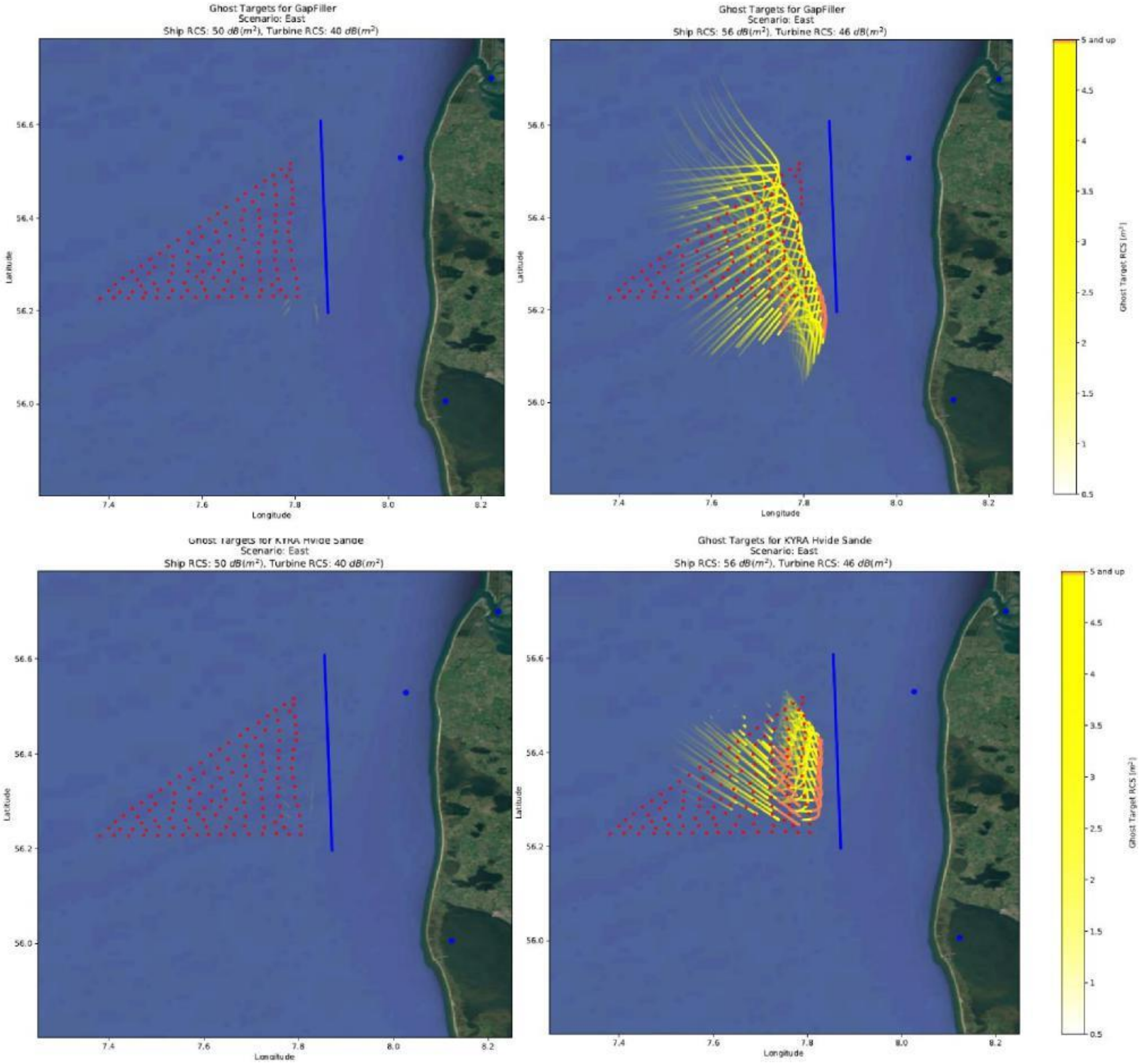

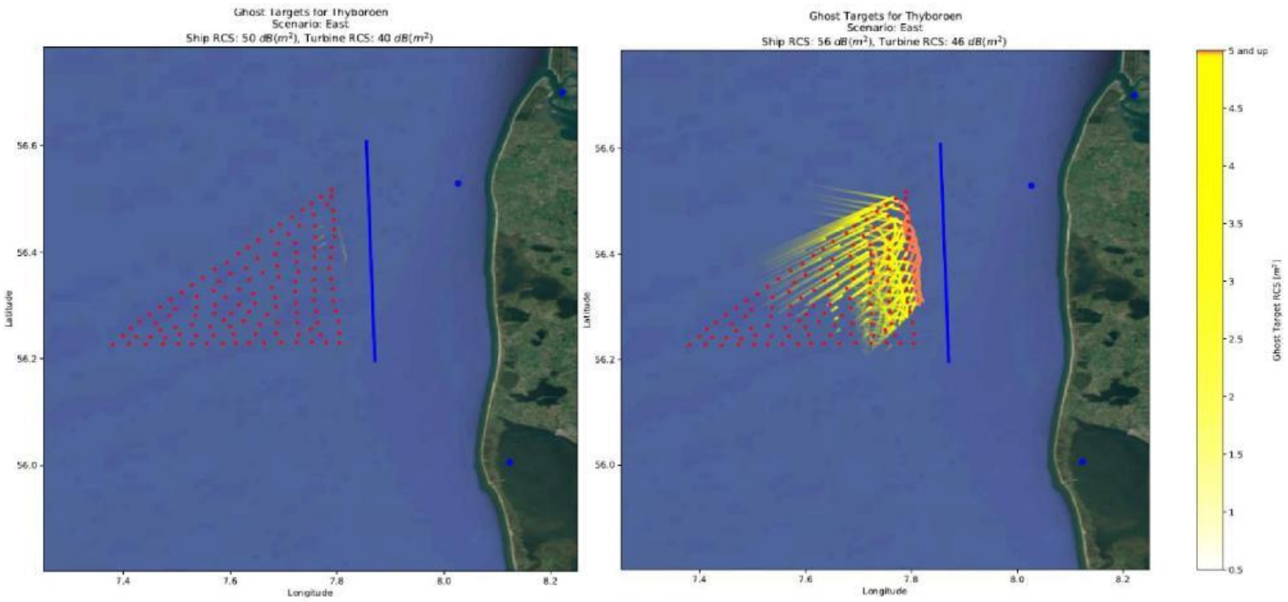

Figure 56 Calculation of ghost targets originating from large vessels, north bound east of Thor Havmøllepark 2 Nautical miles out from the windfarm area. Radar sites from top to bottom are: Gapfiller Radar at Vesterhav Nord, KYRA Hvide Sande, and KYRA Thyborøn. Representative (left) and Worst case (right)

Likelihood of ghosts originating from east bound traffic south of Thor Havmøllepark 2 Nautical miles out from the windfarm area

Below images indicate that there is likelihood of ghosts originating from large ships operating south of Thor Havmøllepark. The ghosts are weak and diffuse for the smaller ships, however in the worst case prominent ghost echoes can be seen (> 5 m2 in RCS) and can therefore cause significant false tracks or significant disturbance on operational displays.

Due to the large distance from the radar to the turbines, KYRA Thyborøn does not indicate prominent ghost echoes.

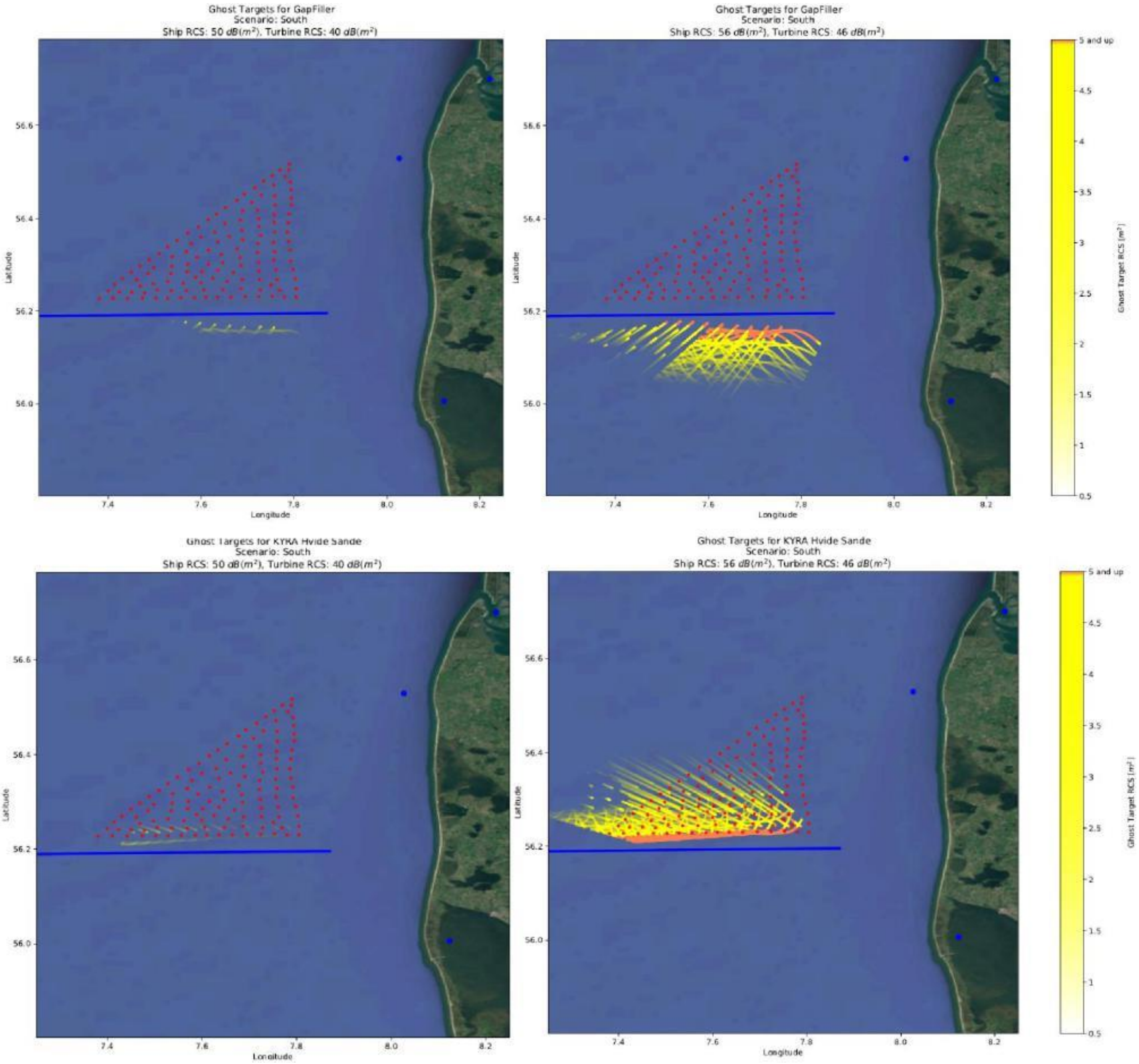

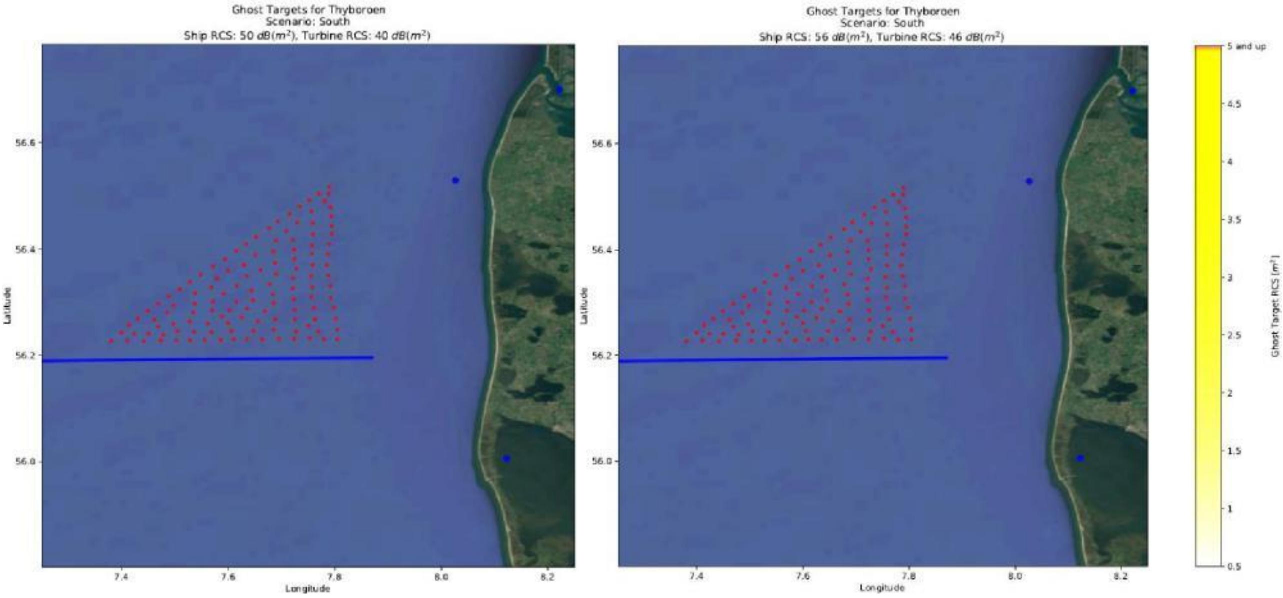

Figure 57 Calculation of ghost targets originating from large vessels, east bound south of Thor Havmøllepark 2 Nautical miles out from the windfarm area. Radar sites from top to bottom are: Gapfiller Radar at Vesterhav Nord, KYRA Hvide Sande, and KYRA Thyborøn. Representative (left) and Worst case (right)

7.1.1 Scenario 4 15MW Windmills

Likelihood of ghosts originating from southwest bound traffic West of Thor Havmøllepark 1 Nautical mile out from the windfarm area

Below images indicate that there is a high likelihood of ghosts originating from ships travelling Northwest of Thor Havmøllepark.

The ghosts may be pronounced (> 5 m2 in RCS) and are therefore likely to cause significant false tracks or significant disturbance on operational displays.

Due to the large distance, KYRA Hvide Sande is calculated to not produce prominent ghost echoes.

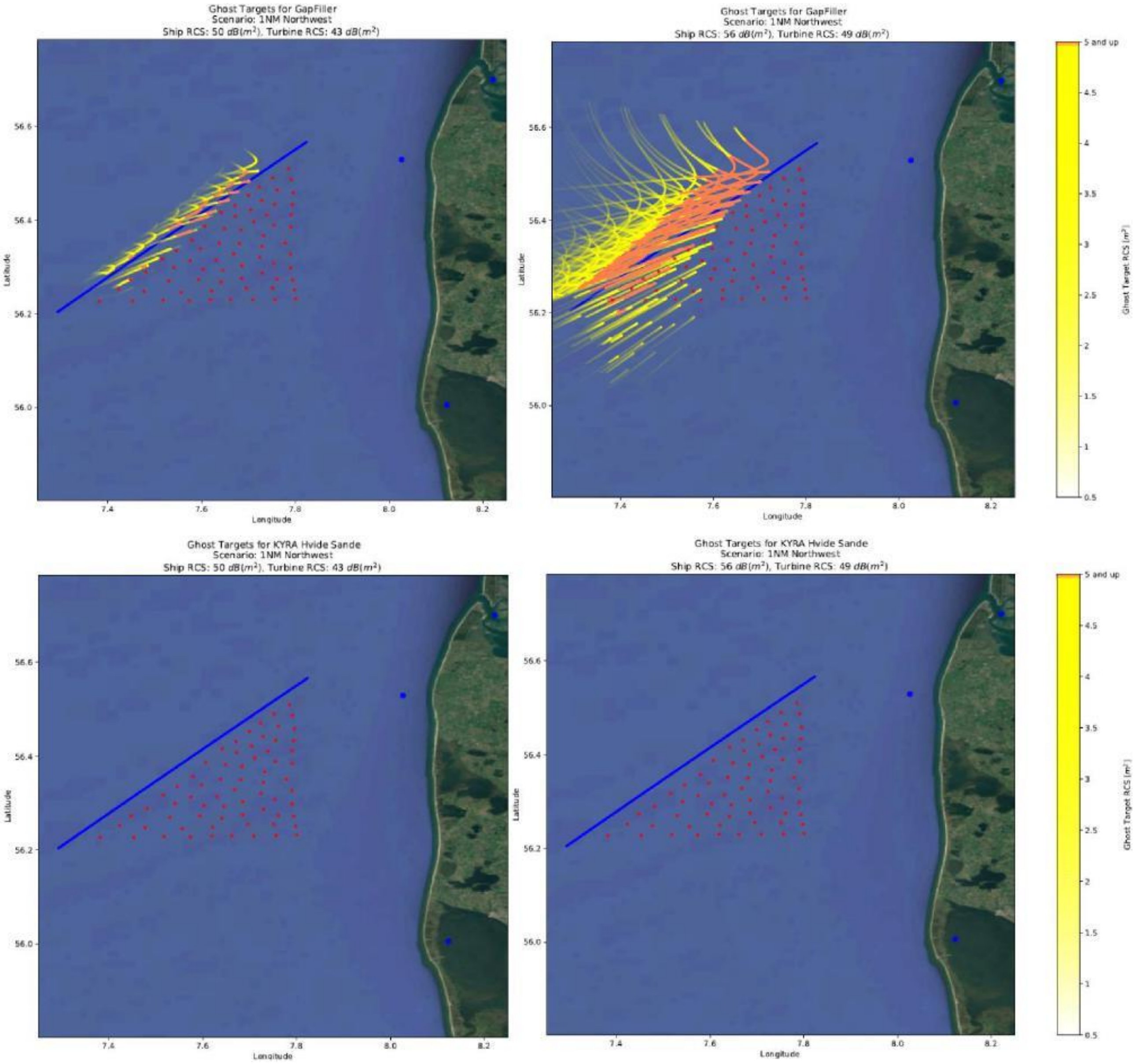

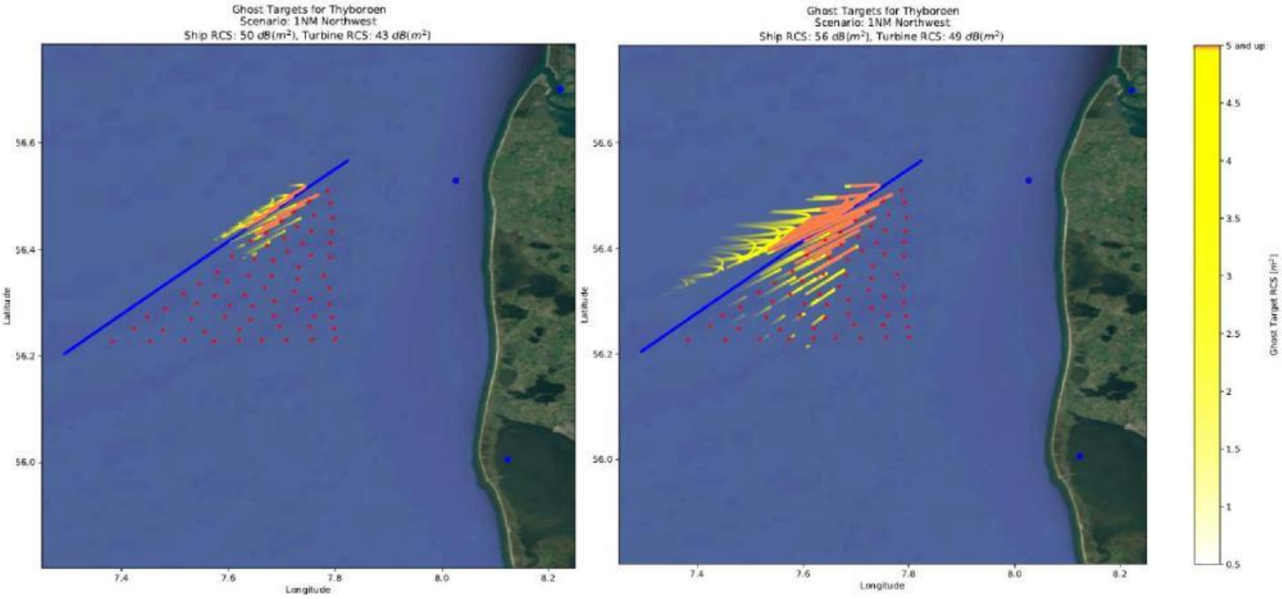

Figure 58 Calculation of ghost targets originating from large vessels, southwest bound west of Thor Havmøllepark 1 Nautical mile out from the windfarm area. Radar sites from top to bottom are: Gapfiller Radar at Vesterhav Nord, KYRA Hvide Sande, and KYRA Thyborøn. Representative (left) and Worst case (right)

Likelihood of ghosts originating from north bound traffic east of Thor Havmøllepark 1 Nautical mile out from the windfarm area

Below images indicate that here is a high likelihood of ghosts originating from ships travelling east of Thor Havmøllepark. Possible ghost echoes are calculated to be prominent and therefore are likely to cause false tracks or to be displayed on operational displays.

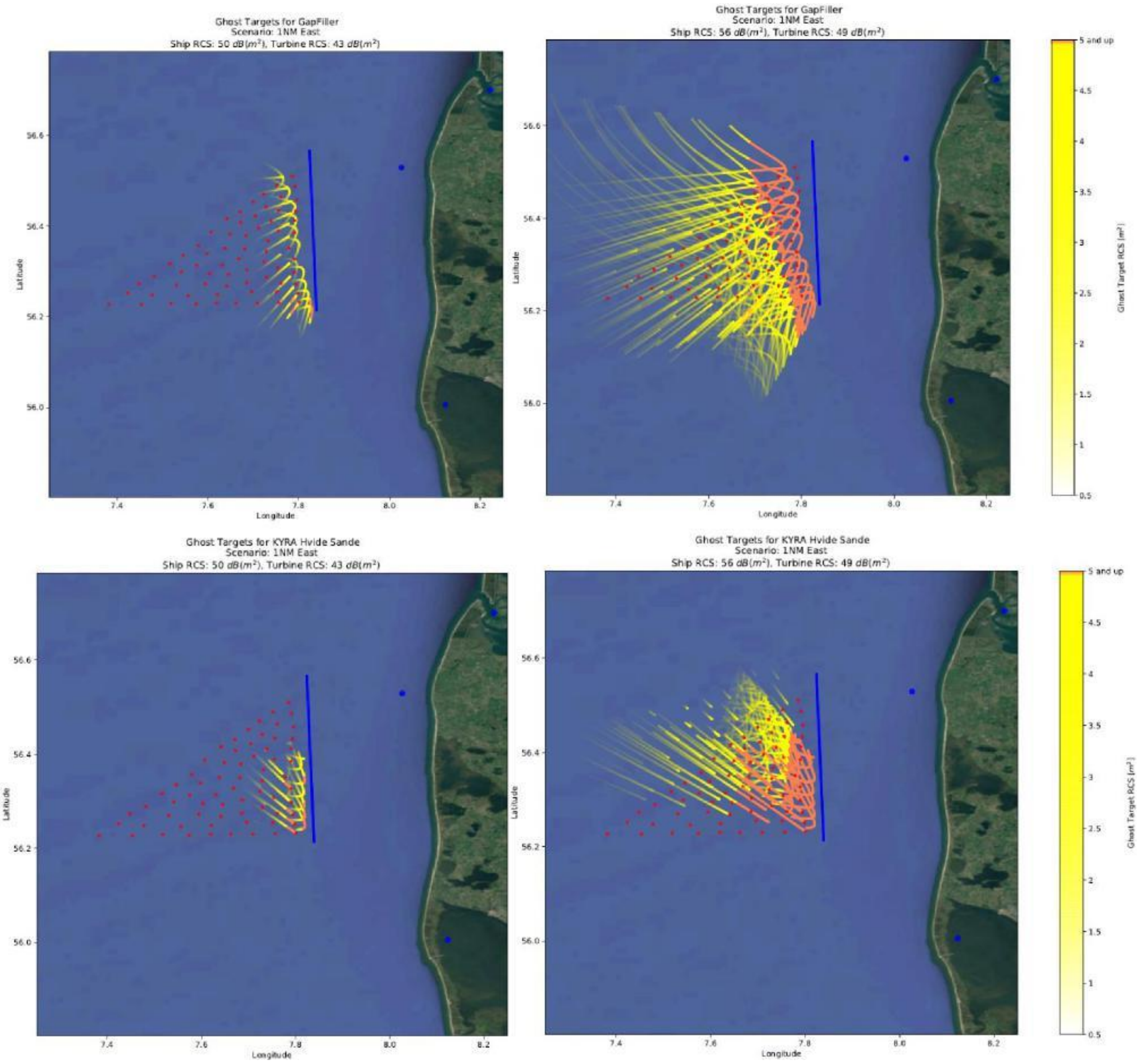

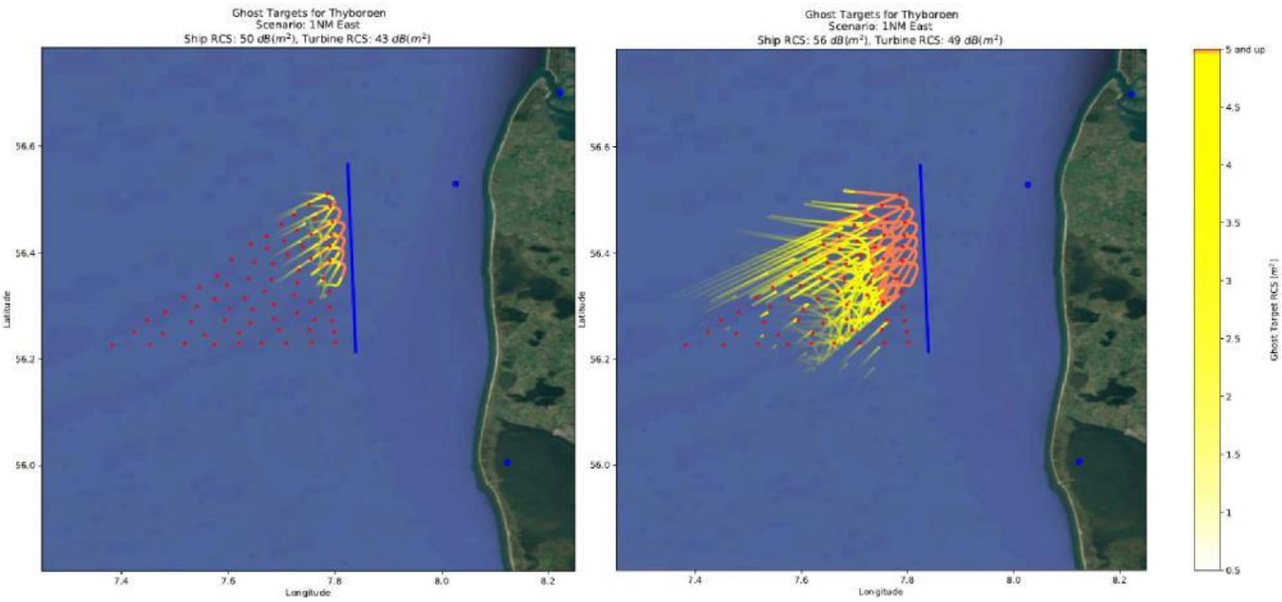

Figure 59 Calculation of ghost targets originating from large vessels, north bound east of Thor Havmøllepark 1 Nautical mile out from the windfarm area. Radar sites from top to bottom are: Gapfiller Radar at Vesterhav Nord, KYRA Hvide Sande, and KYRA Thyborøn. Representative (left) and Worst case (right)

Likelihood of ghosts originating from east bound traffic south of Thor Havmøllepark 1 Nautical mile out from the windfarm area

Below images indicate that here is a high likelihood of ghosts originating from ships travelling south of Thor Havmøllepark. The ghosts may be pronounced (> 5 m2 in RCS) and are thereby likely to cause significant false tracks or significant disturbance on operational displays.

Due to the large distance, KYRA Thyborøn is calculated to not produce prominent ghost echoes.

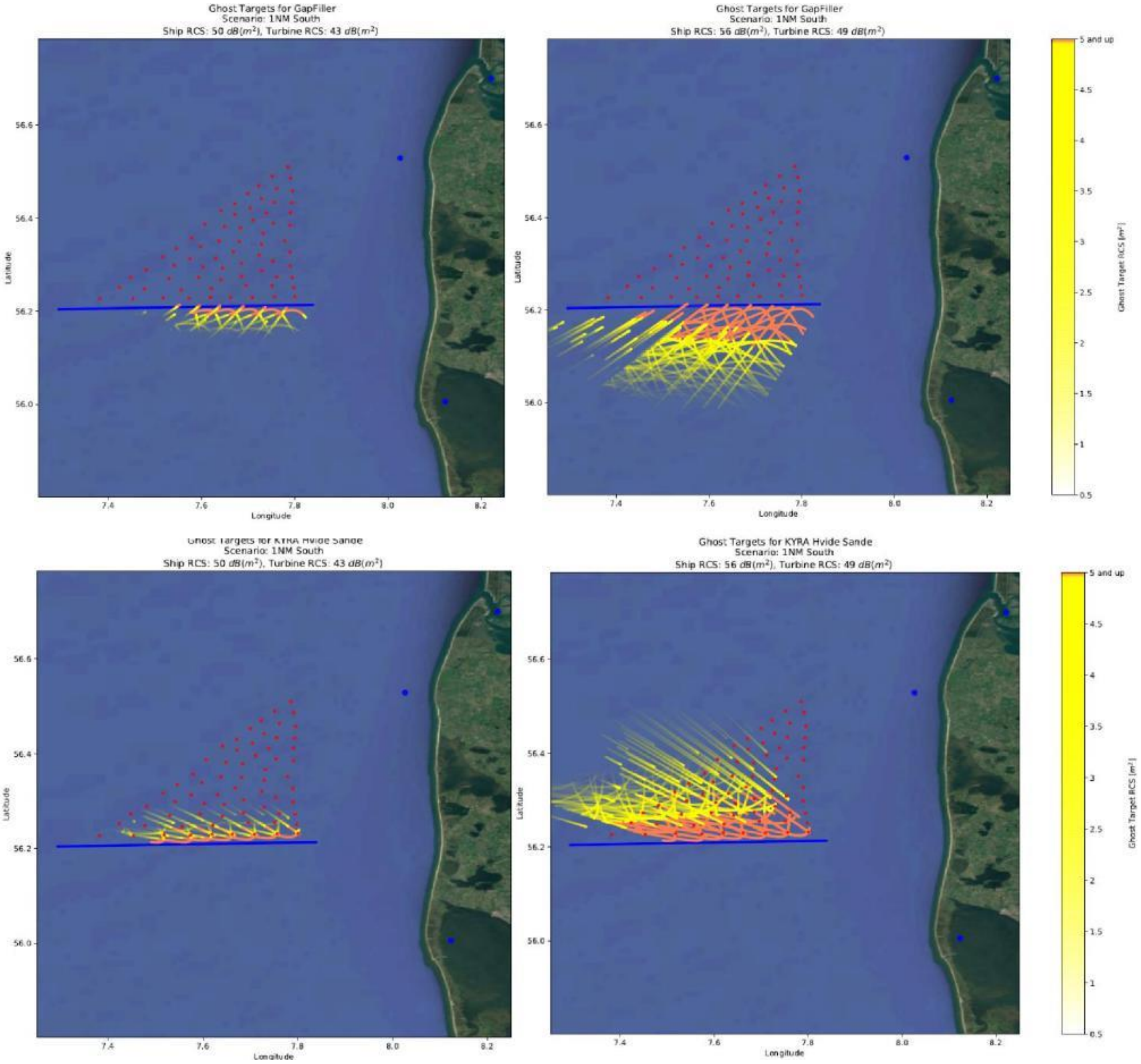

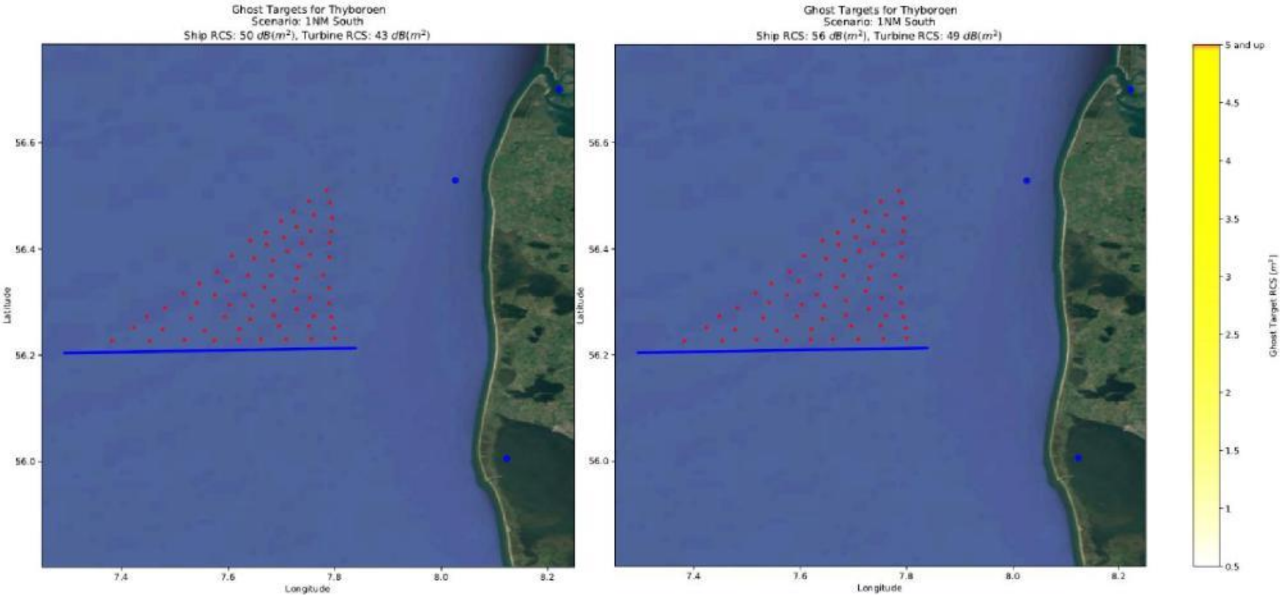

Figure 60 Calculation of ghost targets originating from large vessels, east bound south of Thor Havmøllepark 1 Nautical mile out from the windfarm area. Radar sites from top to bottom are: Gapfiller Radar at Vesterhav Nord, KYRA Hvide Sande, and KYRA Thyborøn. Representative (left) and Worst case (right)

Likelihood of ghosts originating from southwest bound traffic West of Thor Havmøllepark 2 Nautical miles out from the windfarm area

Below images indicate that there is possibility of ghosts originating from ships travelling Northwest of Thor Havmøllepark.

Possible ghost echoes are calculated to be weak and diffuse for smaller ships, however in the worst case, ghost echoes of more than 5 m^2 in RCS are seen and therefore are likely to cause false tracks or to be displayed on operational displays.

Due to the large distance, KYRA Hvide Sande is calculated to not produce prominent ghost echoes.

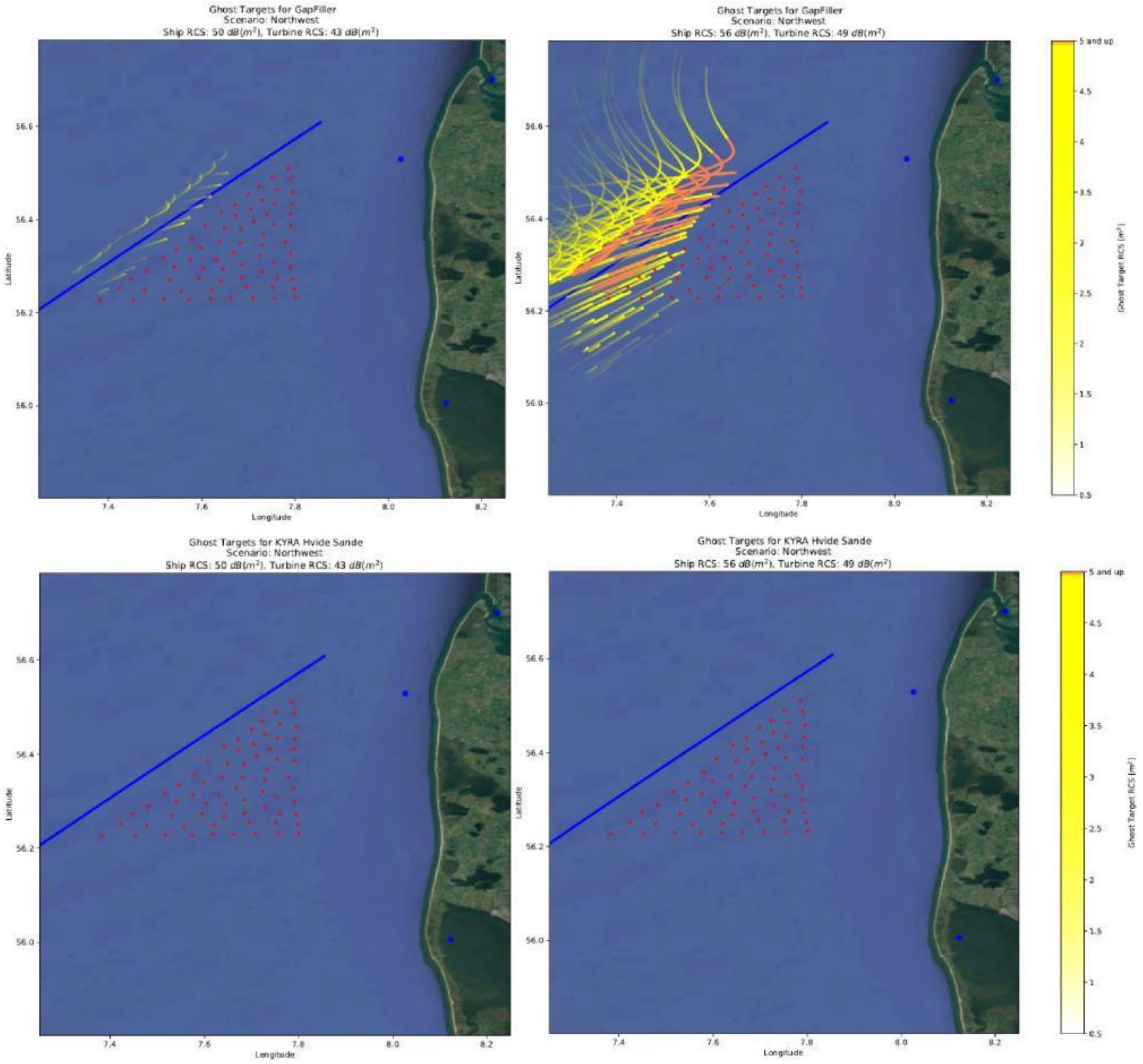

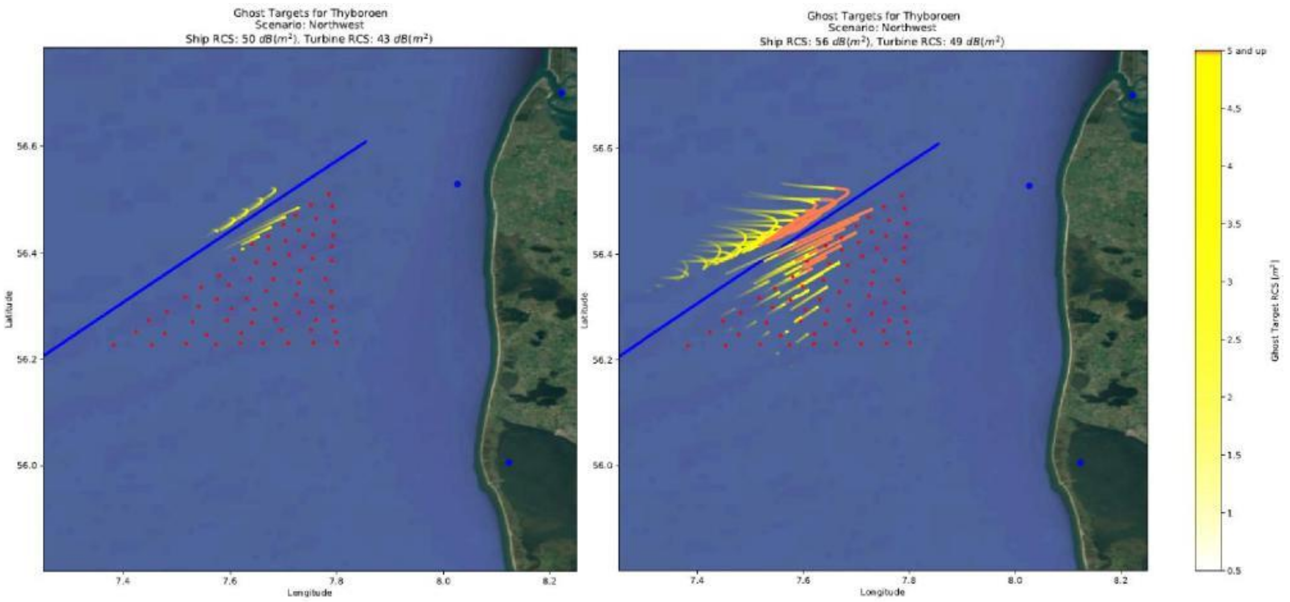

Figure 61 Calculation of ghost targets originating from large vessels, southwest bound north of Thor Havmøllepark 2 Nautical miles out from the windfarm area. Radar sites from top to bottom are: Gapfiller Radar at Vesterhav Nord, KYRA Hvide Sande, and KYRA Thyborøn. Representative (left) and Worst case (right)

Likelihood of ghosts originating from north bound traffic east of Thor Havmøllepark 2 Nautical miles out from the windfarm area

Below images indicate that here is a low likelihood of ghosts originating from ships travelling east of Thor Havmøllepark. Possible ghost echoes are calculated to be weak and diffuse for smaller ships, however in the worst case, ghost echoes of more than 5 m^2 in RCS are seen and therefore are likely to cause false tracks or to be displayed on operational displays.

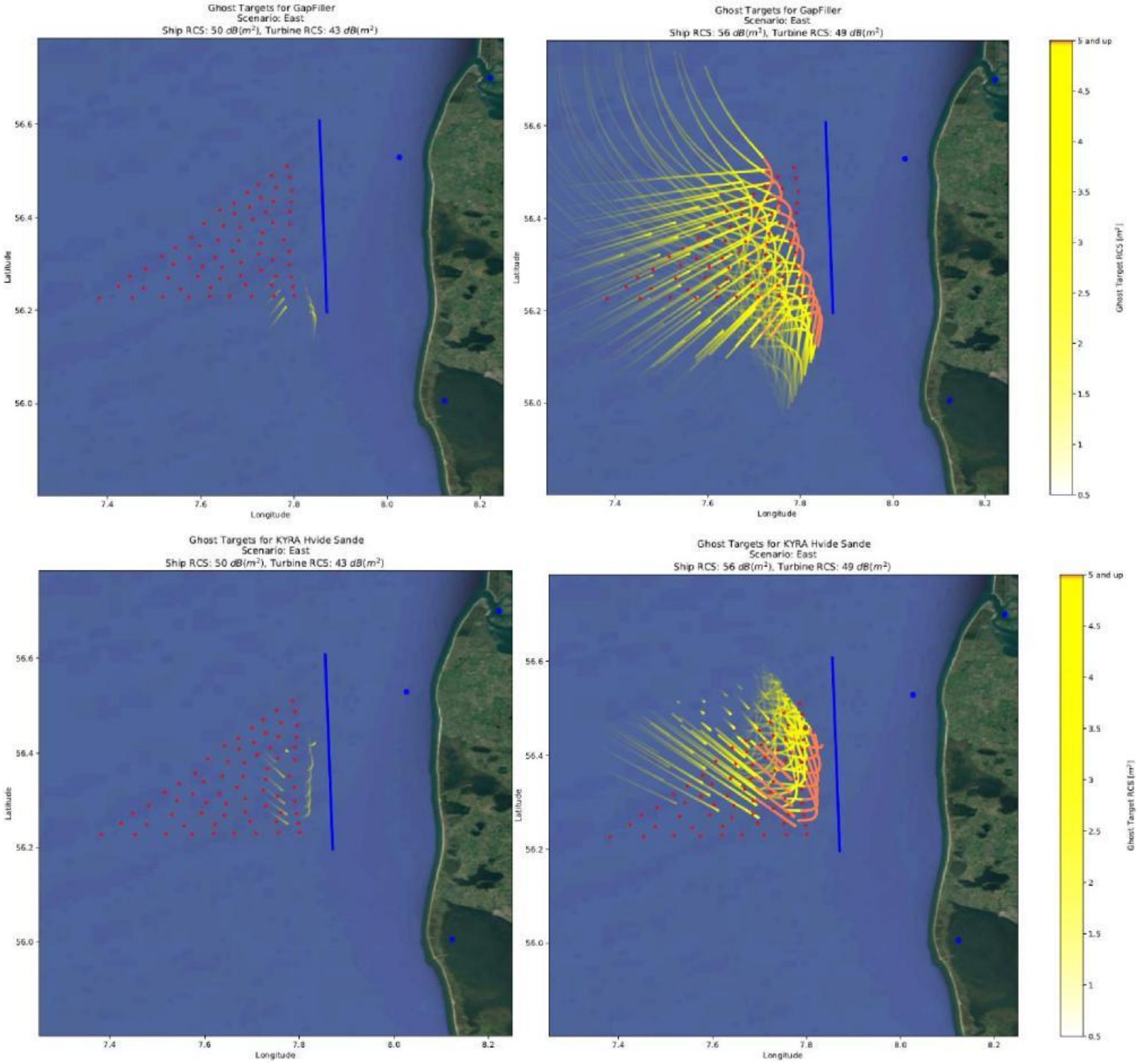

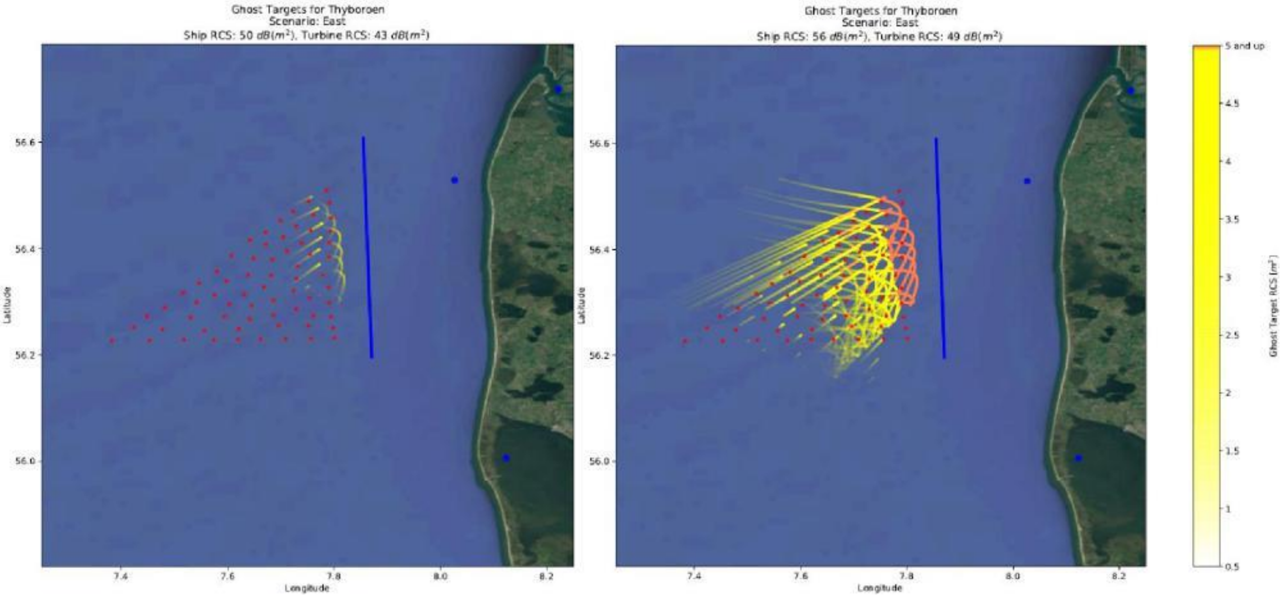

Figure 62 Calculation of ghost targets originating from large vessels, north bound east of Thor Havmøllepark 2 Nautical miles out from the windfarm area. Radar sites from top to bottom are: Gapfiller Radar at Vesterhav Nord, KYRA Hvide Sande, and KYRA Thyborøn. Representative (left) and Worst case (right)

Likelihood of ghosts originating from east bound traffic south of Thor Havmøllepark 2 Nautical miles out from the windfarm area

Below images indicate that there is high likelihood of ghosts originating from large ships operating south of Thor Havmøllepark. The ghosts are in the worst case be prominent (> 5 m2 in RCS) and are therefore likely to cause significant false tracks or significant disturbance on operational displays.

KYRA Thyborøn does not produce prominent ghost echoes due to the large distance.

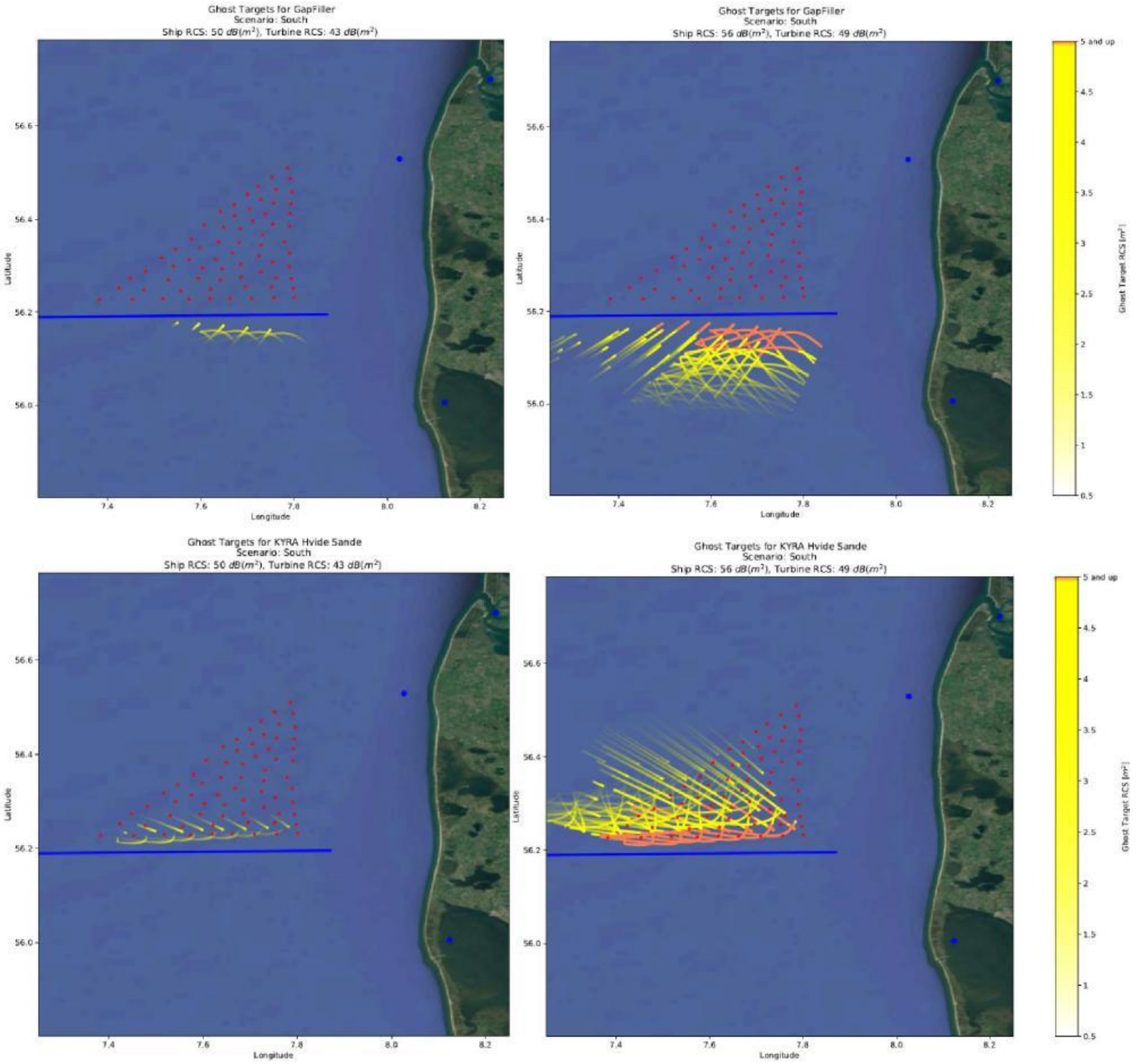

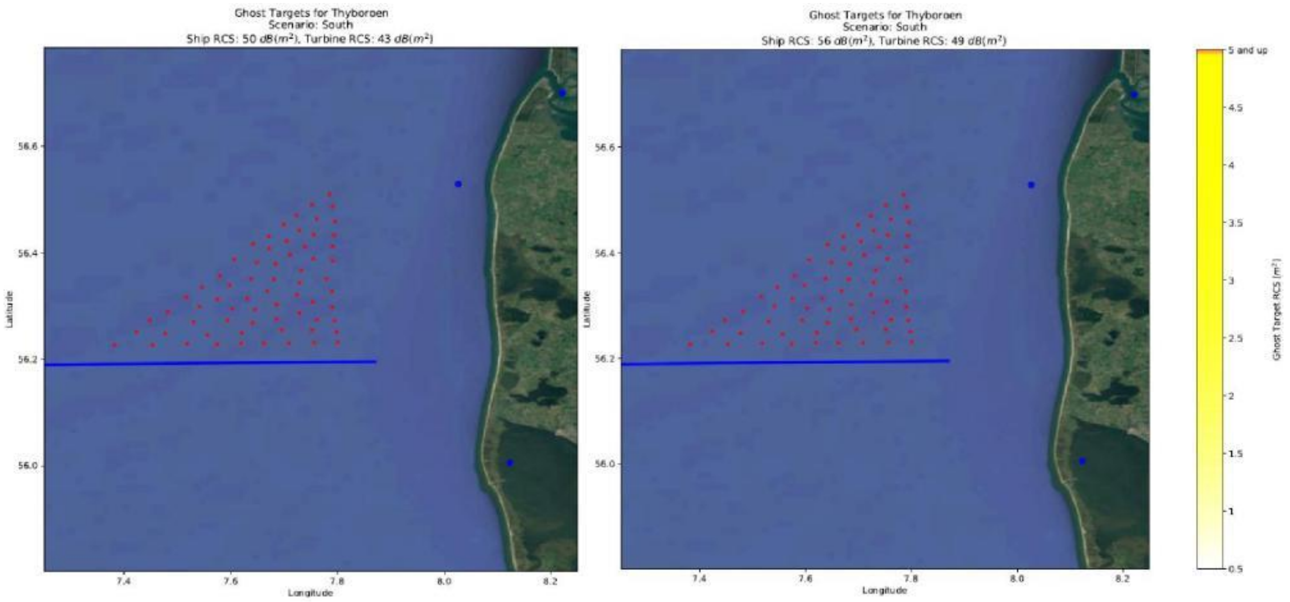

Figure 63 Calculation of ghost targets originating from large vessels, east bound south of Thor Havmøllepark 2 Nautical miles out from the windfarm area. Radar sites from top to bottom are: Gapfiller Radar at Vesterhav Nord, KYRA Hvide Sande, and KYRA Thyborøn. Representative (left) and Worst case (right)

7.2 Side lobes

Considering the distances involved, the impact from side lobes on coastal radars is evaluated to be insignificant.

7.3 Shadowing

In the visual light regime, shadow effects are very distinct i.e. you do not see anything hiding behind an obstacle such as a wind turbine tower. In the radio frequency regime, the shadows are much more blurred out. This is illustrated in Figure 64.

The scales in Figure 64 are in meters, the wind turbine tower is placed at (0,0), the radar is placed in the fair field distance from the antenna (4000 m to the left of the tower in this case).

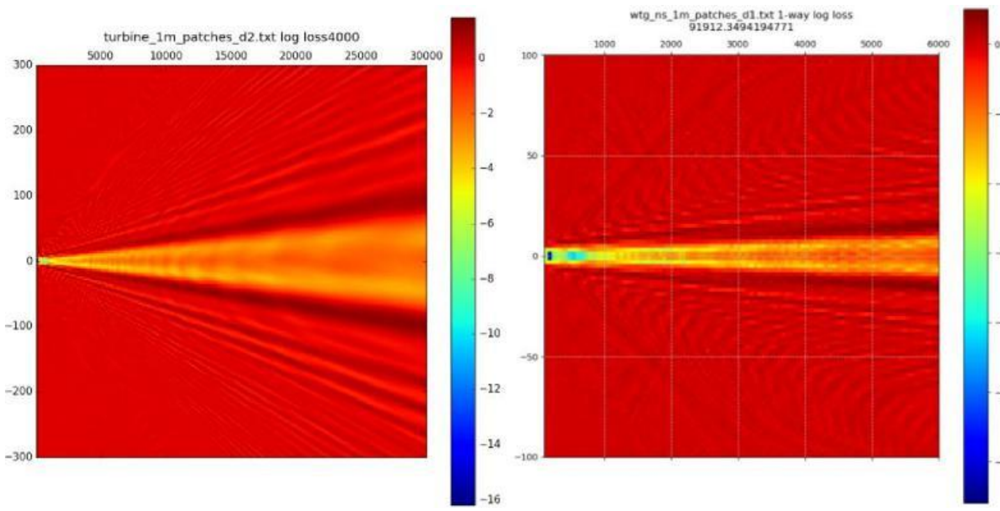

Figure 64 Simulation of shadowing from one wind turbine. Left plot shows the simulated shadowing out to a 30km range, and the right plot is seen closer to the wind turbine, and out to a 6km range. Variations of up to +/- 3dB will only have minor influence and considerable shadowing will only be in a narrow sector stretching about 0,5 NMI beyond the individual turbine.

When the transmission from the radar hits the tower, it gives rise to a diffraction pattern behind (i.e. to the right) of the tower, as illustrated in the figures. The values indicated by the varying colors tell how much the echo of a target will be reduced (or enhanced) as a function of distance behind and to the side of the tower. At very short distances behind the tower, the reduction will be considerable (blue and green colors), while in a narrow fan behind the wind turbine the reduction will be moderate (yellow color). It should also be noted that even 20 km behind the tower, the yellow fan less than 100 m wide. Outside these areas the reduction will be insignificant or there will even be an enhancement of the echo.

In conclusion, the effect of the shadowing will be that only very small targets can be hidden in shadows in small area directly behind the wind turbine towers.

Other targets will not be hidden completely, influence on sensitivity is only affecting small areas and tend to be less than 6dB for all vessels behind wind turbines. The effect may be a marginal variation in the detection probability in accordance with diminished/increased echo power.

7.4 Receiver sensitivity

For the detection of targets, the signal processing of a radar may reduce sensitivity in areas with dense target intensity. [redacted]

The ability to detect small targets, e.g. service boats, inside a windfarm is illustrated in Figure 65 from a previous Terma trial.

In this case the radar system is on-shore, and the service boat is in the left side of the wind farm area, easily discriminated by the red trail. A moving target is also seen to the far right, behind the wind farm area as seen from the radar position.

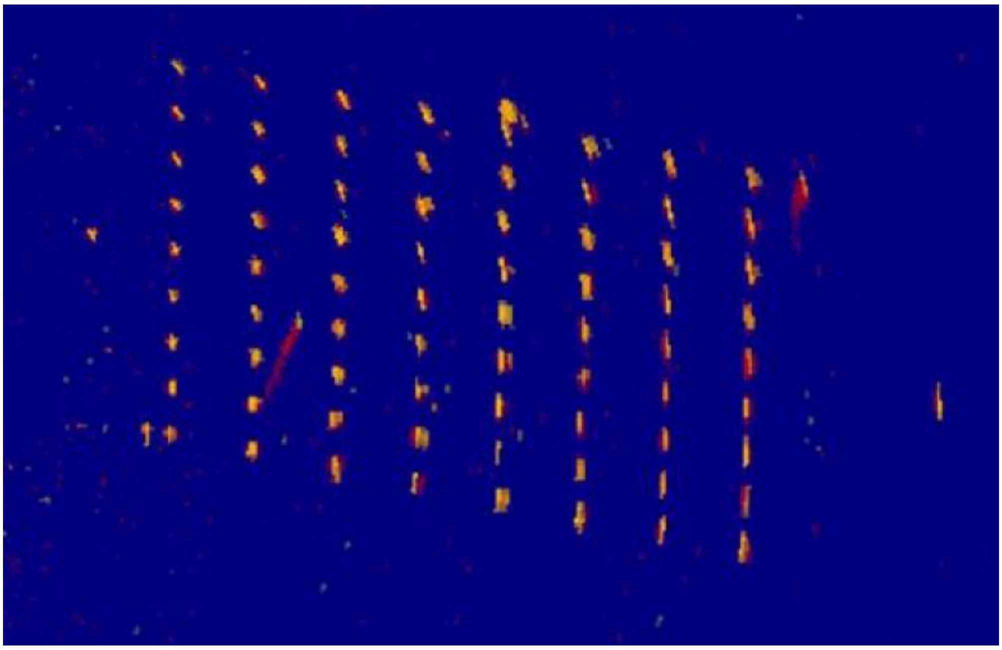

Figure 65 Small service boat inside wind farm.
The radar is placed to the left, outside the figure.

8 Influence on air coverage radars, evaluations and calculations

The following surveillance sensors have been informed relevant by DALO for the assessment:

- Karup (TPS) PSR/SSR

[redacted]

8.1 Overview

The location of the turbines relative to the Karup PSR is summarized in Table 5.

[redacted]

8.2 Radar line of sight assessment

The radar Line-of-Sight prior to building deployment is analyzed to assess the minimum target visibility altitude at the site of the turbines. The overview is generated using a 75m cell size terrain raster where the relevant sector towards the wind park is analyzed using a 10m cell size terrain raster. The below figures only show the initial 60NM range.

[redacted]

Focusing on the area with the wind turbines, it can be seen which sections will be visible to the Karup PSR.

[redacted]

[redacted] the entire area is outside LoS for the 8 MW turbines. For the 15MW turbines, only the northeastern part of the area is within LoS. For the 15MW turbines, only the top part of blades will be visible from the radar, as the hub height is 150m.

Scenario 1

For scenario 1, the turbines were focused on the eastern part of the windfarm area. For the 15MW turbines, [redacted] the turbines were in view of Karup PSR. [redacted]

[redacted]

The PSR LoS is summarized in Table 6.

[redacted]

[redacted]

Scenario 2

[redacted]

The PSR LoS is summarized in Table 6.

[redacted]

[redacted]

Scenario 3

[redacted]

RELEASEABLE FOR PUBLIC USE

Scenario 4

[redacted]

The PSR LoS is summarized in Table 6.

[redacted]

8.3 Top-level engineering assessment – PSR and SSR

8.3.1 Radar Far-Field Monitors (FFM)

It is recommended to protect and mitigate any far-field monitor in azimuth of the FFM in a sector of two times the antenna horizontal beam-width at 3dB according to [1]. The safe-guarding zones are listed in Table 9.

Table 9 – Safe-guarding zone for FFM

[redacted]

Location of relevant FFMs have not been provided. Thus, it cannot be concluded if the turbines will require any FFM to be relocated as a possible mitigation.

8.3.2 Radar data sharing

Information on radar data sharing has not been provided. Thus, this is not considered applicable.

8.3.3 Cumulative impact

Only the wind turbines being constructed at Thor Havmøllepark is considered in this assessment. Terma A/S has not been informed of any other neighboring approved projects that may already affect the performance of the radar.

8.3.4 PSR Processing overload

Information on the plot processing, plot extraction, and overload prevention techniques have not been provided.

8.4 Engineering assessment for PSR

8.4.1 PSR Probability of detection

8.4.1.1 Shadow height

To illustrate the shadow height, the cross-section of the terrain (blue line) in the azimuth angle extending from the radar site towards turbines, named after the previous section, is shown. The PSR radar LoS before (red) shown is based on ArcGIS output. The LoS after deployment of the turbines (yellow) is the shadow height following the formula provided in [1] section A.2. An example for each scenario is shown, with the rest of the images being placed in Annex C ,and a table giving the difference before and after implementation of the turbines at certain distances.

8.4.1.1.1 Scenario 1:

[redacted]

Table 10 – Scenario 1: Karup PSR - Shadow height prior and after deployment

[redacted]

[redacted]

[redacted]

[redacted]

8.4.1.1.2 Scenario 2:

[redacted]

[redacted]

Figure 73 – Scenario 2, Turbine 4: Cross-section of terrain and radar LoS in azimuth angle towards the wind turbines before (red) and after (yellow) deployment for the Karup PSR.

[redacted]

[redacted]

[redacted]

[redacted]

8.4.1.1.3 Scenario 4:

[redacted]

Figure 74 – Scenario 4, Turbine 4: Cross-section of terrain and radar LoS in azimuth angle towards the wind turbines before (red) and after (yellow) deployment for the Karup PSR.

[redacted]

[redacted]

[redacted]

8.4.1.2 Shadow width

The half-width shadow as a function of the range from the radar is listed in Table 13. The half-width shadows are calculated using 1.2 GHz to calculate the worst-case shadow.

[redacted]

[redacted]

[redacted]

Scenario 2

[redacted]

[redacted]

[redacted]

Figure 76 – Half-shadow width of turbine 1 and 4

Scenario 4

[redacted]

[redacted]

Figure 77 – Half-shadow width of turbine 1 and 4

9 Influence on ship navigational radars

Conclusions from experience and tests performed [5] are that the only significant influence of wind farm structures on shipping is the that the large vertical extent of the wind turbine generators return radar responses strong enough to produce interfering side lobe, multiple and reflected echoes (ghosts) on ship borne (navigational) radar systems.

Bearing discrimination was also reduced by the magnitude of the response and hence the cross-range size of displayed echoes. If on passage close to a wind farm boundary or within the wind farm itself, this could in some circumstances affect a vessel's ability to fully comply with the International Regulations for the Prevention of Collisions at Sea.

Clutter in the ships radar display due to the presence of wind turbines was found to be quite considerable. Both ring-around and false plots were observed (referred to by mariners as side-lobe, multiple and reflected echoes). The observed problems could be suppressed successfully by using the gain and range settings of the radar. However, this may have the unwanted side-effect of no longer being able to detect some small targets.

While reducing receiver amplification (gain) would enable individual turbines to be clearly identified from the side lobes - and hence limit the potential of collisions with them - its effect would also be to reduce the amplitude of other received signals such that small vessels, buoys, etc., might not be detectable within or close to the wind farm.

It was also found that the performance of a vessel's automatic radar plotting aid (ARPA), could be adversely affected when tracking targets in or near the wind farm.

With respect to the multiple and reflected echoes produced when wind farm structures lie between the observing radar and a relatively high sided vessel, gain reduction will have similar effects to those described above.

The exact behaviour of false radar returns depends on the layout of the wind farms and the shape of the individual ships. The layout of wind farms, where the individual turbines placed in grids or along lines add to the problem. The most dangerous problem is that ghosts are almost chaotic in nature, and it is practically impossible to predict where they appear in the shipping lanes.

It may furthermore be impossible to distinguish the ghosts from real targets onboard a ship. The nature is that ghosts on ships radar often look like smaller trade vessels, fishing boats or leisure boats.

The risk imposed by the mechanisms described will depend on traffic density and positioning of the wind farms relative to the ships traffic. The risk will be reduced with increasing distance between individual ships and between ships and wind farms.

Returns from side lobes are normally of less risk as they are easy to distinguish based on their symmetrical structure around real objects.

Some of the possible reflection patterns causing ghosts are visualised in Figure 78 where the observing radar is on the yellow ship.

The false echoes will in any case be beyond the targets but may anyway cause confusion.

Tracking of the green ship in the figure is e.g. likely to jump to one of the nearby ghosts as speeds of the real and false echoes will be of the same magnitude. A false track with high speed is also generated.

Alike patterns will exist for radars onboard all 3 ships in the picture.

Calculations and experience show that generation of complete ships images as the one shown on in Figure 78 will require at least one of the ships to be within 0.5 nautical mile distance from a wind turbine.

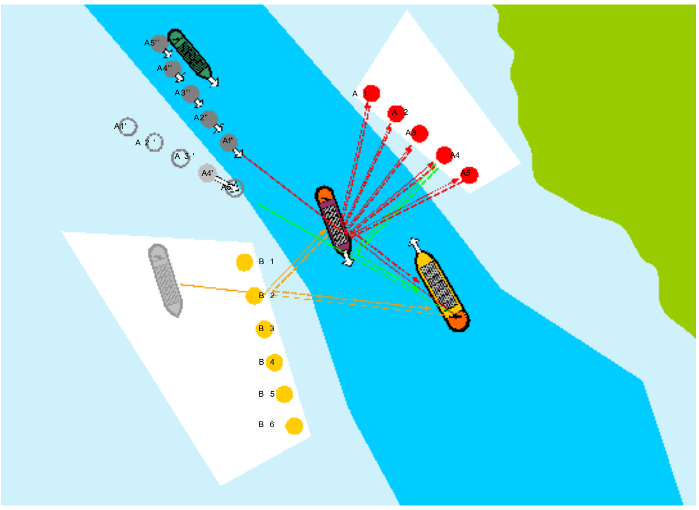

Figure 78 Visualisation of ghost effects (elements not to scale)

9.1 Side lobes

Side lobes are caused by imperfect antenna radiation diagrams and appear on the radar screen as shown in Figure 79. Red and yellow circles illustrate individual wind turbine towers and grey object illustrate false information.

False reflections on typical ships radar will typically occur at angles up to 10 degrees on both sides of the individual wind turbine and at distances up to several nautical miles.

The effect may be even worse on poorly installed ships radars or when the ship is very close to a wind turbine.

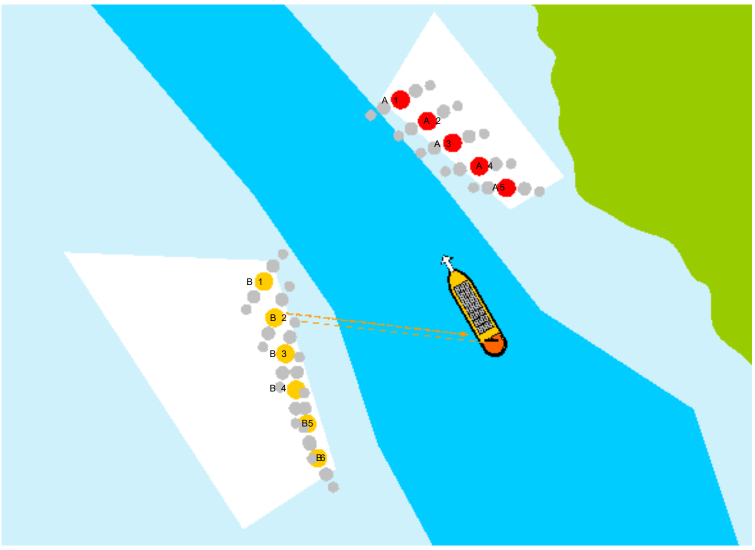

Figure 79 Visualisation of side lobe effects (elements not to scale)

10 Mitigation with additional radar(s)

Taking the reported set-up of existing and planned radars into account, it is unlikely that they will suffer from significant disturbance within their instrumented ranges, however, the risk of

[redacted]

[redacted]

10.1 Radar Coverage

10.1.1 Current coverage and CARPET calculations

[redacted]

[redacted]

Figure 81 Surface Coverage of current and planned radars.

10.1.2 For mitigation of effects west of Thor Havmøllepark.

[redacted]

[redacted]

Annex A Coordinates of Windmills

Table 16: Scenario 1 -The projected coordinates of the wind turbines comprising the wind farm with 8MW turbines

Latitude	Longitude	Hub height AMSL [m]	Output Power [MW]
56.22928	7.658436	105.0	8000
56.22956	7.684317	105.0	8000
56.22983	7.710198	105.0	8000
56.2301	7.73608	105.0	8000
56.23036	7.761963	105.0	8000
56.23062	7.787845	105.0	8000
56.24082	7.658032	105.0	8000
56.24109	7.683921	105.0	8000
56.24137	7.709811	105.0	8000
56.24163	7.7357	105.0	8000
56.2419	7.76159	105.0	8000
56.24215	7.787481	105.0	8000
56.25235	7.657629	105.0	8000
56.25263	7.683526	105.0	8000
56.2529	7.709423	105.0	8000
56.25317	7.73532	105.0	8000
56.25343	7.761218	105.0	8000
56.25369	7.787116	105.0	8000
56.26388	7.657225	105.0	8000
56.26416	7.68313	105.0	8000
56.26443	7.709034	105.0	8000
56.2647	7.73494	105.0	8000
56.26496	7.760845	105.0	8000
56.26522	7.786751	105.0	8000
56.27542	7.656821	105.0	8000
56.27569	7.682733	105.0	8000
56.27597	7.708646	105.0	8000
56.27623	7.734559	105.0	8000

Latitude	Longitude	Hub height AMSL [m]	Output Power [MW]
56.2765	7.760472	105.0	8000
56.27675	7.786386	105.0	8000
56.28695	7.656417	105.0	8000
56.28723	7.682337	105.0	8000
56.2875	7.708257	105.0	8000
56.28777	7.734178	105.0	8000
56.28803	7.760099	105.0	8000
56.28829	7.786021	105.0	8000
56.29848	7.656012	105.0	8000
56.29876	7.68194	105.0	8000
56.29903	7.707868	105.0	8000
56.2993	7.733797	105.0	8000
56.29956	7.759726	105.0	8000
56.29982	7.785655	105.0	8000
56.31002	7.655607	105.0	8000
56.31029	7.681542	105.0	8000
56.31057	7.707478	105.0	8000
56.31084	7.733415	105.0	8000
56.3111	7.759352	105.0	8000
56.31136	7.785289	105.0	8000
56.32155	7.655202	105.0	8000
56.32183	7.681145	105.0	8000
56.3221	7.707089	105.0	8000
56.32237	7.733033	105.0	8000
56.32263	7.758978	105.0	8000
56.32289	7.784923	105.0	8000
56.33308	7.654796	105.0	8000
56.33336	7.680747	105.0	8000
56.33364	7.706699	105.0	8000
56.3339	7.732651	105.0	8000
56.33417	7.758603	105.0	8000

Latitude	Longitude	Hub height AMSL [m]	Output Power [MW]
56.33442	7.784556	105.0	8000
56.34462	7.65439	105.0	8000
56.3449	7.680349	105.0	8000
56.34517	7.706309	105.0	8000
56.34544	7.732268	105.0	8000
56.3457	7.758229	105.0	8000
56.34596	7.78419	105.0	8000
56.35615	7.653984	105.0	8000
56.35643	7.679951	105.0	8000
56.3567	7.705918	105.0	8000
56.35697	7.731886	105.0	8000
56.35723	7.757854	105.0	8000
56.35749	7.783823	105.0	8000
56.36768	7.653577	105.0	8000
56.36796	7.679552	105.0	8000
56.36824	7.705527	105.0	8000
56.3685	7.731503	105.0	8000
56.36877	7.757479	105.0	8000
56.36902	7.783455	105.0	8000
56.37922	7.65317	105.0	8000
56.3795	7.679153	105.0	8000
56.37977	7.705136	105.0	8000
56.38004	7.731119	105.0	8000
56.3803	7.757103	105.0	8000
56.38056	7.783088	105.0	8000
56.39075	7.652763	105.0	8000
56.39103	7.678754	105.0	8000
56.3913	7.704745	105.0	8000
56.39157	7.730736	105.0	8000
56.39183	7.756728	105.0	8000
56.39209	7.78272	105.0	8000

Latitude	Longitude	Hub height AMSL [m]	Output Power [MW]
56.40228	7.652356	105.0	8000
56.40256	7.678354	105.0	8000
56.40284	7.704353	105.0	8000
56.4031	7.730352	105.0	8000
56.40337	7.756352	105.0	8000
56.40363	7.782352	105.0	8000
56.41382	7.651948	105.0	8000
56.41409	7.677954	105.0	8000
56.41437	7.703961	105.0	8000
56.41464	7.729968	105.0	8000
56.4149	7.755975	105.0	8000
56.41516	7.781983	105.0	8000
56.42563	7.677554	105.0	8000
56.4259	7.703569	105.0	8000
56.42617	7.729584	105.0	8000
56.42644	7.755599	105.0	8000
56.42669	7.781615	105.0	8000
56.43744	7.703176	105.0	8000
56.43771	7.729199	105.0	8000
56.43797	7.755222	105.0	8000
56.43823	7.781246	105.0	8000
56.44897	7.702783	105.0	8000
56.44924	7.728814	105.0	8000
56.4495	7.754845	105.0	8000
56.44976	7.780876	105.0	8000
56.46077	7.728429	105.0	8000
56.46104	7.754468	105.0	8000
56.46129	7.780507	105.0	8000
56.47231	7.728043	105.0	8000
56.47257	7.75409	105.0	8000
56.47283	7.780137	105.0	8000

Latitude	Longitude	Hub height AMSL [m]	Output Power [MW]
56.4841	7.753712	105.0	8000
56.48436	7.779767	105.0	8000
56.4959	7.779397	105.0	8000
56.50743	7.779026	105.0	8000

Table 17: Scenario 1 -The projected coordinates of the wind turbines comprising the wind farm with 15MW turbines

Latitude	Longitude	Hub height AMSL [m]	Output Power [kW]
56.231	7.7926	150.0	15000
56.249	7.792	150.0	15000
56.268	7.7914	150.0	15000
56.286	7.7909	150.0	15000
56.305	7.7903	150.0	15000
56.323	7.7897	150.0	15000
56.341	7.7891	150.0	15000
56.36	7.7885	150.0	15000
56.378	7.7879	150.0	15000
56.397	7.7874	150.0	15000
56.415	7.7868	150.0	15000
56.433	7.7862	150.0	15000
56.452	7.7856	150.0	15000
56.47	7.785	150.0	15000
56.489	7.7844	150.0	15000
56.507	7.7838	150.0	15000
56.231	7.7585	150.0	15000
56.249	7.7579	150.0	15000
56.267	7.7573	150.0	15000
56.286	7.7567	150.0	15000
56.304	7.7561	150.0	15000
56.323	7.7555	150.0	15000
56.341	7.7549	150.0	15000
56.359	7.7543	150.0	15000
56.378	7.7537	150.0	15000
56.396	7.7531	150.0	15000
56.415	7.7525	150.0	15000
56.433	7.7519	150.0	15000
56.451	7.7513	150.0	15000

Latitude	Longitude	Hub height AMSL [m]	Output Power [kW]
56.47	7.7507	150.0	15000
56.488	7.7501	150.0	15000
56.23	7.7244	150.0	15000
56.249	7.7238	150.0	15000
56.267	7.7232	150.0	15000
56.286	7.7225	150.0	15000
56.304	7.7219	150.0	15000
56.322	7.7213	150.0	15000
56.341	7.7207	150.0	15000
56.359	7.7201	150.0	15000
56.377	7.7195	150.0	15000
56.396	7.7188	150.0	15000
56.414	7.7182	150.0	15000
56.433	7.7176	150.0	15000
56.451	7.717	150.0	15000
56.23	7.6903	150.0	15000
56.248	7.6896	150.0	15000
56.267	7.689	150.0	15000
56.285	7.6884	150.0	15000
56.304	7.6878	150.0	15000
56.322	7.6871	150.0	15000
56.34	7.6865	150.0	15000
56.359	7.6859	150.0	15000
56.377	7.6852	150.0	15000
56.396	7.6846	150.0	15000
56.414	7.684	150.0	15000
56.432	7.6833	150.0	15000
56.23	7.6562	150.0	15000
56.248	7.6555	150.0	15000
56.266	7.6549	150.0	15000
56.285	7.6542	150.0	15000

Latitude	Longitude	Hub height AMSL [m]	Output Power [kW]
56.303	7.6536	150.0	15000
56.322	7.6529	150.0	15000
56.34	7.6523	150.0	15000
56.358	7.6516	150.0	15000
56.377	7.651	150.0	15000
56.395	7.6503	150.0	15000
56.414	7.6497	150.0	15000

Table 18: Scenario 2 -The projected coordinates of the wind turbines comprising the wind farm with 8MW turbines

Latitude	Longitude	Hub height AMSL [m]	Output Power [MW]
56.274	7.7686	105.0	8000
56.274	7.7918	105.0	8000
56.286	7.7217	105.0	8000
56.286	7.7449	105.0	8000
56.286	7.7682	105.0	8000
56.286	7.7915	105.0	8000
56.298	7.6747	105.0	8000
56.298	7.698	105.0	8000
56.298	7.7213	105.0	8000
56.298	7.7445	105.0	8000
56.299	7.7678	105.0	8000
56.299	7.7911	105.0	8000
56.31	7.6511	105.0	8000
56.31	7.6743	105.0	8000
56.31	7.6976	105.0	8000
56.31	7.7209	105.0	8000
56.311	7.7441	105.0	8000
56.311	7.7674	105.0	8000
56.311	7.7907	105.0	8000
56.321	7.6041	105.0	8000
56.322	7.6273	105.0	8000
56.322	7.6506	105.0	8000
56.322	7.6739	105.0	8000
56.322	7.6972	105.0	8000
56.323	7.7204	105.0	8000
56.323	7.7437	105.0	8000
56.323	7.767	105.0	8000
56.323	7.7903	105.0	8000
56.333	7.5571	105.0	8000

Latitude	Longitude	Hub height AMSL [m]	Output Power [MW]
56.333	7.5803	105.0	8000
56.334	7.6036	105.0	8000
56.334	7.6269	105.0	8000
56.334	7.6502	105.0	8000
56.335	7.6735	105.0	8000
56.335	7.6968	105.0	8000
56.335	7.72	105.0	8000
56.335	7.7433	105.0	8000
56.335	7.7666	105.0	8000
56.336	7.7899	105.0	8000
56.346	7.5566	105.0	8000
56.346	7.5799	105.0	8000
56.346	7.6032	105.0	8000
56.346	7.6265	105.0	8000
56.347	7.6497	105.0	8000
56.347	7.673	105.0	8000
56.347	7.6963	105.0	8000
56.347	7.7196	105.0	8000
56.348	7.7429	105.0	8000
56.348	7.7662	105.0	8000
56.348	7.7895	105.0	8000
56.358	7.5561	105.0	8000
56.358	7.5794	105.0	8000
56.358	7.6027	105.0	8000
56.359	7.626	105.0	8000
56.359	7.6493	105.0	8000
56.359	7.6726	105.0	8000
56.359	7.6959	105.0	8000
56.36	7.7192	105.0	8000
56.36	7.7425	105.0	8000
56.36	7.7658	105.0	8000

Latitude	Longitude	Hub height AMSL [m]	Output Power [MW]
56.36	7.7891	105.0	8000
56.37	7.579	105.0	8000
56.371	7.6023	105.0	8000
56.371	7.6256	105.0	8000
56.371	7.6489	105.0	8000
56.371	7.6722	105.0	8000
56.372	7.6955	105.0	8000
56.372	7.7188	105.0	8000
56.372	7.7421	105.0	8000
56.372	7.7654	105.0	8000
56.373	7.7887	105.0	8000
56.383	7.6018	105.0	8000
56.383	7.6251	105.0	8000
56.384	7.6484	105.0	8000
56.384	7.6718	105.0	8000
56.384	7.6951	105.0	8000
56.384	7.7184	105.0	8000
56.385	7.7417	105.0	8000
56.385	7.765	105.0	8000
56.385	7.7883	105.0	8000
56.396	7.6247	105.0	8000
56.396	7.648	105.0	8000
56.396	7.6713	105.0	8000
56.396	7.6946	105.0	8000
56.397	7.718	105.0	8000
56.397	7.7413	105.0	8000
56.397	7.7646	105.0	8000
56.397	7.7879	105.0	8000
56.408	7.6476	105.0	8000
56.408	7.6709	105.0	8000
56.409	7.6942	105.0	8000

Latitude	Longitude	Hub height AMSL [m]	Output Power [MW]
56.409	7.7176	105.0	8000
56.409	7.7409	105.0	8000
56.409	7.7642	105.0	8000
56.41	7.7875	105.0	8000
56.421	7.6471	105.0	8000
56.421	7.6705	105.0	8000
56.421	7.6938	105.0	8000
56.421	7.7171	105.0	8000
56.421	7.7405	105.0	8000
56.422	7.7638	105.0	8000
56.422	7.7872	105.0	8000
56.433	7.67	105.0	8000
56.433	7.6934	105.0	8000
56.434	7.7167	105.0	8000
56.434	7.7401	105.0	8000
56.434	7.7634	105.0	8000
56.434	7.7868	105.0	8000
56.446	7.693	105.0	8000
56.446	7.7163	105.0	8000
56.446	7.7397	105.0	8000
56.446	7.763	105.0	8000
56.447	7.7864	105.0	8000
56.458	7.7159	105.0	8000
56.458	7.7393	105.0	8000
56.459	7.7626	105.0	8000
56.459	7.786	105.0	8000
56.471	7.7388	105.0	8000
56.471	7.7622	105.0	8000
56.471	7.7856	105.0	8000
56.483	7.7618	105.0	8000
56.484	7.7852	105.0	8000

Latitude	Longitude	Hub height AMSL [m]	Output Power [MW]
56.496	7.7614	105.0	8000
56.496	7.7848	105.0	8000
56.508	7.7844	105.0	8000

Table 19: Scenario 2 -The projected coordinates of the wind turbines comprising the wind farm with 15MW turbines

Latitude	Longitude	Hub height AMSL [m]	Output Power [kW]
56.27	7.7914	150.0	15000
56.286	7.7909	150.0	15000
56.302	7.7903	150.0	15000
56.318	7.7898	150.0	15000
56.335	7.7893	150.0	15000
56.351	7.7888	150.0	15000
56.367	7.7883	150.0	15000
56.383	7.7878	150.0	15000
56.399	7.7873	150.0	15000
56.416	7.7868	150.0	15000
56.432	7.7862	150.0	15000
56.448	7.7857	150.0	15000
56.464	7.7852	150.0	15000
56.48	7.7847	150.0	15000
56.497	7.7842	150.0	15000
56.513	7.7836	150.0	15000
56.286	7.7567	150.0	15000
56.302	7.7562	150.0	15000
56.318	7.7556	150.0	15000
56.334	7.7551	150.0	15000
56.351	7.7546	150.0	15000
56.367	7.7541	150.0	15000
56.383	7.7535	150.0	15000
56.399	7.753	150.0	15000
56.415	7.7525	150.0	15000
56.431	7.7519	150.0	15000
56.448	7.7514	150.0	15000
56.464	7.7509	150.0	15000
56.48	7.7504	150.0	15000

Latitude	Longitude	Hub height AMSL [m]	Output Power [kW]
56.285	7.7225	150.0	15000
56.302	7.722	150.0	15000
56.318	7.7215	150.0	15000
56.334	7.7209	150.0	15000
56.35	7.7204	150.0	15000
56.366	7.7198	150.0	15000
56.383	7.7193	150.0	15000
56.399	7.7188	150.0	15000
56.415	7.7182	150.0	15000
56.431	7.7177	150.0	15000
56.447	7.7171	150.0	15000
56.464	7.7166	150.0	15000
56.301	7.6878	150.0	15000
56.317	7.6873	150.0	15000
56.334	7.6867	150.0	15000
56.35	7.6862	150.0	15000
56.366	7.6856	150.0	15000
56.382	7.6851	150.0	15000
56.398	7.6845	150.0	15000
56.415	7.6839	150.0	15000
56.431	7.6834	150.0	15000
56.317	7.6531	150.0	15000
56.333	7.6525	150.0	15000
56.349	7.652	150.0	15000
56.366	7.6514	150.0	15000
56.382	7.6508	150.0	15000
56.398	7.6502	150.0	15000
56.414	7.6497	150.0	15000
56.317	7.6189	150.0	15000
56.333	7.6183	150.0	15000
56.349	7.6177	150.0	15000

Latitude	Longitude	Hub height AMSL [m]	Output Power [kW]
56.365	7.6172	150.0	15000
56.381	7.6166	150.0	15000
56.398	7.616	150.0	15000
56.332	7.5841	150.0	15000
56.349	7.5835	150.0	15000
56.365	7.5829	150.0	15000
56.348	7.5493	150.0	15000

Table 20: Scenario 3 -The projected coordinates of the wind turbines comprising the wind farm with 8MW turbines

Latitude	Longitude	Hub height AMSL [m]	Output Power [MW]
56.226	7.3924	105.0	8000
56.226	7.4157	105.0	8000
56.227	7.4389	105.0	8000
56.227	7.4621	105.0	8000
56.227	7.4853	105.0	8000
56.228	7.5085	105.0	8000
56.228	7.5317	105.0	8000
56.228	7.555	105.0	8000
56.228	7.5782	105.0	8000
56.229	7.6014	105.0	8000
56.229	7.6246	105.0	8000
56.229	7.6478	105.0	8000
56.229	7.6711	105.0	8000
56.23	7.6943	105.0	8000
56.23	7.7175	105.0	8000
56.23	7.7407	105.0	8000
56.238	7.4152	105.0	8000
56.239	7.4384	105.0	8000
56.239	7.4616	105.0	8000
56.239	7.4848	105.0	8000
56.239	7.5081	105.0	8000
56.24	7.5313	105.0	8000
56.24	7.5545	105.0	8000
56.24	7.5777	105.0	8000
56.241	7.601	105.0	8000
56.241	7.6242	105.0	8000
56.241	7.6474	105.0	8000
56.241	7.6706	105.0	8000
56.242	7.6939	105.0	8000

Latitude	Longitude	Hub height AMSL [m]	Output Power [MW]
56.242	7.7171	105.0	8000
56.25	7.4147	105.0	8000
56.25	7.4379	105.0	8000
56.251	7.4611	105.0	8000
56.251	7.4844	105.0	8000
56.251	7.5076	105.0	8000
56.252	7.5308	105.0	8000
56.252	7.5541	105.0	8000
56.252	7.5773	105.0	8000
56.252	7.6005	105.0	8000
56.253	7.6238	105.0	8000
56.253	7.647	105.0	8000
56.253	7.6702	105.0	8000
56.253	7.6935	105.0	8000
56.254	7.7167	105.0	8000
56.262	7.4374	105.0	8000
56.263	7.4607	105.0	8000
56.263	7.4839	105.0	8000
56.263	7.5071	105.0	8000
56.263	7.5304	105.0	8000
56.264	7.5536	105.0	8000
56.264	7.5769	105.0	8000
56.264	7.6001	105.0	8000
56.265	7.6233	105.0	8000
56.265	7.6466	105.0	8000
56.265	7.6698	105.0	8000
56.265	7.6931	105.0	8000
56.266	7.7163	105.0	8000
56.274	7.4602	105.0	8000
56.275	7.4834	105.0	8000
56.275	7.5067	105.0	8000

Latitude	Longitude	Hub height AMSL [m]	Output Power [MW]
56.275	7.5299	105.0	8000
56.276	7.5532	105.0	8000
56.276	7.5764	105.0	8000
56.276	7.5997	105.0	8000
56.276	7.6229	105.0	8000
56.277	7.6462	105.0	8000
56.277	7.6694	105.0	8000
56.277	7.6927	105.0	8000
56.287	7.483	105.0	8000
56.287	7.5062	105.0	8000
56.287	7.5295	105.0	8000
56.287	7.5527	105.0	8000
56.288	7.576	105.0	8000
56.288	7.5992	105.0	8000
56.288	7.6225	105.0	8000
56.289	7.6457	105.0	8000
56.289	7.669	105.0	8000
56.289	7.6923	105.0	8000
56.299	7.4825	105.0	8000
56.299	7.5058	105.0	8000
56.299	7.529	105.0	8000
56.299	7.5523	105.0	8000
56.3	7.5755	105.0	8000
56.3	7.5988	105.0	8000
56.3	7.6221	105.0	8000
56.3	7.6453	105.0	8000
56.301	7.6686	105.0	8000
56.301	7.6919	105.0	8000
56.311	7.5053	105.0	8000
56.311	7.5286	105.0	8000
56.311	7.5518	105.0	8000

Latitude	Longitude	Hub height AMSL [m]	Output Power [MW]
56.312	7.5751	105.0	8000
56.312	7.5984	105.0	8000
56.312	7.6216	105.0	8000
56.312	7.6449	105.0	8000
56.313	7.6682	105.0	8000
56.323	7.5281	105.0	8000
56.323	7.5514	105.0	8000
56.323	7.5747	105.0	8000
56.324	7.5979	105.0	8000
56.324	7.6212	105.0	8000
56.324	7.6445	105.0	8000
56.324	7.6678	105.0	8000
56.335	7.5276	105.0	8000
56.335	7.5509	105.0	8000
56.335	7.5742	105.0	8000
56.336	7.5975	105.0	8000
56.336	7.6208	105.0	8000
56.336	7.6441	105.0	8000
56.336	7.6673	105.0	8000
56.347	7.5505	105.0	8000
56.347	7.5738	105.0	8000
56.347	7.5971	105.0	8000
56.348	7.6203	105.0	8000
56.348	7.6436	105.0	8000
56.359	7.5733	105.0	8000
56.359	7.5966	105.0	8000
56.36	7.6199	105.0	8000
56.36	7.6432	105.0	8000
56.371	7.5962	105.0	8000
56.371	7.6195	105.0	8000
56.372	7.6428	105.0	8000

Latitude	Longitude	Hub height AMSL [m]	Output Power [MW]
56.383	7.5957	105.0	8000
56.383	7.6191	105.0	8000
56.395	7.6186	105.0	8000

Table 21: Scenario 3 -The projected coordinates of the wind turbines comprising the wind farm with 15MW turbines

Latitude	Longitude	Hub height AMSL [m]	Output Power [kW]
56.231	7.7227	150.0	15000
56.246	7.7222	150.0	15000
56.23	7.6886	150.0	15000
56.246	7.6881	150.0	15000
56.261	7.6876	150.0	15000
56.276	7.6871	150.0	15000
56.291	7.6865	150.0	15000
56.306	7.686	150.0	15000
56.23	7.6545	150.0	15000
56.245	7.654	150.0	15000
56.26	7.6535	150.0	15000
56.275	7.6529	150.0	15000
56.291	7.6524	150.0	15000
56.306	7.6519	150.0	15000
56.321	7.6513	150.0	15000
56.336	7.6508	150.0	15000
56.351	7.6503	150.0	15000
56.366	7.6497	150.0	15000
56.23	7.6204	150.0	15000
56.245	7.6199	150.0	15000
56.26	7.6193	150.0	15000
56.275	7.6188	150.0	15000
56.29	7.6182	150.0	15000
56.305	7.6177	150.0	15000
56.321	7.6171	150.0	15000
56.336	7.6166	150.0	15000
56.351	7.616	150.0	15000
56.366	7.6155	150.0	15000
56.381	7.6149	150.0	15000

Latitude	Longitude	Hub height AMSL [m]	Output Power [kW]
56.396	7.6144	150.0	15000
56.229	7.5863	150.0	15000
56.244	7.5857	150.0	15000
56.26	7.5852	150.0	15000
56.275	7.5846	150.0	15000
56.29	7.5841	150.0	15000
56.305	7.5835	150.0	15000
56.32	7.5829	150.0	15000
56.335	7.5824	150.0	15000
56.35	7.5818	150.0	15000
56.366	7.5813	150.0	15000
56.229	7.5522	150.0	15000
56.244	7.5516	150.0	15000
56.259	7.5511	150.0	15000
56.274	7.5505	150.0	15000
56.289	7.5499	150.0	15000
56.305	7.5493	150.0	15000
56.32	7.5488	150.0	15000
56.335	7.5482	150.0	15000
56.229	7.5181	150.0	15000
56.244	7.5175	150.0	15000
56.259	7.5169	150.0	15000
56.274	7.5163	150.0	15000
56.289	7.5158	150.0	15000
56.304	7.5152	150.0	15000
56.319	7.5146	150.0	15000
56.228	7.484	150.0	15000
56.243	7.4834	150.0	15000
56.258	7.4828	150.0	15000
56.274	7.4822	150.0	15000
56.289	7.4816	150.0	15000

Latitude	Longitude	Hub height AMSL [m]	Output Power [kW]
56.228	7.4499	150.0	15000
56.243	7.4493	150.0	15000
56.258	7.4487	150.0	15000
56.273	7.4481	150.0	15000
56.227	7.4158	150.0	15000
56.242	7.4152	150.0	15000
56.227	7.3817	150.0	15000

Table 22: Scenario 4 -The projected coordinates of the wind turbines comprising the wind farm with 8MW turbines

Latitude	Longitude	Hub height AMSL [m]	Output Power [MW]
56.227	7.3803	105.0	8000
56.228	7.4104	105.0	8000
56.227	7.4415	105.0	8000
56.228	7.4738	105.0	8000
56.228	7.5028	105.0	8000
56.228	7.5281	105.0	8000
56.229	7.5858	105.0	8000
56.23	7.6101	105.0	8000
56.23	7.6354	105.0	8000
56.231	7.6952	105.0	8000
56.231	7.7241	105.0	8000
56.232	7.753	105.0	8000
56.23	7.7796	105.0	8000
56.331	7.792	105.0	8000
56.248	7.8045	105.0	8000
56.23	7.8043	105.0	8000
56.243	7.3994	105.0	8000
56.241	7.4235	105.0	8000
56.239	7.4782	105.0	8000
56.281	7.4857	105.0	8000
56.281	7.5346	105.0	8000
56.244	7.5686	105.0	8000
56.246	7.6059	105.0	8000
56.264	7.6556	105.0	8000
56.229	7.5559	105.0	8000
56.23	7.6639	105.0	8000
56.245	7.7278	105.0	8000
56.245	7.7692	105.0	8000
56.35	7.7883	105.0	8000

Latitude	Longitude	Hub height AMSL [m]	Output Power [MW]
56.27	7.8024	105.0	8000
56.257	7.4139	105.0	8000
56.241	7.4503	105.0	8000
56.259	7.4968	105.0	8000
56.246	7.5051	105.0	8000
56.244	7.5358	105.0	8000
56.261	7.5996	105.0	8000
56.271	7.6253	105.0	8000
56.283	7.6692	105.0	8000
56.248	7.6858	105.0	8000
56.268	7.6884	105.0	8000
56.256	7.7505	105.0	8000
56.268	7.763	105.0	8000
56.37	7.7854	105.0	8000
56.29	7.7979	105.0	8000
56.267	7.4614	105.0	8000
56.254	7.4689	105.0	8000
56.26	7.5618	105.0	8000
56.273	7.5883	105.0	8000
56.285	7.6016	105.0	8000
56.288	7.6356	105.0	8000
56.304	7.6464	105.0	8000
56.246	7.6473	105.0	8000
56.298	7.6855	105.0	8000
56.268	7.7253	105.0	8000
56.289	7.7609	105.0	8000
56.39	7.7875	105.0	8000
56.308	7.7925	105.0	8000
56.264	7.5281	105.0	8000
56.285	7.5696	105.0	8000
56.294	7.4976	105.0	8000

Latitude	Longitude	Hub height AMSL [m]	Output Power [MW]
56.301	7.5713	105.0	8000
56.322	7.6434	105.0	8000
56.315	7.6841	105.0	8000
56.36	7.5997	105.0	8000
56.361	7.6602	105.0	8000
56.286	7.7248	105.0	8000
56.31	7.7564	105.0	8000
56.409	7.7896	105.0	8000
56.297	7.5368	105.0	8000
56.317	7.5377	105.0	8000
56.328	7.5684	105.0	8000
56.331	7.6165	105.0	8000
56.334	7.6778	105.0	8000
56.353	7.6903	105.0	8000
56.374	7.6879	105.0	8000
56.345	7.7219	105.0	8000
56.328	7.7584	105.0	8000
56.429	7.795	105.0	8000
56.338	7.528	105.0	8000
56.301	7.6159	105.0	8000
56.316	7.5911	105.0	8000
56.349	7.6359	105.0	8000
56.389	7.6509	105.0	8000
56.416	7.6899	105.0	8000
56.434	7.709	105.0	8000
56.363	7.7281	105.0	8000
56.348	7.7555	105.0	8000
56.443	7.7945	105.0	8000
56.352	7.5484	105.0	8000
56.345	7.5791	105.0	8000
56.37	7.6297	105.0	8000

Latitude	Longitude	Hub height AMSL [m]	Output Power [MW]
56.396	7.6844	105.0	8000
56.284	7.4493	105.0	8000
56.27	7.4303	105.0	8000
56.423	7.6523	105.0	8000
56.37	7.7584	105.0	8000
56.368	7.5712	105.0	8000
56.324	7.5091	105.0	8000
56.311	7.4885	105.0	8000
56.297	7.4687	105.0	8000
56.45	7.7297	105.0	8000
56.305	7.7232	105.0	8000
56.461	7.7936	105.0	8000
56.397	7.6151	105.0	8000
56.381	7.594	105.0	8000
56.449	7.7589	105.0	8000
56.409	7.6334	105.0	8000
56.471	7.7563	105.0	8000
56.326	7.7211	105.0	8000
56.478	7.7924	105.0	8000
56.439	7.6772	105.0	8000
56.452	7.693	105.0	8000
56.466	7.7156	105.0	8000
56.399	7.7239	105.0	8000
56.407	7.7579	105.0	8000
56.492	7.7525	105.0	8000
56.48	7.7349	105.0	8000
56.382	7.7243	105.0	8000
56.391	7.7575	105.0	8000
56.504	7.7701	105.0	8000
56.428	7.7595	105.0	8000
56.49	7.7815	105.0	8000

Latitude	Longitude	Hub height AMSL [m]	Output Power [MW]
56.417	7.7216	105.0	8000
56.504	7.789	105.0	8000
56.517	7.7899	105.0	8000

Table 23: Scenario 4 -The projected coordinates of the wind turbines comprising the wind farm with 15MW turbines

Latitude	Longitude	Hub height AMSL [m]	Output Power [kW]
56.232	7.8006	150.0	15000
56.298	7.7901	150.0	15000
56.231	7.7565	150.0	15000
56.272	7.7941	150.0	15000
56.321	7.724	150.0	15000
56.327	7.7898	150.0	15000
56.351	7.7785	150.0	15000
56.389	7.7548	150.0	15000
56.23	7.7092	150.0	15000
56.251	7.7981	150.0	15000
56.308	7.7537	150.0	15000
56.287	7.7291	150.0	15000
56.387	7.6068	150.0	15000
56.367	7.7322	150.0	15000
56.385	7.7905	150.0	15000
56.412	7.7908	150.0	15000
56.433	7.7935	150.0	15000
56.487	7.7913	150.0	15000
56.23	7.6618	150.0	15000
56.274	7.7615	150.0	15000
56.339	7.5978	150.0	15000
56.344	7.7289	150.0	15000
56.382	7.6489	150.0	15000
56.379	7.6839	150.0	15000
56.411	7.7389	150.0	15000
56.422	7.7044	150.0	15000
56.453	7.6997	150.0	15000
56.458	7.7952	150.0	15000
56.49	7.7516	150.0	15000

Latitude	Longitude	Hub height AMSL [m]	Output Power [kW]
56.51	7.7852	150.0	15000
56.23	7.6194	150.0	15000
56.255	7.7514	150.0	15000
56.313	7.5752	150.0	15000
56.303	7.6857	150.0	15000
56.335	7.546	150.0	15000
56.35	7.6812	150.0	15000
56.416	7.6418	150.0	15000
56.464	7.7613	150.0	15000
56.434	7.7557	150.0	15000
56.47	7.7229	150.0	15000
56.228	7.5737	150.0	15000
56.293	7.6452	150.0	15000
56.255	7.696	150.0	15000
56.314	7.6308	150.0	15000
56.396	7.7114	150.0	15000
56.351	7.638	150.0	15000
56.408	7.6722	150.0	15000
56.442	7.7287	150.0	15000
56.229	7.5181	150.0	15000
56.275	7.6856	150.0	15000
56.268	7.6412	150.0	15000
56.317	7.5163	150.0	15000
56.328	7.6681	150.0	15000
56.357	7.5798	150.0	15000
56.431	7.6711	150.0	15000
56.248	7.4774	150.0	15000
56.246	7.5563	150.0	15000
56.249	7.6211	150.0	15000
56.295	7.6031	150.0	15000
56.289	7.4816	150.0	15000

Latitude	Longitude	Hub height AMSL [m]	Output Power [kW]
56.27	7.5302	150.0	15000
56.273	7.5942	150.0	15000
56.299	7.5414	150.0	15000
56.273	7.4481	150.0	15000
56.227	7.4531	150.0	15000
56.252	7.4235	150.0	15000
56.227	7.3817	150.0	15000

Annex B Formula symbols of Annex C in [1]

P_{ref}	The power of the reflected signal arriving at the radar (W)
P_t	Transmitted power (W)
P_{thresh}	Radar receiver detection threshold (W)
G_t	Transmit antenna gain
G_r	Receive antenna gain (main beam)
G_{rs}	Receive antenna gain (side lobes)
σ_a	The mono-static RCS of the aircraft (m^2)
σ_w	The mono-static RCS of the wind turbine (m^2)
σ_{a1}	The bi-static RCS of the aircraft from radar to wind turbine (m^2)
σ_{a2}	The bi-static RCS of the aircraft from wind turbine to radar (m^2)
σ_{w1}	The bi-static RCS of the wind turbine from radar to aircraft (m^2)
σ_{w2}	The bi-static RCS of the wind turbine from aircraft to radar (m^2)
$F_{rw} = F_{wr}$	Terrain induced attenuation factor between radar and wind turbine.
$F_{wa} = F_{wa}$	Terrain induced attenuation factor between wind turbine and aircraft.
$F_{ra} = F_{ar}$	Terrain induced attenuation factor between radar and aircraft.
D_{rw}	Distance radar to wind turbine (m)
D_{wa}	Distance wind turbine to aircraft (m)
D_{ra}	Distance radar to aircraft (m)
λ	Signal wavelength (m)

Annex C Shadow Height Illustrations

[redacted]

[redacted]

[redacted]

[redacted]

[redacted]

 Scenario 2

[redacted]

[redacted]

[redacted]

[redacted]

[redacted]

[redacted]

[redacted]

[redacted]

[redacted]